

AD-A121 172

MANUFACTURING METHODS AND TECHNOLOGY (MANTECH) PROGRAM
MANUFACTURING TECH.: (U) HUGHES HELICOPTERS INC CULVER
CITY CA J V ALEXANDER ET AL. OCT 81 HHI-81-367

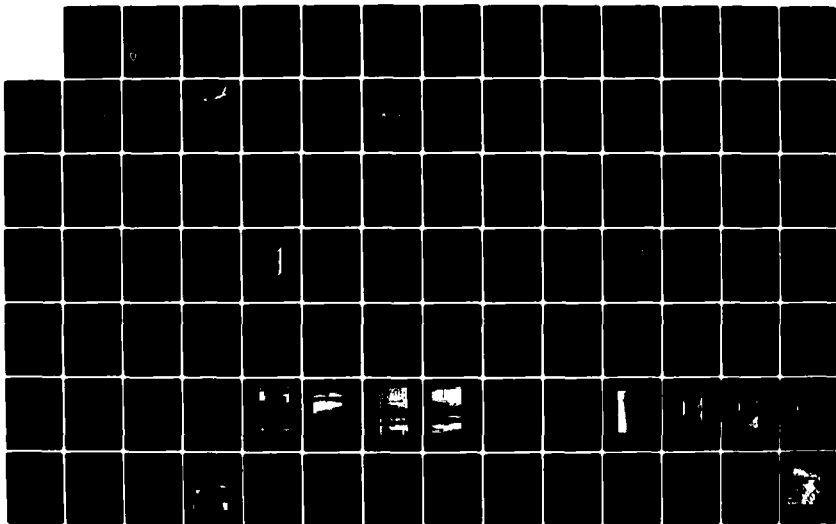
1/3

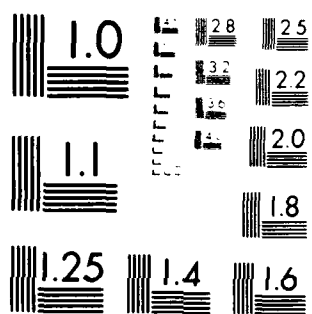
UNCLASSIFIED

USAAVRADCOM-TR-82-F-1 DAAK50-78-G-0004

F/G 1/3

NL





MICROCOPY RESOLUTION TEST CHART
NATIONAL BUREAU OF STANDARDS-1963-A

AVRADCOM
Report No. TR-82-F-1

AD

**MANUFACTURING METHODS AND TECHNOLOGY
(MANTECH) PROGRAM MANUFACTURING
TECHNIQUES FOR A COMPOSITE TAIL SECTION FOR
THE ADVANCED ATTACK HELICOPTER**

AD A 121172

J.V. ALEXANDER
R.E. HEAD

October 1981

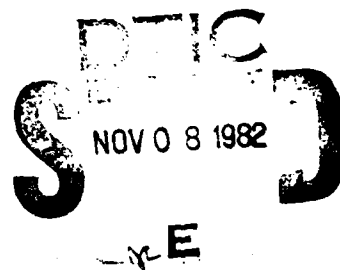
FINAL REPORT

Contract No. DAAK50-78-G-0004
DO 0002



Approved for public release;
distribution unlimited

UNITED STATES ARMY
AVIATION RESEARCH AND DEVELOPMENT COMMAND



UNCLASSIFIED

SECURITY CLASSIFICATION OF THIS PAGE (When Data Entered)

REPORT DOCUMENTATION PAGE		READ INSTRUCTIONS BEFORE COMPLETING FORM
1. REPORT NUMBER USAAVRADCOM TR-32-F-1	2. GOVT ACCESSION NO.	3. RECIPIENT'S CATALOG NUMBER
4. TITLE (and Subtitle) Manufacturing Techniques for a Composite Tail Section for the Advanced Attack Helicopter		5. TYPE OF REPORT & PERIOD COVERED Final Report Sept. 1979 - April 1981
		6. PERFORMING ORG. REPORT NUMBER HHI 81-367
7. AUTHOR(s) J. V. Alexander R. E. Head		8. CONTRACT OR GRANT NUMBER(s) DAAK50-78-G-0004 (DO-0002)
9. PERFORMING ORGANIZATION NAME AND ADDRESS Hughes Helicopters, Inc. Centinela and Teale Streets Culver City, CA 90230		10. PROGRAM ELEMENT, PROJECT, TASK AREA & WORK UNIT NUMBERS Project No. 7333
11. CONTROLLING OFFICE NAME AND ADDRESS U.S. Army Aviation Research and Development Command, Attn: DRDAV-EGX, 4300 Goodfellow Blvd., St. Louis, MO 63120		12. REPORT DATE October 1981
		13. NUMBER OF PAGES
14. MONITORING AGENCY NAME & ADDRESS (if different from Controlling Office)		15. SECURITY CLASS. (of this report) Unclassified
		15a. DECLASSIFICATION/DOWNGRADING SCHEDULE
16. DISTRIBUTION STATEMENT (of this Report) Approved for public release; distribution unlimited		
17. DISTRIBUTION STATEMENT (of the abstract entered in Block 20, if different from Report)		
18. SUPPLEMENTARY NOTES		
19. KEY WORDS (Continue on reverse side if necessary and identify by block number) Fuselage Antenna Pattern Fabrication Kevlar Empennage Lightning Protection Resin Nomex Composite Structure Tooling Graphite Electrolysis Ballistic Survivability		
20. ABSTRACT (Continue on reverse side if necessary and identify by block number) This manufacturing methods and technology program involved the study of establishing manufacturing methods for a Composite Tail Section (CTS) for the AH-64A Advanced Attack Helicopter by the wet filament wound, cocure process. The CTS was meant to replace equivalent metal components on the AH-64A while providing potential weight and cost savings. Ballistic tolerance against 23mm HEI-T was demonstrated, and VHF antenna		

DD FORM 1 JAN 73 1473

EDITION OF 1 NOV 65 IS OBSOLETE

UNCLASSIFIED

SECURITY CLASSIFICATION OF THIS PAGE (When Data Entered)

UNCLASSIFIED

SECURITY CLASSIFICATION OF THIS PAGE(When Data Entered)

20. performance was shown to be unaffected by the change to composite construction. The program was terminated for fiscal reasons just when the CTS design was completed and the tooling design was within one month of completion. This CTS concept offers significant benefits to the AH-64A helicopter program and should be reinstated at the earliest opportunity. '

UNCLASSIFIED

SECURITY CLASSIFICATION OF THIS PAGE(When Data Entered)

PREFACE

This report was prepared by Hughes Helicopters, Inc. (HHI) under U. S. Army Basic Ordering Agreement DAAK50-78-G-0004, Delivery Order 0002. The contract was sponsored by the U. S. Army Aviation Research and Development Command (AVRADCOM) and administered under the technical direction of Mr. James Tutka, AVRADCOM, with assistance from Mr. Nicholas Calapodas, Applied Technology Laboratory, Ft. Eustis, VA.

The technical tasks were conducted under the direction of HHI's program managers, Messrs. Nicholas Mocerino and Robert Head, and Mr. Sherwood Twitchell, the project engineer at Fiber Science, Inc., the major sub-contractor for tooling and fabrication.

Accession For	
NTIS GRA&I	<input checked="checked" type="checkbox"/>
DTIC TAB	<input type="checkbox"/>
Unannounced	<input type="checkbox"/>
Justification	
By	
Distribution/	
Availability Codes	
Dist	Avail and/or Special
A	



TABLE OF CONTENTS

	<u>Page</u>
PREFACE	3
LIST OF ILLUSTRATIONS	6
LIST OF TABLES	11
INTRODUCTION	13
DESIGN REQUIREMENTS	17
DESIGN REFINEMENT	27
Tailboom	29
Vertical Tail	37
Stabilator	46
Environmental Protection	49
WEIGHT ANALYSIS	51
RELIABILITY ASSESSMENT	55
STRUCTURE VERIFICATION TESTS.....	57
BALLISTIC VULNERABILITY TESTING	65
LIGHTNING PROTECTION EVALUATION (HHI SPONSORED TEST) .	76
ANTENNA INTEGRATION EVALUATION	83
MANUFACTURING TECHNOLOGY REFINEMENT	93
Wet Filament Winding Methodology	93
Tailboom	96
Vertical Tail Spar	98
Stabilator	98
Resin Cure Cycle.....	100

TABLE OF CONTENTS (CONT)

	<u>Page</u>
FABRICATION REFINEMENT	102
Tailboom Tooling	102
Vertical Tail Tooling	107
Stabilator Tooling	111
Final Assembly	119
NON-DESTRUCTIVE EVALUATION (NDE)	121
DESIGN TO UNIT PRODUCTION COST	133
LABORATORY AND FLIGHT TEST PLANS	149
Laboratory Tests	149
Flight Tests	150
IMPLICATIONS FOR PRODUCTION	159
CONCLUSIONS	163
REFERENCES	165
CTS ASSEMBLY AND SUBASSEMBLY DRAWINGS	166

LIST OF ILLUSTRATIONS

<u>Figure</u>		<u>Page</u>
1	AH-64A - Initial CTS Configuration	13
2	AH-64A - Final CTS Configuration	15
3	AH-64A Lines Drawing	18
4	Flight Load Factors Versus Airspeed (Basic Structural Design Gross Weight Except Where Noted)	20
5	Sideslip Envelopes	21
6	Tailboom Stiffness	22
7	Vertical Tail Stiffness	23
8	Stabilator Stiffness	24
9	Composite Tail Section with Adjacent Fairings, Closeouts, and Internal Hardware	28
10	Tail Boom Configuration	30
11	Tail Boom - Structure Details	32
12	Metal/Composite Manufacturing Splice, Sta 370	33
13	Tail Boom	35
14	Aft End of Tailboom	36
15	Vertical Tail Spar Box Structure	38
16	Vertical Tail Cross Sections	40
17	Vertical Stabilizer Skin Thickness	41
18	Root Fitting	42
19	Upper Gearbox Assembly	44

LIST OF ILLUSTRATIONS (CONT)

<u>Figure</u>		<u>Page</u>
20	Step/Hand Hold	45
21	Stabilator Structure	47
22	Lightning Protection	50
23	AH-64A Longitudinal Center-of-Gravity with CTS	54
24	Tension/Compression Specimen	58
25	Torsion Test Specimen	59
26	Bearing Test Specimen Type III-1	60
27	Bearing Test Specimen Type III-2	61
28	Tubular Static Tension Test Schematic	63
29	Tubular Static Compression Test Schematic	64
30	Tubular Static Shear (Torsion) Test Schematic	64
31	Ballistic Test Specimen Construction	70
32	Ballistic Test Setup and Impact Location	70
33	Ballistic Damage Zones	71
34	Ballistic Specimen #1 -- Undamaged	72
35	Specimen #1 -- Front View With Damage	72
36	Specimen #1 -- Rear View With Damage	73
37	Ballistic Specimen #2 -- Undamaged	74
38	Specimen #2 -- Front View With Damage	74
39	Specimen #2 -- Close-up Front View With Damage	75

LIST OF ILLUSTRATIONS (CONT)

<u>Figure</u>		<u>Page</u>
40	Specimen #2 -- Rear View With Damage.	75
41	Test Arrangement for Stationary 200,000 Ampere Discharge.	76
42	Test Arrangement for Swept Stroke Tests.	77
43	Stationary Discharge Damage -- Specimen 1.	78
44	Stationary Discharge Damage -- Specimen 2.	79
45	Swept Stroke Discharge Damage -- Specimen 3.	80
46	Swept Stroke Discharge Damage -- Specimen 4.	81
47	YAH-64 Graphite Tail Section Mockup Installed on Antenna Tower/Positioner.	85
48	Radiation Pattern Test Setup.	86
49	AH-64A Trailing Edge Antenna on Aluminum Mockup.	87
50	AH-64A Trailing Edge Antenna on Graphite Mockup.	88
51	Antenna Pattern -- 30 MHz.	90
52	Antenna Pattern -- 40 MHz.	90
53	Antenna Pattern -- 50 MHz.	91
54	Antenna Pattern -- 60 MHz.	91
55	Antenna Pattern -- 70 MHz.	92
56	Antenna Pattern -- 76 MHz.	92
57	Tubular Element Filament Winding Process.	94
58	Resin Impregnator.	95

LIST OF ILLUSTRATIONS (CONT)

<u>Figure</u>		<u>Page</u>
59	Tailboom Mandrel Geometry	96
60	Tailboom Mandrel - Main Section (Toolproofing)	97
61	Tailboom Mandrel - Removable Sections (Toolproofing) . .	97
62	Vertical Tail Spar Winding Pattern Study	99
63	Bead-Stiffening Study for Stabilator Skin.	100
64	Resin Cure Cycle	101
65	Tailboom Mandrel	103
66	Frame Assembly Fixture Schematic	104
67	Frame Mold Section Schematic	105
68	Helical Winding Machine	106
69	Angle Mold Schematic	107
70	Tailboom Fabrication Sequence.	108
71	Vertical Tail Spar Mandrel	109
72	Frame Subassembly Tool Schematic	110
73	Tip Cap Mold Schematic	112
74	T-Bar Mold Section Schematic	113
75	T-Bar Bonding Jig Schematic	113
76	Vertical Tail Fabrication Sequence	114
77	Stabilator Skin Winding Mandrel Schematic	115
78	Stabilator Skin Mold Schematic	115

LIST OF ILLUSTRATIONS (CONT)

<u>Figure</u>		<u>Page</u>
79	Tip Cap Mold Schematic	116
80	Stabilator Skin Bonding Jig Schematic	117
81	Stabilator Fabrication Sequence	118
82	Final Assembly Fixture Functions	120
83	Composite Tailboom Inspection Zones	122
84	Composite Vertical Tail Inspection Zones	126
85	Composite Stabilator Inspection Zones	129
86	Schematic Static/Fatigue Test Setup	151
87	Strain Gage Installation FS 375.	152
88	Strain Gage Installation - Tail Boom FS 539	153
89	Strain Gage Installation - Vertical Stabilizer Fitting FS 530.09	154
90	Strain Gage Installation - Rear Frame FS 547.	155
91	Strain Gage Installation - Vertical Stabilizer Spar	156
92	Strain Gage Installation - Stabilator Spar	157
93	Tail Section Weight Comparison	161
94	Unit Production Cost Comparison 536 Shipsets - 1981 Dollars	162
95	Tailboom Assembly	167
96	Tailboom Subassembly	173
97	Vertical Tail Assembly	181
98	Vertical Tail Subassembly	183
99	Stabilator Assembly	187

LIST OF TABLES

<u>Table</u>		<u>Page</u>
1	Examples of Structural Failures	26
2	CTS Weight Analysis.	52
3	CTS Weight Status Summary	53
4	Tension/Compression Specimens	58
5	Torsion Specimen	59
6	Stacking Sequence for Type II Specimens	62
7	Fabrication Notes for Type III Specimens	63
8	Tension/Compression Test Results	66
9	Torsion Test Results	67
10	Bearing Test Results	68
11	Tailboom Critical Disbond and Delamination Limits	123
12	Potential NDE Techniques - Tailboom	124
13	Vertical Tail - Center Box Critical Disbond and Delamination Limits	125
14	Potential NDE Techniques - Vertical	127
15	Stabilator Critical Disbond and Delamination Limits	130
16	Potential NDE Techniques - Stabilator	132
17	Labor for Tailboom (S/N-010)	134
18	Labor for Stabilator (S/N-010)	136
19	Labor for Vertical Tail (S/N-010)	138

LIST OF TABLES (CONT)

<u>Table</u>		<u>Page</u>
20	Composite Material for CTS (Second Quarter 1981 Dollars)	141
21	Components Other Than Structural Composites (Second Quarter 1981 Dollars)	142
22	Design to Unit Production Cost (Second Quarter 1981 Dollars)	144
23	DTUPC Summary (1981 Dollars) (Second Quarter 1981 Dollars)	148
24	Flight Profile	158
25	CTS Design Changes to Achieve "Mix-and-Match"	160

INTRODUCTION

In August, 1979, Hughes Helicopters, Inc. (HHI) was awarded a contract under a Manufacturing Methods and Technology (MM&T) program to develop and refine the manufacturing processes necessary to fabricate and test a set number of Composite Tail Sections (CTS) for the AH-64A Advanced Attack Helicopter (AAH). Anticipated benefits resulting from this MM&T program were reduced weight and cost, and improved survivability, reliability, and maintainability.

The CTS program as initially defined required that the aft portion of the tailboom, the vertical tail spar, and the horizontal tail be the primary composite structure. See Figure 1. Existing fairings from the prototype design such as those for the leading and trailing edges of the vertical tail, driveshaft cover, and aft tailboom fairing were to be transferred to the CTS. The CTS was to accommodate all existing mounts for the gearboxes, controls, tail wheel, etc.

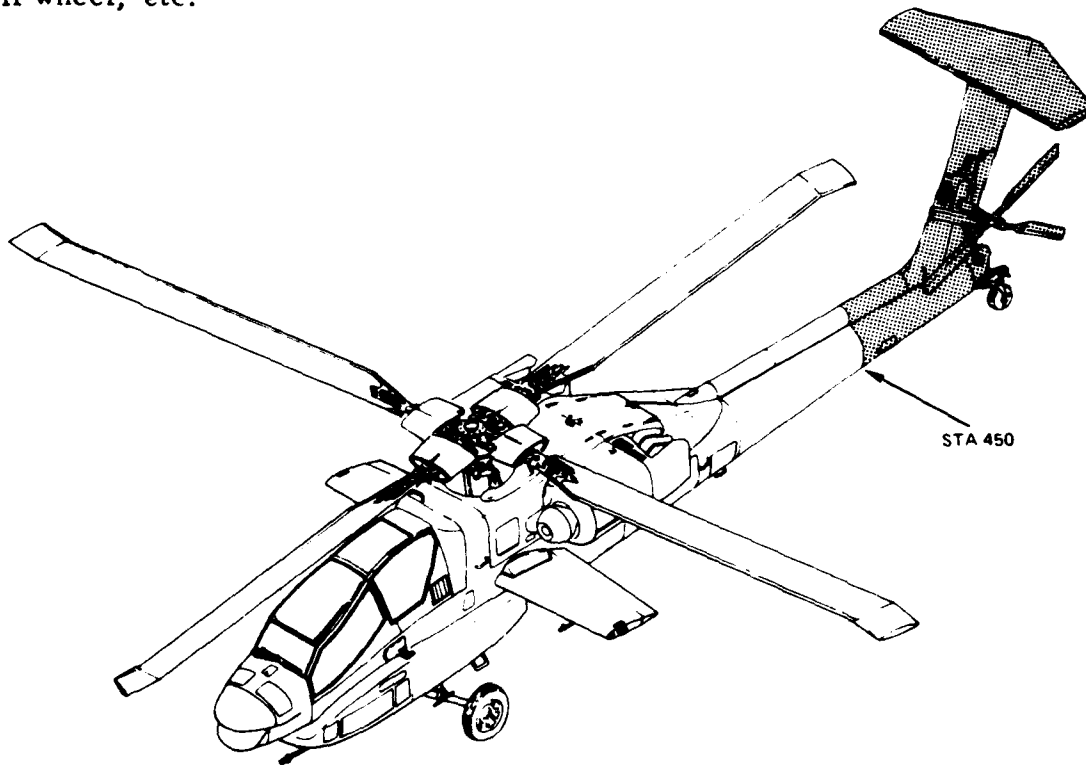


Figure 1. AH-64A - Initial CTS Configuration

The CTS technology was based on work HHI had done previously in concert with Fiber Science, Inc. (FSI) for a composite tail assembly for the AH-1G helicopter (Reference 1), a composite main rotor blade for the AH-1G (Reference 2), and a composite landing gear for the AH-64A (Reference 3). These components were fabricated by the wet filament winding, cocure process and this process was to be carried over into the CTS program. HHI had overall program responsibility, did the design refinement work, and was to conduct all laboratory and flight testing. FSI was responsible for optimizing the tooling and fabrication processes for the CTS components.

When the CTS program was proposed, the prototype metal tailboom for the AH-64A had a fold joint at Fuselage Station (Sta) 450 to aid in an air transportability in C-141 cargo planes. However, the Air Force lengthened the fuselages of all its C-141s making the AH-64A tail folding no longer needed. In the interest of structural efficiency, the fold joint was replaced by a tension bolt attachment. The prototype tail assembly was a T-tail configuration with the horizontal stabilizer rigidly attached to the top of the vertical tail.

This was to be the configuration for the composite tail assembly -- a geometric copy of the prototype metal tail section.

AH-64A flight tests that were made just before the CTS design work began showed that the helicopter's flying qualities could be markedly improved by changing from the T-tail configuration to one having a controllable stabilator mounted at the base of the vertical tail. When this change was made, the tail rotor was moved up the vertical tail to have clearance from the new position of the stabilator. The composite tail design matched this flight test configuration from the beginning (see Figure 2).

As the design work progressed, it became apparent that important benefits could be attained if the composite portion of the tailboom was extended further forward. A contract modification was negotiated to extend the composite structure 80 inches forward and make the metal-to-composite joint at Sta 370. This was the farthest forward point the composite structure could go without compromising the existing design of equipment bays, access doors, etc. It was determined that a shear bolt attachment at this point would be a production manufacturing break.

Other modifications were made to the CTS design to accommodate the findings of the prototype flight test program and the composite flexbeam tail rotor design program that were going along in parallel. These included softening the torsional stiffness of the tailboom to avoid a resonance with the main rotor 4-per-rev frequency, increasing the torsional strength of the tailboom and the sideward bending strength of the vertical tail to support

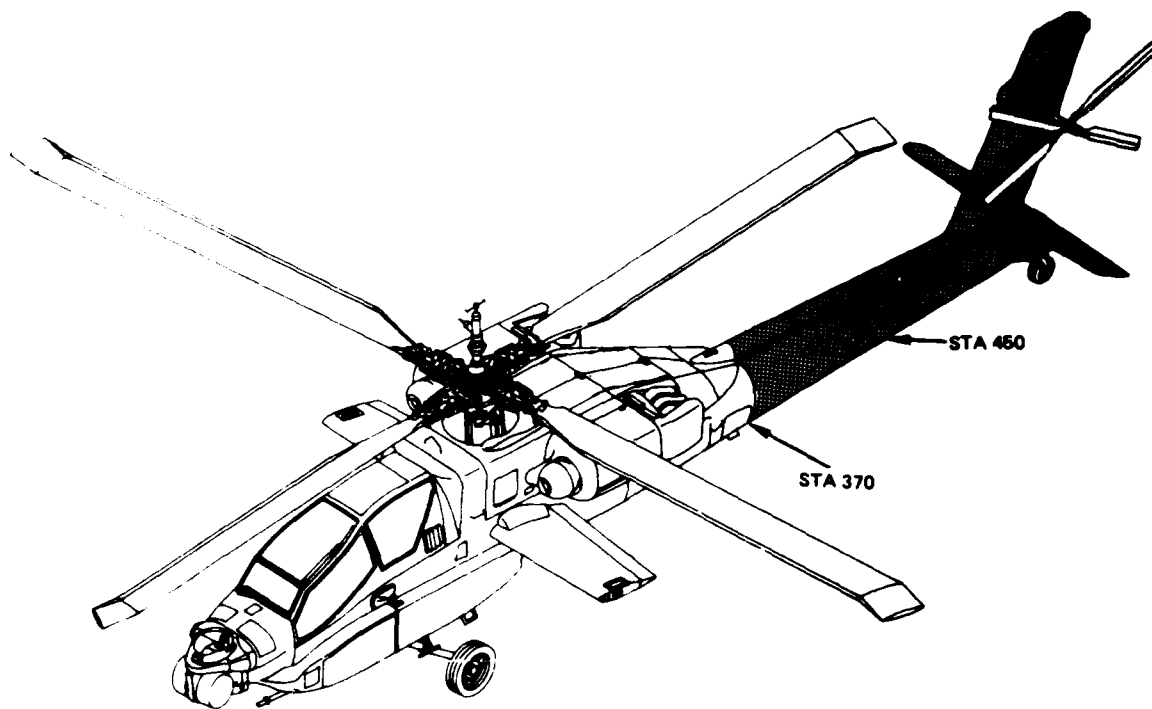


Figure 2. AH-64A Final CTS Configuration

the composite tail rotor that had 16 percent more thrust capability than the flight test metal tail rotor, and changing the vertical tail incidence and camber to unload the tail rotor in cruise flight to reduce its flapping motion for better fatigue life.

So what started out to be essentially a one-for-one replacement of metal by composites turned into a sophisticated CTS design that improved dynamics, permitted the use of the larger tail rotor needed for high altitude controllability when the T700-GE-701 engine is installed, and made a spectacular reduction in parts count while reducing the weight and cost. In this CTS configuration, the gearbox, control system, and tail wheel mount points were held inviolate, and the drive shaft covers and vertical tail leading edge fairing were retained. A new trailing edge fairing for the vertical tail spar was required by the modified incidence and camber.

A tradeoff study was made to determine the best design concepts for the three CTS components: tailboom, vertical tail, and stabilator. For the tailboom and vertical tail spar, a monocoque honeycomb sandwich shell with

frames located at high load points was determined to be optimum, consistent with good design practice and the wet filament winding manufacturing process. The skins of these components were selected to be hybrid graphite/Kevlar/epoxy. The best stabilator configuration proved to be a skin/spar/rib arrangement with graphite/epoxy used for the spars and central ribs, and Kevlar/epoxy for the skin and for the nose and tail portions of the ribs.

In parallel with this design refinement work, FSI established refined processes for fabricating the three CTS components, predominantly by the wet filament winding, cocure process that had been used successfully in a wide variety of previous programs. This work included analytical and experimental assessment of mandrel shapes to accommodate the specified winding angles, frame and hardpoint inserts, etc. Based on these activities, tooling suitable for building 50 shipsets of the components was designed.

At the time that the CTS program was terminated, the design was complete. The tooling design was in the final stages, and tool fabrication was ready to start. Material properties tests in support of design had been completed. Antenna pattern tests had been conducted to show that the composite structure had no appreciable influence on the radiation characteristics. Ballistic damage tests, conducted at the Army's Ballistic Research Laboratory, had shown that simulated composite tailboom components were survivable against 23mm HEI-T projectiles equipped with MG-25 fuzes. Lightning survivability tests had demonstrated the suitability of the design. Both the ballistic and lightning tests were sponsored by HHI.

The analysis of the CTS showed that in comparison with the metal* components it would replace, there would be:

- 71 pounds weight saving
- \$41,000 design to unit production cost saving (1981 dollars)
- 269 parts count saving
- 9047 fastener count saving
- 55 feet per minute vertical rate of climb increase from weight reduction
- \$1.1 million fuel saving over life of the fleet

*AH-64A weight and cost values for metal components are those quoted for the second quarter of 1981.

DESIGN REQUIREMENTS

The Composite Tail Section (CTS) consists of three major components:

- Tailboom
- Stabilator
- Vertical Tail

plus fairings, covers, steps, handholds, lights, and antennas.

The basic geometry of the CTS is shown in the lines drawing, Figure 3.

The strategy for optimizing the design of the CTS to match optimized techniques used in building it is to create a low cost, light-weight configuration while providing:

- External Geometric Similarity
- Accommodation of Existing Gearboxes, Controls and Tailwheel
- Maximum Incorporation of Filament-Reinforced Plastic Structure
- Aerodynamic Compatibility
- 4500-Hour Service Life
- Ballistic Survivability
- Lightning Survivability
- Reduced Parts and Fastener Count
- Interchangeability at Fuselage Station 370
- Accommodation of Existing Antennas, Lights, Mission Equipment Kits

In addition, the configuration must accept either the 112-inch diameter composite flexbeam tail rotor or the 110-inch diameter prototype metal tail rotor.

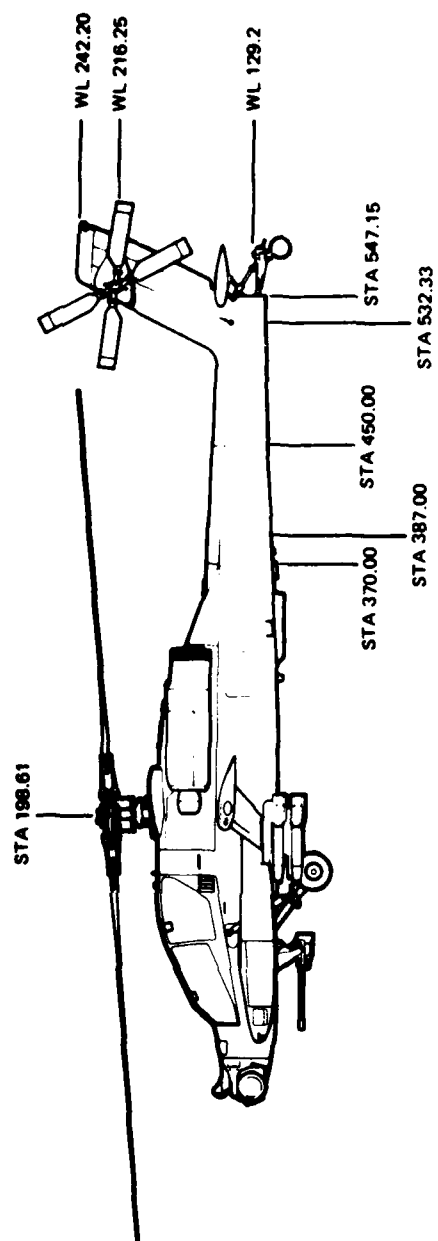
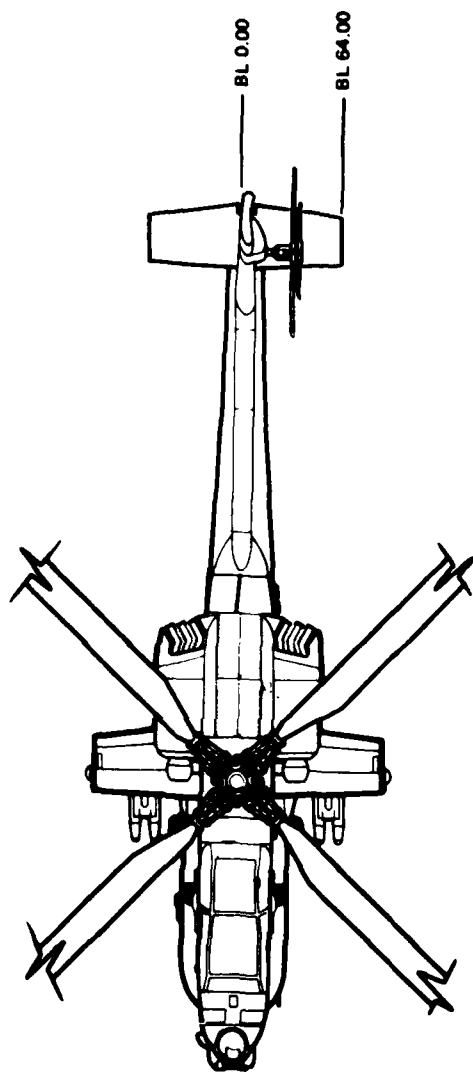


Figure 3. AH-64A Lines Drawing

The basic AH-64A description and all its design criteria remain the same as those described in Reference 4, the Design Criteria Report for AH-64A vehicle, with the exception of minor geometry changes to the stabilator and vertical tail (see Design Refinement section).

For reference, the flight envelope for weights at or below the Basic Structural Design Gross Weight (BSDGW) is presented in Figure 4. For weights above the BSDGW, the maximum vertical load factor is reduced by the ratio of the BSDGW divided by the gross weight for the particular condition up to the maximum alternate gross weight. In no case is the load factor less than 2.0. The sideslip envelopes for the AH-64A are presented in Figure 5 for the static limit, transient limit, and emergency limit.

The requirements for CTS stiffness to assure good dynamic properties are given in Figures 6, 7, and 8. These are chosen to place the stabilator roll and yaw asymmetric natural frequencies at 30 Hz while avoiding the main rotor 4P, main rotor 8P, and tail rotor 1P excitation frequencies that occur at 19.3, 38.6, and 23.5 Hz, respectively.

The basic external loads for the composite tail section are used for static and failsafe analysis and, where specified, for weighted fatigue. Oscillatory load levels from the flight strain survey weighted fatigue level of ± 10 percent of limit load for the fuselage and ± 30 percent for the vertical stabilizer and stabilator are used. These loads are the same as those specified for the basic AH-64A and are calculated for the flight maneuver conditions specified in Reference 5, and in Army-approved deviations to Reference 5.

One of the driving forces behind the increased use of composites is the increase in reliability; i.e., the decrease in failure rate. Structural failures can be classified according to severity and cause.

Severity of failures can be classified as minor, major, and critical. Minor failures merely require maintenance, and can generally be termed discrepancies. Major failures represent a threat to personnel and equipment and may result in a degradation of performance. Critical failures may result in loss of control of the aircraft.

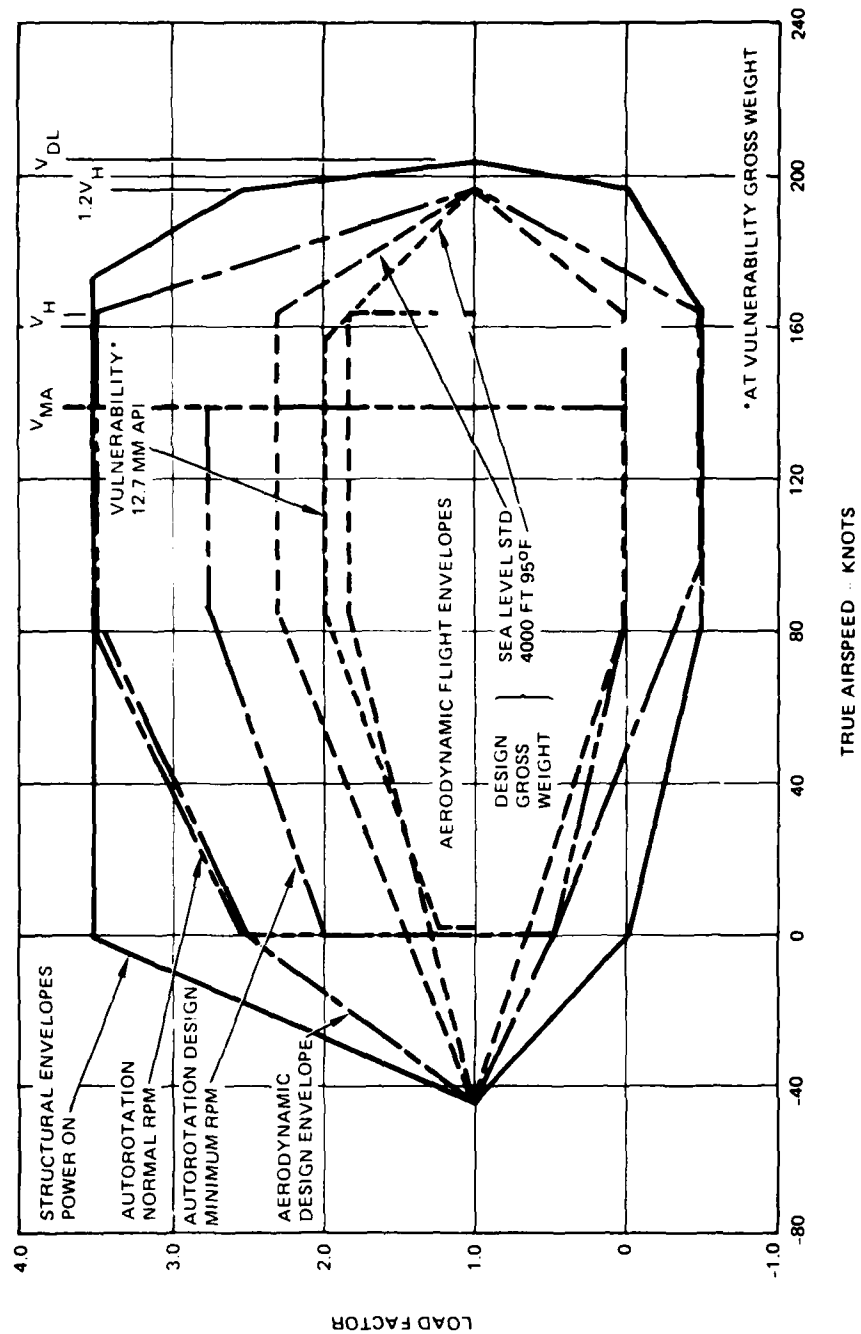


Figure 4. Flight Load Factors Versus Airspeed (Basic Structural Design Gross Weight Except Where Noted)

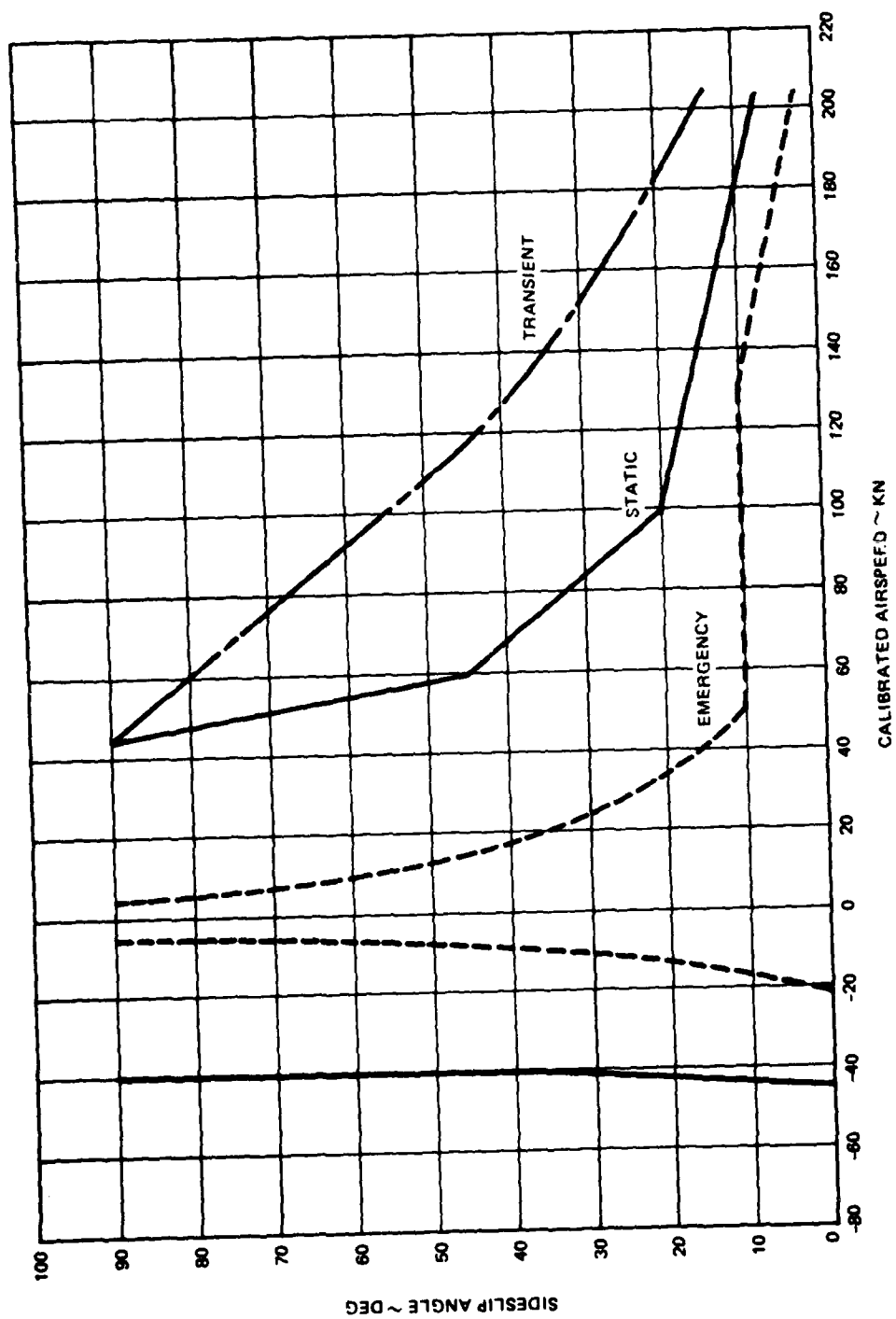


Figure 5. Sideslip Envelopes

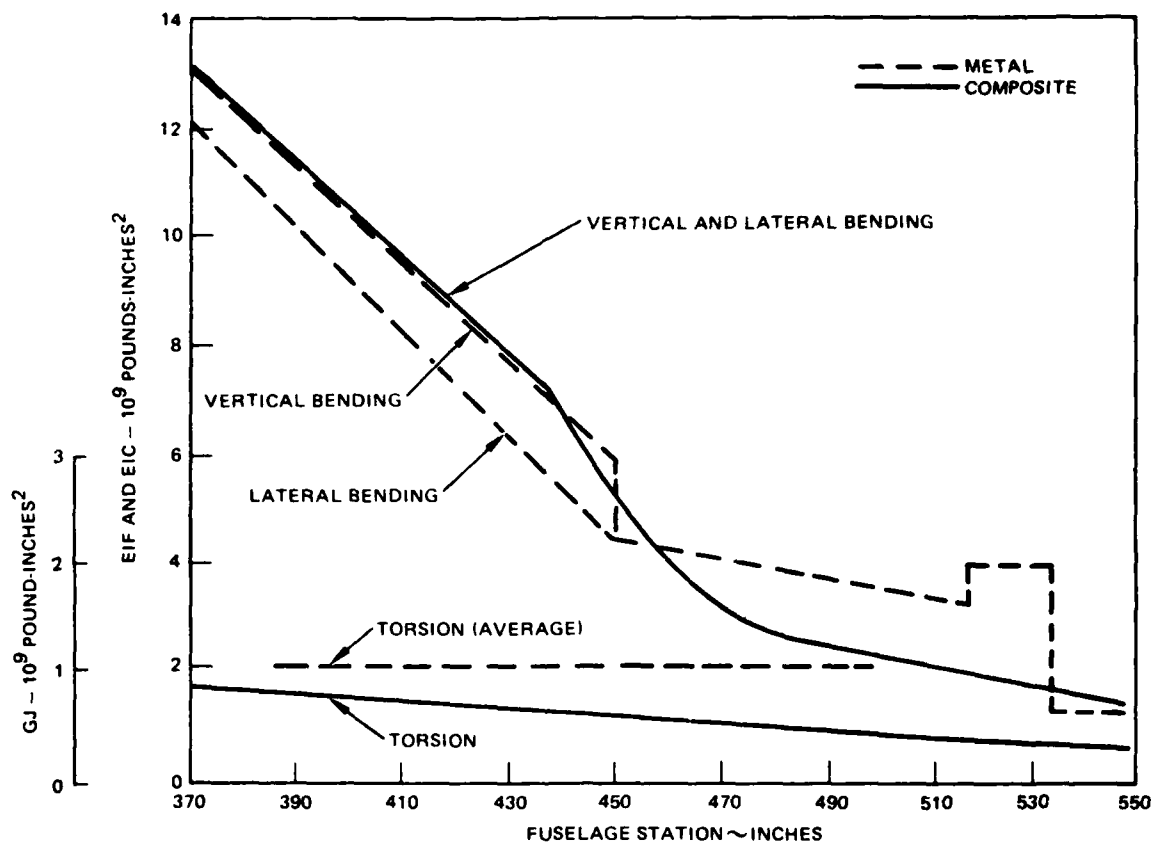


Figure 6. Tailboom Stiffness

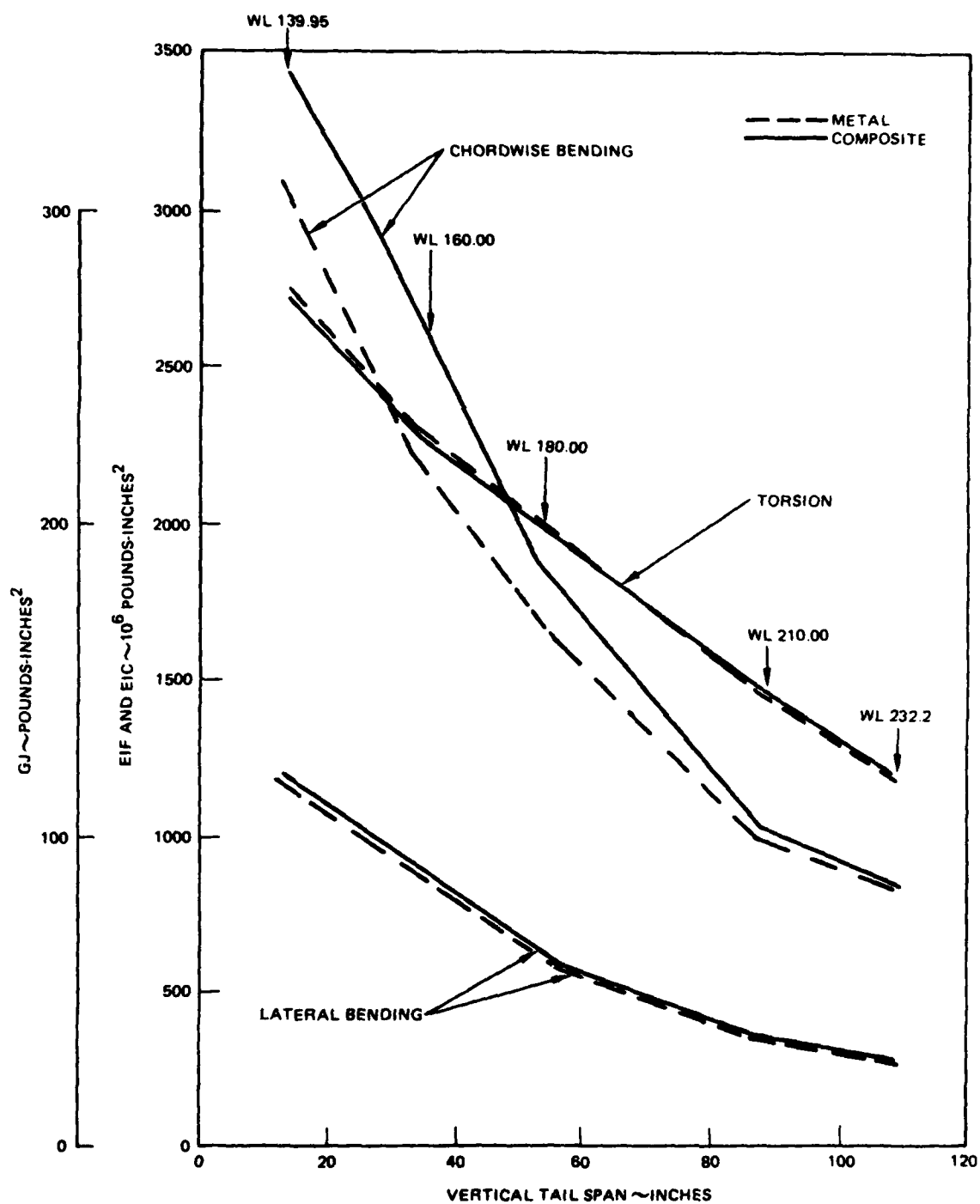


Figure 7. Vertical Tail Stiffness

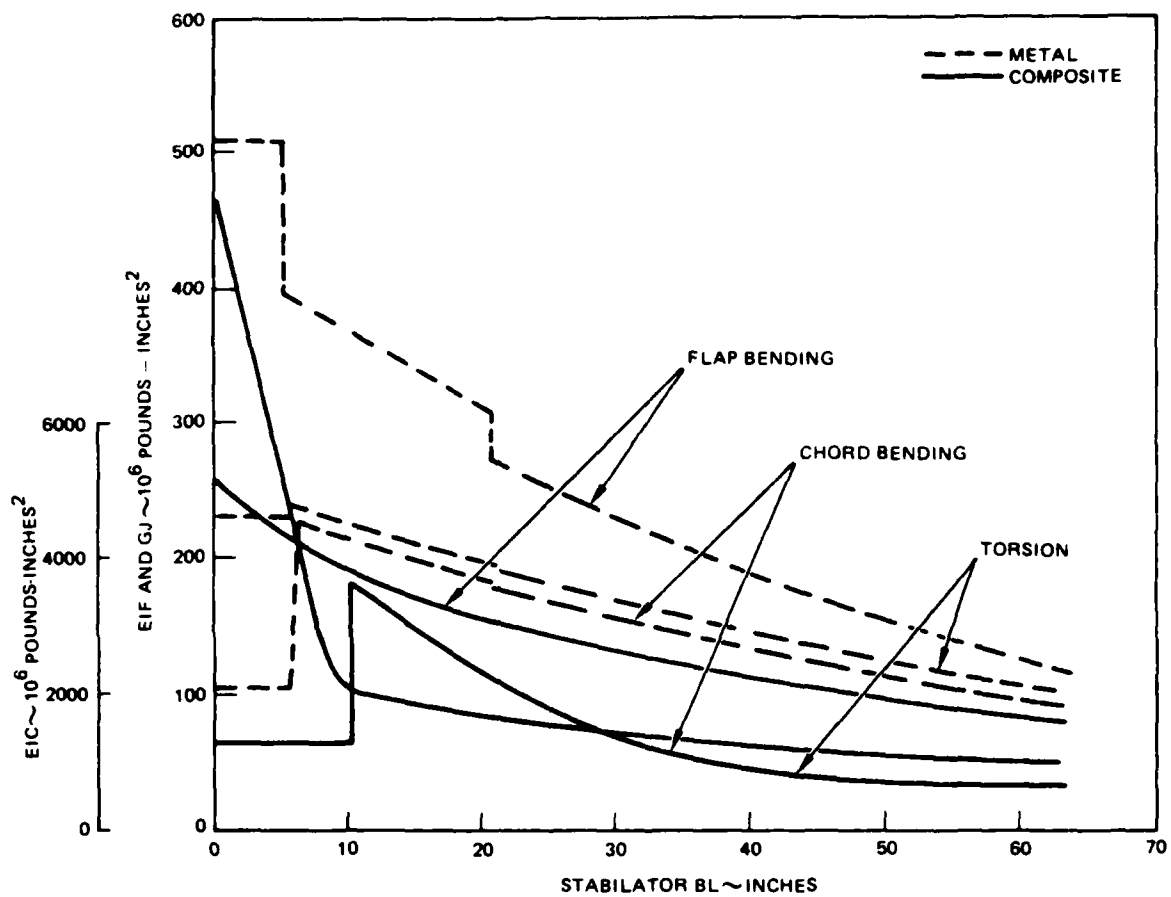


Figure 8. Stabilator Stiffness

Classification by cause divides failure into inherent or induced modes. Induced failures generally include any damage caused by external influences such as foreign objects, by certain environmental factors, or by conditions outside of the design envelope (such as overload conditions). Inherent failures include anything that is not induced such as fretting, cracking, etc., that occur at load levels within the design envelope. Examples of induced and inherent failures are given in Table 1.

TABLE 1. EXAMPLES OF STRUCTURAL FAILURES

Inherent Failures

Minor

- Fretting
- Delaminations
- Change in bolt preload

Major

- Formation of small crack
- Loss of primary fastener

Critical

- Loss of multiple primary fastener
- Growth of large crack

Induced Failures

Minor

- Scratch or gouge
- Delamination
- Lightning damage

Major

- Deep gouge
- Small ballistic perforation

Critical

- Large Ballistic perforations

DESIGN REFINEMENT

The AH-64A Composite Tail Section (CTS) is designed according to the existing metal tail section design criteria. Based on the success that HHI had experienced with wet filament winding in other aircraft primary structure programs for the Army, this process was selected for fabricating all the major components.

Design refinements include optimization of weight, mass distribution, inertial properties, stiffness distributions, natural frequencies, vibratory loads, fuselage vibrations, ballistic survivability/tolerance, anticipated service life, maintainability/reliability, acquisition cost, and life cycle cost. The design is in accordance with the AH-64A system specification AMC-SS-AAH-H10000A and meets the following restraints:

- The aluminum fuselage/CTS interface is a permanent joint at Fuselage Station (Sta 370).
- CTS stiffness distributions are dynamically compatible with the test aircraft.
- The CTS interfaces with existing operational hardware of the AH-64A (i.e., gearboxes, tail rotor drive shaft, control components, landing gear, etc.).
- The external geometry of the aluminum baseline configuration is maintained.
- The antennas are functionally integrated within the tailboom and vertical tail.

This section describes the design features of the CTS.

The CTS that consists of three major components -- tailboom, stabilator, and vertical tail -- mates with the AH-64A airframe in a manufacturing splice at Sta 370. Figure 9 is an isometric sketch that shows the configuration of the CTS and the associated fairings, covers, and external hardware that mate with it. Assembly and major subassembly drawings of these components may be found at the back of this report (Figures 95 through 99).

Before this configuration that is based primarily on sandwich wall monocoque construction was selected, a predesign study investigated other structural concepts. The primary contender was a skin, stringer, frame design of

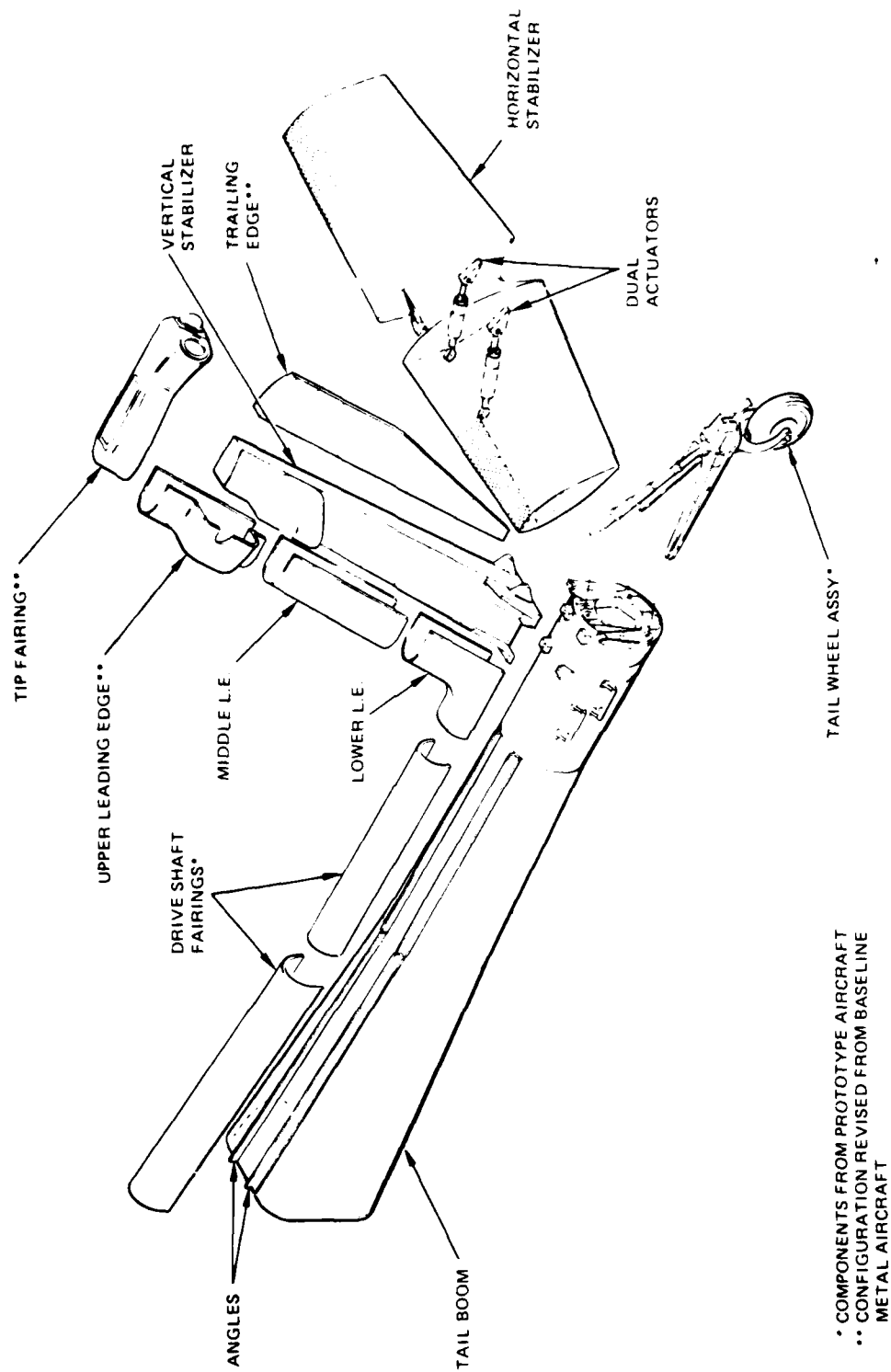


Figure 9. Composite Tail Section with Adjacent Fairings, Closeouts, and Internal Hardware

the tailboom and vertical tail spar. Structurally, this alternate design was equally acceptable, but the sandwich concept was selected as being more amenable to the wet filament winding manufacturing process.

TAILBOOM

The composite tailboom shown in Figure 10 retains most of the baseline metal fuselage configuration. It transitions from a flat-topped ovaloid at Sta 370 to a circular cone from Sta 450 to Sta 530. From Sta 530 aft, the composite tailboom maintains a constant diameter, differing from the continuing cone shape of the baseline configuration.

The composite tailboom is composed of the following major components (see Figures 95 and 96:

- Structural Shell
- Station 387 Frame
- Forward Fitting Assembly
- Intercostal, Upper
- Intercostal, Lower (2)
- Intercostal, Jack Fitting
- Rear Frame

Other details that are attached onto this assembly are:

- Access Steps, Upper and Lower
- Angle Fairing, Right and Left
- Jack Point Fitting

Hard points (local reinforcement and/or core filled honeycomb) are provided for the following details that are common to both CTS and metal baseline:

- Drive Shaft Fairing Hinges
- Drive Shaft Bearing Support Bracket

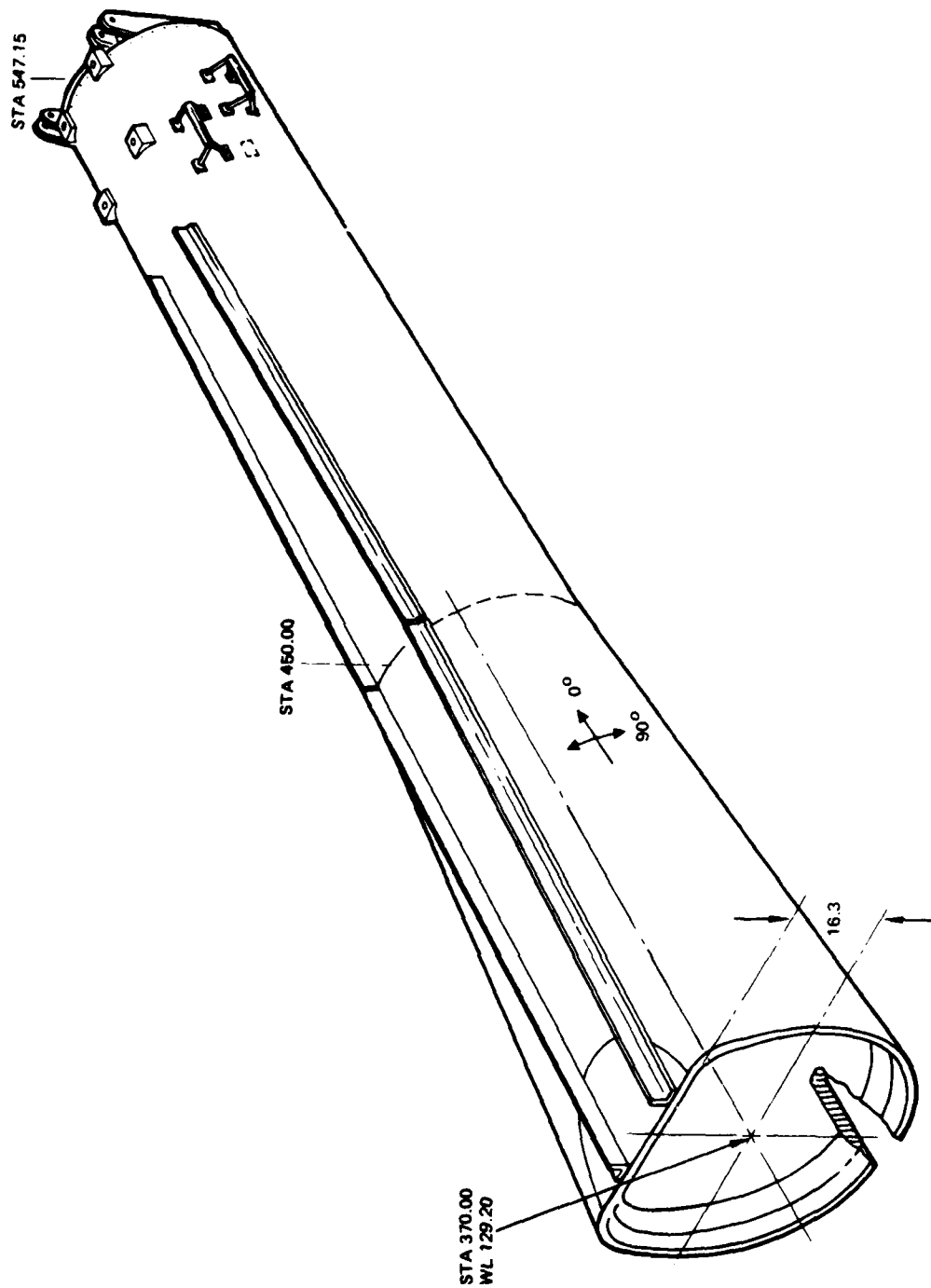


Figure 10. Tail Boom Configuration

- Drive Shaft Anti-Flail and Damper Support
- Flare Dispenser

The structural shell of the tailboom is a graphite-Kevlar/epoxy sandwich with balanced helically wound skins and 0.50 inch thick Nomex core. The inner and outer skins converge at the front end of the tailboom (Sta 370) and at the aft, constant diameter section to form solid laminates as Figure 11 shows.

The base sandwich skin thickness is 0.043 inch and the winding angle is $8^{\circ} \pm 1^{\circ}$ at Sta 370. Skin thickness and wrap angle increase from the forward to aft end of the tailboom. Hoop windings (90°) stabilize the spiral windings. The skin is wound from a 50-50 ratio of graphite/Kevlar rovings. This winding pattern is tailored to provide the required bending and torsional stiffness and strength.

The solid laminate attach flange at Sta 370 is interwound with $\pm 45^{\circ}$ graphite fabric and 90° E-glass to a total flange thickness of 0.172 inches. The interwound plies, in addition to providing the necessary bearing area, are structurally balanced in thickness and elastic modulus to evenly distribute load into the two skins. Figure 12 shows how this solid laminate region is attached to the forward airframe by splice plates and a double row of HiLok fasteners.

The solid laminate at the aft end of the tailboom (sta 530, aft) is also made up of interwound fabric plies tailored for bearing strength and balanced load distribution.

Local attach points and cut-outs employ additional interwound plies of fabric to provide load-carrying structure in these high stress areas. The honeycomb core in these areas is filled with syntactic foam to stabilize the core, anchor the fasteners, or provide compressive strength to support fastener loads.

The materials used to fabricate the tailboom are:

- Graphite Roving: T-300, 3000 Filament Count
- Kevlar Roving: Kevlar-49, 1420 Denier
- Graphite Fabric: T-300, 3000 Filament count, Eight Harness, Satin Weave
- E-glass Fabric: 1581 Glass Fabric

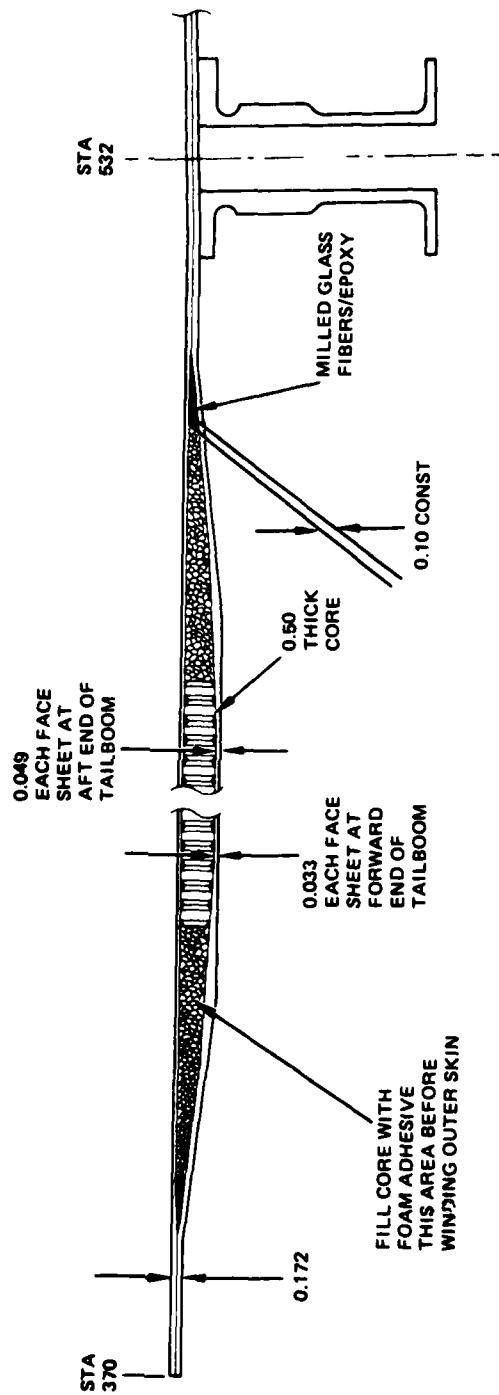


Figure 11. Tail Boom - Structure Details

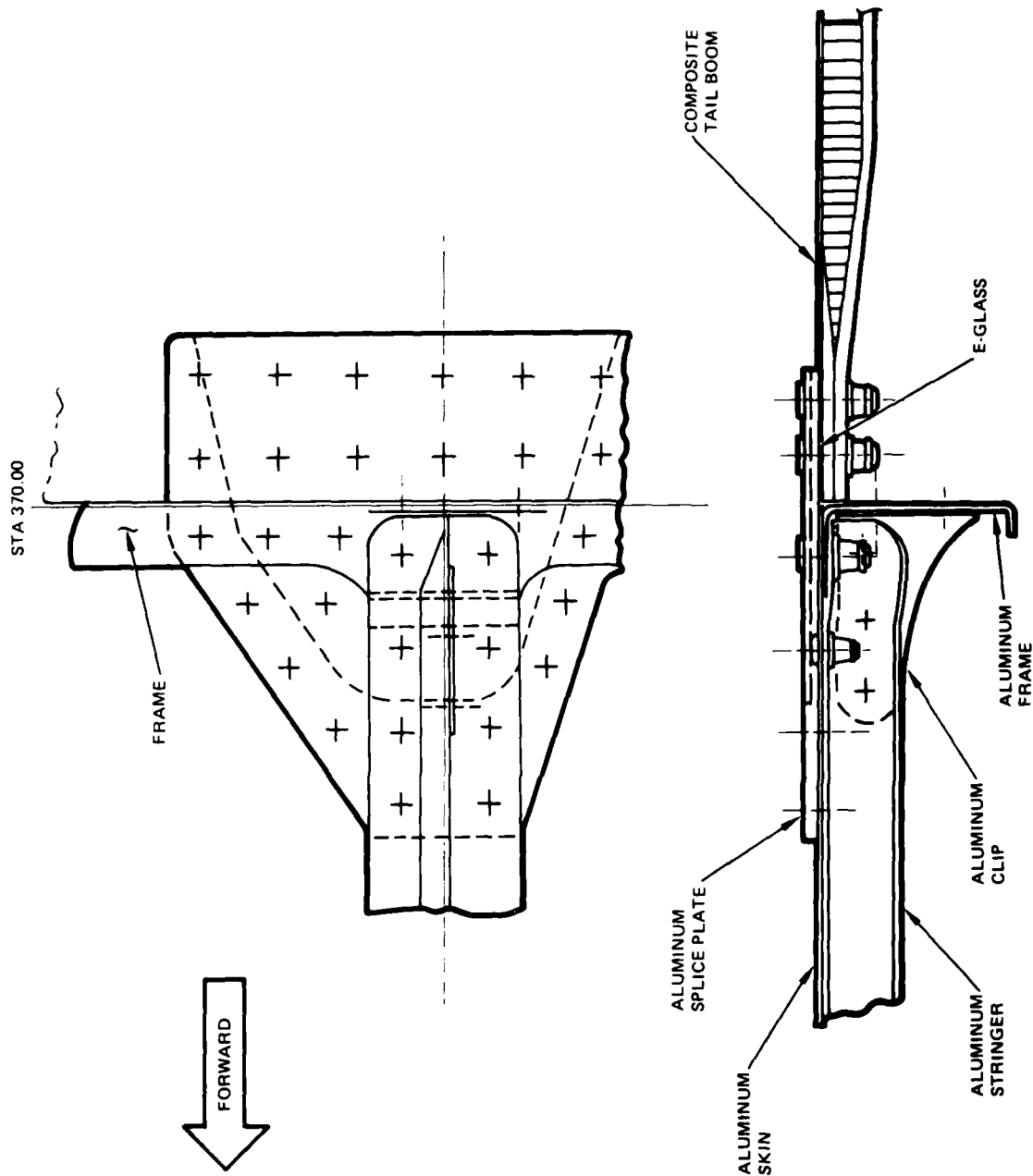


Figure 12. Metal/Composite Manufacturing Splice, Sta 370

- Epoxy Resin: APCO 2434/2347
- Core Adhesive: FM 123-5 Film Adhesive
- Core: Nomex HRH - 10/0X - 3/16

There are three graphite/epoxy frames that are molded separately and then assembled into the tailboom. The forward one at Sta 387 is provided to stiffen the tail rotor shaft bearing support at this location. It is installed by a secondary bonding process. The two back-to-back frames centered at Sta 532.33 are made into a subassembly unit consisting of these two frames, a connecting strap bonded around them, and four graphite/epoxy intercostals that distribute tail wheel loads into the tailboom. This subassembly unit is wound into the tailboom shell structure to become an integral part of it. The tailboom in the region of this subassembly unit is shown in Figure 13.

A machined aluminum fitting is bolted between the two back-to-back composite frames after the tailboom is cured (see Figure 14). This is the fitting to which the forward bolts for the vertical tail attach.

The materials for the frames are:

- Fitting: 7075-T6 Aluminum Alloy
- Frames: Graphite Fabric: T-300, 3000 Filament Count, Eight Satin Weave

Glass Fabric: 1581 Glass Cloth

Resin: APCO 2434/2347

Four graphite/epoxy intercostals are located between the forward/frame assembly and the rear frame, (see Figure 13). Three of these intercostals transfer most of the tail wheel shock and strut loads into the skin. The balance of the load goes into the forward frame assembly through a row of shear bolts. The fourth intercostal transfers jacking and tie-down loads into the tailboom. The materials for the intercostals are :

- Graphite Fabric: T-300, 3000 Filament Count, Eight Harness, Satin Weave
- Epoxy Resin: APCO 2434/2347

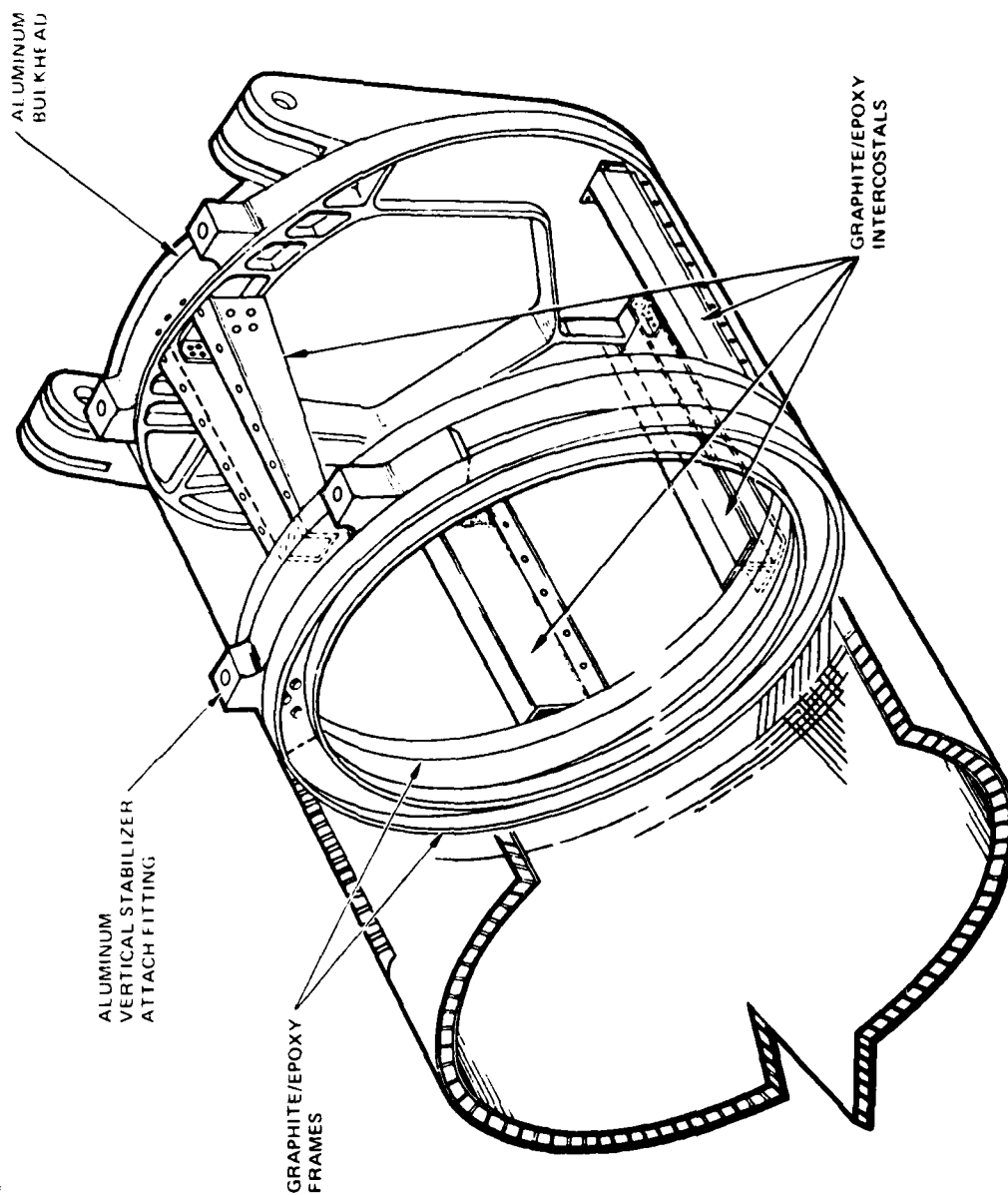


Figure 13. Tail Boom

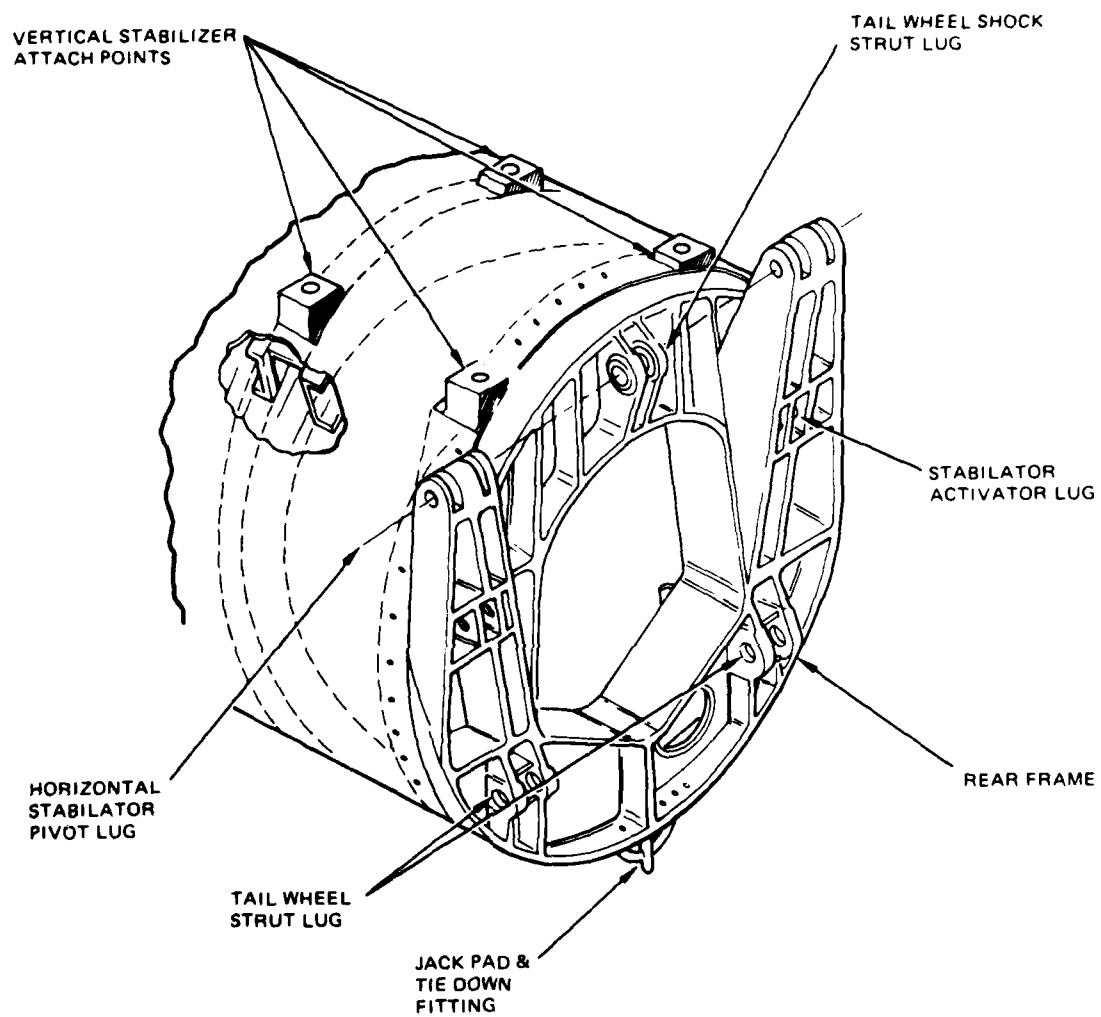


Figure 14. Aft End of Tailboom

The rear frame, Figure 14, is a machined aluminum fitting that has multiple functions. It contains the tail wheel assembly attach points, stabilator pivot points, and the stabilator actuator attach points. It provides the two aft points for vertical tail attachment and anchors the aft jacking fitting. The frame, made from 7075-T6 aluminum alloy, is bolted into the tailboom with HiLok fasteners.

VERTICAL TAIL

The geometry of the composite vertical tail is:

Area (from boom \bar{C}_L) - ft ²	32.2
Span (from boom \bar{C}_L) - in.	113.0
Tip chord - in.	35.1
Chord of section at W.L. 196.0 - in.	43.5
Root chord (at boom \bar{C}_L) - in.	44.0
Geometric aspect ration (based on span from boom \bar{C}_L)	2.5
Airfoil	NACA 4415 modified
Leading edge sweep - deg	29.4
Rudder - (mean) percent chord	55.0
Rudder deflection - deg	4.0
Rudder tab - (mean) percent chord	25.0
Rudder tab deflection (from rudder chord line) - deg	18.0
Geometric incidence - deg	0.0
Aerodynamic incidence - deg	9.4

The major structural element in the vertical tail is the spar box shown in Figure 15. Leading and trailing edge fairings and tip cap as shown in Figure 9 complete the assembly. The vertical tail's planform is unchanged

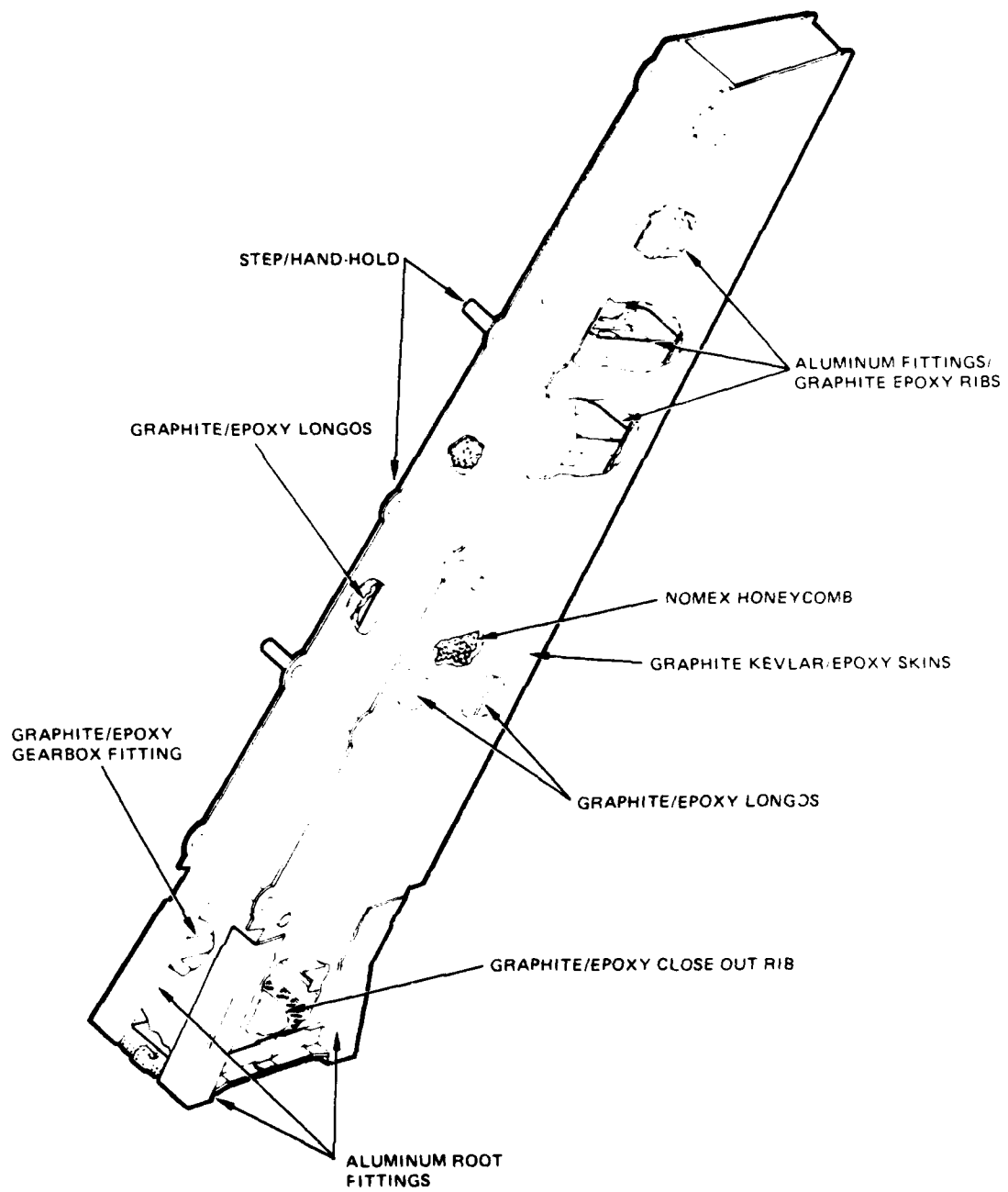


Figure 15. Vertical Tail Spar Box Structure

from that of the prototype AH-64A, but the vertical incidence is increased four degrees to partially unload the tail rotor in high speed flight and minimize its flapping motion for improved fatigue life. Figure 16 shows this incidence change. Note that the front face of the spar remains unchanged while the rear face is moved to the left. This keeps the gear box attach points in the same location as the metal baseline, allowing all driveshaft and control hardware to be interchangeable. The leading edge, trailing edge, and tip closure fairings are the same as the baseline except where contours are impacted in a minor way by the four-degree vertical tail incidence change. Steps and hand-hold locations are the same as the metal baseline. See Figure 15.

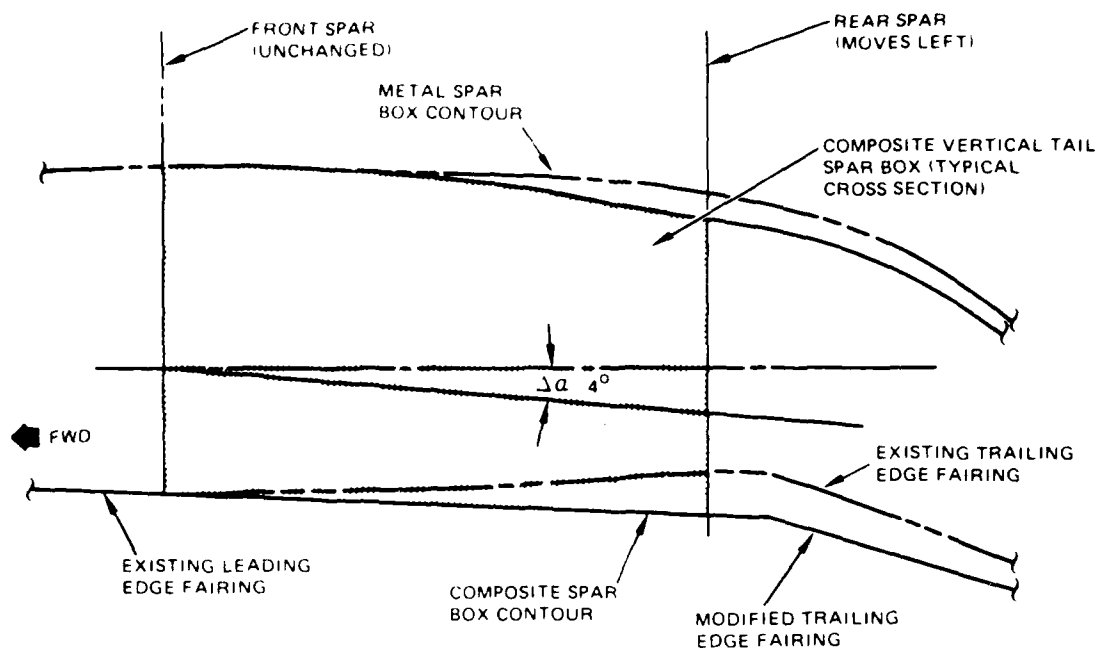
The composite vertical tail is composed of the following components (see Figures 97 and 98):

- Spar box
- Root Fittings
- Upper Gearbox Support Assembly
- Lower Gearbox Support Frames
- Upper Closure Rib
- Steps and Handholds

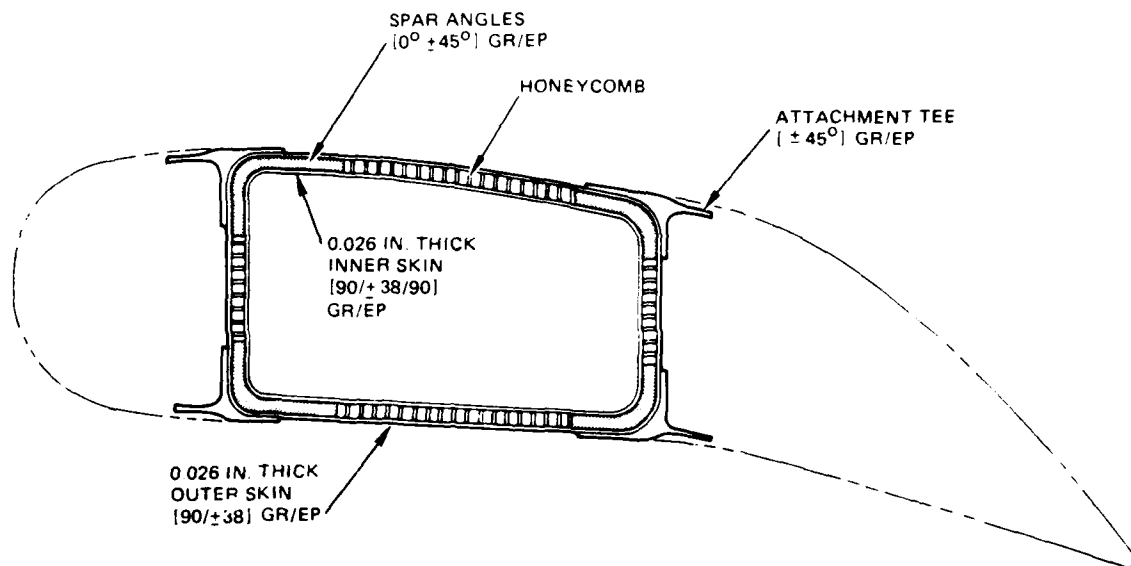
Hardpoints for attaching hardware are provided for the following:

- Tip Fairing
- Leading Edge
- Trailing Edge
- Tail Rotor Brace (2)

The basic structure of the box is a graphite/Kevlar/epoxy filament wound honeycomb sandwich. The skins are ± 38 -degree helical windings over a 0.250 inch thick Nomex honeycomb core. Graphite/epoxy spar angles ($0^\circ \pm 45^\circ$ plies) are incorporated in the four corners between the inner and outer skins. The helical windings provide the necessary torsional strength and stiffness, with the corner spar angles supplying bending strength and stiffness. See the lower portion of Figure 16.



VERTICAL STABILIZER INCIDENCE ANGLE MODIFICATION



LEADING AND TRAILING EDGE FAIRING ATTACHMENT TEES

Figure 16. Vertical Tail Cross Sections

The honeycomb sandwich is a balanced structure with each skin 0.020 inch thick. The skins converge to form solid laminates at the root fitting attach region and at the tip end just below the tip cap. Local skin thickness is sized to accommodate the local load requirements. The skin thickness, including laminae and honeycomb core is illustrated in Figure 17. In the center of the spar the sandwich is 0.301 inch thick. The ends taper to 0.060 inch solid laminate.

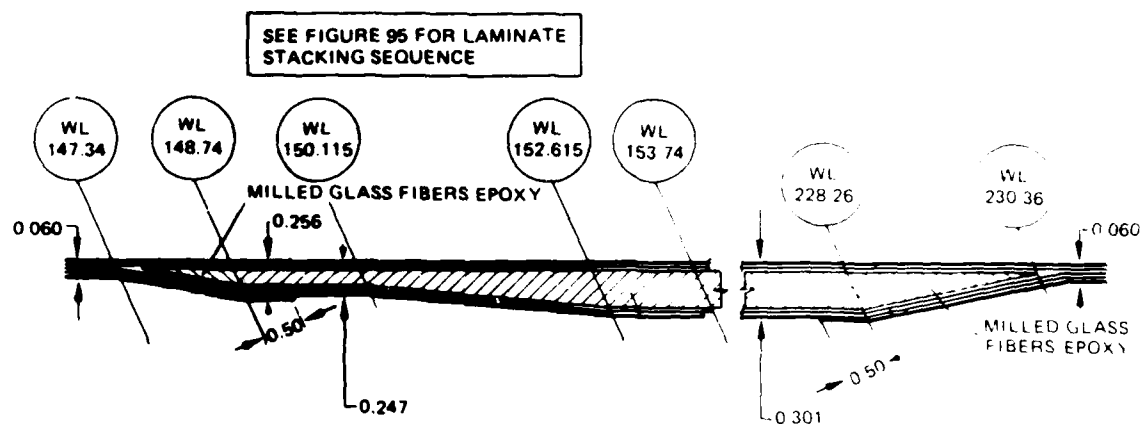


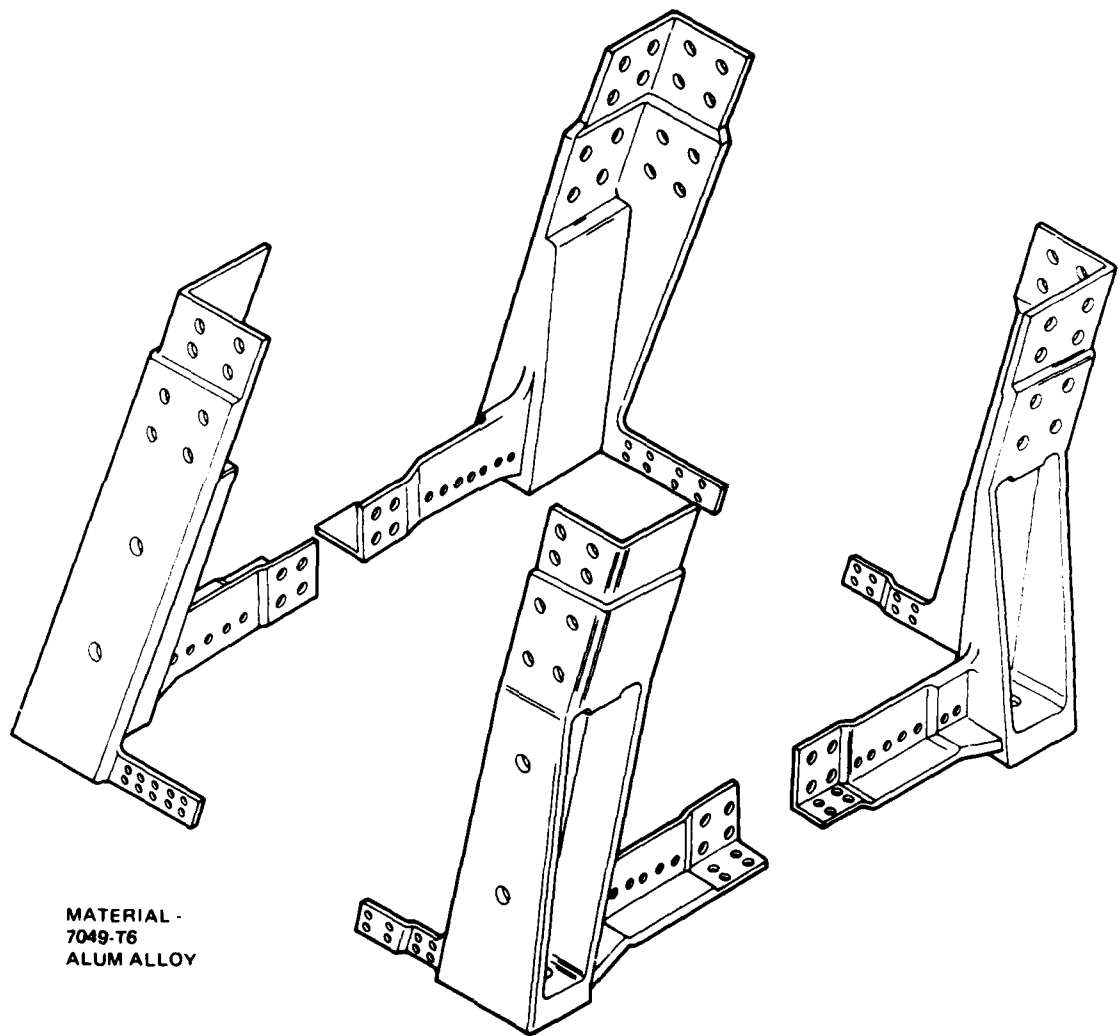
Figure 17. Vertical Stabilizer Skin Thickness

The leading and trailing edge attachment tees are bonded to the box as indicated in Figure 16.

The materials used to fabricate the spar box are:

- Graphite Roving: T300, 3000 filament count
- Kevlar Roving: Kevlar-49, 1420 Denier
- Graphite Fabric: T300, 3000 filament count, eight harness, satin weave
- Epoxy resin: APCO 2434/2347
- Core Adhesive: FM 123-5 film adhesive
- Honeycomb Core: HRH-10 -1/4, 0.250 inch thick

The composite vertical tail attaches to the tailboom with the four-piece aluminum fitting shown in Figure 18. This split fitting attaches to the composite box with HiLok fasteners and carries the bosses for the four 5/8-inch diameter attach bolts. The forward portions of the root fitting also incorporates the intermediate gearbox attach bosses. The root fitting is made from 7049-T6 aluminum alloy.



MATERIAL -
7049-T6
ALUM ALLOY

Figure 18. Root Fitting

The upper gearbox mount shown in Figure 19 consists of three graphite/epoxy ribs that have aluminum reinforcing bars bonded in. Self-locking anchor nuts mount the gearbox. The three ribs are connected with a strap to form a prefabricated unit that is assembled with the winding mandrel and wound into the spar box structure. HiLok fasteners are also used to anchor these ribs to the spar box. The lower gearbox supporting rib (Figure 15) is a pre-molded/graphite/epoxy rib that is bolted in place with HiLok fasteners. An aluminum reinforcing bar supports the intermediate gearbox.

The materials used for the ribs are:

- Rib Assemblies: Graphite/epoxy: T300, 3000 filament, eight harness, satin weave, preimpregnated
- E-glass/Epoxy: 1581 glass cloth, preimpregnated
- Adhesive: FM 123-5
- Inserts: 2024-T6: Aluminum alloy

The upper closure is made from graphite/epoxy - T-300, 3000 filament count, eight harness, satin weave, preimpregnated.

The steps and handhold are graphite/epoxy tubes fixed on the vertical tail spar box as shown in Figure 15. That portion extending into the air stream is elliptically shaped for reduced drag (See Figure 20).

The materials for the steps are:

- Graphite/epoxy: T-300, 3000 Filament count, eight harness, satin weave, preimpregnated
- Graphite roving: T-300, 3000 filament count
- Epoxy resin: APCO 2434/2347

The leading and trailing edge fairings attach to flanges that are bonded to the corners of the spar box. These are T-section flanges as indicated in Figure 16. They are made from:

- Graphite/epoxy: T-300, 3000 Filament Count, eight harness, satin weave, preimpregnated

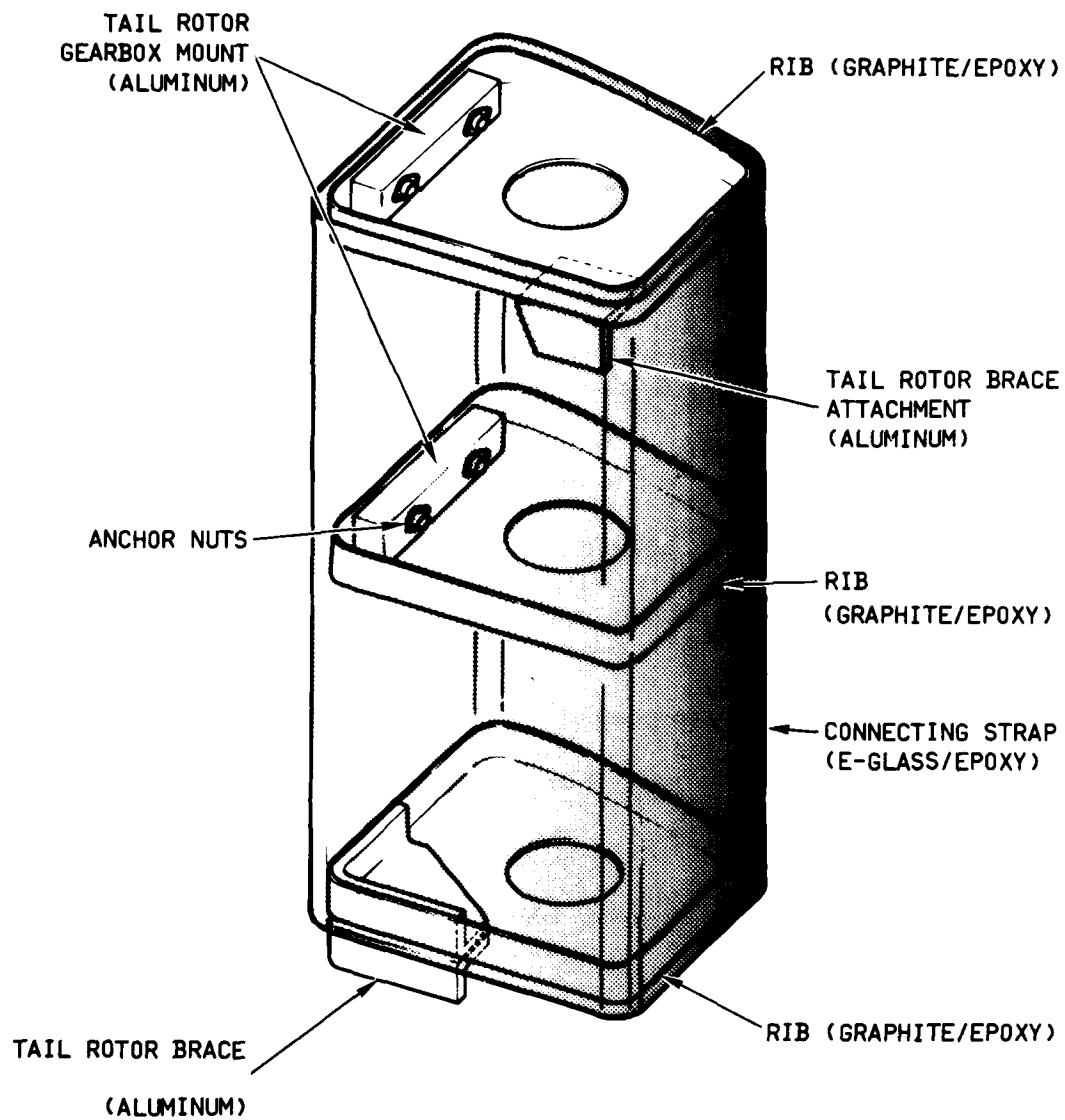


Figure 19. Upper Gearbox Assembly

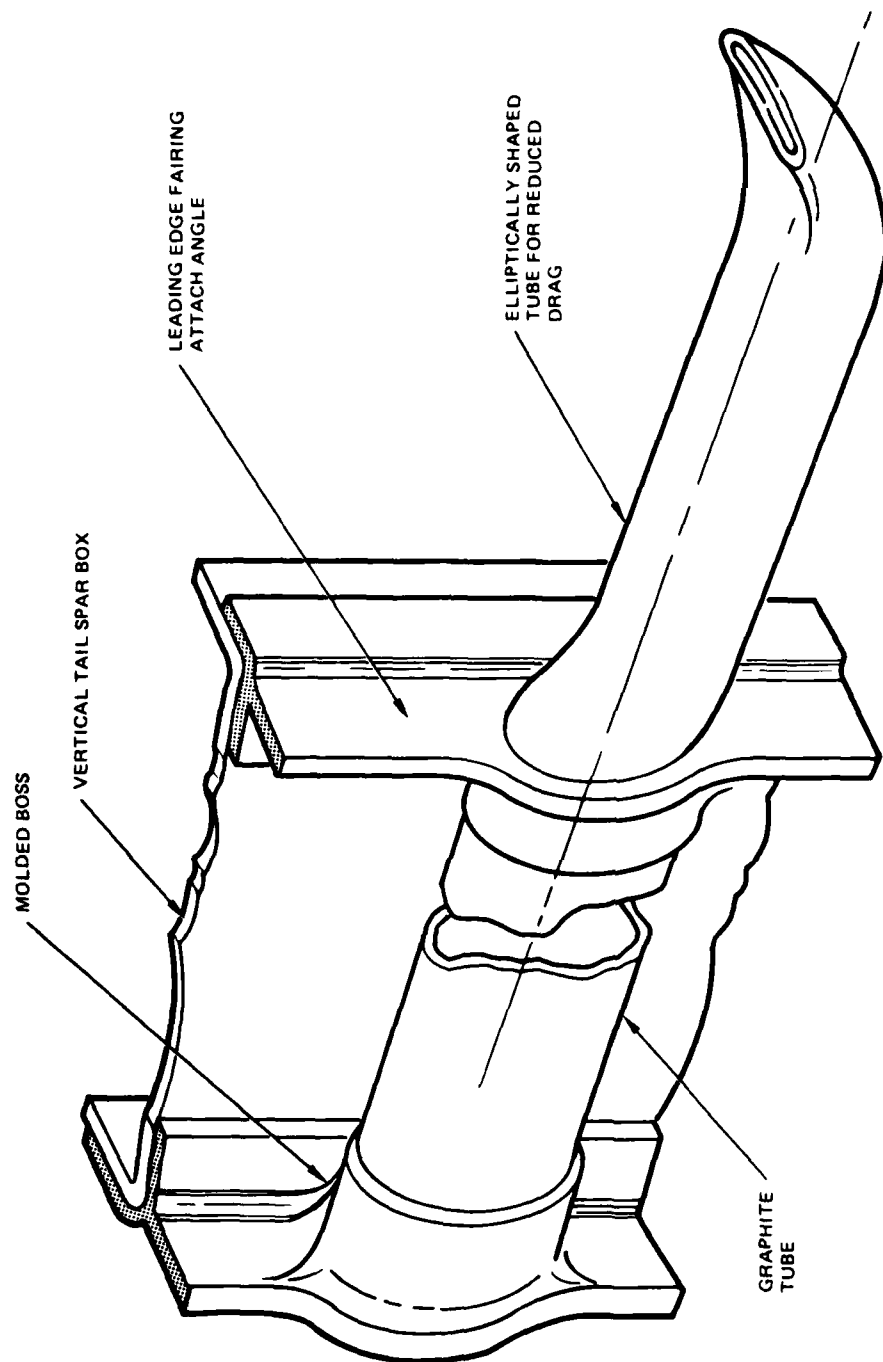


Figure 20. Step/Hand Hold

STABILATOR

The composite stabilator's geometry is:

Area - ft ²	33.36
Span - in.	128.0
Tip chord - in.	31.85
Root chord - (at centerline) - in.	43.2
Airfoil	NACA 0018
Aspect ratio	3.41
Chordline for zero sweepback, percent	50

The composite stabilator is shown in Figure 21. It has the same outside contour as the AH-64A metal stabilator, but with added leading edge sweepback. The pivot point and actuator locations are changed to facilitate hinging the stabilator to the tailboom instead of to the vertical tail. This change permits decoupling of the vertical tail/stabilator dynamic responses and also allows the hinge spacing to be increased, thus reducing the hinge loads. An improved actuation system replaces the prototype helicopter's tandem electric actuator by a pair of side-by-side hydraulic actuators attached to the tailboom aft bulkhead. The hinge is also part of the aft bulkhead.

The stabilator is made up of the following structural members (see Figure 99):

- Skins (left, right, and center)
- Spars (forward and aft)
- Ribs (left and right, 3 each)
- Nose ribs (left and right, 3 each)
- Reinforcing ribs (left and right, 1 each)
- Tip closures (2)

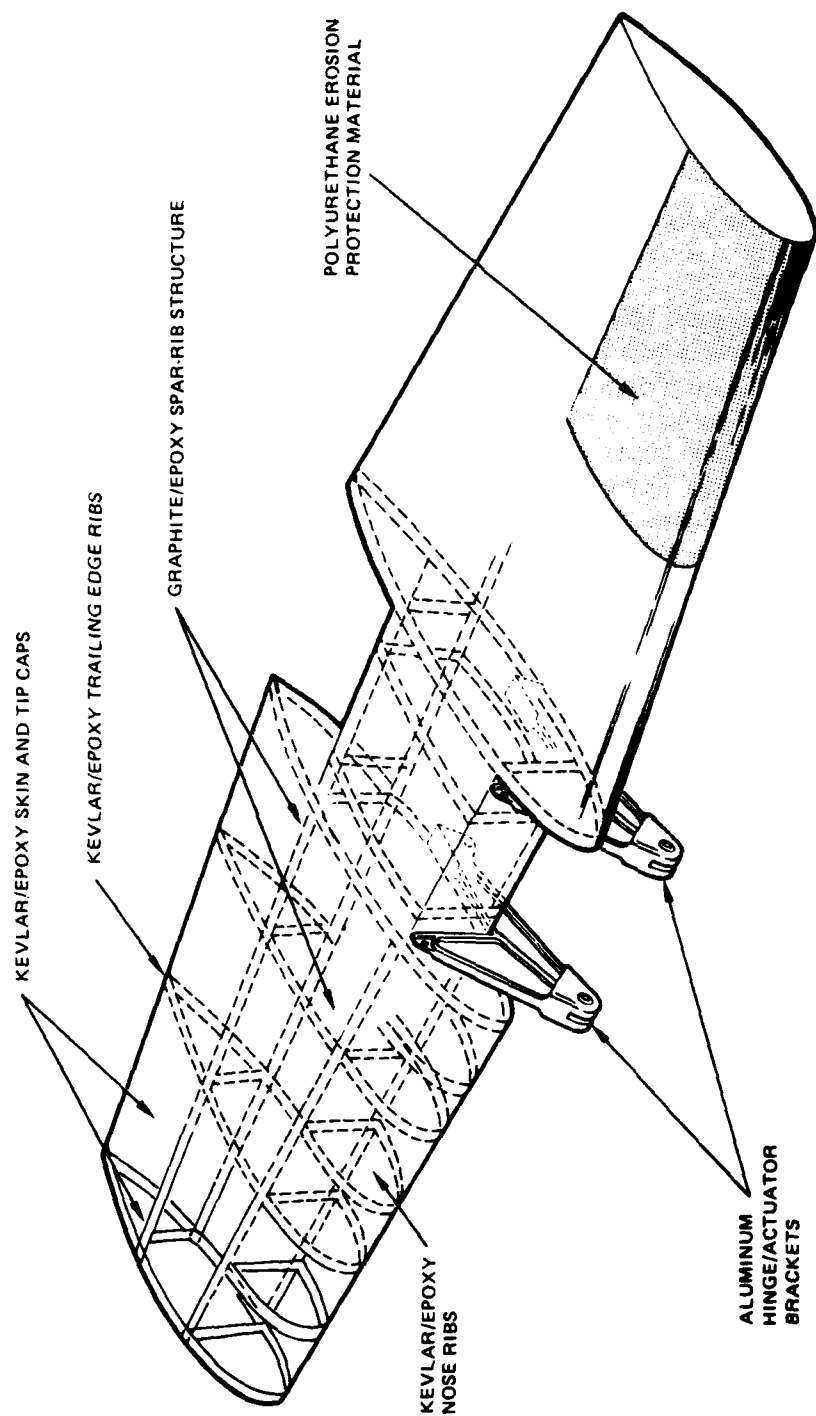


Figure 21. Stabilator Structure

Attach details are:

- Pivot/actuator fitting (left and right)
- Bathtub fitting (left and right)

In addition, the stabilator is protected from rocket debris by a polyurethane cover.

The skin is made of four pieces, (left, right, upper center, lower center). The skin provides the torsional stiffness and shear tie for the spars. The spars provide axial bending stiffness and resist air loads and diagonal tensions loads caused by thin skin shear buckling. The left and right-hand skins are premolded to the airfoil shape, fit over the spar/rib structure, and are bonded to it. The skin is reinforced in the center section for torsional requirements. The total skin thickness is 0.030 inch with an additional 0.030 inch thickness in the center box area between the root end ribs.

The skin material is:

- Kevlar roving: Kevlar-49 roving, 1420 Denier
- Epoxy Resin: APCO 2434/2347

The forward and aft spars consist of C-section beams. Spanwise bending stiffness is provided by unidirectional fiber in the caps oriented in the spanwise direction. The spars are made of:

- Graphite roving: T300, 3000 Filament Count
- Epoxy Resin: APCO 2434/2347

The ribs are molded as three element boxes with flanges all around their peripheries. The portions of the ribs that lie between the spars are graphite/epoxy, while the leading and trailing edge portions are Kevlar/epoxy. The materials used to make the ribs are:

- Graphite Roving: T300, 3000 filament count
- Kevlar Roving: Kevlar-49 Roving, 1420 Denier
- Epoxy Resin: APCO 2434/2347

The tip closures provide a shear rib at the outboard end of the airfoil and serve to shield the edges of the skin and the substructure from environmental effects. The material is the same Kevlar/epoxy used for the skins.

The pivot/actuator fittings are two aluminum alloy fittings attached to the stabilator assembly with stainless steel bolts. The pivot holes are bushed with TFE-lined stainless steel bushings. The materials for these fittings that are shown in Figure 21 are:

- Fitting: 7049-T411 aluminum alloy
- Bushing: CRES steel, TFE coated

Rocket debris protection is provided by a polyurethane cover 0.050 inch thick extending over the outboard 23.5 inches of the span on both sides. This material wraps around the leading edge and covers the forward five inches of the upper surface and all but the aft six inches of the lower surface.

ENVIRONMENTAL PROTECTION

Extensive investigation during the advanced composites programs has established that there will be no corrosion problem with the composite components. However, suppression of galvanic corrosion between aluminum fittings and adjacent graphite/epoxy laminates requires the use of a layer of E-glass/epoxy for electrical isolation at all interfaces.

All steel parts are cadmium plated and all aluminum parts are chromic acid anodized. All fasteners are corrosion-resistant steel. Final painting consists of a urethane top coat over a suitable primer for protection against ultraviolet radiation.

Figure 22 shows how lightning protection is provided by a grounding system that extends from a lightning collector in the tip cap of the vertical tail, down through the aluminum ground plane for the antennas in the trailing edge fairing of the vertical tail, and out through the tailboom's aluminum frame at Sta 547 and the tail landing gear strut. A grid of aluminum foil around the leading and trailing edges and tip to two discharge wicks on each stabilator tip and through a jumper into the aluminum rear frame in the tailboom provides lightning protection for the stabilator.

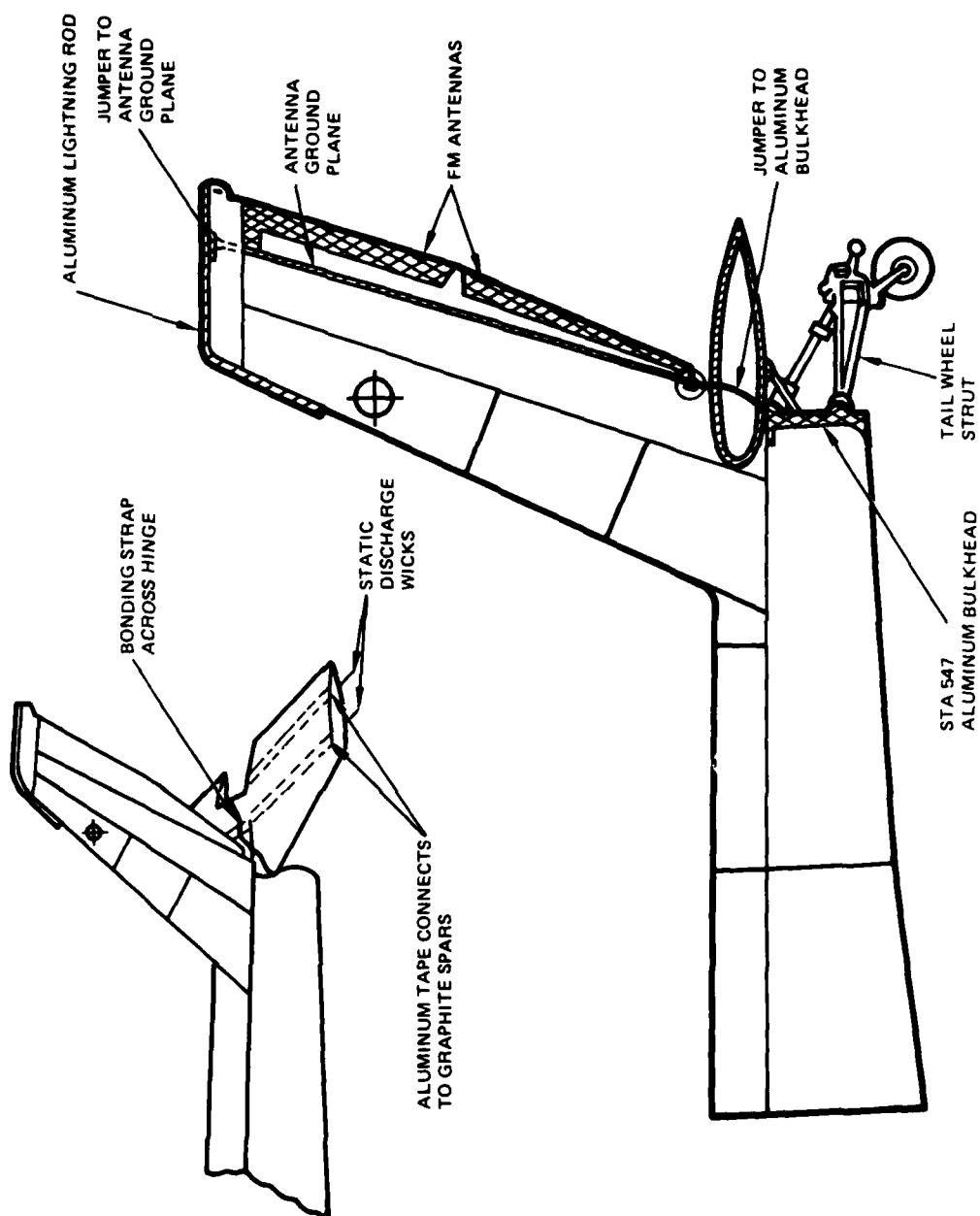


Figure 22. Lightning Protection

WEIGHT ANALYSIS

The weight analysis for the CTS is given in detail in Table 2 per MIL-STD-1374 Part III for the three components -- stabilator, vertical tail, and tailboom. The calculations for these weights are based on released drawings (84 percent by weight), and on pre-release drawings for the remaining details and installation. The component weights are summarized in Table 3 and are compared with their counterparts in the basic metal helicopter. The weight saving is shown to be 72.4 pounds.

Two adjustments are needed. First, a calculation for a preliminary layout of the metal-to-composite splice joint at Sta 370 shows an incremental weight increase of 7.6 pounds relative to a structure without a manufacturing break at this point. Second, the CTS is designed to accept the Composite Flexbeam Tail Rotor (CFTR) that increases the load on the tailboom by six percent relative to the metal tail rotor. A weight analysis of a strengthened metal tailboom to accept this load indicates a weight increase of 6.0 pounds is needed. Hence, the total adjustment for the Sta 370 splice and the CFTR yields an overall weight reduction of 70.8 pounds for the CTS versus the metal tail section modified to accept the CFTR.

The longitudinal center of gravity for the AH-64A equipped with the CTS is given in Figure 23. For comparison, the normal envelope portion of the chart for the helicopter with the metal tail section is shown as a dotted line in Figure 23. Note that the lighter weight CTS results in a more forward center of gravity for the vehicle.

TABLE 2. CTS WEIGHT ANALYSIS

	Original Goal	Current Status	Basis For Current Data	
			% EST	% CALC
<u>Stabilator - Basic</u>	(58.0)	(52.0)	(18)	(82)
Upper - Cover	3.0	3.2	0	100
Lower - Cover	3.0	3.2	0	100
Spars	7.0	15.2	0	100
Interspar - Ribs	4.0	6.0	0	100
- Chordwise Stiff.	0.0	0.0	0	0
Leading Edge - Cover	7.0	3.6	0	100
- Ribs	2.0	1.4	0	100
- Fasteners	1.0	0.0	0	0
Trailing Edge - Cover	14.0	3.6	0	100
- Ribs	4.0	0.6	0	100
- Fasteners	2.0	0.0	0	0
Fitting - Hinge (pivot)	5.0	8.0	100	0
- Actuator	2.0	1.0	0	100
Attachments - Misc. & Fasteners	2.0	2.3	50	50
Tips	2.0	0.0	0	0
Debris Protection	0.0	3.8	0	100
Lightning Protection	0.0	0.1	0	100
<u>Vertical Tail - Basic</u>	(79.0)	(90.0)	(22)	(76)
Cover	26.0	0.0	0	0
Spar Webs	21.0	0.0	0	0
Spar Box Assembly	0.0	34.2	0	100
Interspar Ribs	10.0	9.5	26	74
Leading Edge - Cover	7.0	11.5	0	100
- Ribs	2.0	2.2	0	100
- Fasteners	1.0	2.5	0	100
Trailing Edge - Cover	3.0	4.3	0	100
- Ribs	1.0	0.6	0	100
- Fasteners	0.0	2.1	0	100
Attachments - Tail to Fuselage	2.0	12.0	100	0
- Miscellaneous	1.0	3.0	100	0
Tips	3.0	3.5	0	100
Steps & Grips	2.0	2.0	100	0
Tail Rotor Gear Box Fittings	0.0	2.6	0	100
<u>Tailboom - Basic</u>	(117.6)	(139.5)	(12)	(88)
Bulkheads + Frames	16.0	27.2	48	52
Joints, Splices + Fasteners	8.6	3.4	70	30
Monocoque Sandwich	89.0	100.4	0	100
Intercostals	0.0	4.4	0	100
Stabilator Actuator Fitting	2.0	0.0	0	0
Jack Fitting	2.0	1.2	100	0
Steps + Grips	0.0	1.4	0	100
Tail Rotor Fairing Angles	0.0	1.5	0	100

TABLE 3. CTS WEIGHT STATUS SUMMARY

Item	Metal Weight (lb.)	Composite Weight (lb.)	Weight Savings (lb.)
Stabilator	73.1	52.0	21.1
Vertical Tail	120.0	90.0	30.0
Tailboom	160.8	139.5	21.3
Totals	<u>353.9</u>	<u>281.5</u>	<u>72.4</u>
Estimated increase in weight at fuselage station 370 to install CTS (reduced weight savings)			- 7.6
Net Weight Savings			<u>64.8</u>
Estimated weight increase of metal tailboom to accommodate CFTR			+ 6.0
Adjusted Weight Savings			<u>70.8</u>

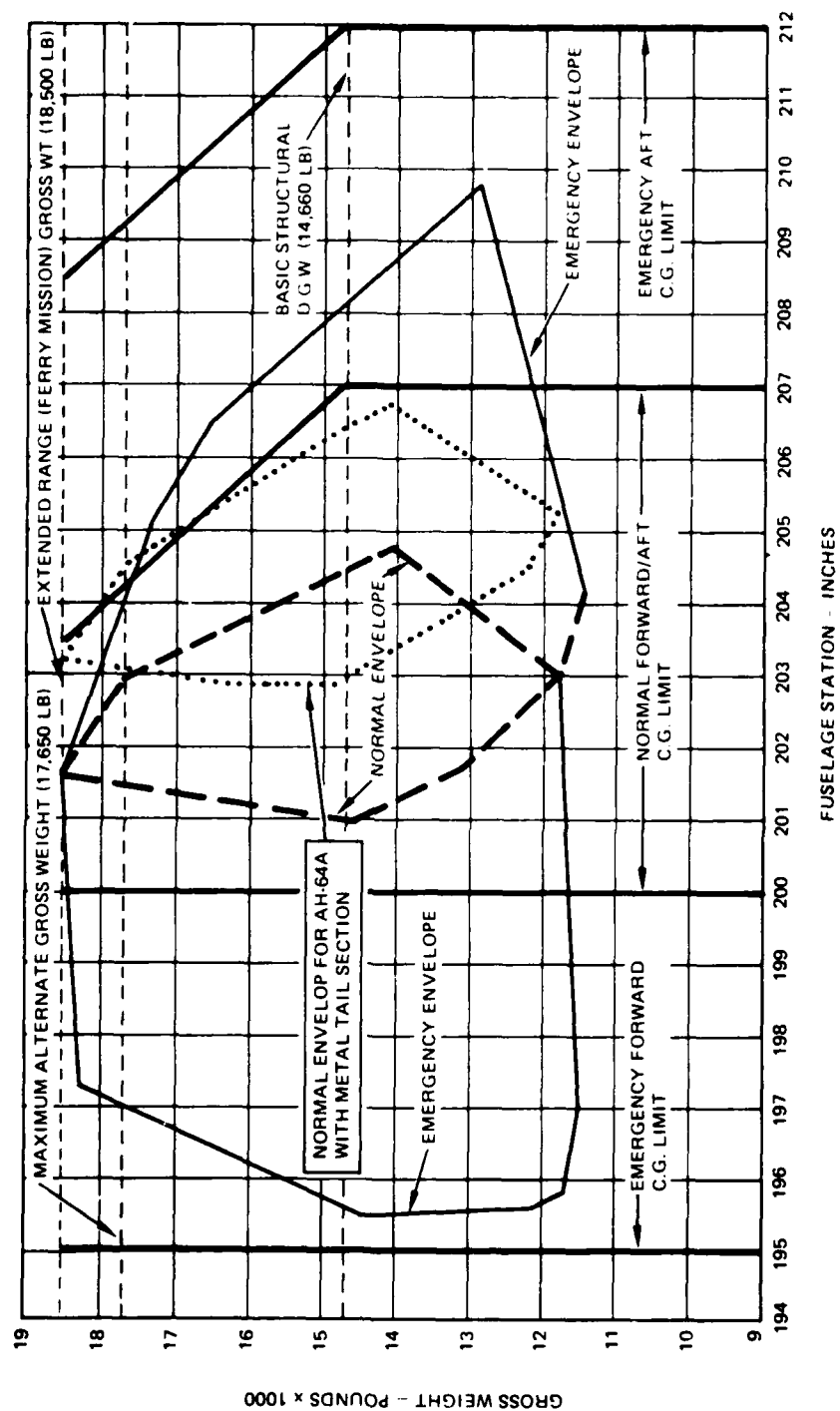


Figure 23. AH-64A Longitudinal Center-of-Gravity with CTS

RELIABILITY ASSESSMENT

Reliability assessment of the CTS is based on the results of a preliminary systemized Failure Modes, Effects, and Criticality Analysis (FMECA), a review of program requirements, and a review of reliability studies conducted for other composite programs at HHI. The analysis considers the degradation of reliability that may occur as a result of manufacturing defects, storage, environmental conditions, in-service conditions, and production techniques. Specific areas of concern include delamination and disbonding, porosity and voids, resin rich and resin starved areas, internal geometry and bond lines, resistance to impact, and defects in metal attach fittings. These studies show that the hazards imposed by air vehicle operation and maintenance are the primary reliability considerations. Detection through such nondestructive inspection techniques as X-ray or Bondoscope permits these problems to be detected and cured.

Cracking occurs primarily at fastener interfaces and is easily detectable. The CTS is designed to use a minimum of fasteners and the composite structure is adequately designed to accept fasteners. Degradation due to limited cracking is expected to be minor.

Resin-starved/resin-rich areas can contribute to structural degradation and loss of effective performance. Resin starvation can fail to support the filaments properly and result in delamination; this can result in geometric misplacement of the fibers to cause unanticipated load paths. Resin richness means either that not enough filaments are present to carry the loads or that the resin/filament matrix is oversized and, hence, out of its desired position in the structure -- in either case structural integrity is jeopardized. These conditions occur only during manufacturing not during in-service operation and are discovered during nondestructive evaluation. A resin-rich or resin-starved defect is not considered to be a failure mode in the FMECA because it is a failure mechanism (cause) of a delamination failure mode.

Ultraviolet light, rain erosion, moisture entrapment, extreme temperatures, snow, wind, and lightning contribute greatly to reliability degradation. The resin matrix material degrades considerably when exposed to ultraviolet light. Protection from ultraviolet light is provided by a suitable coating of the exposed skins. Although moisture entrapment cannot be avoided, the composite tail section is designed for the worst case condition as is true with the rest of the environmental extremes. Extremely rare incidents such as heavy hail or hurricane velocity winds are not considered since these environments should be avoided when operating the air vehicle.

The significant contributors to reliability degradation of the CTS are hazards induced during air vehicle operation and maintenance. These include thermal cycling, shock, vibration, aircraft fluids, rotor downwash (induced airborne particles and FOD), rocket debris, rough handling, impact with terrain objects, maintenance, and contact with work stands and ground vehicles. Design allowables may compensate for some of these hazards and the resultant degradation may be readily visible. However, the resultant degradation of those hazards, not readily visible, can only be determined by an effective and adequate nondestructive evaluation or nondestructive test technique. Based on results of previous testing and for equivalent material thickness, the order of damage tolerance is as follows. Fiberglass is the most damage tolerant, Kevlar is next best, and graphite has low damage tolerance. Sandwich construction has poorer impact resistance than monolithic construction and tends to suffer reductions in strength due to subsurface damage. Nomex sandwich construction is protected by Kevlar/graphite facing sheets on the composite tail section and Nomex has shown to have better damage tolerance than aluminum. Finally, simple field-type repair methods have been shown to be effective for many types of routine impact damage. At the time that the program was terminated, a Failure Modes, Effects, and Criticality Analysis (FMECA) had not been made for comparison with the metal empennage of the basic AH-64A helicopter.

STRUCTURE VERIFICATION TESTS

Tests were made to determine the properties of the particular laminates used in the tailboom, vertical stabilizer, and stabilator of the CTS. The testing included tension, compression, shear, and bearing of typical configurations found in the CTS to verify strength, elasticity, and strain allowables.

Two types of test specimens were investigated: helically wound tubular specimens used for tension, compression, and torsional shear tests and flat panel specimens laminated from wet-filament-wound broadgoods with fabric reinforcing plies. Test fixture end reinforcement was applied to the wet specimens at each end. Specimen identification, material description, and type of test as well as number of specimens are presented for tubular tension and compression specimens in Figure 24 and Table 4, for tubular torsion specimens in Figure 25 and Table 5, and for bolt bearing test specimens in Figures 26 and 27 and Tables 6 and 7. All of the specimens were wet-filament wound using Kevlar-49 and Thornel 300 graphite fibers with APCO 2434/2347 (7.5 PPHR) resin. The fiber volume ratio was 0.50 for all specimens.

All specimens were tested in a room temperature (70°- 75°F), dry condition. Each tension and compression tubular specimen was installed in a test machine as shown in Figures 28 and 29 in a manner to prevent any bending loads from being applied. (A stabilizing bar was installed in the compression specimens to prevent buckling.) A two-inch extensometer was mounted to each specimen to measure deflection. A load-deflection strip-chart recorder monitored the applied load and deflection. The load-deflection curve was used to calculate the modulus of elasticity of the specimen. The load was applied at an average rate of 0.05 inches per minute for the moving head of the test machine. All specimens were tested to failure.

Each tubular torsion test specimen was installed in a test fixture designed to apply shear loads to the test section of the specimen as shown in Figure 30 with a stabilizing bar installed to prevent buckling. Holes were drilled in the end pieces of the specimens to firmly attach them in the test fixture.

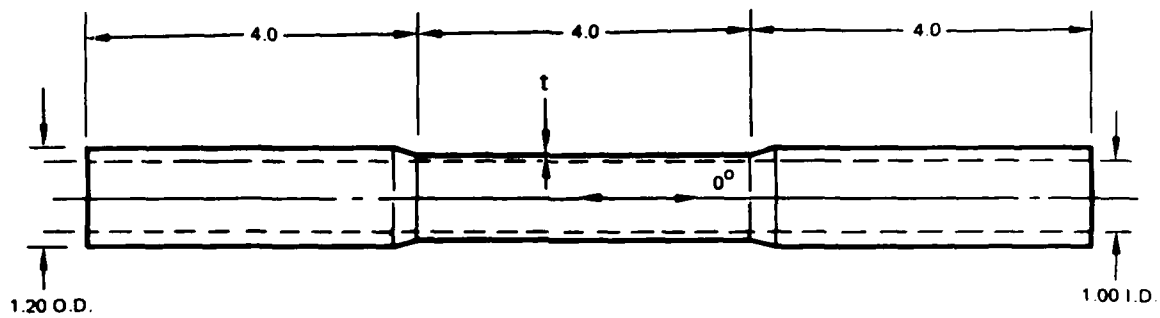


Figure 24. Tension/Compression Specimen

TABLE 4. TENSION/COMPRESSION SPECIMENS

Specimen No.	Component	Layup Composition	Total Thickness	Condition
I-1	Stabilator Skin	$[\pm 45^\circ / 0^\circ / \pm 45^\circ]$ Kevlar (KV)	.020/.020/.020 .060	Tension Compression
I-2	Vertical Tail Skin	$[\pm 30^\circ / 90^\circ / \pm 30^\circ]$ Graphite (GR)	.020/.020/.020 .060	T C
I-3	Stabilator & Vertical Tail Spar Caps	$\pm 45^\circ / 0^\circ_{12} / \pm 45^\circ$ GR	.014/.085/.014 .113	T C
I-4	Tailboom	$\pm 45^\circ / 0^\circ_{12} / \pm 45^\circ$ GR/KV 50-50	.014/.083/.014 .111	T C
I-5	Tailboom	$[90^\circ, (\pm 13.5^\circ)_2, 90^\circ]$ GR/KV 50-50	.007/.038/.007 .052	T C
I-6	Tailboom	$[90^\circ (\pm 8^\circ)_2 90^\circ]$ GR/KV 50-50	.007/.032/.007 .046	T C

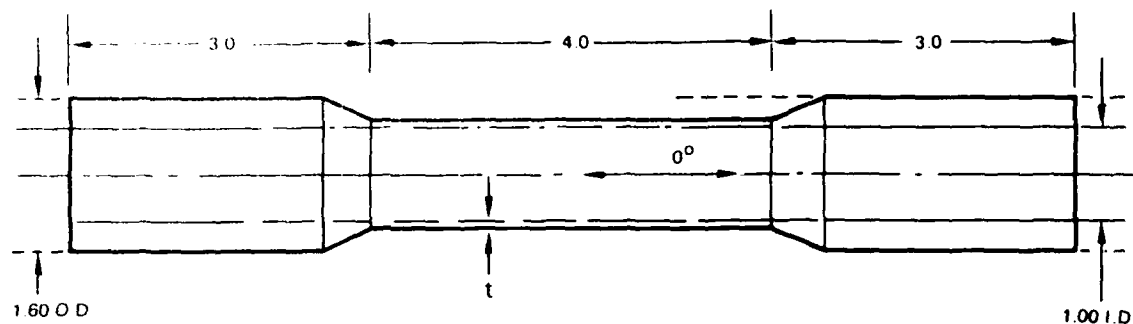


Figure 25. Torsion Test Specimen

TABLE 5. TORSION SPECIMEN

Specimen No.	Component	Layup Composition	Skin Thickness
II-1	Stabilator Skin	$[\pm 45^\circ / 0^\circ / \pm 45^\circ]$ KV	.020/.020/.020 .060
II-2	Vertical Tail Skin	$[\pm 30^\circ / 90^\circ / \pm 30^\circ]$ GR	.020/.020/.020 .060
II-3	Tailboom	$[90^\circ, (13.5^\circ)_2, 90^\circ]$ GR/KV 50-50	.0066/.0382/.0066 .051
II-4	Tailboom	$[90^\circ, (\pm 8^\circ)_2, 90^\circ]$ GR/KV 50-50	.0066/.0320/.0066 .0452
II-5	Tailboom	$[90^\circ, (\pm 9^\circ)_2, 90^\circ]$ GR	.010/.032/.010 .052
II-6	Tailboom	$[90^\circ, (\pm 15^\circ)_2, 90^\circ]$ GR	.010/.034/.010 .054

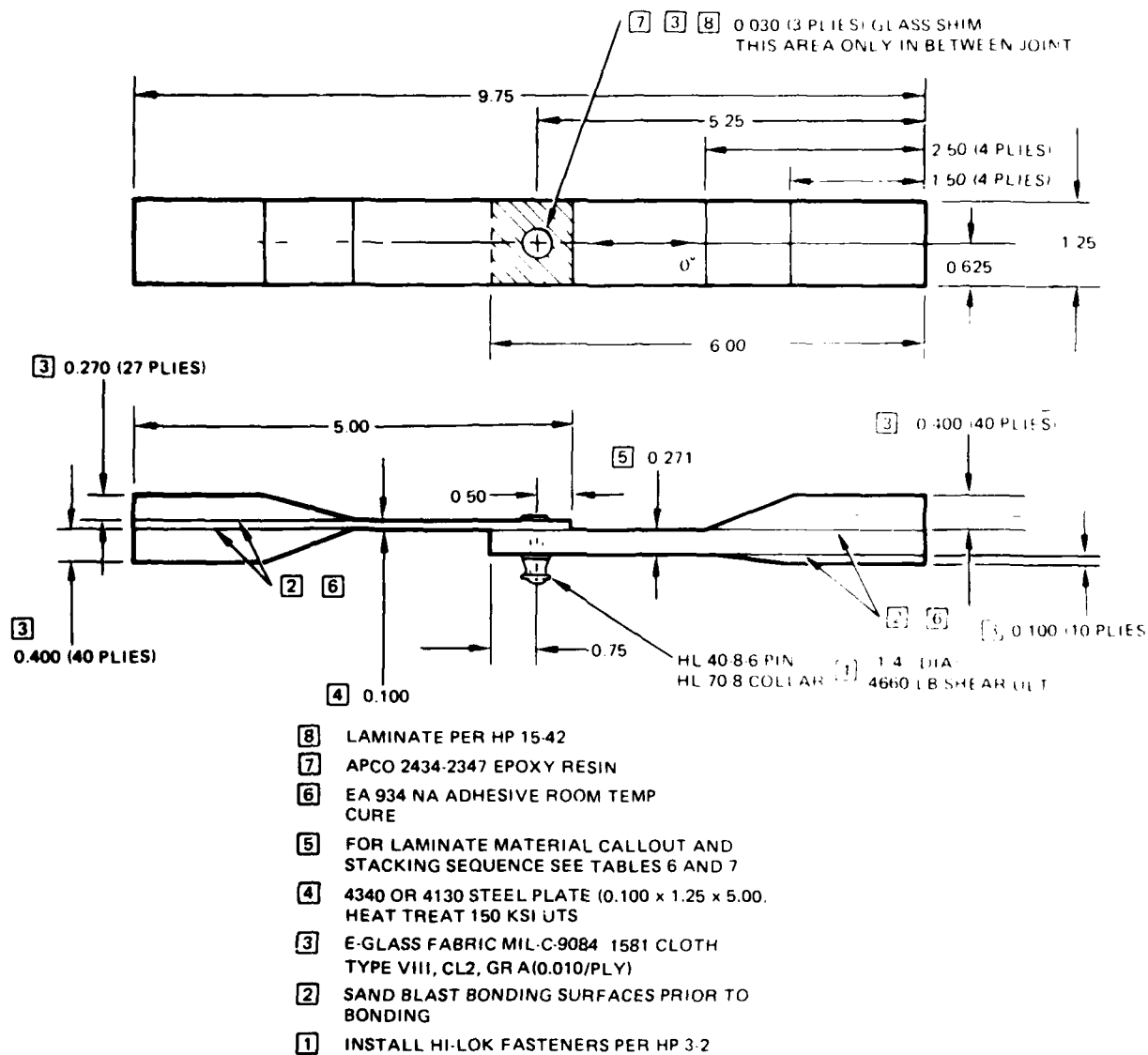


Figure 26. Bearing Test Specimen Type III-1.

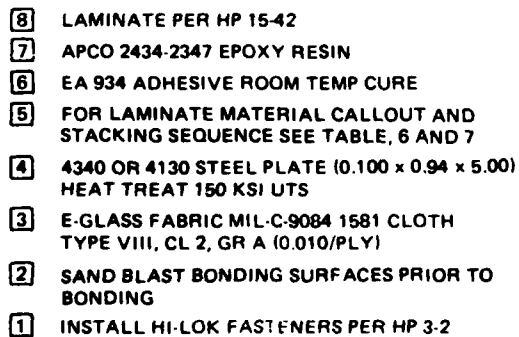


Figure 27. Bearing Test Specimen Type III-2.

TABLE 6. STACKING SEQUENCE FOR TYPE III SPECIMENS

Ply Number	Angle	Material*	Ply Thickness
P15	90°	⑥ ⑧	.011
P14	±45°	④	.013
P13	±8°	⑤ ⑥	.022
P12	±45°	④	.013
P11	90°	⑦	.020
P10	±45°	④	.013
P9	90°	⑦	.020
P8	±45°	④	.026
P7	90°	⑥	.011
P6	±45°	④	.026
P5	90°	⑥	.011
P4	±45°	④	.026
P3	±8°	⑤ ⑥	.022
P2	±45°	④	.026
P1	90°	⑥ ⑧	.011

*See Table 7.

TABLE 7. FABRICATION NOTES FOR
TYPE III SPECIMENS

- ⑧ APCO 2434-2347 Epoxy Resin
HMS 16-1115 Type I, CL 1
- ⑦ E-Glass, Roving
MIL-R-60346 Type I, CL 1
- ⑥ T300 3000 Fil Count, Roving
HMS 16-1163 Type I, CL 1
- ⑤ Kevlar 49, Roving 1420 Denier
HMS 16-1164 Type I, CL 3
- ④ T300 3000 Fil Count, Fabric
HMS 16-1163 Type II, CL 1, GRA
- ③ Filament wind per HP 15-67
- ② Layup per HP 15-42
- ① First Ply goes Against Tool Face

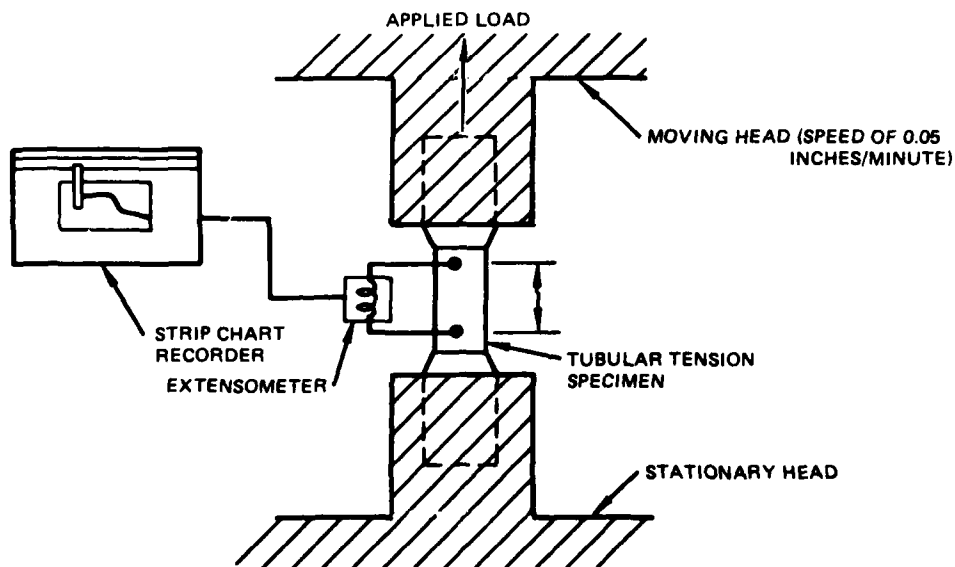


Figure 28. Tubular Static Tension Test Schematic

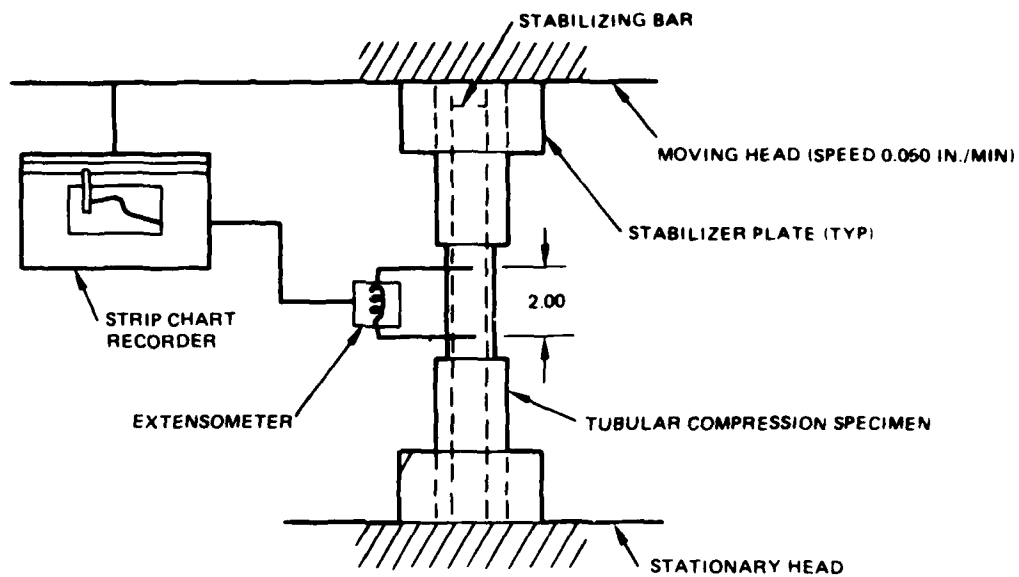


Figure 29. Tubular Static Compression Test Schematic.

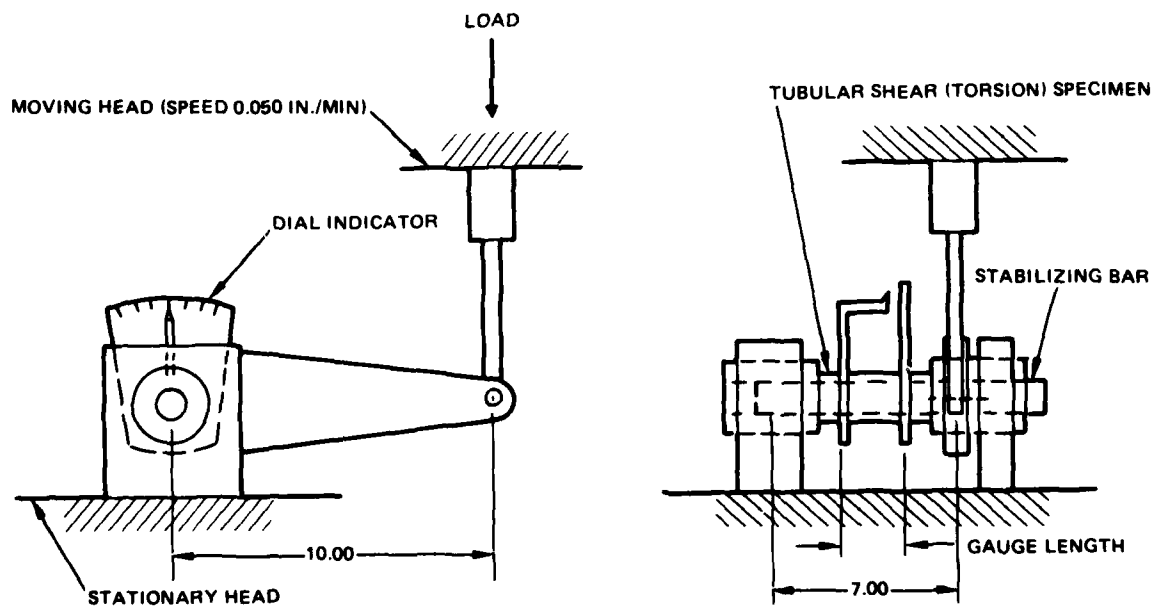


Figure 30. Tubular Static Shear (Torsion) Test Schematic.

A gage indicator was mounted to the test section of the specimen to measure angular displacement during testing. A torque arm was mounted to one end of the specimen and attached to the moving head of the test machine while the other end of the test specimen was fastened to the fixed head of the machine. The torque arm was designed to preclude the application of bending loads to the specimen. The load was applied to the torque arm at the rate of 0.05 inches per minute as for the other tests with each specimen loaded to failure. Angular deflection was measured at periodic intervals during the test. The bolt bearing test specimens were tested in a manner similar to the tension specimens except the deflections were not monitored.

A total of 64 specimens were tested. Test results are given in Tables 8, 9 and 10 for tension/compression, torsion, and bearing tests respectively. The dimensions, ultimate load, ultimate stress, and modulus of elasticity for each specimen are given.

TABLE 8. TENSION/COMPRESSION TEST RESULTS

Specimen		I. D. (in.)	O. D. (in.)	Area (in. ²)	Applied Load		Tens. Str. (%)	Elong. (%)
Type	No.				Type	lb.		
1-1	1	0.991	1.100	0.195	Tension	1000	0.000	0.0
	2	0.993	1.100	0.190	T	10000	0.000	0.0
	3	0.993	1.110	0.200	T	10140	0.000	0.0
	4	0.993	1.109	0.192	Comp.	9500	1.00	4.0
	5	0.993	1.110	0.204	C	9500	1.00	4.0
	6	0.992	1.109	0.193	C	9500	1.00	4.0
1-2	7	0.990	1.115	0.197	T	7000	0.000	0.0
	8	0.995	1.114	0.197	T	7000	0.000	0.0
	9	0.990	1.111	0.190	T	7000	0.000	0.0
	10	0.990	1.113	0.194	C	1434	0.00	0.0
	11	0.995	1.118	0.204	C	1434	0.00	0.0
	12	0.994	1.108	0.188	C	1434	0.00	0.0
1-3	15	1.017	1.236	0.369	C	1888	0.00	0.0
	16	1.010	1.237	0.391	C	1884	0.00	0.0
	17	1.017	1.235	0.388	C	1888	0.00	0.0
1-4	19	0.990	1.208	0.307	C	10340	0.00	0.0
	20	0.990	1.201	0.353	C	10800	0.00	0.0
	21	0.990	1.199	0.350	C	10800	0.00	0.0
	22	0.995	1.208	0.302	C	10480	0.00	0.0
	23	0.994	1.203	0.301	C	10440	0.00	0.0
	24	0.994	1.194	0.344	C	10880	0.00	0.0
1-5	25	1.018	1.073	0.0900	T	7700	0.000	0.0
	26	1.019	1.070	0.0837	T	8800	0.000	0.0
	27	1.019	1.074	0.0904	T	9000	0.000	0.0
	28	1.018	1.078	0.0980	C	8700	0.000	0.0
	29	1.020	1.070	0.0922	C	8028	0.000	0.0
	30	1.020	1.077	0.0939	C	8820	0.000	0.0
1-6	31	1.018	1.107	0.149	T	11840	0.000	0.0
	32	1.018	1.103	0.142	T	10840	0.000	0.0
	33	1.019	1.103	0.140	T	11080	0.000	0.0
	34	1.020	1.104	0.140	C	11800	0.000	0.0
	35	1.019	1.102	0.147	C	10700	0.000	0.0
	36	1.019	1.102	0.138	C	9100	0.000	0.0

See Table 4.

TABLE 9. TORSION TEST RESULTS

Specimen		I. D. (in.)	O. D. (in.)	Area (in. ²)	Ult. Load (in. - lb.)	G (10 ⁶ psi)	Ult. Stress (psi)
Type	No.						
II-1	37	1.011	1.125	0.191	1730	1.5	17,793
	38	1.013	1.125	0.188	1700	1.7	17,749
	39	1.011	1.125	0.191	1680	1.7	17,279
II-2	40	0.996	1.108	0.185	2650	2.6	28,589
	41	0.995	1.115	0.199	2200	2.6	22,094
	42	0.996	1.114	0.195	2400	2.5	24,491
II-3	43	0.994	1.050	0.090	630	0.91	14,079
	44	0.993	1.050	0.091	590	0.90	12,972
	45	0.995	1.050	0.088	740	0.92	16,813
II-4	46	1.018	1.100	0.136	980	0.65	14,073
	47	1.017	1.102	0.141	990	0.77	13,718
	48	1.018	1.100	0.136	1080	0.73	15,508
II-5	49	1.002	1.134	0.221	2580	0.77	18,371
	50	1.001	1.132	0.219	2280	0.69	16,418
	51	1.000	1.131	0.219	2090	0.73	16,440
	52	1.006	1.139	0.224	2100	0.70	15,973
	53	1.006	1.129	0.206	2120	0.63	14,545
II-6	54	1.000	1.074	0.121	1110	1.65	23,078
	55	1.000	1.076	0.124	1020	1.56	20,603
	56	1.002	1.084	0.134	1110	1.54	18,921
	57	1.001	1.084	0.136	1090	1.56	18,490
	58	1.002	1.091	0.146	1070	1.62	20,300

* See Table 5.

TABLE 10. BEARING TEST RESULTS

Specimen		Thickness (in.)		Pin Dia.	Ultimate Load (lbs)	Ult Bearing Stress (psi)
Type*	No.	Steel	Comp.			
III-1	59	0.10	0.258	3/16	2,475	51,000
	60	0.10	0.260	3/16	2,535	51,800
	61	0.10	0.258	3/16	2,500	51,500
	62	0.10	0.257	1/4	3,910	60,900
III-2	63	0.10	0.257	1/4	3,625	56,400
	64	0.10	0.257	1/4	3,825	59,500

*See Figures 26 and 27.

BALLISTIC VULNERABILITY EVALUATION (HHI-SPONSORED TEST)

A ballistic vulnerability test was undertaken to determine the vulnerability of the CTS to the 23mm HEI-T projectile threat. The tests on two simulated tailboom shells determined the suitability of design refinements to be incorporated in the CTS. The test articles consisted of two tapered cylindrical specimens designed to simulate the CTS structural shell from Sta 450 to 547. Both specimens were of sandwich construction with adapters used to interface with the metal tailboom ballistic test fixture. The specimens were honeycomb sandwich construction with composite face sheets and Nomex core. Figure 31 shows the details of construction. Specimen #1 had 0° graphite/±60° E-glass/90° Kevlar skins with 200 x 200 aluminum wire mesh on the outside surface for lightning protection. Specimen #2 had 90°/±12.5°/90° all graphite skins with no lightning protection. Instrumentation consisted of a set of photoelectric velocity screens and electronic time interval counters for determining the impact velocity of the projectiles, and a load cell to verify load conditions. Both high speed and still photographic records were made.

An equivalent hover load was applied to the loading fixture (approximately 1,500 lbs) during and after ballistic impact. Each test specimen was subjected to one Soviet 23mm HEI-T projectile with an MG-25 delay fuze at 1,500 ±50 ft per sec in an aligned attitude at Station 510. Figure 32 shows the test setup and impact location.

Specimen #1 shows less severe damage than Specimen #2 due to the excellent energy absorption capacity of the Kevlar and E-glass, although both specimens are considered successful in defeating the 23mm threat.

Ballistic damage to Specimen #1 consists of a clean entrance hole and three zones of exit damage. See Figure 33 through 36. Zone 1 consists of an area of approximately 8 inches in diameter on the back side of the specimen on the shot line. Damage in this area consists of approximately five holes ranging in size from one to two inches in diameter. One hole is accompanied by a torn face sheet approximately 2 by 6 inches. Zone 2 consists of an area approximately 24 inches in diameter on the back side of the specimen. Damage in this area consists of a large number of small perforations (less than one inch in diameter) spaced relatively widely. Zone 3 consists of two areas approximately 30 by 6 inches along the top and bottom of the specimen just forward of the center line. Damage in this area is most severe with a multitude of small (less than one inch) holes accompanied by some local tearing and delamination of the outer face sheet. Delaminations and tears range up to approximately 3 by 4 inches, maximum. No large holes or delaminations appear in the specimen and sufficient cross section remains intact to assure safe flight.

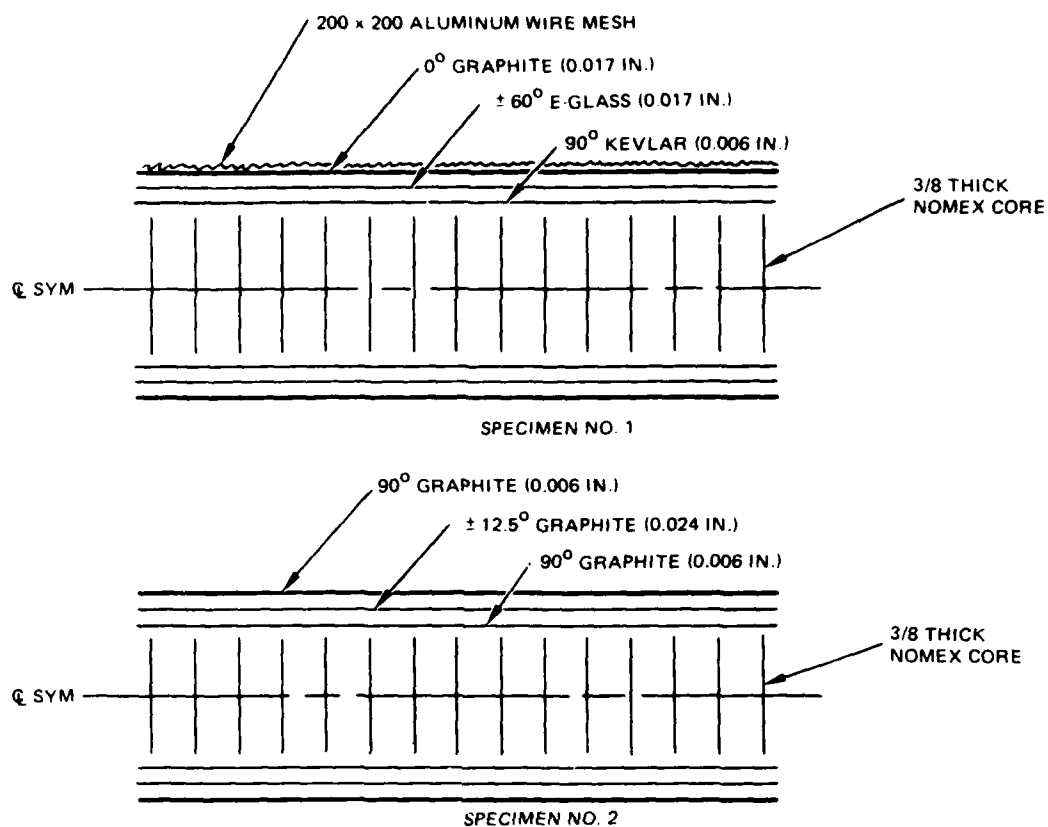


Figure 31. Ballistic Test Specimen Construction

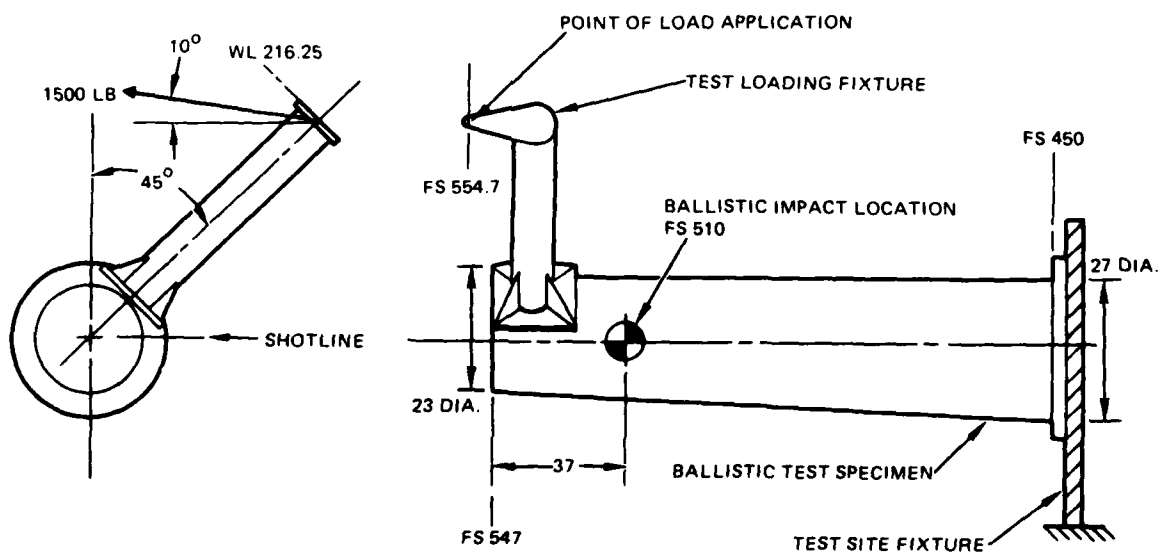


Figure 32. Ballistic Test Setup and Impact Location

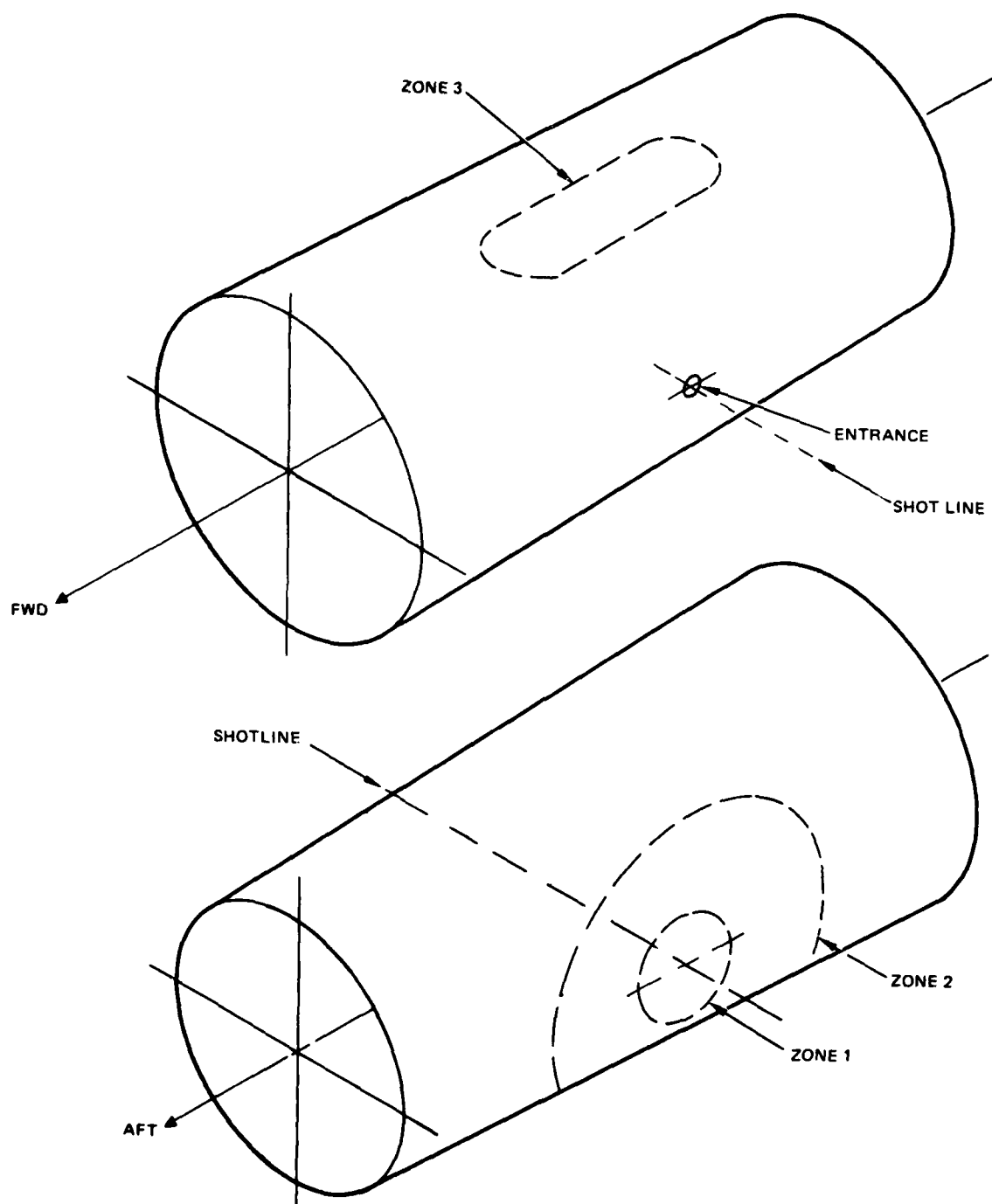


Figure 33. Ballistic Damage Zones.



Figure 3.2

Figure 3.3



Figure 3.4

Figure 3.5



Figure 36. Specimen #1 -- Rear View With Damage

Damage to Specimen #2 is more severe than to Specimen #1. However, residual strength of the specimen is not reduced sufficiently to prevent carrying the hover load. See Figures 37 through 40. Referring to the same zone designations as for Specimen #1, Zone 1 damage is quite similar with slightly more delaminations of the skin. Zone 2 damage is also very similar to that for Specimen #1, although the perforations through the all-graphite skin are much cleaner due to the brittleness of the graphite fibers compared to the Kevlar and fiberglass fibers. Several of the holes are accompanied by minor local delaminations of the skin. Zone 3 damage to Specimen #2 is much more severe than Specimen #1. Although the majority of the holes are smaller, several large holes are present with an area of approximately 6 by 18 inches torn away from the honeycomb core on the lower side.

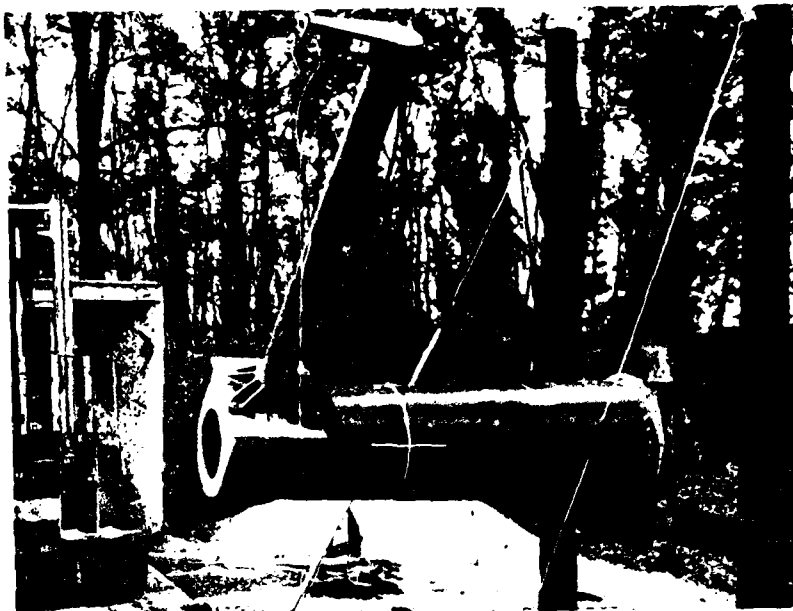


Photo 80-10881-13

Figure 57. Ballistic Specimen #2 -- Undamaged

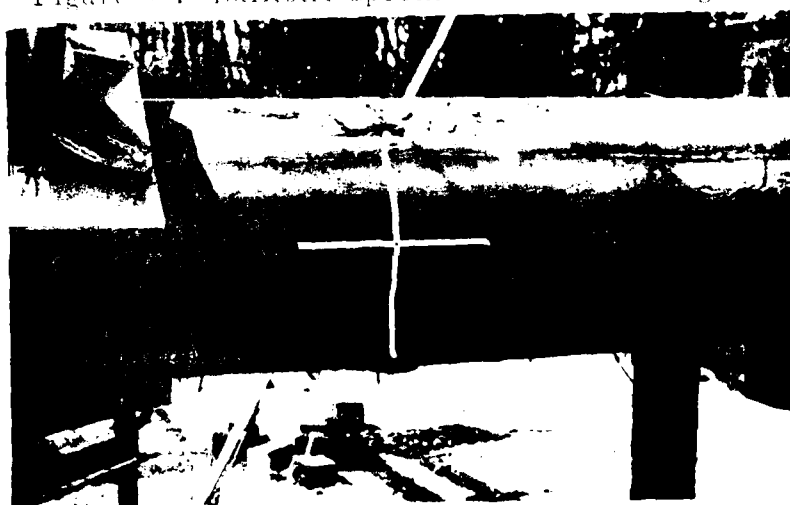


Photo 80-10881-22

Figure 58. Specimen #2 -- Front View With Damage



Photo 80-10881-25

Figure 39. Specimen #2 -- Close-up Front View With Damage



Photo 80-10881-23

Figure 40. Specimen #2 -- Rear View With Damage

LIGHTNING PROTECTION EVALUATION (HHI-SPONSORED TEST)

Preliminary lightning tests were conducted on two graphite/Kevlar 12- x 24-inch flat test panels that were representative of the tailboom laminated sandwich in the Sta 370 region (see stacking sequence in Table 2 of Figure 9). The tests consisted of high current tests in which 200 kiloamperes (or as much as the specimen would pass) was fired through the sample from end to end, and a 100 kiloampere discharge fired as a restrike into an inboard area of the specimens.

The test arrangement is shown in Figures 41 and 42. The test results are summarized as follows:

- A 150,000 ampere end-to-end discharge on these flat panels causes only very slight damage, but the current is limited by the resistance of the graphite. An additional discharge across half the panel (to lower the resistance) also causes only slight damage. See Figures 43 and 44.
- A 100,000 ampere discharge inboard on the sections representing a swept stroke causes delamination of the outer skin of both test samples over an area approximately ten inches square. The damage appears to be severe at first, but it is determined not be flight critical. See Figures 45 and 46.

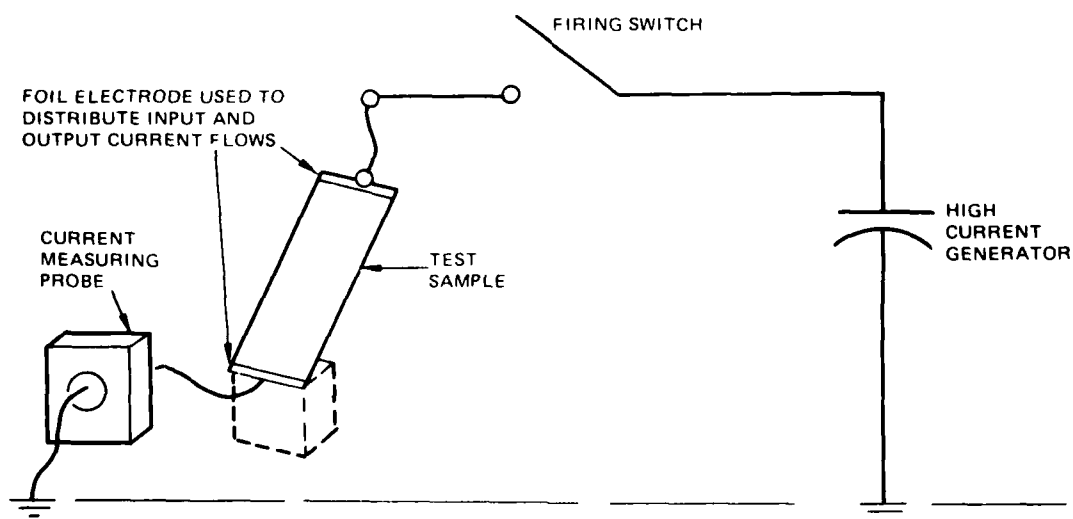


Figure 41. Test Arrangement for Stationary 200,000 Ampere Discharge)

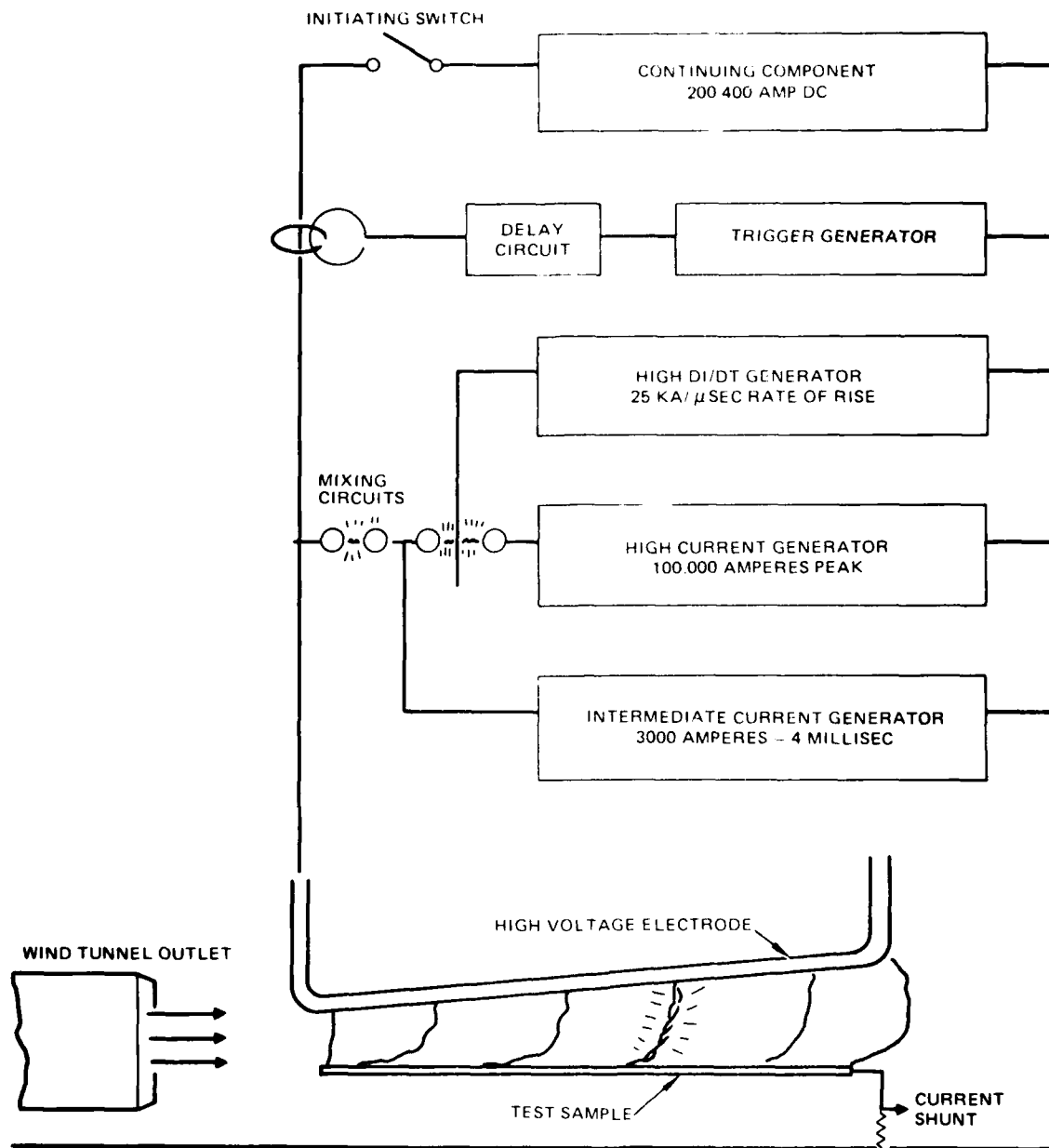


Figure 42. Test Arrangement for Swept Stroke Tests

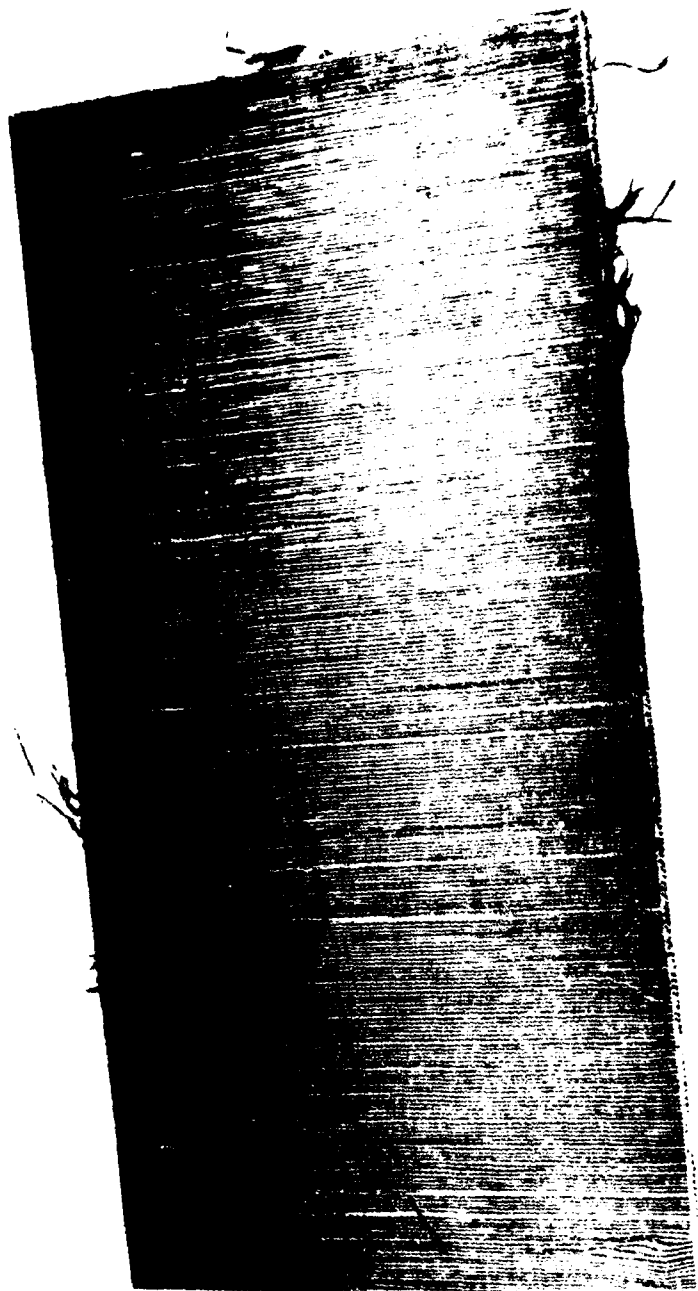


Photo 46-4740

Figure 46. Stationary Discharge Damage -- Specimen 1



Photo 80-4742

Figure 44. Stationary Discharge Damage -- Specimen 2



Photo 80-4741

Figure 45. Swept Stroke Discharge Damage -- Specimen 3



Figure 1. A view of the Dugway Dam, showing the spillway.

Figure 1. A view of the Dugway Dam, showing the spillway.

The tests may be summarized as having caused little damage from discharges of 150,000 amperes from end-to-end of the test section, but inward discharges cause extensive delamination of the outer skin from direct contact with the arc. The damage in the latter case is less severe than the ballistic damage caused by a 23mm HEI-T projectile, and this is considered to be non-flight critical. In either case, the damage is considered repairable, even in the event of a swept lightning strike directly to the tailboom.

It is concluded that because the skin can withstand a swept lightning stroke (which is noted as an unlikely event) that further protection need not be provided.

ANTENNA INTEGRATION EVALUATION

A feasibility study was conducted for the #1 FM antenna that is integrated into the trailing edge of the vertical tail to determine if its operation is compatible with the composite tail section. The study included testing of the various composite materials proposed for use, and included comparative impedance, patterns, and gain measurements in the FM frequency band for both aluminum and graphite/epoxy composite tail section mockups. Antenna impedance, pattern, and gain were measured. The purpose of the study was to determine if the existing FM #1 Vertical Stabilizer Trailing Edge Antenna designed for installation on a metal tail section could provide acceptable performance when installed on a composite tail section, and to provide recommendations for antenna redesign if so indicated by the study.

The electrical properties of materials were studied to determine the construction of the composite mockup to simulate the electrical characteristics of the tail structure closely and with reasonable cost. Unidirectional graphite fabric was used in an epoxy resin wet layup to electrically simulate the semiconducting members of the mockup. Since structural strength was not needed for the mockup, part thicknesses were chosen to simulate the R. F. properties of the structure. Graphite parts were reduced to 0.06 inch thickness, thereby limiting the cost of the mockup and shortening fabrication time. This amounts to six plies of the unidirectional graphite fabric use. (90% unidirectional graphite fabric, T-300, 3000 filament count with 10% glass fill fibers. Woven Structures Style No. ES 1505.)

One composite material designated for study and test was a Thorstrand (aluminized fiberglass)/Kevlar/graphite/epoxy laminate. The electrical properties of this candidate are very difficult to analyze and test because the Kevlar dielectric layer separates the two semiconducting layers. Resistance measurements were made on the Thorstrand alone and on graphite epoxy alone. Manufacturer's resistivity data was also obtained. Composite materials providing improved strength-to-weight characteristics over aluminum fall in the category of electrically non-conducting (dielectric) or semi-conducting materials, whereas aluminum is highly conductive to direct electrical current (DC) and is known as a good conductor. Based on these materials, electrical tests, and the lightning tests, it was determined that the Thorstrand was not needed for the mockup, and only graphite and fiberglass were selected for its construction.

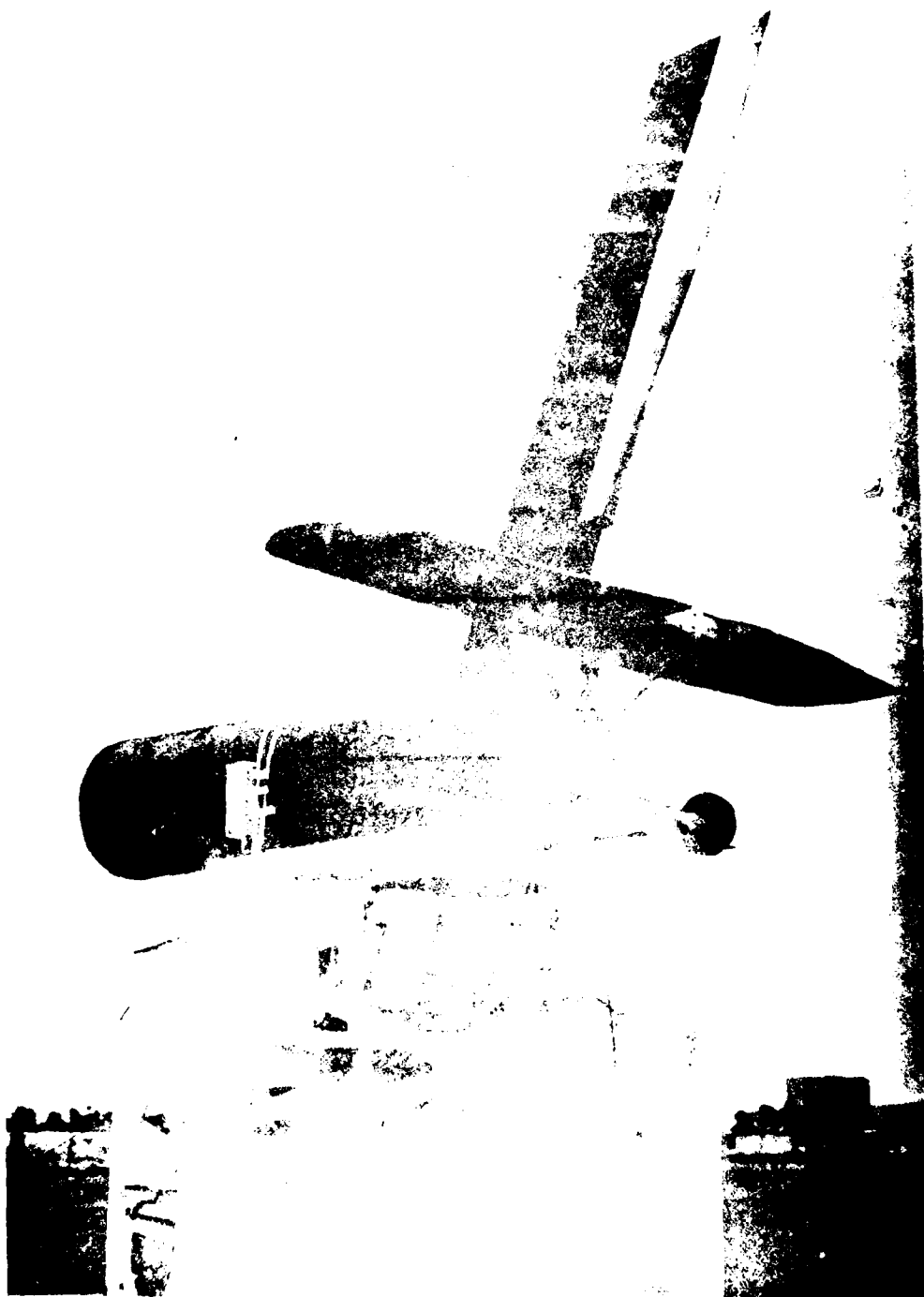
For antennas in the VHF frequency region and below, the airframe on which they are installed form a part of the antenna and contribute to its impedance, radiation pattern, and gain characteristics. The degree to which this is true depends upon the antenna configuration as well as the airframe configuration and the physical relation between antenna and airframe. If the airframe is highly conductive to the RF energy, these characteristics can vary widely when compared to a nonconducting or semi-conducting airframe.

To satisfy the requirements of this study, it was necessary to have two full scale AH-64A tail mockups. Since the trailing edge antenna is designed to operate on the metal version of the tail section, a metal mockup from the AH-64A program was provided for this purpose. All parts of the tail structure from Sta 450 aft that are necessary to electrically simulate the AH-64A metal tail section are included. The composite tail section mockup includes the tailboom skin, vertical spar box skin, and the ribs and spars within the stabilator. Stacking angles and the number of plies are maintained as closely as possible. The stabilator skin is fabricated of epoxy fiberglass. Additional parts of the tail section included in the mockup are tail rotor shaft and gearbox, vertical rotor driveshaft, and tail landing gear. The stabilator is movable in elevation within the $+10^{\circ}$ to -45° limits. Figure 47 shows the AH-64A graphite tail section mockup installed on the tower/positioner. Figure 48 is a schematic of the equipment.

The Vertical Tail Trailing Edge (VSTE) Antenna (P/N 7-211122630) is a *folded dipole antenna* integrated into the trailing edge fairing of the AH-64A helicopter vertical tail. An aluminum sheet metal spar at the forward side of the antenna and forms the "folded" portion of the antenna element.

Swept frequency impedance measurements were performed in the 30 to 70 MHz frequency range of the trailing edge antenna installed on both the aluminum and composite tail section mockups. These measurements enable a judgement to be made as to the comparative level of difficulty to be anticipated in impedance matching the antenna to the 50-ohm transmission line in the two different installation environments. A network analyzer was used to measure the antenna impedance.

Figures 49 and 50 show the impedance plots on impedance coordinates of the Smith Chart, with Several Frequency points in the FM band marked. These impedance plots show that the antenna impedance variation between the two installations is small. As a result, major impedance matching network compensation is not required to provide antenna impedance performance compatibility on the metal and composite tail sections. At most, some circuit component value changes in the matching network may be required. Antenna impedance is not appreciably affected by changing stabilator position on the metal mockup.



Mockup

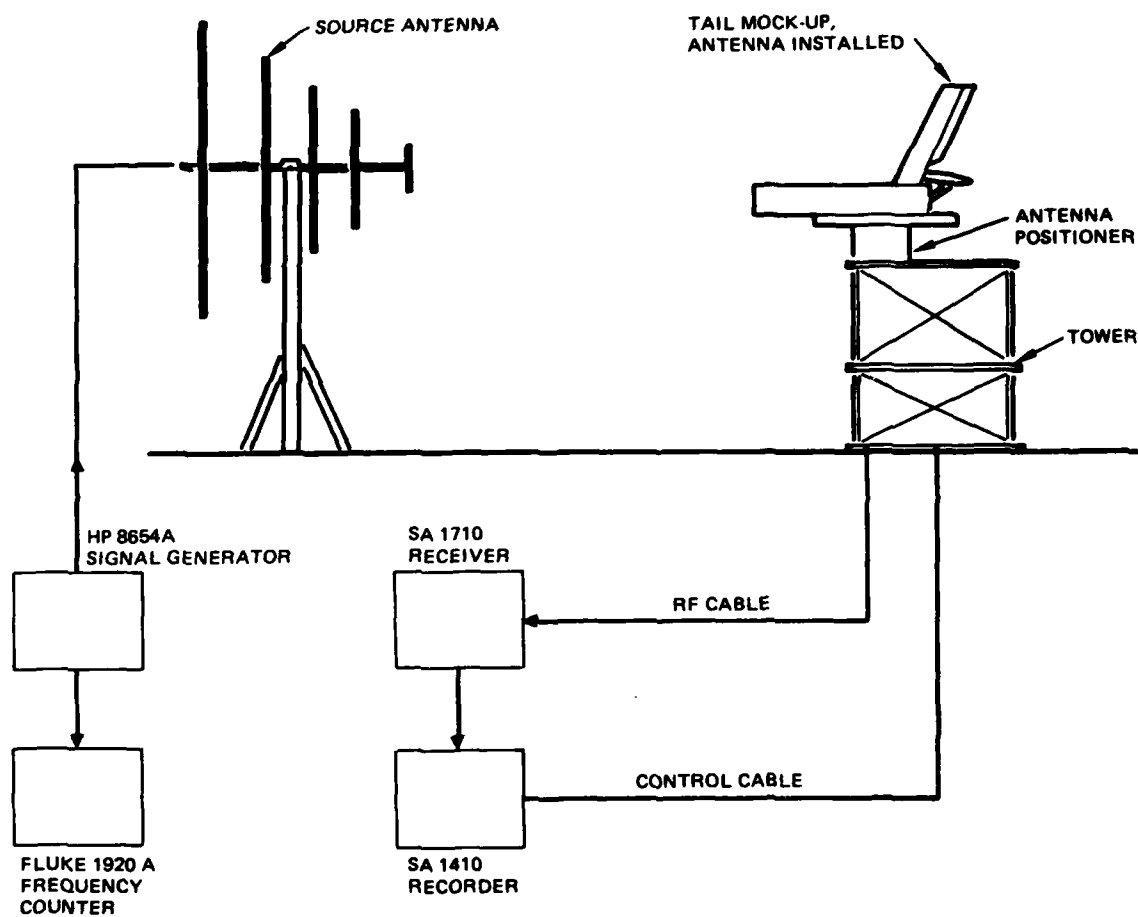


Figure 48. Radiation Pattern Test Setup.

IMPEDANCE COORDINATES—50-OHM CHARACTERISTIC IMPEDANCE

CORRECTED

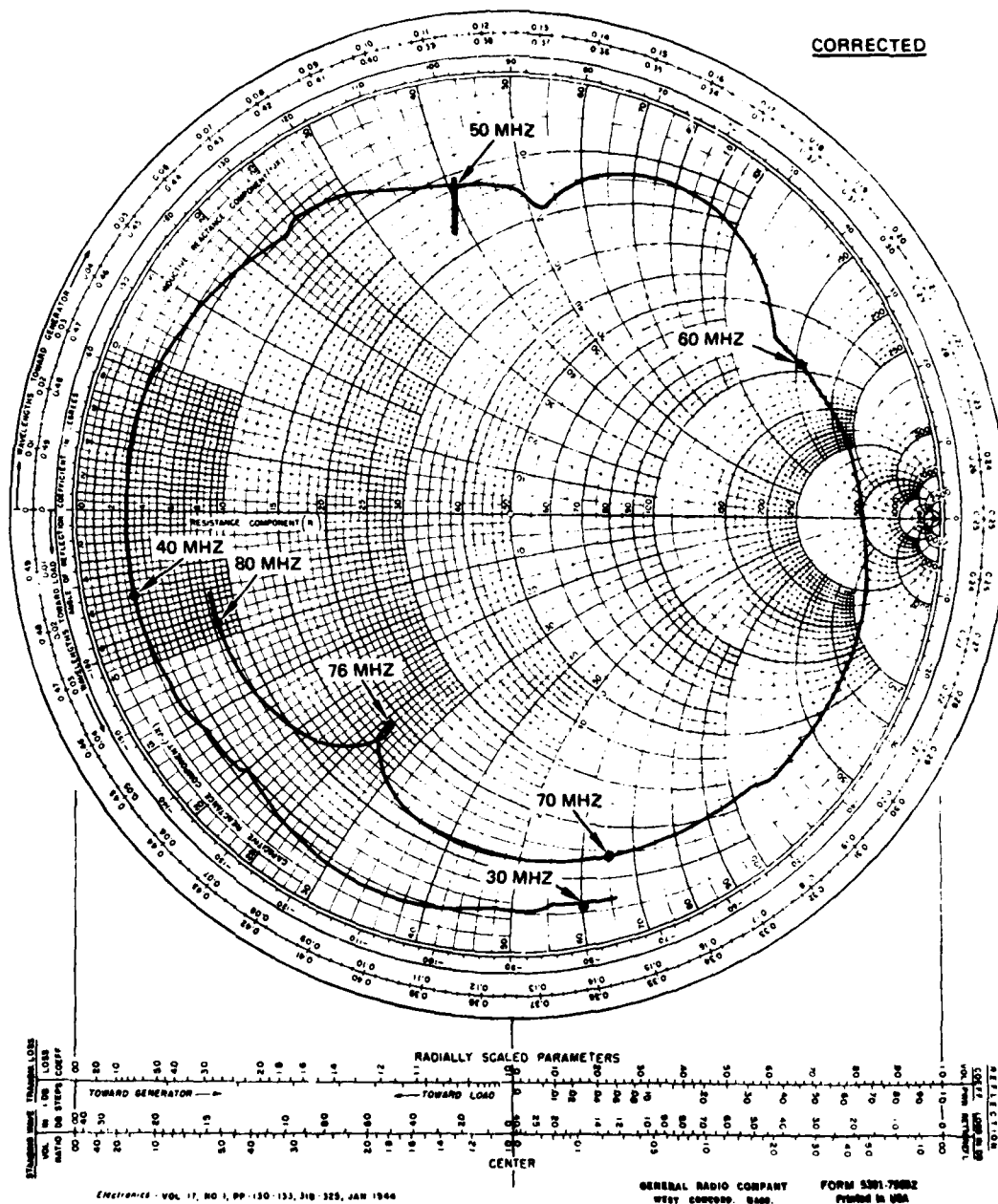


Figure 49. AH-64A Trailing Edge Antenna on Aluminum Mockup

IMPEDANCE COORDINATES—50-OHM CHARACTERISTIC IMPEDANCE

CORRECTED

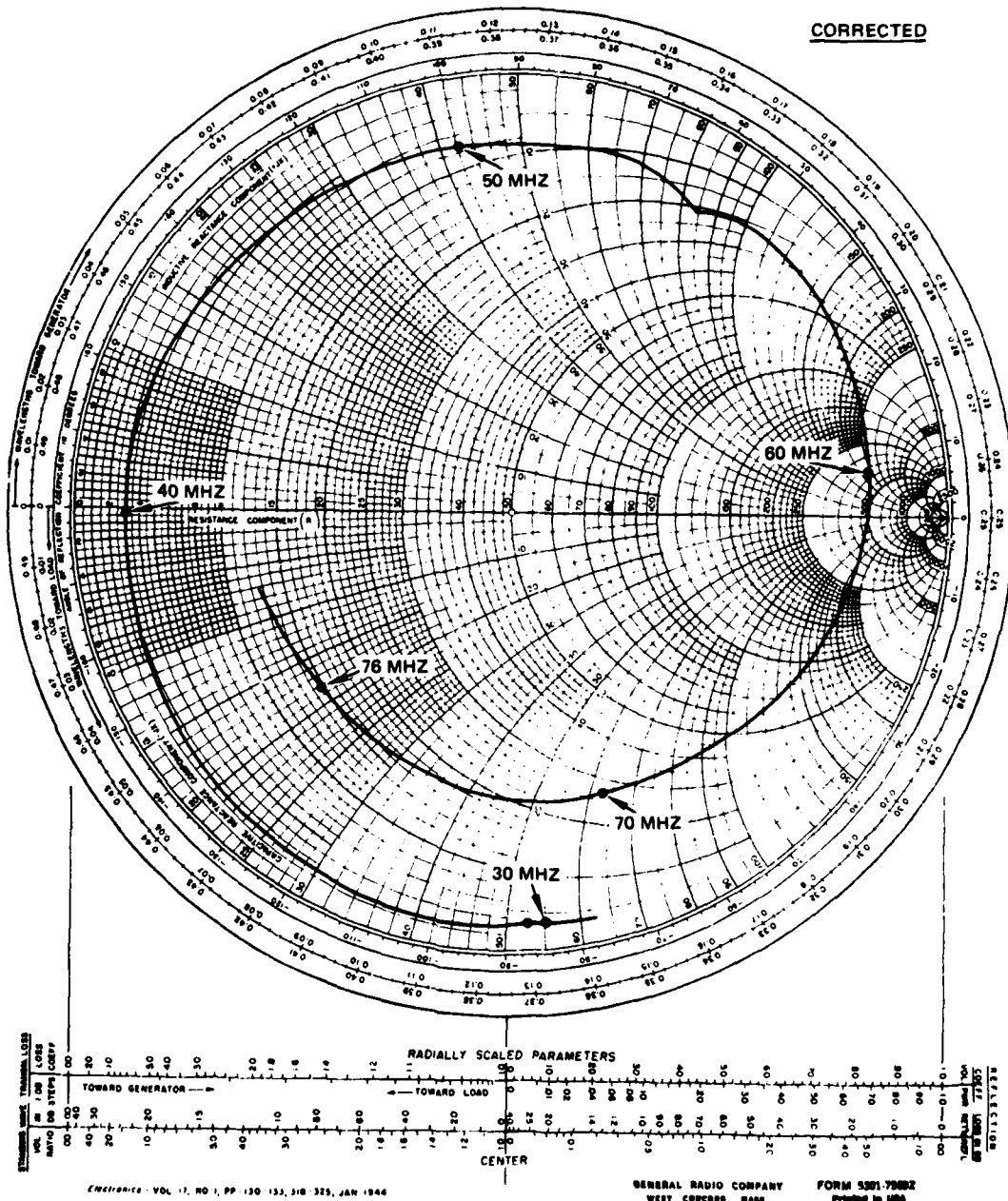


Figure 50. AH-64A Trailing Edge Antenna on Graphite Mockup.

Azimuth radiation pattern and gain measurements were performed at six frequencies in the VHF-FM band on the trailing edge antenna installed on both the aluminum and graphite tail mockups. The test setup is shown in Figure 48. The radiation patterns are shown in Figures 49 and 50. Each pattern contains a gain reference to allow the relative gain of the antenna on the graphite mockup to be compared to that of the antenna on the aluminum mockup. No attempt has been made to measure the absolute antenna gain for this program, since relative gain provides the necessary data for comparison. As shown by the patterns, the major difference is found in the 50 MHz pattern for the graphite mockup. This pattern contains a deep azimuth null and exhibits much lower gain than that for the metal mockup pattern. This condition is not characteristic of this antenna. The deep null can be caused by a parasitic element located on the mockup forward of the antenna. Since the only part of the mockup that has this characteristic is the tail rotor vertical driveshaft, it was removed and the patterns were rerun at one MHz intervals from 40 to 60 MHz. The null remained at frequencies of 49, 50, and 51 MHz, indicating that it is not caused by the driveshaft. This pattern and gain deficiency is believed to be caused by the test environment.

The test tower contains metal positioner, supporting structure, and connecting cables that can act as parasitic elements and are resonant at one or more frequencies. Resulting radiation patterns can contain both azimuth and elevation nulls. The azimuth null is evident in the azimuth pattern. An elevation null located on or near the horizon can also result in the lowered gain. But, as shown by the 50 MHz pattern for the aluminum mockup, a null is not present. The metal skin of the mockup is responsible for this change. The conducting skin has most likely upset the parasitic arraying effect of the test structure to eliminate the null entirely or shift it to a frequency not tested when the antenna is installed on the aluminum mockup. A less severe pattern deficiency occurs at 60 MHz on the metal model. The two deeper side nulls and lower relative gain are caused by the parasitic arraying effect of the antenna tower structure and the aluminum mockup.

Antenna pattern tests were run on the metal mockup with stabilator up 10 degrees and down 45 degrees for comparison with the 0 degree position. Negligible differences were noted at the six test frequencies. These tests were not repeated for the composite mockup because the less conductive stabilator (graphite spar/rib -- Kevlar skin) is anticipated to cause an even smaller effect.

Antenna impedance data for both mockup installations shows only minor antenna impedance variation between the two mockups. Impedance tests also show that antenna impedance is not appreciably affected by changing stabilator position. Hence, major impedance matching compensation is not required.

The comparative gain performance of the trailing edge antenna installed on the two mockups is quite favorable as Figures 51 through 56 show. For four out of the six test frequencies, the gain difference is 2 dB maximum. At the two remaining test frequencies, the gain varies 6 to 8 dB due to the effects of the test environment. It was concluded that this trailing edge antenna installed in the graphite/epoxy tail section meets the Contract requirements for the #1 VHF-FM antenna.

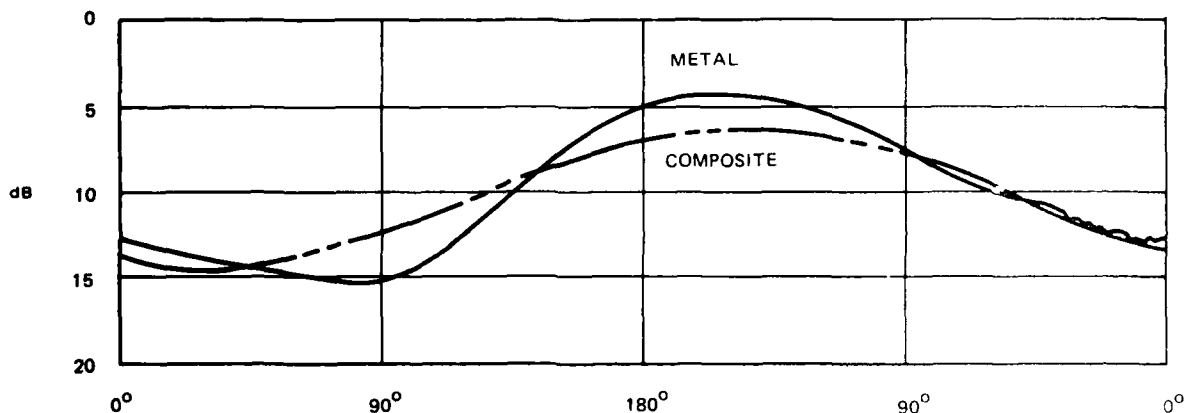


Figure 51. Antenna Pattern -- 30 MHz

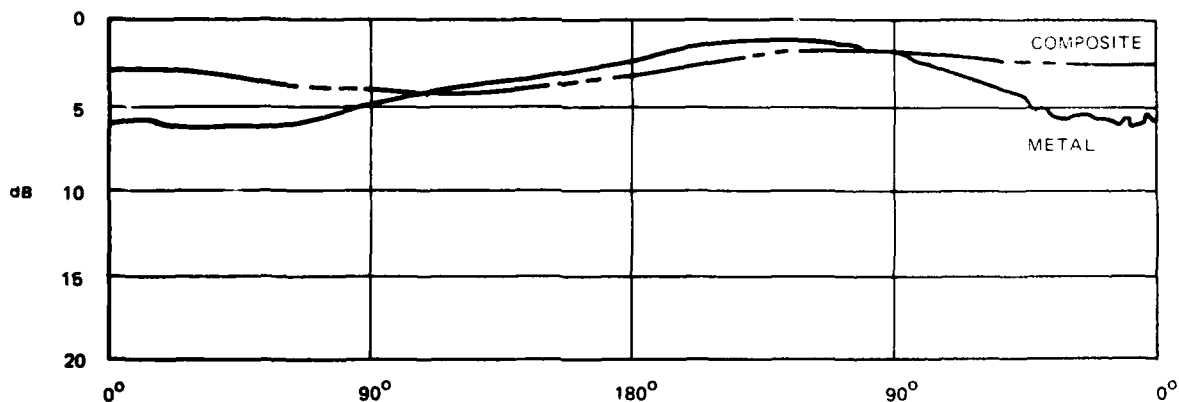


Figure 52. Antenna Pattern -- 40 MHz

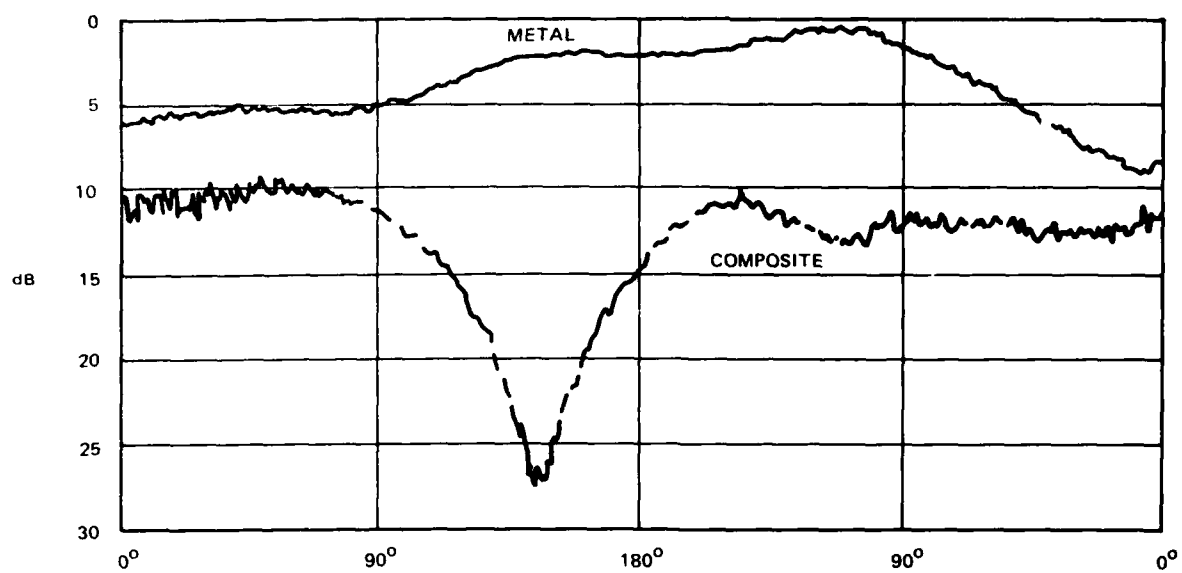


Figure 53. Antenna Pattern -- 50 MHz

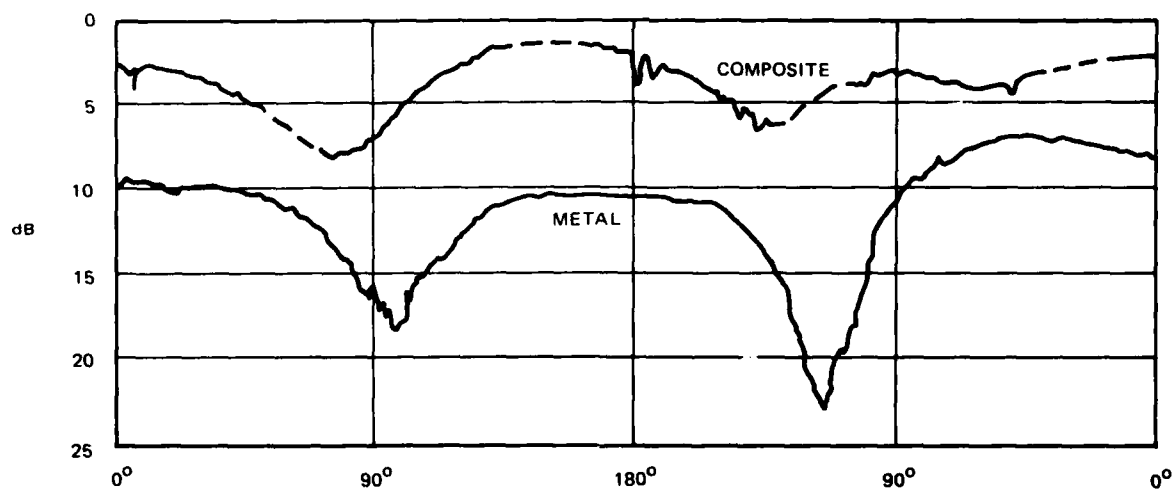


Figure 54. Antenna Pattern -- 60 MHz

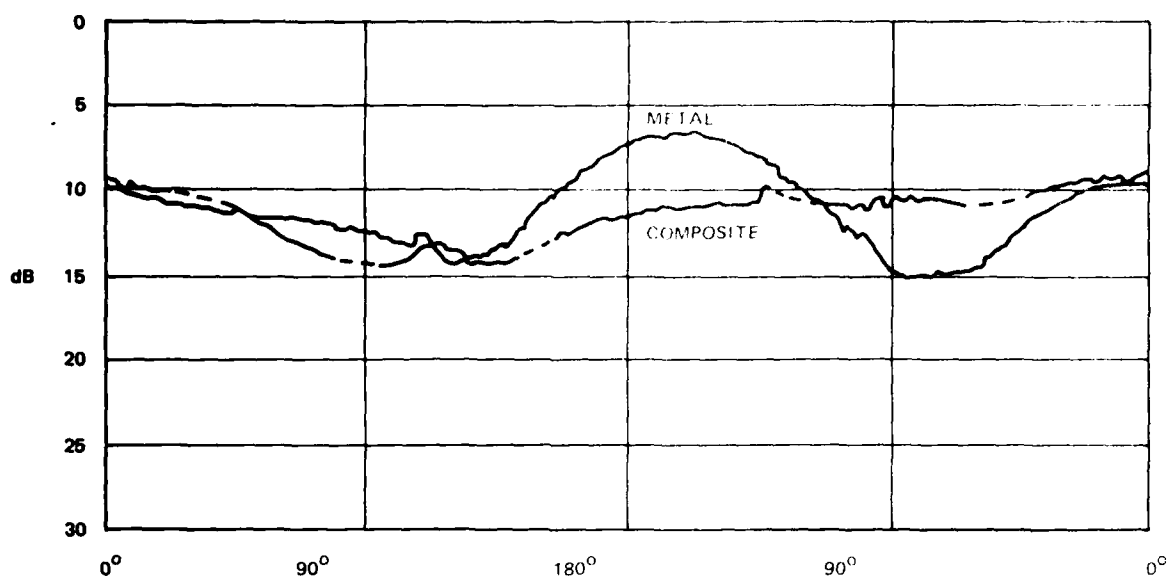


Figure 55. Antenna Pattern -- 70 MHz

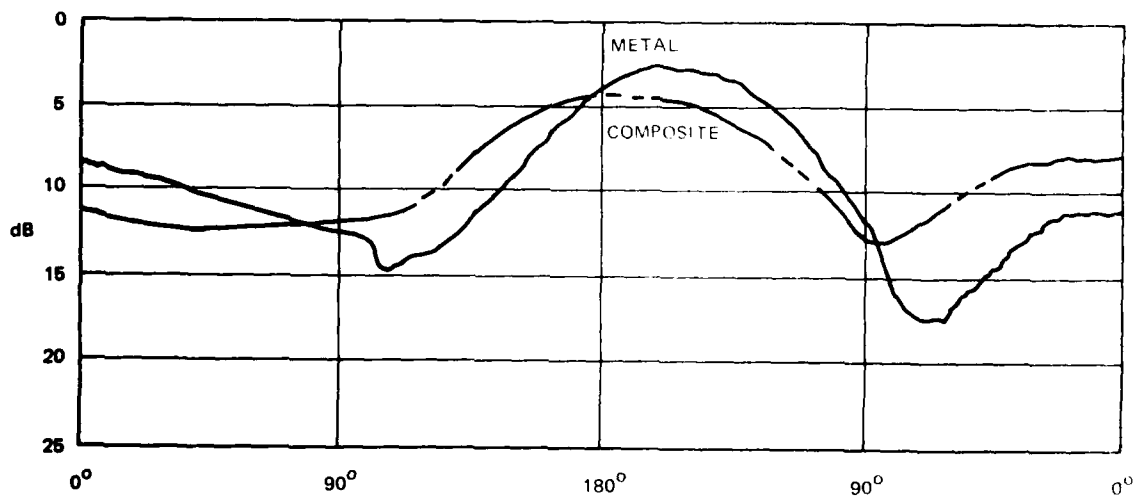


Figure 56. Antenna Pattern -- 70 MHz

MANUFACTURING TECHNOLOGY REFINEMENT

WET FILAMENT WINDING METHODOLOGY

The previous work that HHI and FSI had accomplished in the field of advanced composites primary structures was primarily in the field of the wet filament winding (WFW) cocure process. The CTS MM&T program was structured to continue the use of this process to the greatest extent possible, and refine it for the special requirements of the three CTS components.

The WFW process is summarized in Figure 57. This figure shows how bands of rovings are laid onto a rotating mandrel along geodesic paths until the entire surface of the mandrel is covered with a layer of filaments oriented in a \pm angle pattern. This process can lay filaments onto a mandrel at any angle between approximately ± 5 degrees and 90 degrees relative to the axis about which the mandrel rotates. Because the roving band follows a geodesic path to avoid slipping, the angular orientation is constant \pm angle from end to end on a cylindrical mandrel. But it is a variable from end to end if the mandrel is conical (small \pm angle at the large end to large \pm angle at the small end). Each end of the mandrel has a suitably shaped dome for securing the filaments and guiding them smoothly as they turn around to make the reverse pass along the mandrel. It has been demonstrated that the mandrel need not have a circular cross section - rectangular and triangular cross sections are readily wound.

The band of wet rovings is created by passing a number of dry filament rovings (approximately 16 in number) through a resin impregnator such as that shown in Figure 58. It meters resin into the filaments to achieve a fixed fiber volume ratio. All of the filaments may be alike, such as graphite, or they may alternate, for example graphite and Kevlar, to form a hybrid composite. A dispensing eye whose travel along the mandrel is geared to the rotation of the mandrel guides the band of wet filaments onto the mandrel at the desired angle.

The tailboom and the vertical tail spar of the CTS are approximately cylindrical in shape and so are prime candidates for filament winding. The stabilator skin is also appropriate for WFW since its stacking sequence is 90/ ± 45 /90 degrees (90 degrees being the chordwise direction) and can be wound on a cylindrical mandrel, cut off, and formed to shape over an airfoil-shaped mandrel. With the basic concept of WFW being well established, the primary manufacturing development work for the CTS was the refinement of the details of how to wind each component.

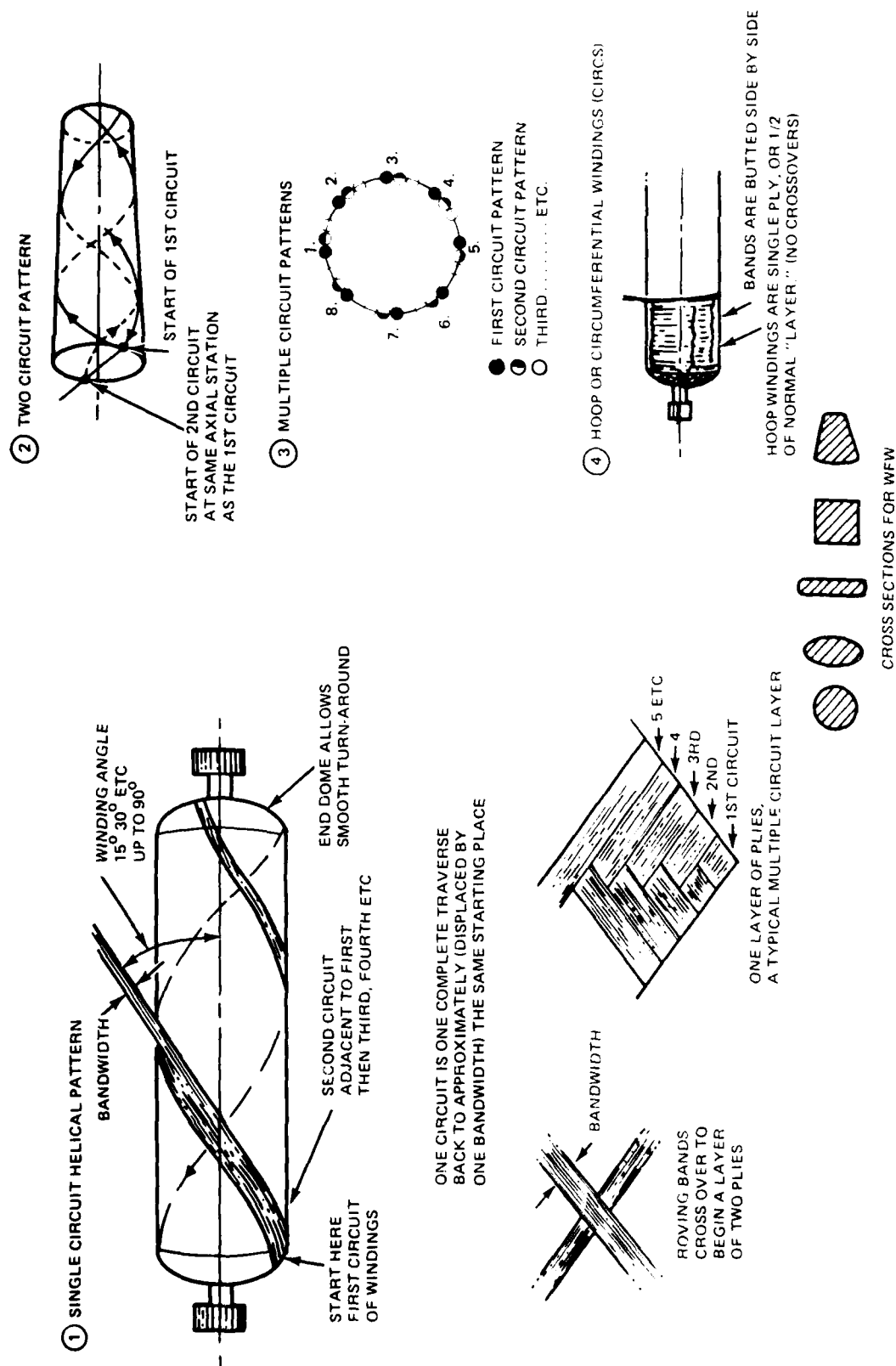


Figure 57. Tubular Element Filament Winding Process

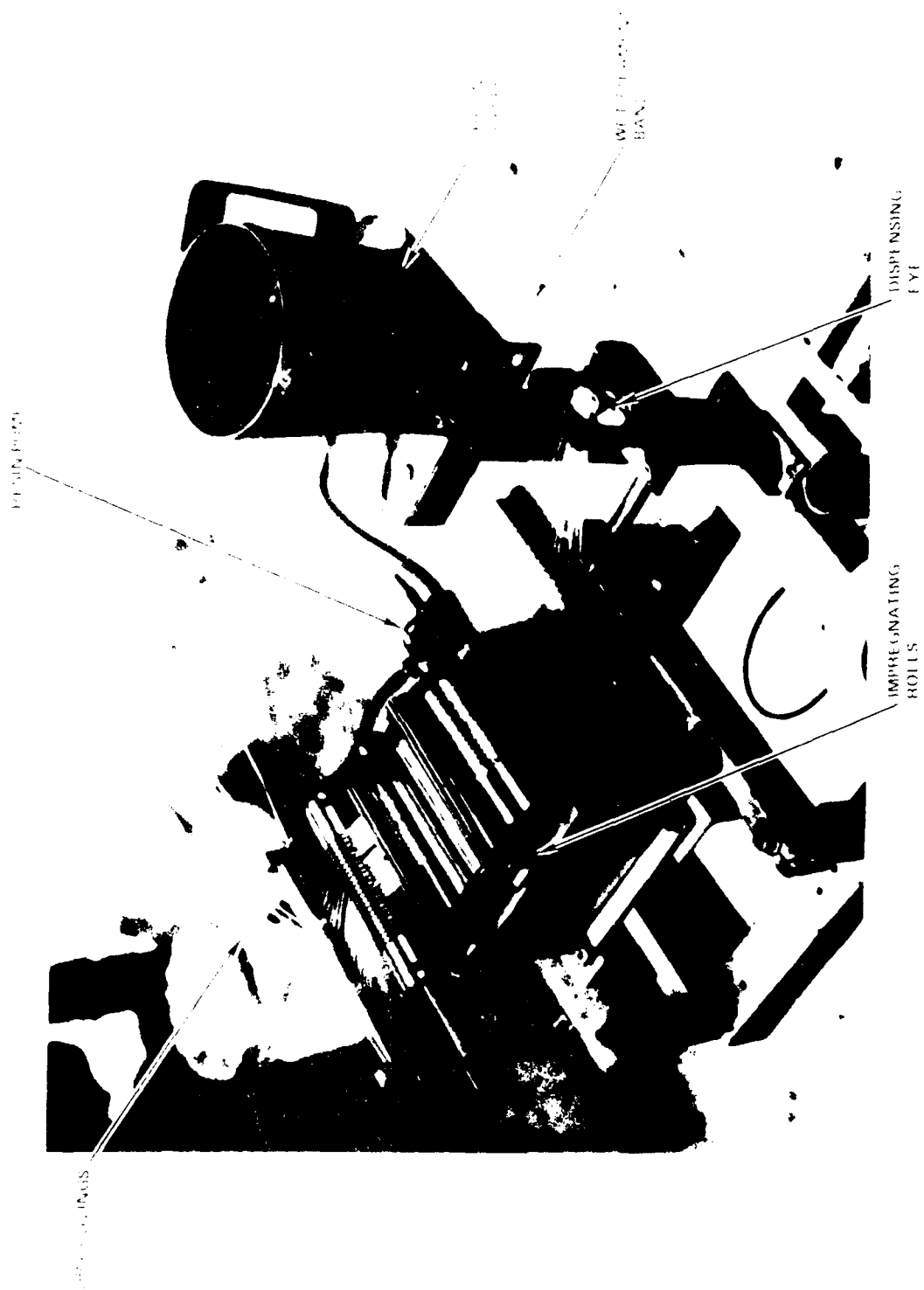


Figure 38. Resin Impregnator

AD-A121 172

MANUFACTURING METHODS AND TECHNOLOGY (MANTECH) PROGRAM
MANUFACTURING TECH.. (U) HUGHES HELICOPTERS INC CULVER
CITY CA J V ALEXANDER ET AL. OCT 81 HHI-81-367

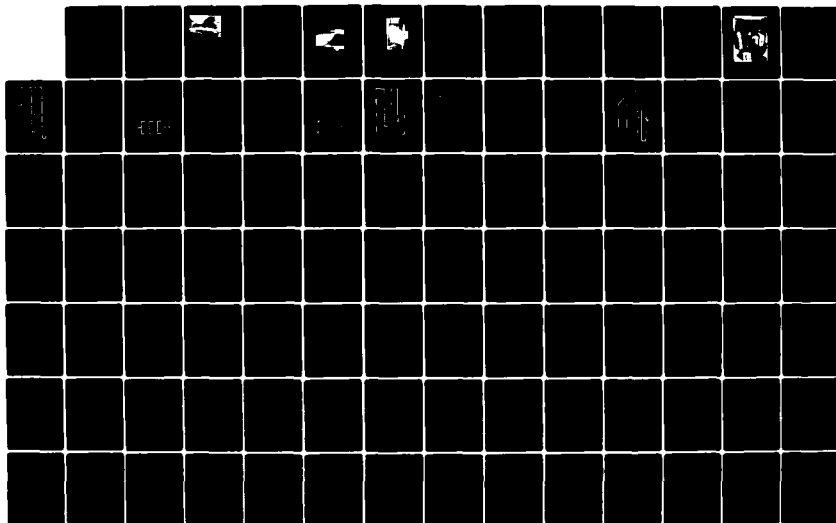
2/3

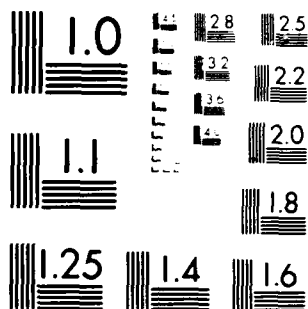
UNCLASSIFIED

USAAVRADCOM-TR-82-F-1 DAAKSO-78-G-0004

F/G 1/3

NL





MICROCOPY RESOLUTION TEST CHART
NATIONAL BUREAU OF STANDARDS-1963-A

TAILBOOM

The tailboom is a sandwich wall, hollow cone with the honeycomb filler deleted at both ends of the structure to make the walls a solid laminate in these regions. The configuration of the mandrel on which the tailboom would be wound is indicated in Figure 59. From Sta 370 to 450 the diameter tapers and the cross section varies smoothly from an essentially rectangular shape at the front to a circle at Sta 450. It is a circular cone between Stations 450 and 529, and then is cylindrical to the end of the tailboom. The shape of the end dome on the large end of the mandrel is critical for guiding the filament turnaround and also to guard against the ± 8 degree filaments bridging over the flat region on the top of the forward end of the tailboom. The mandrel's geometry was worked out on the full-scale toolproofing mandrel shown in Figure 60. (This was lightweight fiberglass mandrel adequate for the development work but not suitable for CTS fabrication.) Figure 61 shows the removable segment that aligned the four intercostals that lie in the aft end of the tailboom, and the end domes. The ring frames that are centered on Sta 532.33 are clamped between the right end of the mandrel shown in Figure 60 and the left end of the slotted mandrel shown in Figure 61. The three ring frames (Sta 387.00, 531.23, and 533.43) and the four intercostals are hand layups. They are made in metal female molds to provide accurate contours for matching the interior of the tailboom, using silicon blocks to supply the molding pressure. This technology was considered to be well enough understood that it was not necessary to undertake a special manufacturing development program.

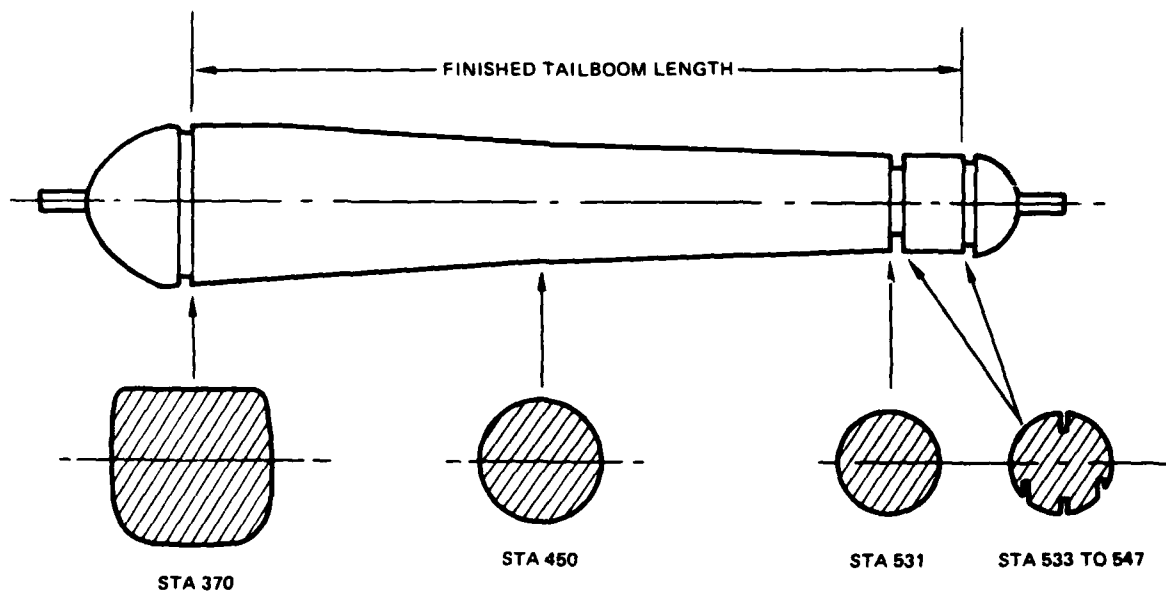


Figure 59. Tailboom Mandrel Geometry



Figure 60. Tailboom Mandrel - Main Section (Toolproofing)

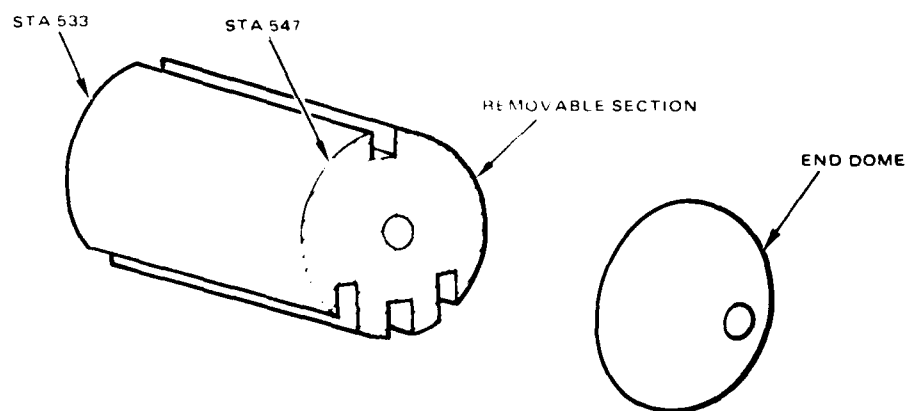


Figure 61. Tailboom Mandrel - Removable Sections (Toolproofing)

VERTICAL TAIL SPAR

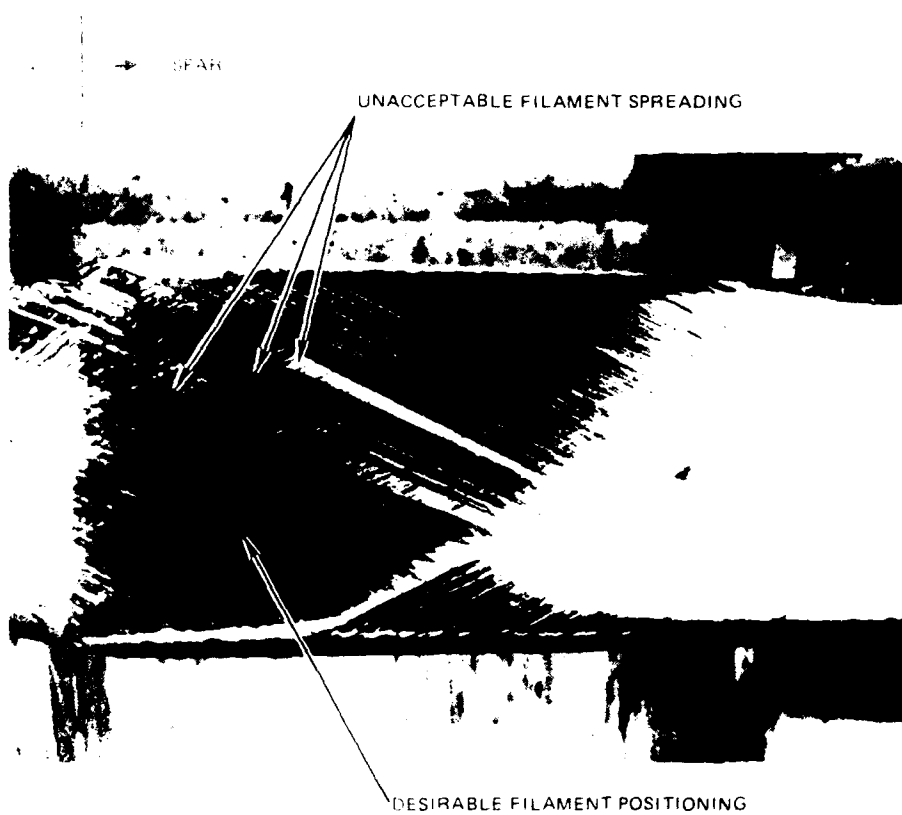
The structure of this spar is similar to that of the tailboom - solid laminate walls at the ends and sandwich wall in the center. The major difference is that its periphery is smaller, and its cross section is generally trapezoidal in shape. This spar, too, has frames for the tail rotor gearbox support wound into the spar.

A full-scale toolproofing mandrel was made of fiberglass and was used for determining the winding procedure (see Figure 60). The development work included determining the manner of holding the composite frames in place in the mandrel, developing the configuration of the end domes, and determining how to remove the mandrel from the cured spar box. Figure 62 shows the results of winding on an early, unsatisfactory end dome configuration. Note how the filaments are spread in an unacceptable manner.

The frames that go into the vertical tail spar were proposed to be made in female metal molds with silicone blocks for pressurization. This technology was considered to be well enough understood that toolproofing studies were not needed.

STABILATOR

An early stabilator configuration had two spars, four ribs, and a bead-stiffened skin. A tooling development study was made of the skin which is shown in Figure 63. HHI had previous experience with a beaded skin for a composite stabilator for the OH-58A in which a flat, wet skin was worked onto an airfoil-shaped mandrel that had ridges to form the beads. While this was successful for the small size of the OH-58A, it was determined to be inappropriate for the AH-64A stabilator because of the size, and because of the filament distortion that was caused by forcing the flat skin to form around the deep beads. A second step, which is shown in Figure 63, consisted of forming beads separately and cocuring them to the skin that was draped over a single curvature mold. Based on the toolproof skin, this too appeared impractical from an overall skin stability standpoint and the design concept was changed to the spar/rib/skin structure described in the Design Refinement section. The technology for forming the spars and ribs in female metal molds with silicone blocks for pressure was considered well enough known not to need special development.



Vertical Tail Spar Winding Pattern Study

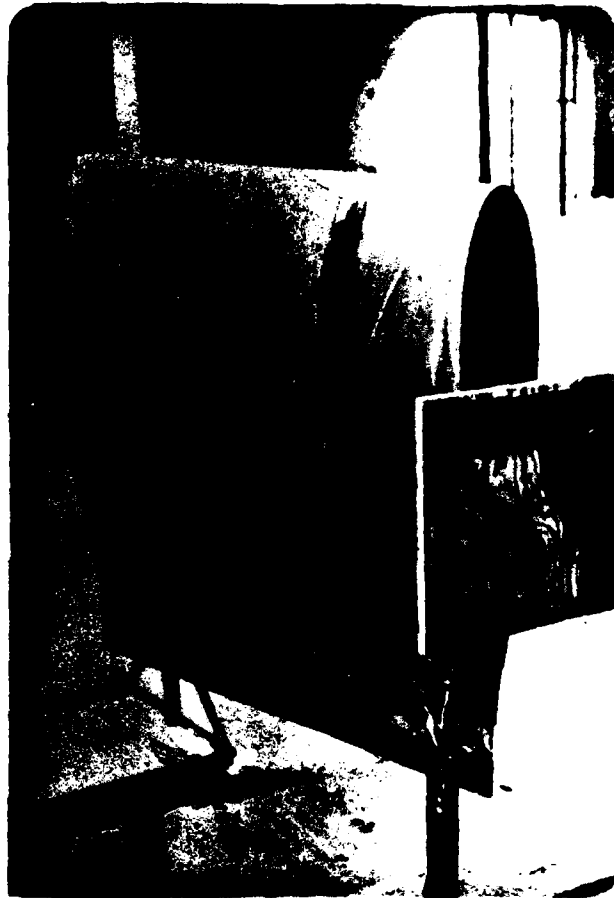


Figure 63. Bead-Stiffening Study for Stabilator Skin

RESIN CURE CYCLE

HHI and FSI recommended that Applied Plastics Corporation resins and hardeners be used as the epoxy matrix for the structure:

- 2434 - epoxy resin
- 2347 - 300°F cure hardener
- 2340 - room temperature cure hardener

The 300°F cure hardener, 2347, would be used for all filament winding of major structural elements. The 2340 hardener would be used for small, noncritical parts. The 2347 hardener is formulated to have a 24-hour pot life at room temperature. This time can be extended to 72 hours if stored at temperatures below 40°F, and to two weeks if stored at 0°F.

The cure cycle for the APCO resins has been determined through evaluation tests to be as shown in Figure 64. The Phase I cure is analogous to "B-staging" in conventional preregs. This cycle rigidizes a component by partially cross-linking the resin so that the component is rigid enough to be handled, mounted in winding mandrels so wet filaments may be wound over it, or positioned in assembly fixture for final assembly by cocuring.

The "final assembly by cocuring" cycle that goes to 300°F raises the glass transition temperature above the range of normal operating temperatures for strength at elevated temperatures, and produces a structure that is free of micro-cracking.

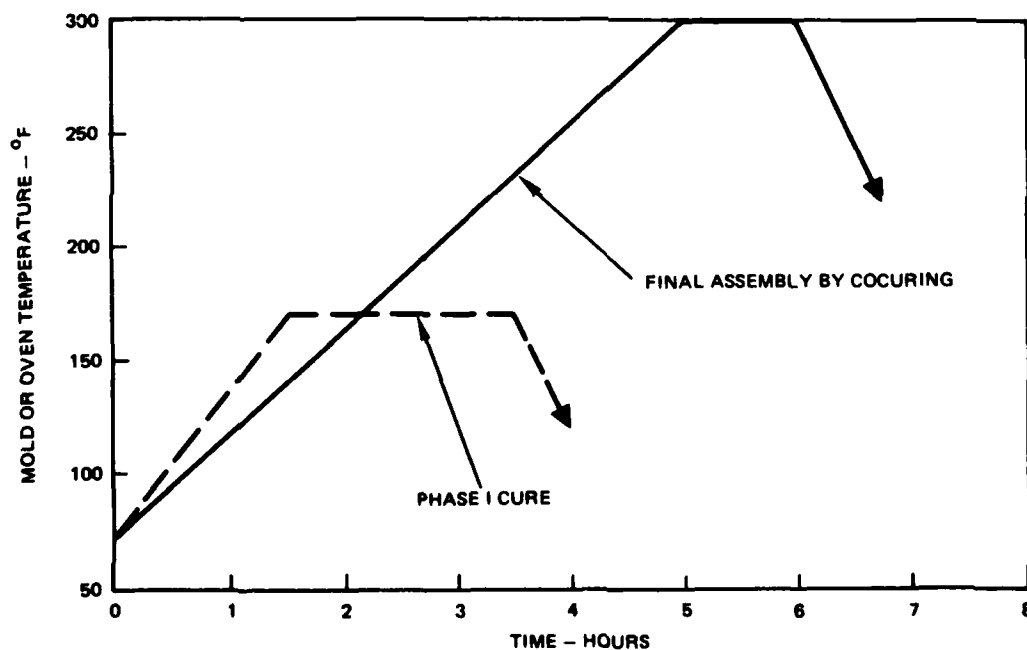


Figure 64. Resin Cure Cycle

FABRICATION REFINEMENT

At the time that the program was terminated, no production tooling had been built. The concept and approximately 60 percent of the drawings for it had been completed. The three components of the CTS were to be built on aluminum tooling to fulfill the requirement that the tools be satisfactory for fabricating a minimum of 50 shipsets of the CTS. The jig for assembling and aligning the three CTS components as an assembly was to use the tailboom winding mandrel as the base, with jigs and fixtures added to support the various components for bonding or bolting them together.

TAILBOOM TOOLING

The proposed tailboom mandrel is shown schematically in Figure 65. It consists of five major parts, plus two clamps to lock it together. The main section is generally conical in shape and has a shaft extending out of each end. It is shaped to the inside contour of the tailboom from Sta 370 to 429 and is an aluminum monocoque structure stiffened with bulkheads and longerons. The shafts are supported by the two bulkheads nearest to each end. The shafts and the bulkheads are perforated so that hot air may be circulated inside the mandrel while the resin cures in the oven.

The large end turn-around dome slips over the shaft of the main mandrel and is pinned to it so they will turn together. A wedge-type clamp anchors the dome to the shaft. The dome is contoured to guide the filaments smoothly as they leave and reapproach the mandrel, and to prevent bridging of the filaments across the flat spot on the mandrel. The dome has a channel all around it where it touches the main mandrel to serve as a cutoff guide for trimming the cured tailboom. This channel is to be filled with plastic foam during the winding process to present a smooth winding surface.

The cylindrical segment adjacent to the small end of the main mandrel slips over the shaft, is pinned to the main mandrel, is held against the main mandrel by the small end dome, and is locked to the shaft by a wedge lock at the outboard end of the end dome. This cylindrical mandrel is spaced away from the end of the main mandrel far enough to enclose the two graphite/epoxy frames that are bonded together as an assembly with aluminum tooling blocks between, and are centered at Sta 532.33. The tooling for this assembly is indicated in Figure 66. The cylindrical section of the mandrel has four lengthwise channels formed into its surface to accept the four graphite/epoxy intercostals that lie in the aft end of the tail boom. The end dome has a channel around its periphery where it touches the cylindrical mandrel to serve as a cutoff guide. This channel is filled with foam to provide a fair surface for winding.

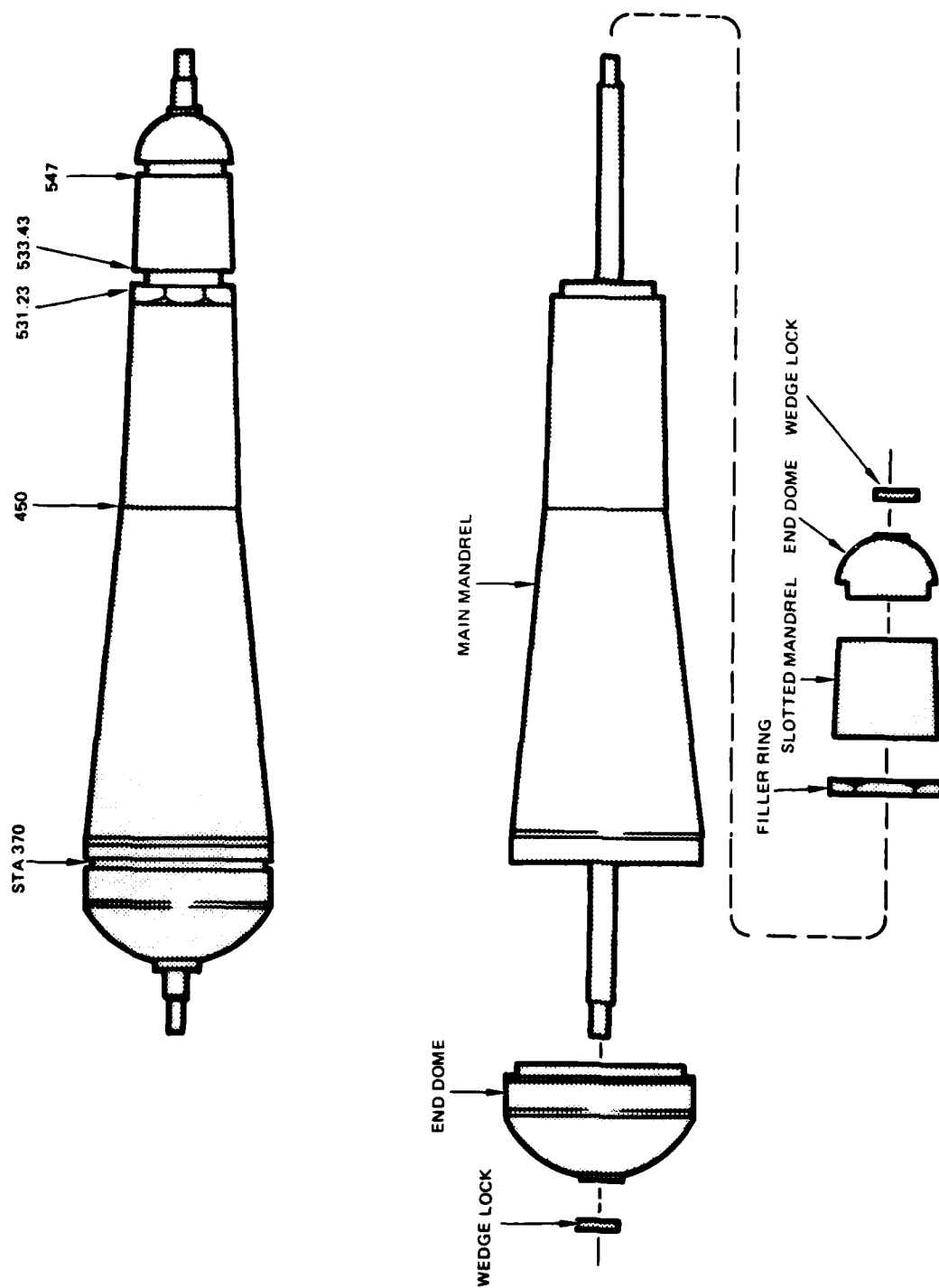


Figure 65. Tailboom Mandrel

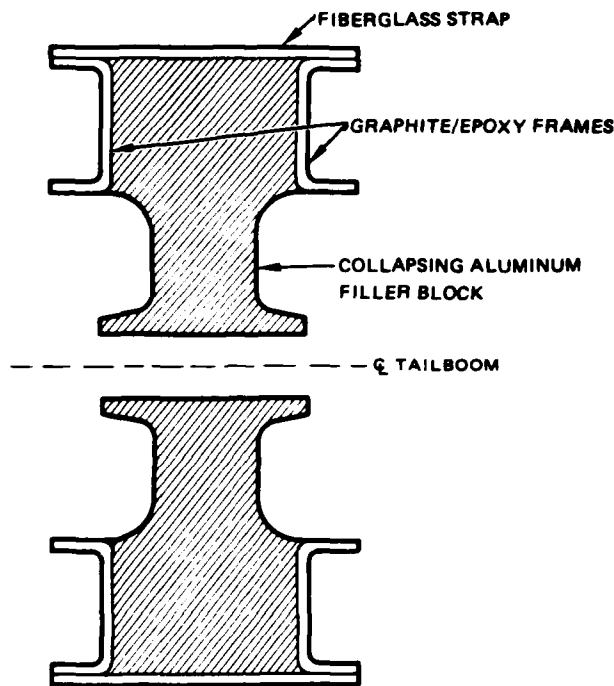


Figure 66. Frame Assembly Fixture Schematic

The filler ring indicated in Figure 65 is a removable, tapered aluminum ring that fits closely onto the main mandrel and is shaped to the tapered aft end of the honeycomb filler. This ring must be able to slip off of the aluminum mandrel so that the cured tailboom will not be mechanically locked to the mandrel.

The graphite/epoxy frames at Sta 387.66, 531.23, and 533.43 and the four graphite/epoxy intercostals are formed in matched metal dies using trapped silicone rubber to furnish the molding pressure during the cure cycle. Figure 67 is a schematic cross section of such a mold. The design shows the Sta 533.43 frame and the intercostals attached to each other by HyLoc fasteners. This subassembly is located in the mandrel as the mandrel is being assembled.

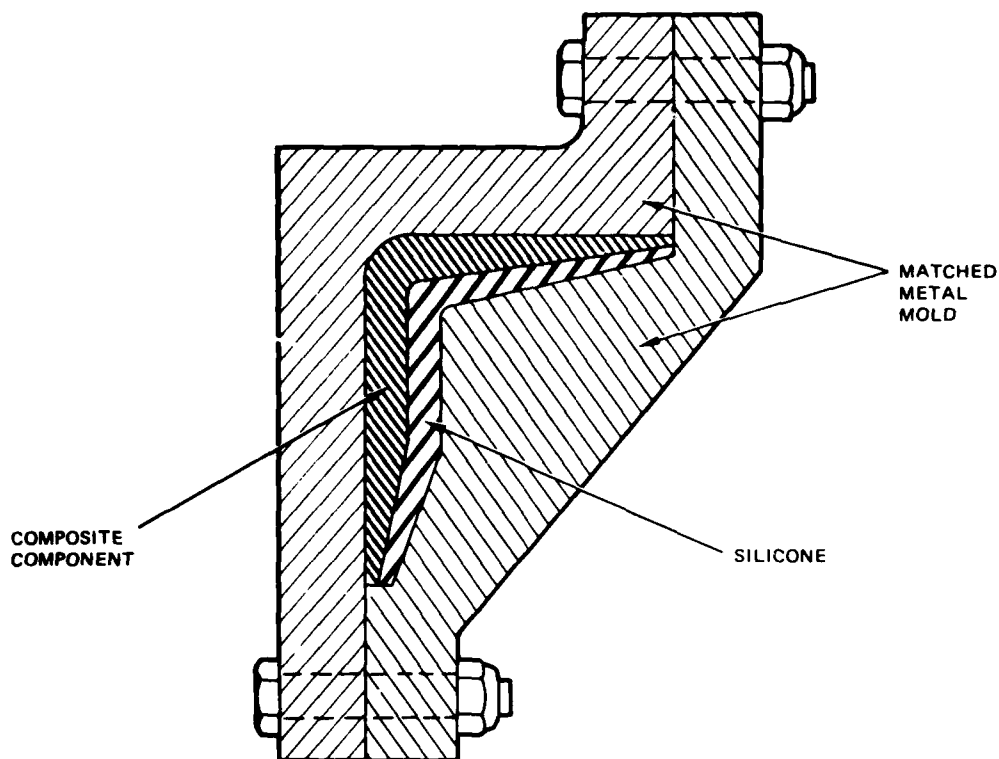


Figure 67. Frame Mold Section Schematic

Flat-pattern metal templates are provided for cutting out the honeycomb filler for the sandwich portion of the tailboom, and for the individual sheets of prepreg material that are laid up to form the ring frames, intercostals, and tailboom skin reinforcements. Metal jigs that key to the mandrel serve to locate the reinforcements.

A conventional router is set up to bevel the ends of the honeycomb panels.

A wet filament winding machine similar to the one shown in Figure 68 is used to wet filament wind the tailboom. This machine takes dry composite rovings, impregnates them with a metered amount of resin, and winds them onto the mandrel at the spiral angles required by the design.

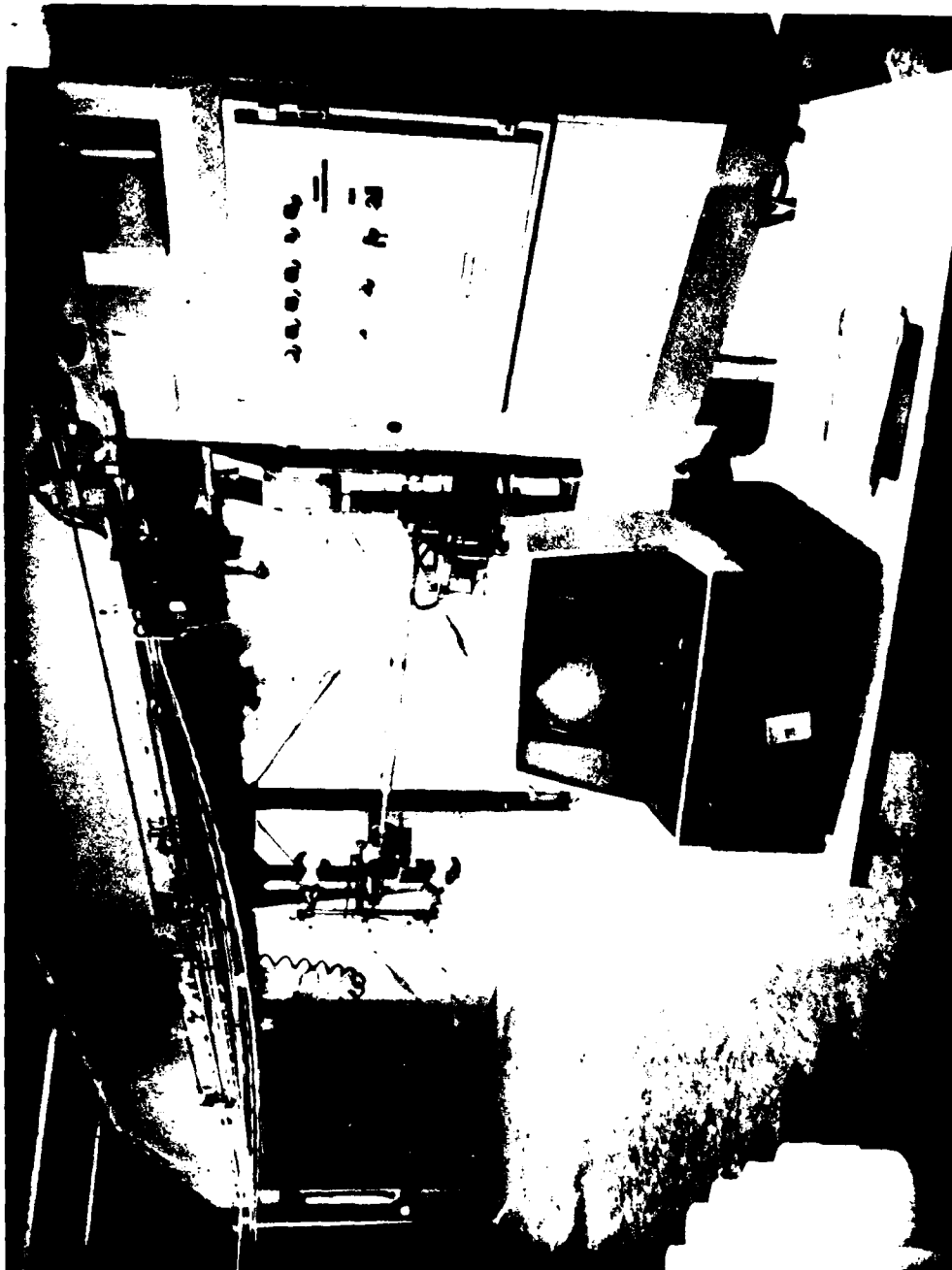


Figure 68. Helical Winding Machine

Aluminum male molds (Figure 69) are used to lay up prepreg material to form the angles that attach the tail rotor driveshaft cover.

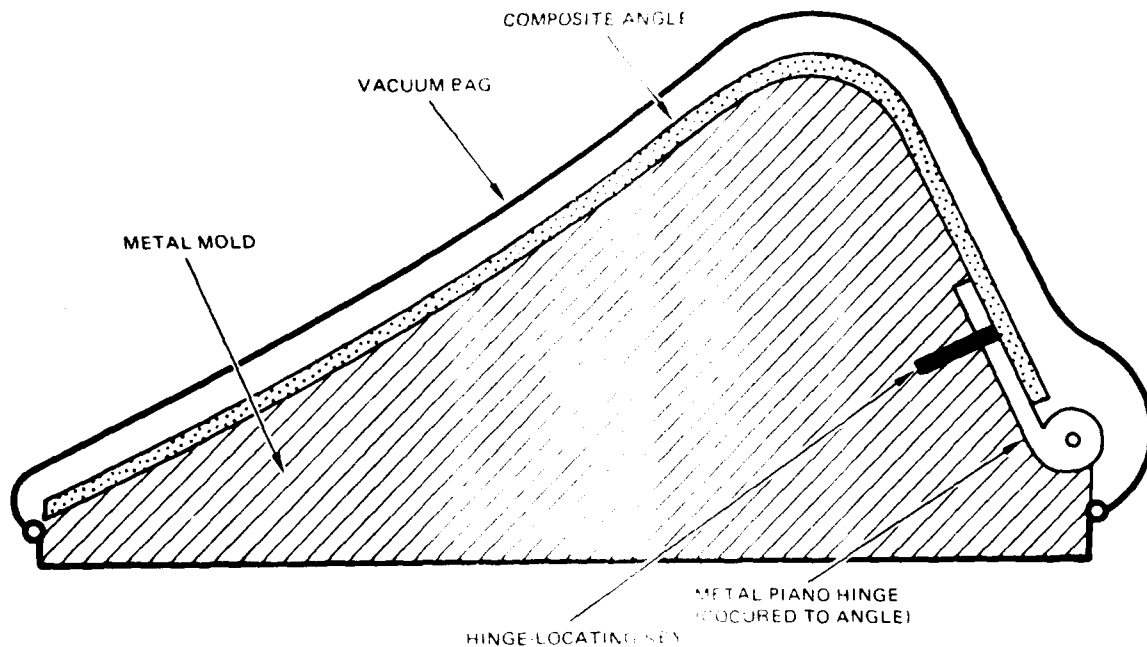


Figure 69. Angle Mold Schematic

The proposed sequence for fabricating the composite components of the tailboom is laid out in Figure 70. It begins with the fabrication of premolded frames, goes through filament winding, curing, and subassembly of miscellaneous parts. From this operation it goes on to final assembly that is described below.

VERTICAL TAIL TOOLING

The mandrel for the hollow box structure of the vertical tail spar is the same in concept as that for the tailboom, except that it has a trapezoidal cross section. See Figure 71. The main part of the mold is an aluminum monocoque box with a shaft extending from each end. This mandrel is formed to the inside contour of the spar box. An end dome that is shaped to

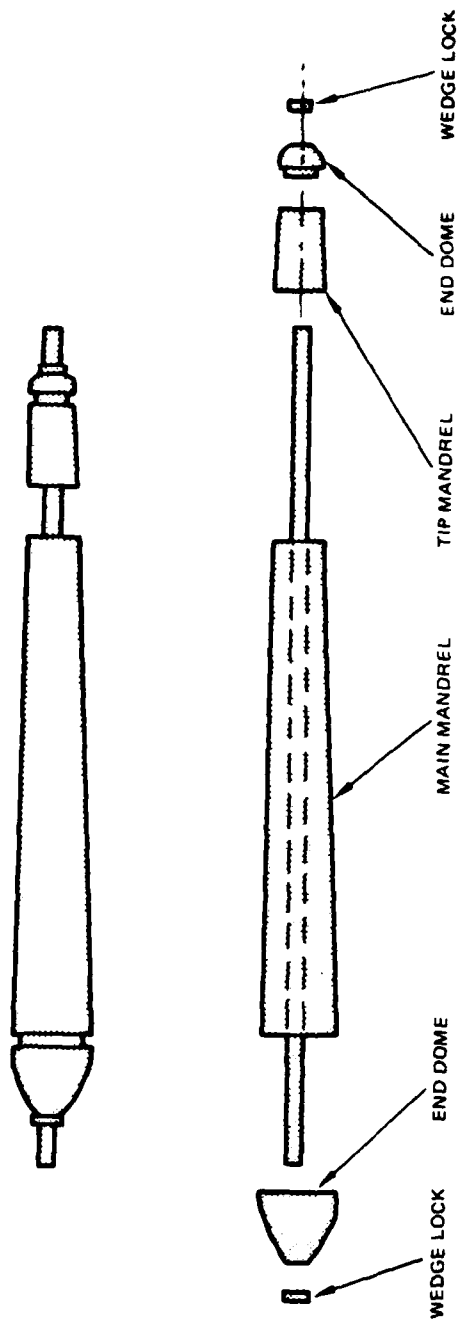


Figure 71. Vertical Tail Spar Mandrel

perform the filament turnaround function and guide the filaments off of and onto the four-sided mandrel slips over the extension shaft at the big end of the mandrel. It is pinned to it to force them to rotate together and is secured by a wedge-type clamp. The tip end portion of the mandrel slides over the main mandrel's extension shaft and is pinned to it. A suitable end dome is mounted beyond this portion of the mandrel and is attached by another clamp. The tip-end portion of the mandrel is spaced away from the upper end of the main mandrel to allow insertion of the upper frame sub-assembly so that it may be wet filament wound into the vertical tail spar. Provisions are made for keying this subassembly to the mandrel.

The five composite frames (three upper frames to support the tail rotor gearbox and two lower frames to support the intermediate gearbox) are formed in matched metal molds with trapped silicone rubber furnishing the molding pressure.

The three frames that support the tail rotor gearbox are formed into an assembly that goes into the spar box mandrel. A three part wash-out mold locates the three frames while a prepreg shell is wrapped around them and cured. See Figure 72.

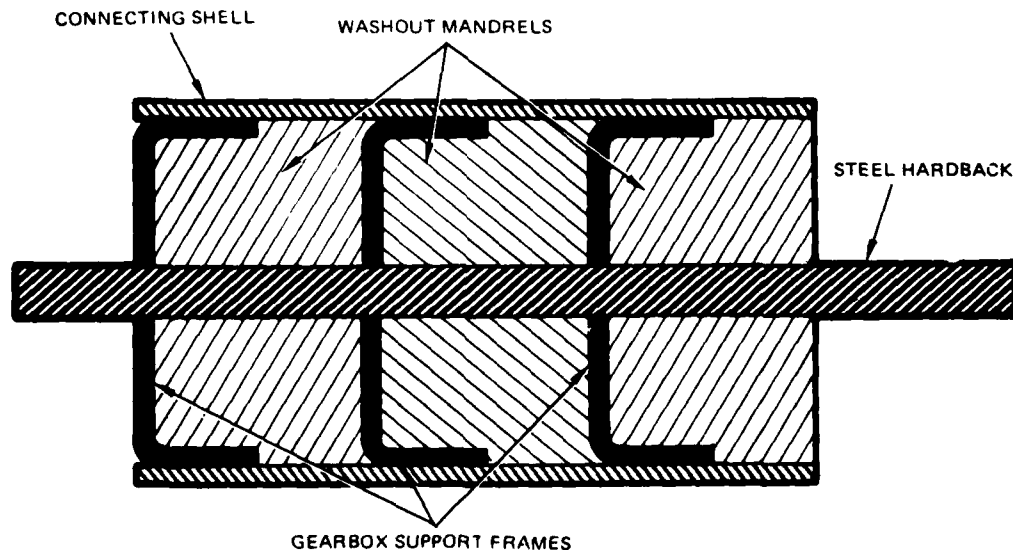


Figure 72. Frame Subassembly Tool Schematic

Flat pattern metal templates are used to cut out the honeycomb filler for the spar box, and for the laminates that make up the frames, doublers, and fairings.

A routing fixture is clamped to the spar box and the top and bottom ends of the box are cut to shape. A support fixture holds the spar box and provides jig points for positioning the two lower bulkheads, and the four aluminum lower attachment fittings. These are held in place while HyLoc fasteners secure the components. A conventional milling machine faces off the attachment lugs and precisely bores holes in them for the vertical tail attachment bolts.

A female metal mold is used to form the vertical tail's tip cap, and contains appropriate keys for locating the navigation lights, radar warning antennas, and lightning protection strip. It is shown schematically in Figure 73.

The trailing edge fairing is a purchased part that contains communications antennas and is furnished by the antenna subcontractor. The leading edge fairing is taken unchanged from the prototype vertical tail.

A closed cavity metal mold with silicone rubber pressurizing blocks is used for forming each of the T-bars that are placed at the corners of the spar box for attaching the leading and trailing edge fairings. Figure 74 is a schematic cross section of such a mold.

The T-bars are bonded to the four corners of the vertical tail spar in a bonding jig similar to that shown in Figure 75. Trapped silicone rubber is used to supply the bonding pressure.

Figure 76 shows the proposed sequence for fabricating the vertical tail spar by the wet filament winding process. This spar assembly goes into the CTS final assembly process as described below.

STABILATOR TOOLING

The stabilator skin is wet filament wound on a cylindrical aluminum mandrel (Figure 77), cut off, and cured on an aluminum male mold shaped to the airfoil contour as Figure 78 indicates.

The spars and ribs are laid up in matched metal molds with silicone rubber pressurization in a manner similar to that described for the tailboom frames in Figure 67.

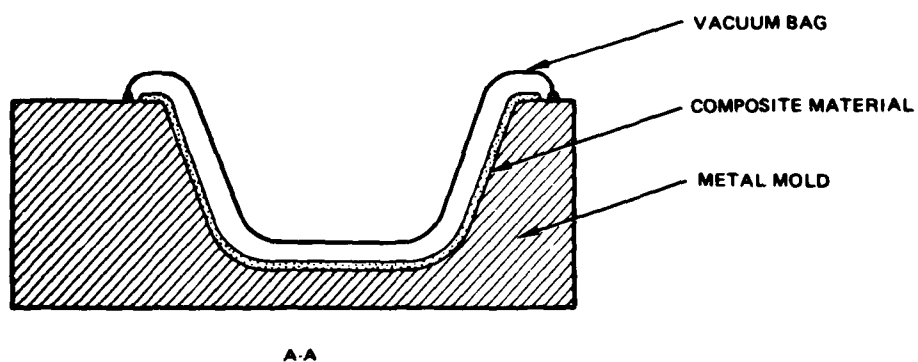
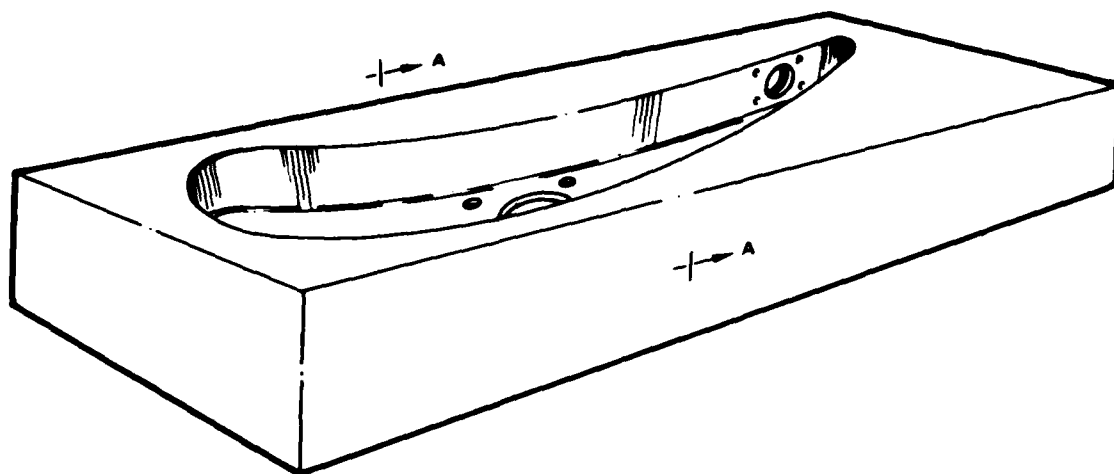


Figure 73. Tip Cap Mold Schematic

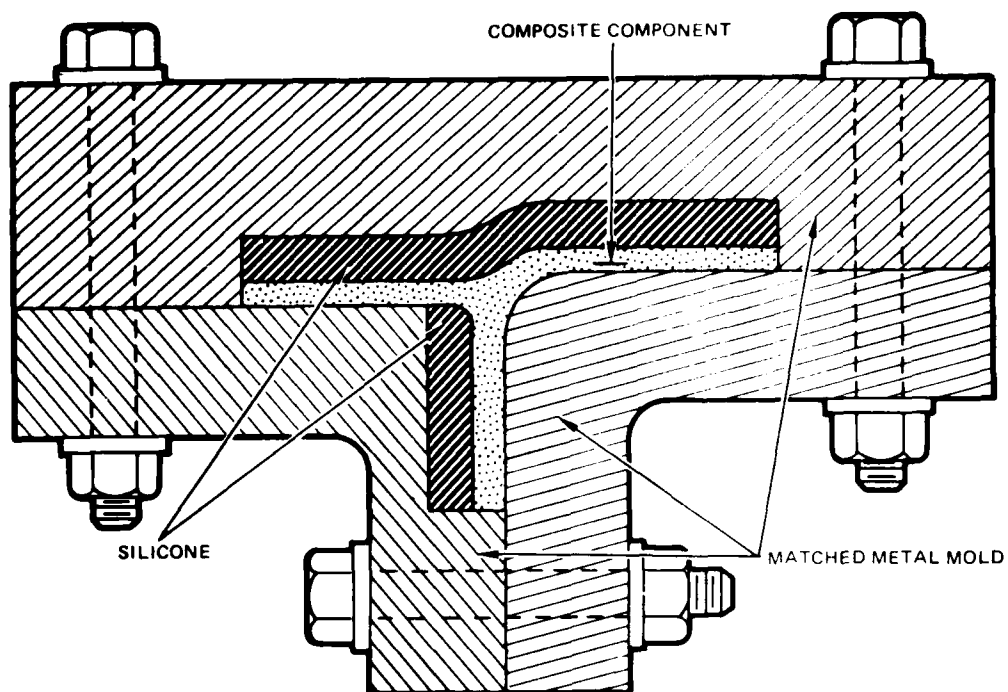


Figure 74. T-Bar Mold Section Schematic

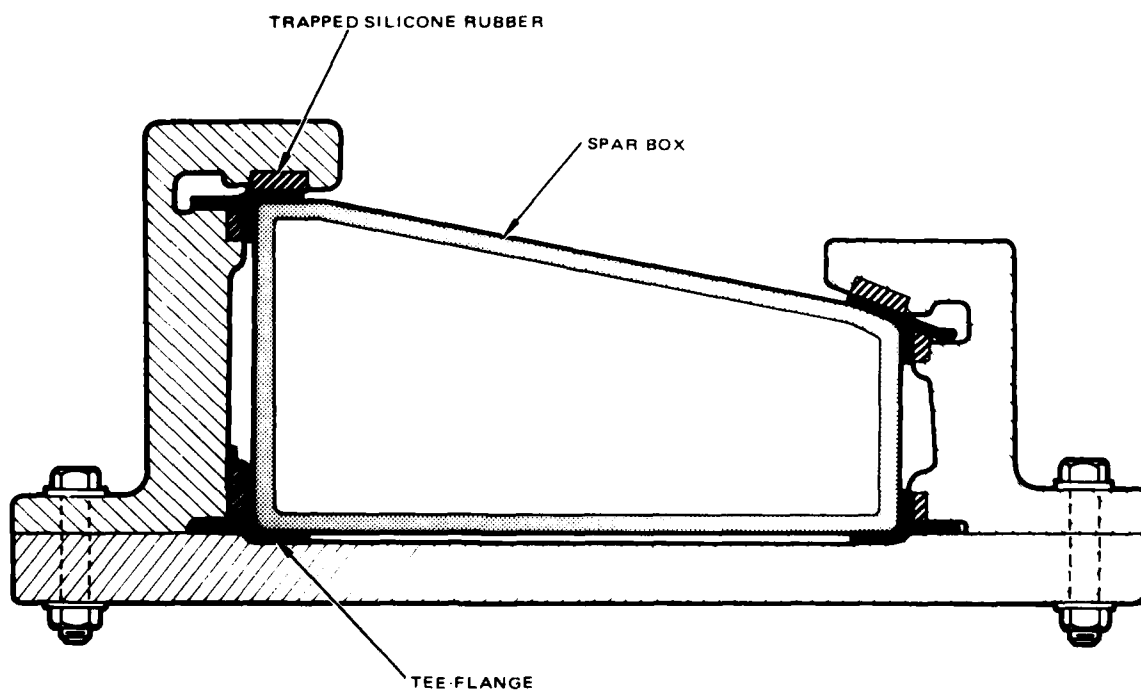
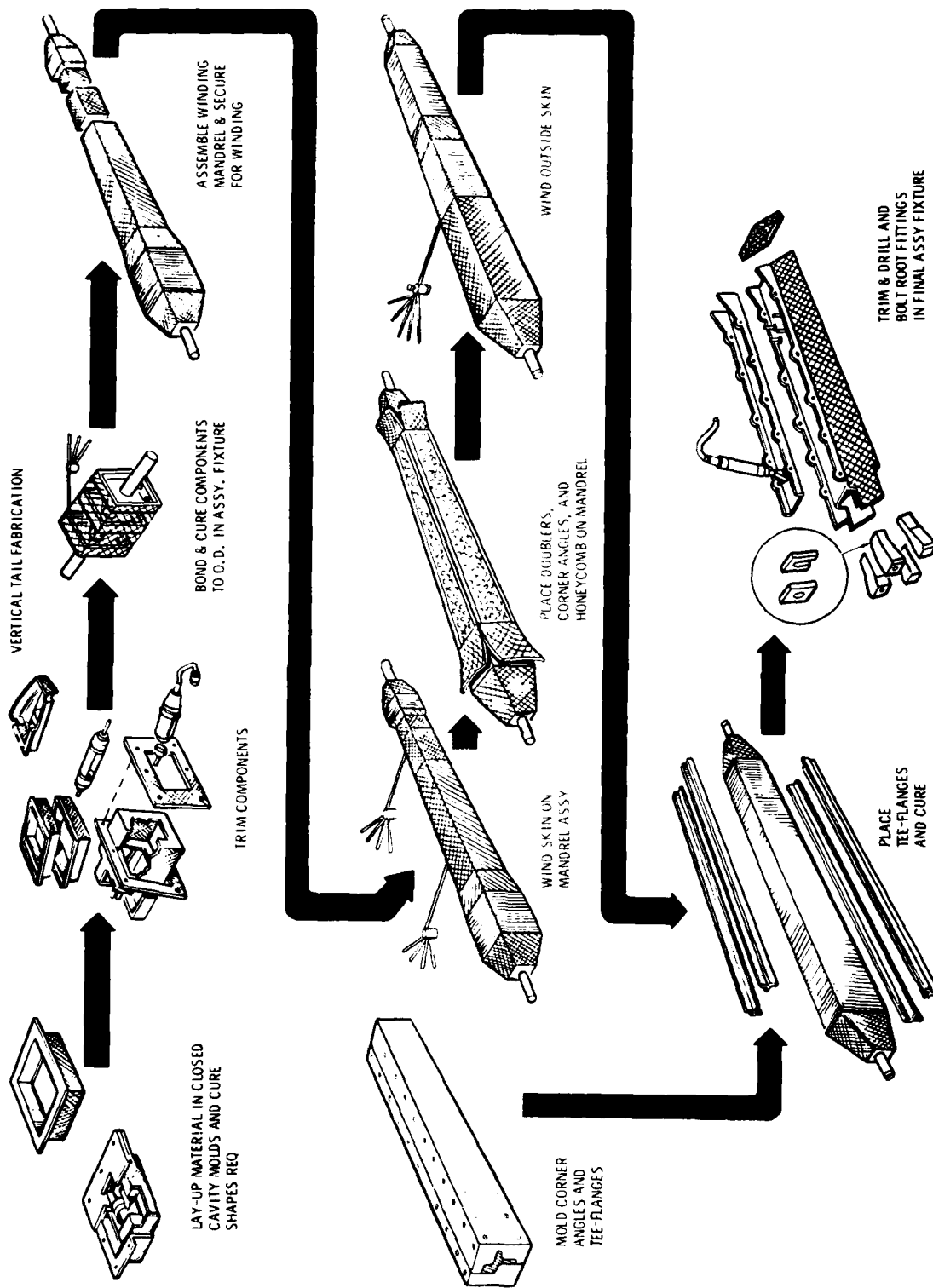


Figure 75. T-Bar Bonding Jig Schematic



010426-175

Figure 7b. Vertical Tail Fabrication Sequence

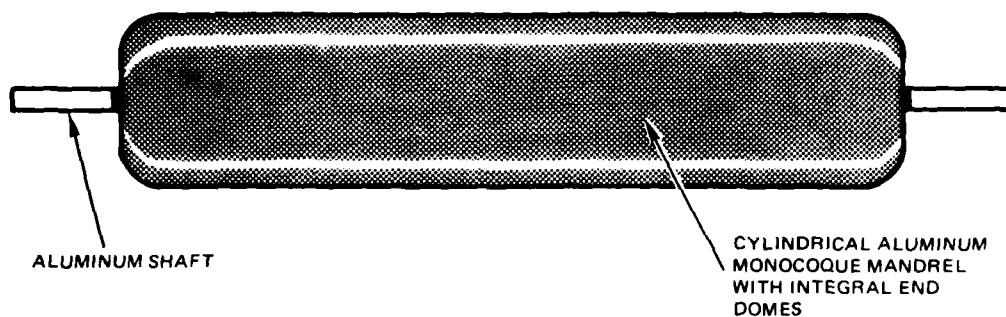


Figure 77. Stabilator Skin Winding Mandrel Schematic

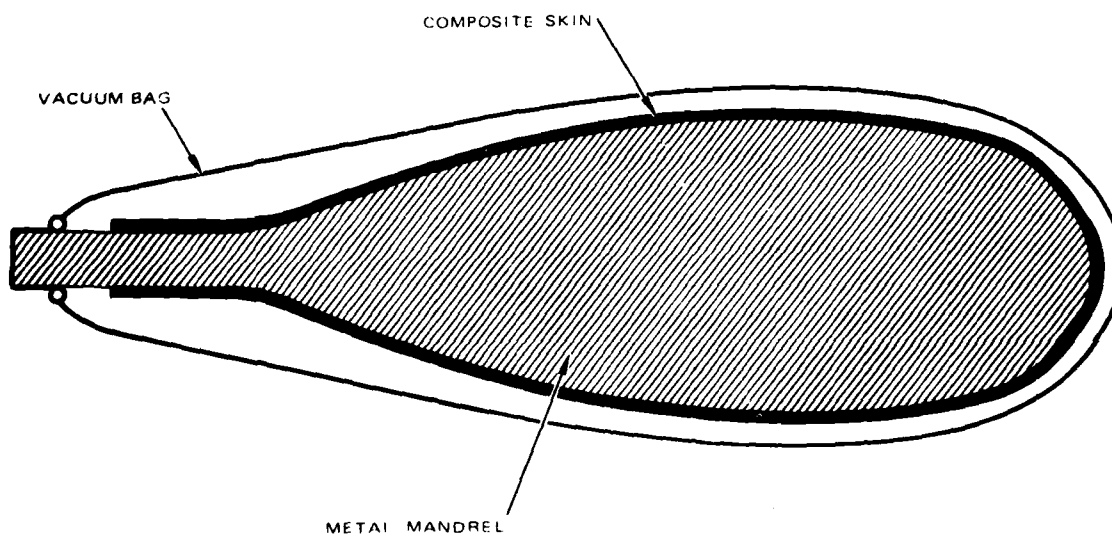


Figure 78. Stabilator Skin Mold Schematic

The tip caps are laid up on metal male mold as shown in Figure 79.

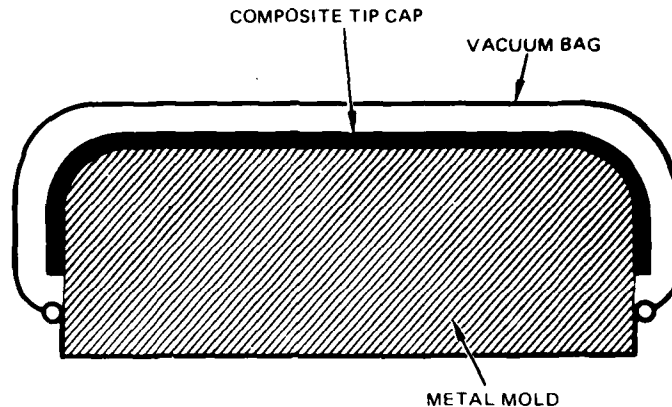


Figure 79. Tip Cap Mold Schematic

The stabilator's interior structure is assembled in a fixture that locates the spars, ribs, and tip caps. It includes clamping devices to apply bonding pressure where the ribs and tip caps bear against the spar. The stabilator final assembly jig (Figure 80) is basically a grid structure that locates the skin segments over the internal structure of the stabilator and has an array of elastomeric pads that provide the bonding pressure. They press the skin against the spars and ribs, and the upper and lower skins together at the trailing edge. A single blind rivet at the nose of each rib aligns the skin and ribs positively. This jig also has provisions for aligning the stabilator hinge fittings with respect to the stabilator, so that they may be attached with mechanical fasteners.

The process shown in Figure 81 is the proposed fabrication sequence for the stabilator. Final assembly into the CTS is described below.

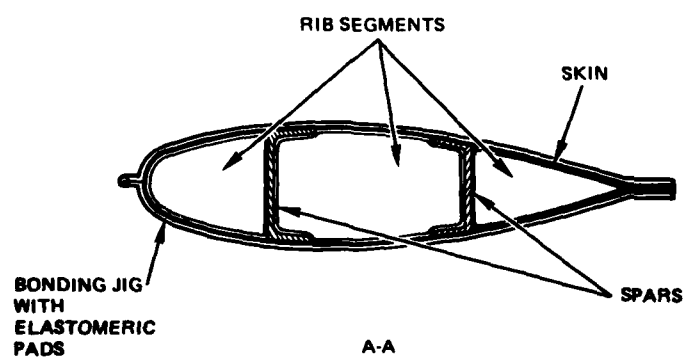
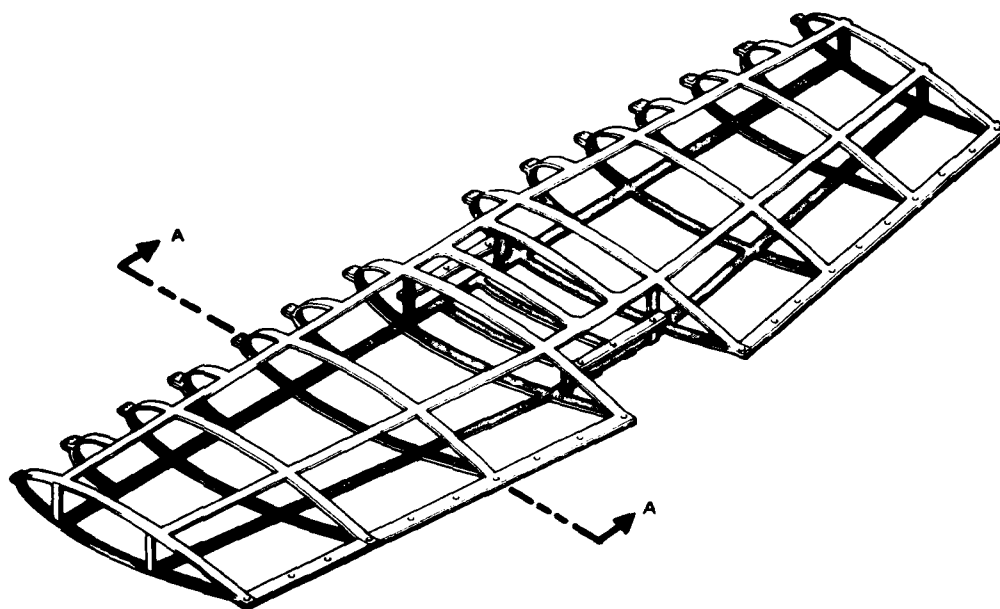


Figure 80. Stabilator Skin Bonding Jig Schematic

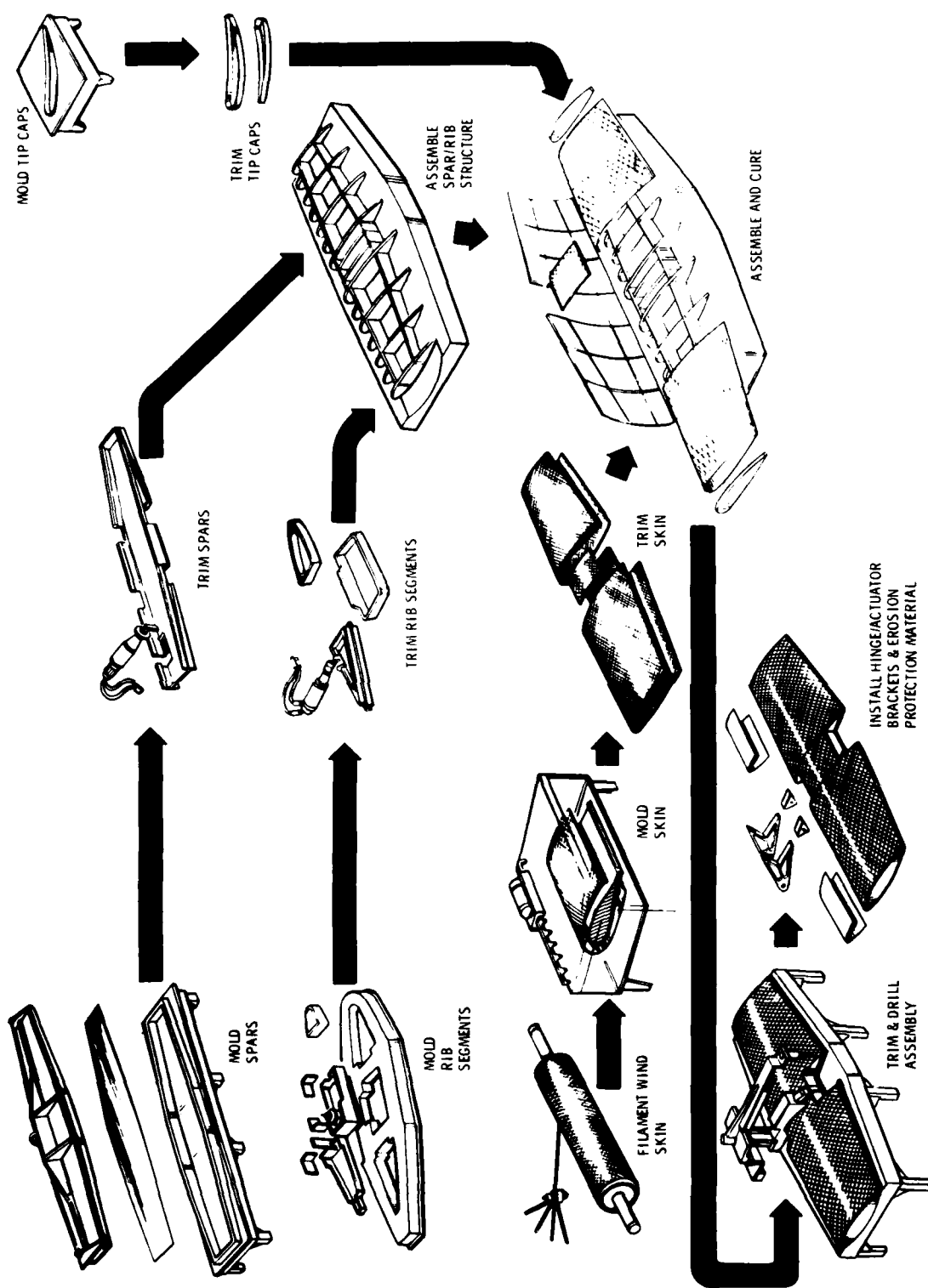


FIGURE 81

Figure 81. Stabilator Fabrication Sequence

FINAL ASSEMBLY

Final assembly of the CTS is accomplished in the fixture that is shown schematically in Figure 82. Its first purpose is to locate the aluminum rear bulkhead in the tailboom and hold it while it is bolted in place. Next it serves as a jig for drilling the four bolt holes that attach the vertical tail, for milling off the top of the vertical tail attach bosses, and for locating the jacking/tiedown fitting. It has drill jig plates for locating the tail rotor driveshaft bearing and anti-flail supports and for mounting the steps and flare dispenser. It holds the vertical tail in alignment while the gearboxes and controls are installed. It positions the stabilator while its actuators are adjusted.

When the CTS assembly is taken out of this fixture, it is ready to be mounted on the AH-64A airframe. An alignment jig is needed for attaching the CTS to the metal fuselage at Sta 370; a jig that is not a part of the MM&T program tooling but is to be provided by the AH-64A project organization under AVRADCOM Contract DAAJ01-77-C-0064, Modification P00108.

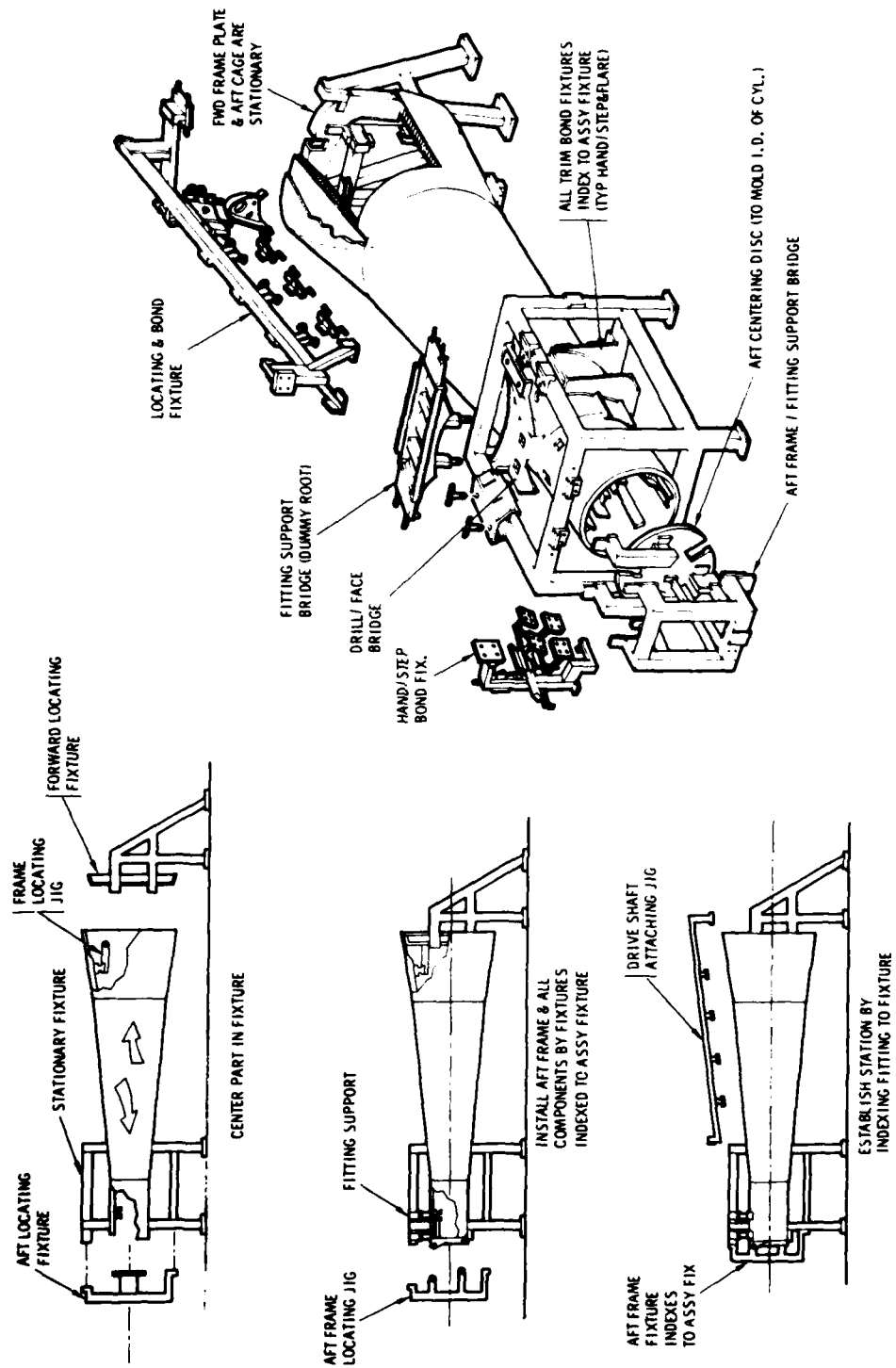


Figure 82. Final Assembly Fixture Functions

NON-DESTRUCTIVE EVALUATION (NDE)

NDE is planned to ensure that all CTS components meet the design criteria, that they are free of internal defects, and that they have the proper internal geometry. Reports of all NDE activities are maintained by component serial number for permanent record.

Types of defects that could degrade the components' performance are:

- Delaminations
- Unbonded areas
- Porosity or voids
- Resin rich or resin starved areas
- Geometry of internal spars
- Thick bond lines
- Foreign objects
- Defects in metal attach fittings

The importance of these defects varies with their location and size in components. Tentative criteria for various areas and sections of the CTS components are given below.

Figure 83 indicates critical zones A, B, and C of the tailboom. Allowable limits for disbonds and delaminations that may occur in the ring stiffener, sandwich wall of the shell mainframe, frames, intercostals, and fairing hinge supports are detailed in Table 11. NDE techniques scheduled for use on tailboom hardware are listed in Table 12.

Figure 84 delineates critical zones A and B of the vertical tail. Table 13 lists the limits for disbonds and delaminations allowed in the preassembly structure and in the completed item. Table 14 is a matrix of NDE techniques scheduled for vertical tail components.

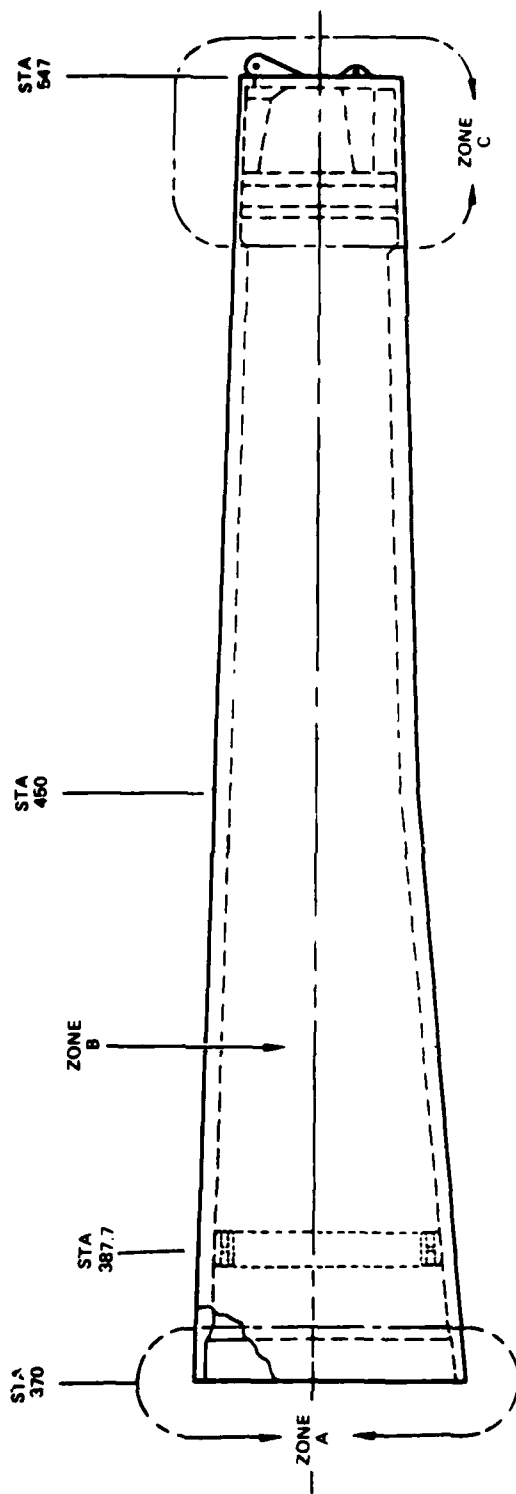


Figure 83. Composite Tailboom Inspection Zones

TABLE 11. TAILBOOM CRITICAL DISBOND AND
DELAMINATION LIMITS

Zone A	
1. Solid Laminate:	<p>No single delamination to be larger than 0.5 inch in diameter.</p> <p>No delaminated areas to be within 3.0 inches of each other.</p> <p>No more than 10 percent delamination allowed.</p>
2. Sandwich Wall:	<p>No single delamination or disbond to be larger than 1.0 inch in diameter.</p> <p>No delaminated or disbanded areas to be within 3.0 inches of each other.</p> <p>No more than 10 percent delamination or disbond allowed.</p>
Zone B	
1. Sandwich Wall:	<p>No single delamination or disbond to be larger than 1.0 inch in diameter.</p> <p>No delaminations or disbanded areas to be within 3.0 inches of each other.</p> <p>No more than 10 percent delamination or disbond allowed.</p>
2. Fairing Hinge Supports:	<p>No more than 20 percent disbond allowed.</p> <p>No single disbond to be more than 1.0 square inch.</p> <p>No two disbanded areas to be within 2.0 inches of each other.</p>
Zone C	
1. Shell:	<p>No single delamination to be larger than 1.0 inch in diameter.</p> <p>No delaminated areas to be within 3.0 inches of each other.</p> <p>No more than 1.0 percent delamination allowed.</p>
2. Frame:	<p>No single disbond to be more than 1.0 square inch.</p> <p>No two delaminated areas to be within 2.0 inches of each other.</p> <p>No more than 10 percent disbond allowed.</p>
3. Intercostals:	<p>No single disbond to be more than 1.0 square inch.</p> <p>No two delaminated areas to be within 2.0 inches of each other.</p> <p>No more than 10 percent disbond allowed.</p>

TABLE 12. POTENTIAL NDE TECHNIQUES - TAIL BOOM

Section	X-ray	Acoustic Emission (1)	Ultrasonic			Impulse Response	Visual (2)	Stiffness Test
			Harmonic Bond Tester	C-Scan	Bondscope			
Conical Section	X	X	X	X	X	X	X	X
Frames / Intercostals			X		X	X	X	

(1) During static, dynamic and fatigue testing.
(2) Cut edges, exterior bond surfaces, etc.

TABLE 13. VERTICAL TAIL - CENTER BOX CRITICAL
DISBOND AND DELAMINATION LIMITS

Zone A	
1. Laminate:	<p>No delamination to be over 1.0 inch in diameter.</p> <p>No skin delamination to be within 3.0 inches of another.</p> <p>No more than 15 percent delamination allowed.</p>
Zone B	
1. Preassembly Sandwich Structure:	<p>No single void to be more than 0.5 inch in any direction, and not tangent to any edge.</p> <p>No two void areas to be within 3.0 inches of each other.</p> <p>No more than 10 percent delamination allowed.</p>
2. Integrally Fabricated Attach Brackets:	<p>No disbond to be over 0.5 inch in diameter.</p> <p>No two disbond areas to be within 3.0 inches of each other.</p> <p>No more than 10 percent disbond allowed.</p>

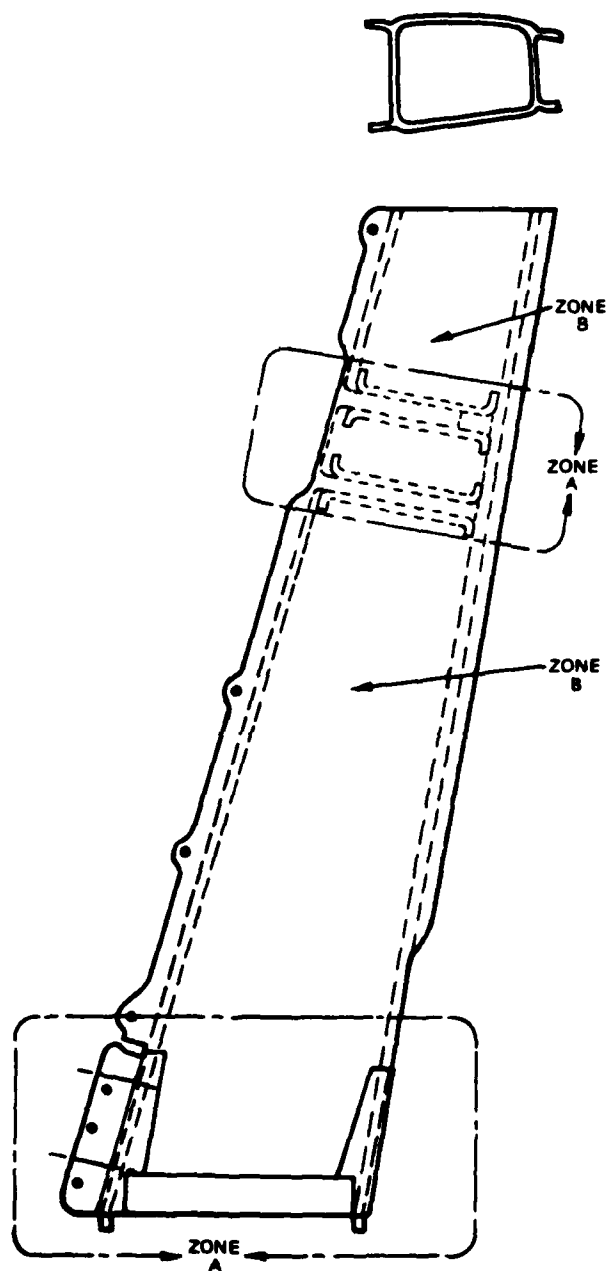


Figure 84. Composite Vertical Tail Inspection Zones

TABLE 14. POTENTIAL NDE TECHNIQUES - VERTICAL

Section	X-ray	Acoustic Emission (1)	Ultrasonic			Impulse Response	Visual (2)	Stiffness Test
			Harmonic Bond Tester	C-Scan	Bondscope			
Spar Box	X	X	X	X	X	X	X	X
Ribs			X		X		X	
T-Flanges			X		X		X	

(1) During static, dynamic, fatigue testing.
 (2) Cut edges, exterior bond surfaces, etc.

The stabilators' critical zones A and B are defined in Figure 85. Tolerances for bond and laminate defects permitted in preassembly components, attachable details, and the completed structure are delineated in Table 15. Table 16 presents the NDE procedures to be used to evaluate the integrity of stabilator structural parts.

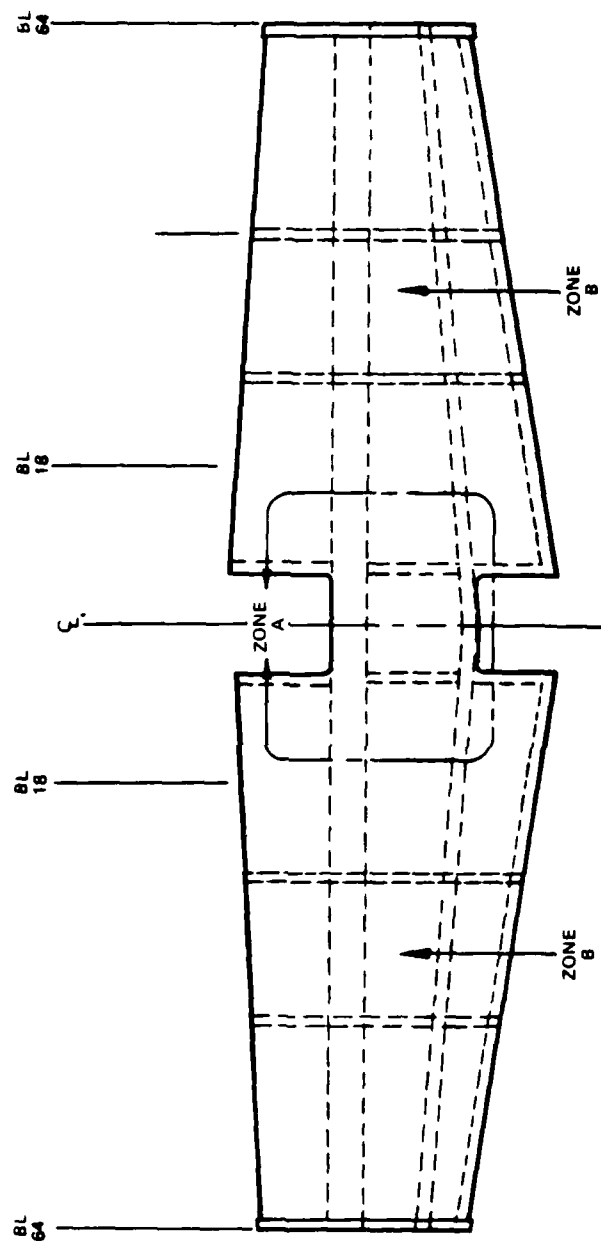


Figure 85. Composite Stabilator Inspection Zones

TABLE 15. STABILATOR CRITICAL DISBOND AND
DELAMINATION LIMITS

Preassembly and Attachable Details	
1. Skin:	<p>No single delamination to be over 1.0 square inch.</p> <p>No delamination to be within 3.0 inches of another.</p> <p>No more than 10 percent delamination allowed.</p>
2. Forward and Aft Spar Assemblies:	<p>No delamination to be over 1.0 square inch.</p> <p>No single delaminations to be within 3.0 inches of each other.</p> <p>No more than 10 percent delamination allowed.</p>
3. Ribs and Caps:	<p>No skin delamination to be over 1.0 square inch.</p> <p>No single delamination to be within 3.0 inches of another.</p> <p>No more than 10 percent delamination allowed.</p>

TABLE 15. STABILATOR CRITICAL DISBOND AND
DELAMINATION LIMITS (CONT)

Final Assembly	
Zone A	
1. Forward and Aft Spar Assembly Bonds:	<p>No more than 10 percent disbond allowed.</p> <p>No disbond to be larger than 1.0 square inch.</p> <p>No disbanded area to be within 3.0 inches of another.</p>
2. Ribs and Closeouts:	<p>No more than 10 percent for ribs and 20 percent for closeout disbonds allowed along attach flanges.</p> <p>No area of disbond to extend across bonding flange.</p>
Zone B	
1. Forward and Aft Spar Assembly Bond:	<p>No more than 10 percent disbond allowed.</p> <p>No single disbond to be more than 1.0 square inch.</p> <p>No disbanded area to be within 3.0 inches of another.</p>
2. Trailing Edge Bond Joint:	<p>No more than 10 percent disbond allowed.</p> <p>No voids allowed 0.5 inch from trailing edge.</p>
3. Ribs and Caps:	<p>No more than 10 percent disbond allowed.</p> <p>No disbond to extend across bonding flange.</p>

TABLE 16. POTENTIAL NDE TECHNIQUES - STABILATOR

Section	X-ray	Ultrasonic			Impulse Response	Visual (1)	Stiffness Test
		Harmonic Bond Tester	C-Scan	Bondascope			
Spars	X	X	X	X		X	
Ribs		X	X	X		X	
Assembly		X		X	X	X	X
(1) Cut edges, exterior bond surfaces, etc.							

DESIGN TO UNIT PRODUCTION COST

The design to unit production cost (DTUPC) assessment (in Second Quarter 1981 dollars) is based on HHI's experience with procuring and fabricating composites and metal components, and assembling them. The estimate for fabricating composite components is divided into those that are labor-intensive and labor non-intensive. Different process improvement factors are used for each category. The procurement of the metal components is related to similar components in the prototype AH-64A helicopter. The initial estimates are made for the Serial Number (S/N) 010 unit. The costs are worked backward to the S/N-001 unit and then forward to the average for the 536 shipset production base.

The labor required to fabricate the three major composite components is estimated in Tables 17, 18, and 19 for each step in the process. The composite materials required for three CTS components are listed in Table 20.

The fabricated metal components that go into each of the three CTS components and connect them together are estimated in Table 21.

The production improvement factors used in this analysis are:

- Composite fabrication (labor intensive) 80 percent
- Composite fabrication (labor non-intensive) 85 percent
- Purchased metal components 95 percent
- Purchased composite materials 100 percent

The mathematical ratios for these factors relative to the first unit, tenth unit, and cumulative average for 536 units are:

<u>Improvement Factor</u>	<u>S/N-001</u>	<u>S/N-010</u>	<u>Cumulative Average, 536</u>
80 percent	1.0000	0.3286	0.1373
85 percent	1.0000	0.4636	0.2291
95 percent	1.0000	0.8193	0.6281
100 percent	1.0000	1.0000	1.0000

TABLE 17. LABOR FOR TAILBOOM (S/N-010)

		Manminutes	
		Labor Intensive	Labor Non-Intensive
Clean and prepare tailboom mandrel	2 men, 1 hour	120	-
Clean and prepare frame and intercostal molds	7 molds, 1 man per mold per 1/4 hour	105	-
Cut out fabric	2 men, 1/2 hour	60	-
Layup frames and intercostals	7 molds, 2 men per mold per 1/2 hour	420	-
Cure frames and intercostals	1 man, 6 hours	360	-
Trim and prepare honeycomb	2 men, 1 hour	120	-
Trim and assemble frames and intercostals	2 men, 2 hours	240	-
Assembly tailboom mandrel	2 men, 1/2 hour	60	-
Mount mandrel in winding machine	2 men, 1/4 hour	-	30
Wind inner skin	1 man, 50 lb, 8 lb/hour	-	375
Place film adhesive	2 men, 1/4 hour	-	30
Place honeycomb	2 men, 1/2 hour	-	60

TABLE 17. LABOR FOR TAILBOOM (S/N-010) (CONT)

		Manminutes	
		Labor Intensive	Labor Non-Intensive
Place film adhesive	2 men, 1/4 hour	-	30
Place doublers and fillers	2 men, 1/2 hour	60	-
Wind outer skin	1 man, 50 lb, 8 lb/hour	-	375
Install peel ply	2 men, 1/4 hour	-	30
Overwind	1 man, 1 ft/min, 20 ft	-	20
Phase I cure	1 man, 6 hours	-	360
Remove tailboom from mandrel	2 men, 3/4 hour	-	90
Install frames, etc.	2 men, 1 hour	120	-
Post cure	1 man, 6 hours	-	360
Trim, drill, install metal fittings, finish machine	3 men, 8 hours	1440	-
Inspect	1 man, 2 hours	-	120
Paint	1 man, 2 hours	-	120
Weigh	2 men, 1/4 hour	-	30
Pack for shipment	2 men, 1/4 hour	-	30
	TOUCH TIME	3105	2060

TABLE 18. LABOR FOR STABILATOR (S/N-010)

		Manminutes	
		Labor Intensive	Labor Non-Intensive
Clean and prepare skin and broadgoods mandrels	2 men, 1 hour	120	-
Clean and prepare rib, spar and skin molds	32 molds, 1 man, 1/4 hour	480	-
Wind broadgoods	1 man, 40 lb, 8 lb/hour	-	300
Cut out fabric and broadgoods	2 men, 2 hours	240	-
Lay up ribs and spars	16 molds, 1 man/mold, 1/2 hr	480	-
Wind skins	1 man, 30 lb, 8 lb/hour	-	225
Cut out skins	2 men, 1/2 hour	60	-
Lay up skins	2 men, 1 hour	120	-
Phase I cure ribs, spars and skins	(A)	-	0
Trim ribs, spars and skins	2 men, 3 hours	-	960
(A) Coincide with tailboom and vertical fin			

TABLE 18. LABOR FOR STABILATOR (S/N-010) (CONT)

		Manminutes	
		Labor Intensive	Labor Non-Intensive
Assembly ribs and spars	2 men, 2 hours	-	240
Cure rib/spar assembly	(A)	-	0
Assemble skins	2 men, 1/2 hour	60	-
Cure stabilator	(A)	-	0
Trim, drill, install metal fittings	2 men, 3 hours	960	-
Inspect	1 man, 1 hour	-	60
Paint	1 man, 1 hour	-	60
Weigh	2 men, 1/8 hour	-	15
Pack for shipment	1 man, 1/4 hour	-	15
TOUCH TIME		2520	1875
(A) Coincide with tailboom and vertical fin			

TABLE 19. LABOR FOR VERTICAL TAIL (S/N-010)

		Manminutes	
		Labor Intensive	Labor Non-Intensive
Clean and prepare spar mandrel	1 man, 1 hour	60	-
Clean and prepare bulkhead and angle molds	8 molds, 1 man, 1/4 hour	120	-
Cut out fabric	1 man, 1 hour	60	-
Lay up bulkheads and angles	8 molds, 2 men/mold, 1/2 hour	480	-
Cure bulkheads	ⓑ	-	0
Trim bulkheads and prepare bulkheads and angles	2 men, 2 hours	240	-
Assemble fin spar mandrel	2 men, 1 hour	120	-
Wind inner skin	1 man, 10 lb, 8 lb/hour	-	75
Place film adhesive	2 men, 1/8 hour	-	15
Place honeycomb	2 men, 1/4 hour	-	30
Place film adhesive	2 men, 1/8 hour	-	15
ⓑ Coincide with tailboom and stabilator			

TABLE 19. LABOR FOR VERTICAL TAIL (S/N-010) (CONT)

		Manminutes	
		Labor Intensive	Labor Non-Intensive
Wind outer skin	1 man, 10 lb, 8 lb/hour	-	75
Place peel ply	2 men, 1/8 hour	15	-
Place caul sheets	2 men, 1/4 hour	-	-
Overwind	1 man, 1 ft/min, 9 ft	-	10
Phase I Cure	(B)	-	0
Remove spar from mandrel	2 men, 1/4 hour	30	-
Install bulkheads and angles	2 men, hour	240	-
Post cure	(B)		
Trim, drill, install metal fittings, and finish machine	2 men, hours	480	-
Inspect	1 man, 1 hour	-	60
Paint	1 man, 1 hour	-	60
(B) Coincide with tailboom and stabilator			

TABLE 19. LABOR FOR VERTICAL TAIL (S/N-010) (CONT)

		Manminutes	
		Labor Intensive	Labor Non-Intensive
Install leading and trailing edge fairings	2 men, 1/2 hour each	120	-
Weigh	2 men, 1/8 hour	-	15
Pack for shipping	1 man, 1/4 hour	<u>-</u>	<u>15</u>
	TOUCH TIME	1995	370

TABLE 20. COMPOSITE MATERIAL FOR CTS
(SECOND QUARTER 1981 DOLLARS)

	Pounds	Square Feet	\$ per Pound	\$ per Square Foot	\$
<u>TAILBOOM</u>					
Graphite	34.1		26.00		887
Kevlar	27.4		9.00		245
Resin	61.0		1.20		73
Honeycomb	13.0		150.00		1950
Film Adhesive		105		1.30	137
Miscellaneous Process Materials					150
25% Allowance for Scrap, Turnaround, etc.					861
				TOTAL	\$4303
<u>STABILATOR</u>					
Graphite	11.3		26.00		294
Kevlar	7.0		9.00		63
Resin	18.0		1.20		22
Urethane	3.8		15.00		57
Film Adhesive		15.0		1.30	20
Miscellaneous Process Materials					100
25% Allowance for Scrap, Turnaround, etc.					139
				TOTAL	\$ 695
<u>VERTICAL TAIL</u>					
Graphite	16.0		26.00		416
Resin	16.0		1.20		19
Honeycomb	3.0		150.00		450
Film Adhesive		40		1.30	52
Miscellaneous Process Materials					100
25% Allowance for Scrap, Turnaround, etc.					259
				TOTAL	\$1296
GRAND TOTAL					\$6294

TABLE 21. COMPONENTS OTHER THAN STRUCTURAL COMPOSITES
(SECOND QUARTER 1981 DOLLARS)

<u>Tailboom</u>		
One Sta 547 Frame	Based on \$3800 Phase II frame + 40 percent inflation + added complexity and HHI material + machining estimate)	\$ 5,700
Two Sta 532 Fittings	Based on size and complexity relative to 547 frame	700
Four Intercostal Clips	Based on size and complexity relative to 547 frame	400
One Jack Fitting	Based on \$700 Phase II titanium fitting redesigned into stainless steel	400
One Set of Tail Rotor Shaft Supports	Phase II quote + 40 percent inflation	1,400
One Set of Maintenance Steps	HHI estimate	600
Miscellaneous Hardware, Fasteners, etc.	HHI estimate	<u>1,200</u>
TOTAL		\$10,400
<u>Stabilator</u>		
Two Stabilizer Hinge Fittings	Based on size and complexity relative to 547 frame	\$ 1,000
Six Bathtub Fittings	Based on size and complexity relative to 547 frame	900
Two Actuator Fittings	Based on size and complexity relative to 547 frame	300
Miscellaneous Hardware, Fasteners, etc.		<u>200</u>
TOTAL		\$ 2,400
<u>Vertical Tail</u>		
Four Fin Attach Fittings	Based on size and complexity relative to 547 frame	\$ 3,200
Nine Gearbox Attach Fittings	Based on size and complexity relative to 547 frame	2,000
Leading Edge, Trailing Edge, and Tip Fairings	Phase II quote	5,000
Four Maintenance Steps	HHI estimate	300
Miscellaneous Hardware, Fasteners, etc.	HHI estimate	<u>800</u>
TOTAL		\$11,300
GRAND TOTAL		\$22,800

A burdened labor rate of \$35 per hour is assumed for composites fabrication and final assembly.

The DTUPC for the CTS is calculated in Table 22 and is summarized in Table 23. At the time that the CTS program was terminated, the AH-64A DTUPC for the comparable metal components was quoted by Teledyne Ryan Aeronautical (the AH-64A airframe subcontractor) as shown in Table 23. (Both composite and metal DTUPC's are rounded to the nearest \$500.)

TABLE 22. DESIGN TO UNIT PRODUCTION COST
(SECOND QUARTER 1981 DOLLARS)

Tailboom

S/N-010 Labor Intensive + Support = $1\text{-}2/3 * \times 3105 = 5175 \text{ mm}$

Labor Non-Intensive + Support =

$$1\text{-}2/3 * \times 2060 = 3433 \text{ mm}$$

Metal, etc. = \$9100

Composites = \$4303

S/N-001 Labor Intensive + Support =

$$\frac{5175}{60 \times 0.3286} = 262 \text{ mh}$$

Labor Non-Intensive + Support =

$$\frac{3433}{60 \times 0.4636} = \frac{123}{385 \text{ mh}}$$

$$\text{Metal, etc.} = \frac{\$10,400}{0.8193} = \$12,694$$

$$\text{Composite} = \frac{\$4303}{1.0000} = \$4,303$$

*2/3 factor for nonproductive personnel time

TABLE 22. DESIGN TO UNIT PRODUCTION COST (CONT)
(SECOND QUARTER 1981 DOLLARS)

<u>Tailboom (Cont)</u>				
Cumulative Avg for 536	Labor Intensive	=	$262 \times 0.1323 \times \35	= \$ 1,213
	Labor Non-Intensive	=	$123 \times 0.2291 \times \35	= 986
	Metal	=	$\$12,694 \times 0.6281$	= 7,973
	Composite	=	$\$4,303 \times 1.0000$	= <u>4,303</u>
TOTAL				\$14,475
<u>Stabilator</u>				
S/N-010	Labor Intensive + Support = $1-2/3^* \times 2520 = 4200$ mm			
	Labor Non-Intensive + Support =			
	$1-2/3^* \times 1875 = 3125$ mm			
	Metal, etc. = \$2400			
	Composites = \$695			
*2/3 factor for nonproductive personnel time				

TABLE 22. DESIGN TO UNIT PRODUCTION COST (CONT)
(SECOND QUARTER 1981 DOLLARS)

<u>Stabilator (Cont)</u>				
S/N-001	Labor Intensive + Support =			
	$\frac{4200}{60 \times 0.3286} = 213 \text{ mh}$			
	Labor Non-Intensive + Support =			
	$\frac{3125}{60 \times 0.4636} = \frac{112}{325 \text{ mh}}$			
	Metal, etc. = $\frac{\$2400}{0.8193} = \2929			
	Composite = $\frac{\$695}{1.0000} = \695			
Cumulative Avg for 536	Labor Intensive	=	$213 \times 0.1323 \times \35	= \$ 986
	Labor Non-Intensive	=	$112 \times 0.2291 \times \35	= 898
	Metal	=	$\$2929 \times 0.6281$	= 1,840
	Composite	=	$\$695 \times 1.0000$	= 695
	TOTAL			\$ 4,419

TABLE 22. DESIGN TO UNIT PRODUCTION COST (CONT)
(SECOND QUARTER 1981 DOLLARS)

Vertical Tail

S/N-010 Labor Intensive + Support = $1\text{-}2/3^* \times 1995 = 3325 \text{ mm}$

Labor Non-Intensive + Support =

$$1\text{-}2/3^* \times 370 = 617 \text{ mm}$$

Metal, etc. = \$11,300

Composites = \$1296

S/N-001 Labor Intensive + Support =

$$\frac{3575}{60 \times 0.3286} = 168 \text{ mh}$$

Labor Non-Intensive + Support =

$$\frac{617}{60 \times 0.4636} = \frac{22}{190 \text{ mh}}$$

Metal, etc. = $\frac{\$11,300}{0.8193} = \$13,792$

Composite = $\frac{\$1296}{1.0000} = \1296

*2/3 factor for nonproductive personnel time

TABLE 22. DESIGN TO UNIT PRODUCTION COST (CONT)
(SECOND QUARTER 1981 DOLLARS)

<u>Vertical Tail (Cont)</u>			
Cumulative Avg for 536	Labor Intensive	= 168 x 0.1323 x \$35	= \$ 778
	Labor Non-Intensive	= 22 x 0.2291 x \$35	= 176
	Metal	= \$13,792 x 0.6281	= 8,663
	Composite	= \$1296 x 1.0000	= <u>1,296</u>
	TOTAL		\$10,913

TABLE 23. DTUPC SUMMARY
(SECOND QUARTER
1981 DOLLARS)

Component	Metal	Composite	Saving
Tailboom	28,000	14,500	13,500
Stabilator	13,500	4,500	9,000
Vertical Tail	32,000	11,000	21,000
Airframe Modification to Accommo- date CTS	<u>-</u>	<u>2,500</u>	<u><2,500></u>
	73,500	32,500	41,000

LABORATORY AND FLIGHT TEST PLANS

The CTS program did not progress far enough to conduct any structural testing. The plan was to conduct static, dynamic, fatigue, ballistic, and local impact tests to a level that would demonstrate safety of flight for a 25-hour flight test to be conducted under the MM&T program. When this was demonstrated to be successful, full airworthiness qualification in the laboratory and in flight would have been conducted.

LABORATORY TESTS

The CTS laboratory test article consists of the main structural elements of the CTS assembly including the tailboom, vertical tail spar, and stabilator. Fairings, etc., that have no influence on strength and/or stiffness are deleted from the test article.

Criteria for the laboratory tests include:

- | | |
|---------|--|
| Static | The factor of safety is 1.5 for all conditions, with negligible permanent set at limit load, and no failure at ultimate load. The minimum margin of safety for all flight and ground loading conditions is zero for all structures, but in such cases where the analytical margin of safety is less than zero, a positive margin is to be demonstrated by static test. |
| Dynamic | The natural frequency of the CTS when installed on the AH-64A fuselage is such that the modal separation from the excitation frequencies is better than or equal to that of the metal tailboom and empennage to reduce CTS loads and vibration. |
| Fatigue | The CTS is designed to require no major overhaul in less than 4500 flight hours. Prior to determination of oscillatory load levels from flight strain surveys, weighted fatigue level of 10 percent of limit load for the tailboom and 30 percent for the stabilator and vertical tail is used for design purposes. The distribution of maneuver load cycles used in the fatigue analysis calculations is derived from the flight profile shown in Table 24. |

- | | |
|-----------|--|
| Ballistic | The CTS ballistic survivability test consists of impacting the structure with a 23mm HEI-T projectile while the CTS is under load, and then applying static loading to destruction. |
| Impact | After static test failure, a local impact test that simulates anticipated service abuse will be conducted on the tailboom and stabilator. Type, location, and extent of damage will be recorded. |

The test article shown in Figure 86 is mounted at Station 370 on a steel fixture. Straps, loading frames, or whiffletrees are attached to the CTS for introducing loads. Hydraulic loading jacks apply the test loads between the airframe attachments and the support framework. The tare weight of the attachments, linkages, and dummy fixtures is counterbalanced by hydraulic compensation in the loading system as well as by counterweights, pulleys, and cable.

Instrumentation includes strain and rosette gages mounted as shown in Figures 87 through 92. The same gages and locations are used in the laboratory test and in flight. Prior to test and at specified times during the tests, all gages are calibrated against standards.

Predicted loading conditions are established based on AH-64A flight tests, and *modes of failure are predicted for comparison with actual test results.*

FLIGHT TESTS

Limited flight tests are conducted on the load survey air vehicle for a total of 25 hours and to a level of 80 percent of the AH-64A flight envelope. Flight conditions are summarized in Table 24.

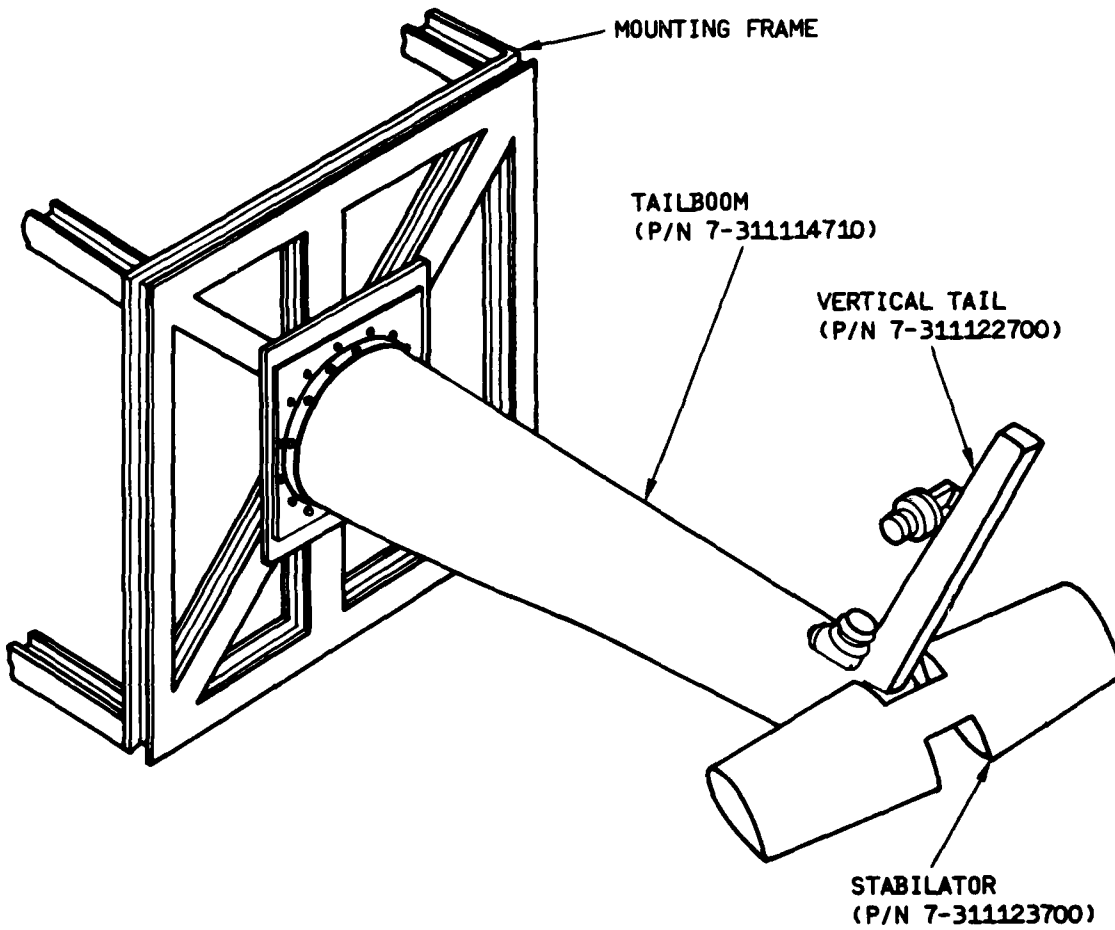


Figure 86. Schematic Static/Fatigue Test Setup

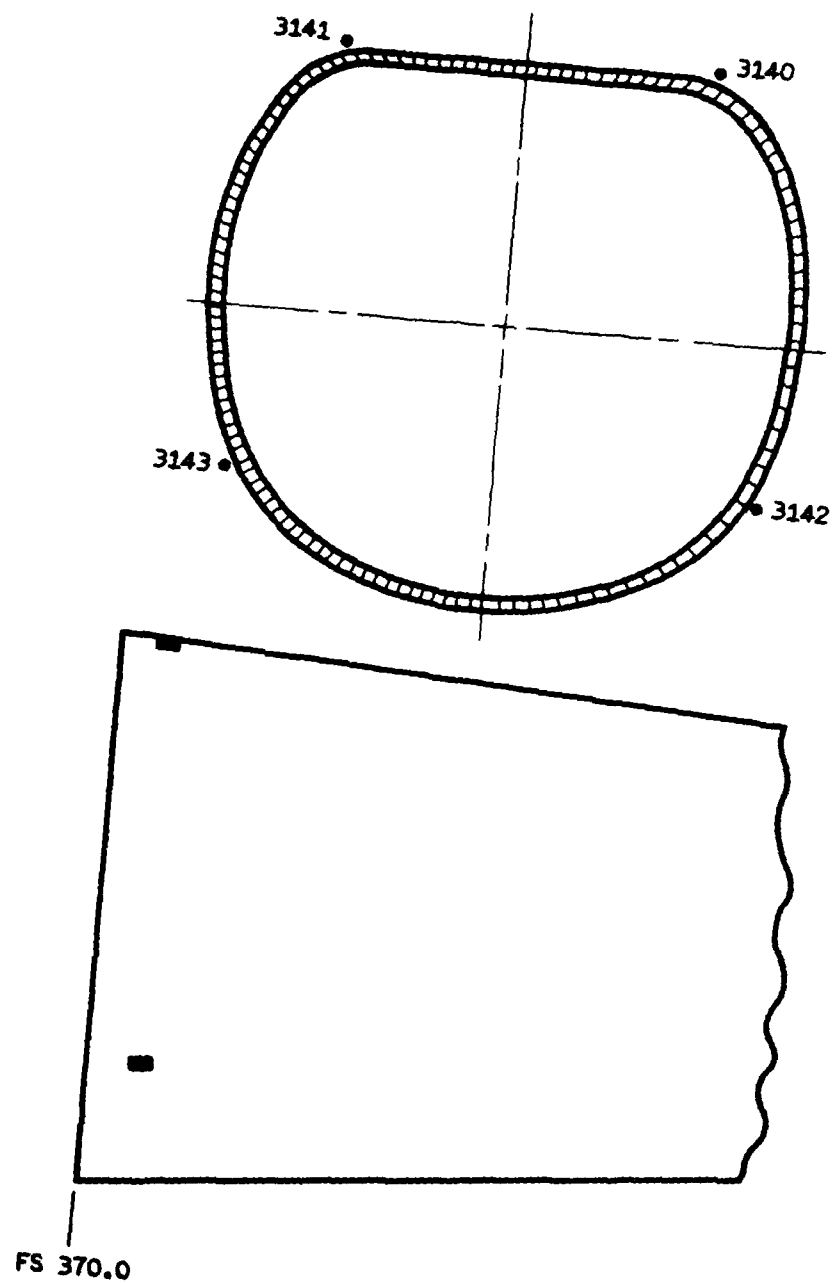


Figure 87. Strain Gage Installation FS 375

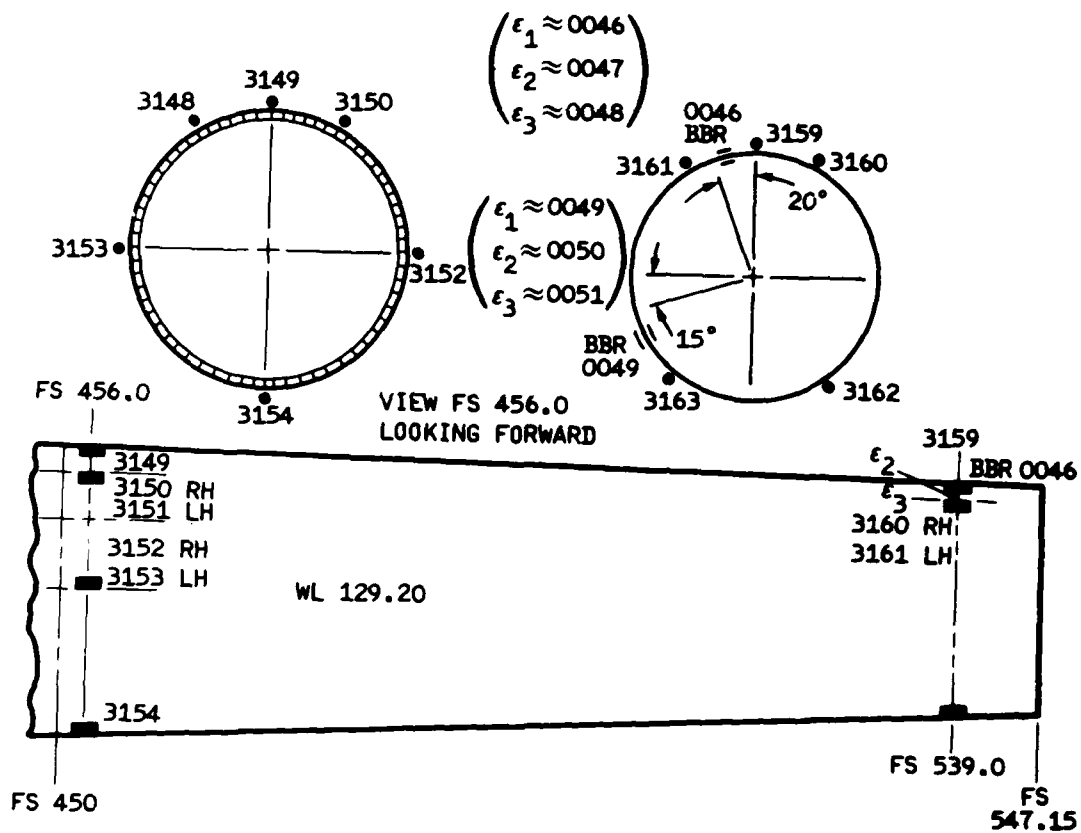


Figure 88. Strain Gage Installation - Tail Boom FS 539

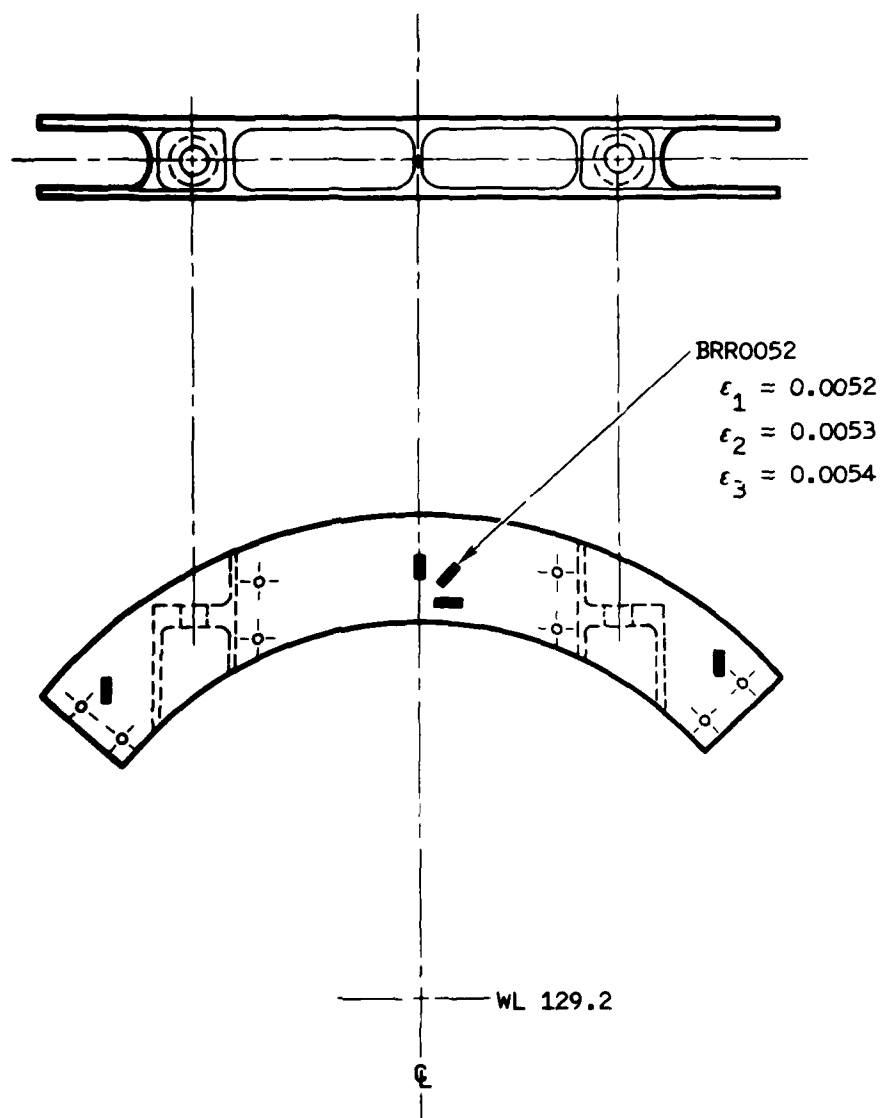
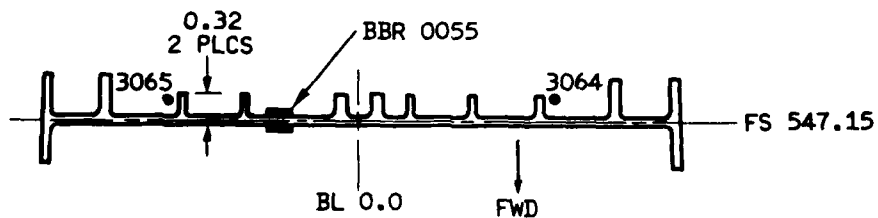
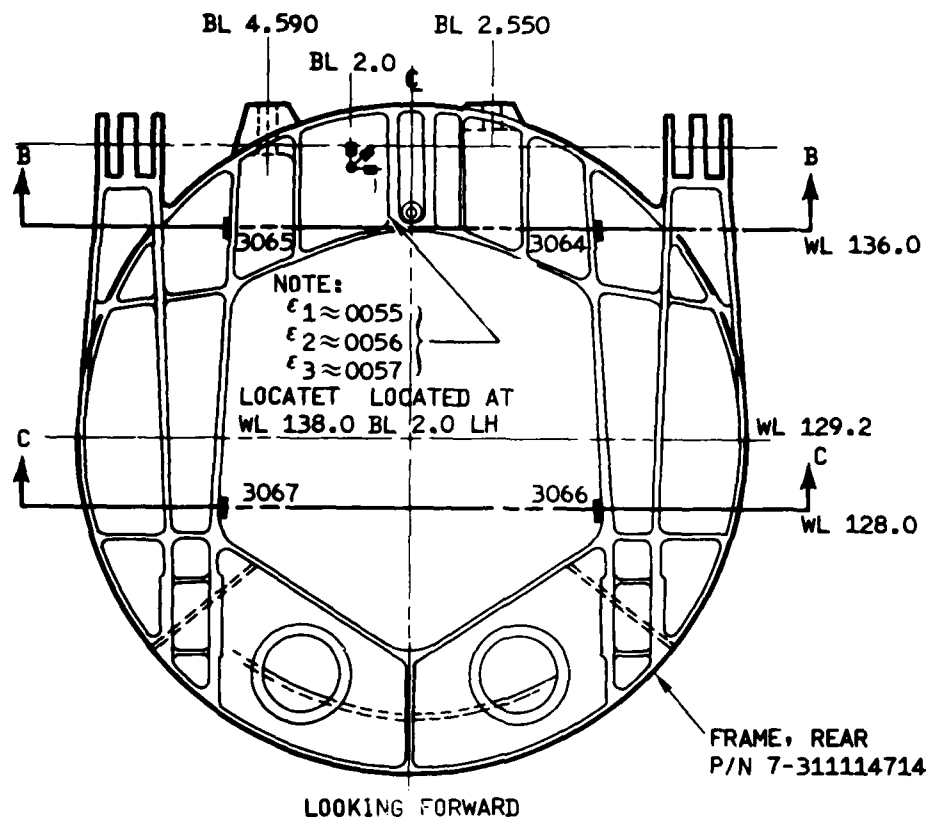
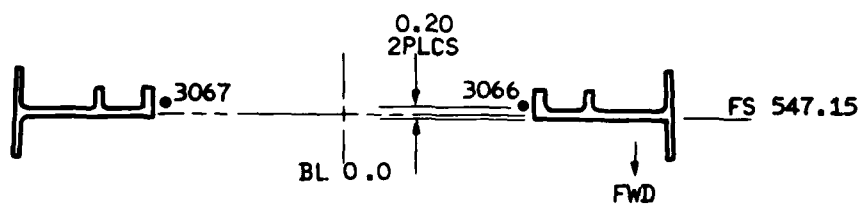


Figure 89. Strain Gage Installation - Vertical Stabilizer Fitting FS 530.09



VIEW B-B



VIEW C-C

Figure 90. Strain Gage Installation - Rear Frame FS 547

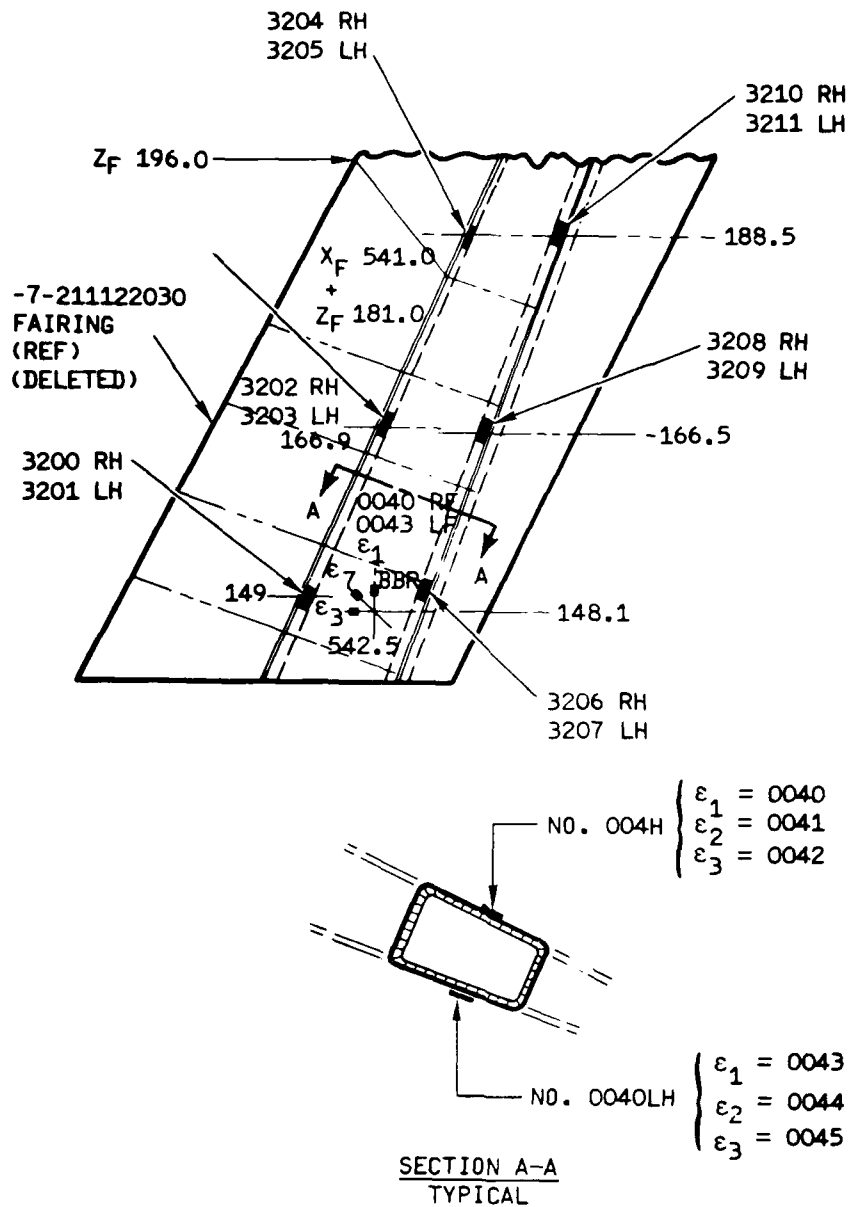


Figure 91. Strain Gage Installation - Vertical Stabilizer Spar

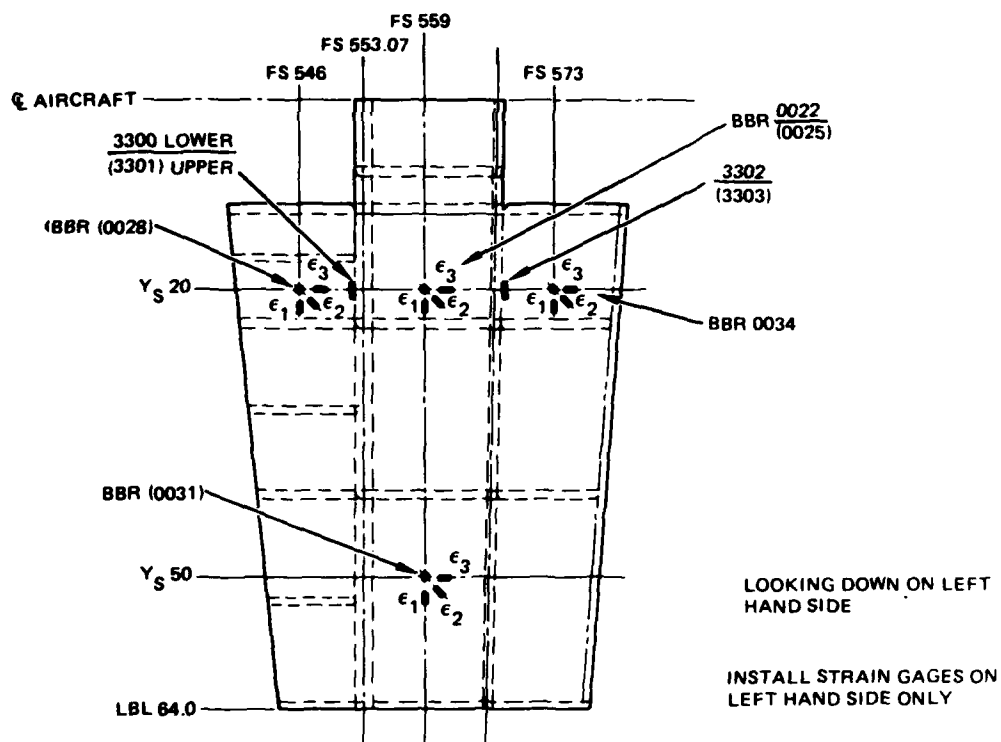


FIGURE 107. STRAIN GAGE INSTALLATION - STABILATOR SPAR 4 AXIAL STRAIN GAGE, SKIN 5 BBRs

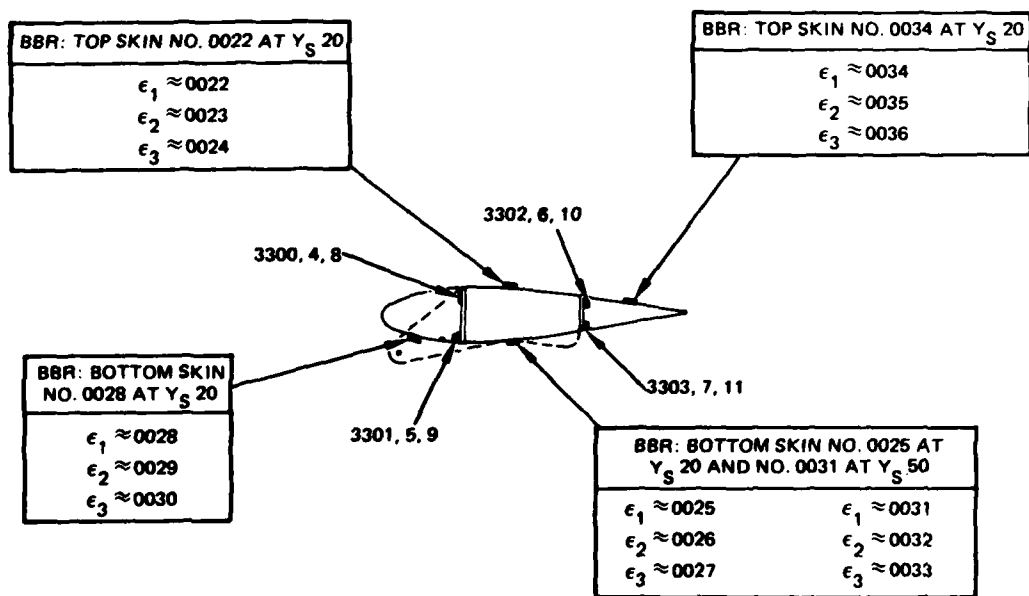


Figure 92. Strain Gage Installation - Stabilator Spar

TABLE 24. FLIGHT PROFILE

Speed Spectrum		Maneuver Spectrum		
Speed	Speed Envelope % Life	Peak Nz at cg	Time at g (sec)	Cumulative Exceedances per 4500 hours
Hover	23.0	3.00	0.8	200
(HOGE)		2.75	1.2	500
0.5 V _H	3.0	2.50	1.7	1,000
0.6 V _H	6.0	2.25	2.8	2,000
0.7 V _H	15.0	2.00	4.0	5,000
0.8 V _H	15.0	1.75	6.0	10,000
0.9 V _H	15.0	1.50	10.0	20,000
1.0 V _H	10.0	1.25	12.0	150,000
1.2 V _H	3.0			
Sideward Flight	7.0	0.75	4.2	60,000
Rearward Flight		0.50	2.8	8,000
Vertical Flight		0.25	2.5	1,000
Ground	3.0	0	2.0	200
Total	100.0			

NOTES:

- 60 percent of maneuvers shall be unsymmetrical maneuvers.
40 percent of maneuvers shall be symmetrical maneuvers.
- Climb and descent time shall be distributed as follows:
5 percent of level flight/moderate maneuvering time in ascending mode.
8 percent of level flight/moderate maneuvering time in descending mode.
- Gross weight shall be distributed as follows:
40 percent of life at basic structural design gross weight.
40 percent of life at basic structural design gross weight minus payload and 50 percent fuel.
20 percent of life at maximum alternate gross weight.
- The average time per maneuver considering all types of maneuvers shall be in accordance with the time at g column.
- Life shall be divided approximately as follows:
70 percent level flight with moderate maneuvering (0.75-1.25 g).
20 percent pull up and turn maneuvers.
10 percent other maneuvers (control reversals, auto rotation, accelerations/decelerations).
- Firing loads shall be additive to the above profile. Assume 810 firing anti-armor missions with 55 percent of mission ordnance (MO) expended during HOGE. Assume 875 firing escort or covering missions with 20 percent of MO expended during HOGE. Distribution of remaining MO should be in accordance with the forward flight spectrum.
- The altitude spectrum shall be:
80 percent at sea level-STD (representing low altitude flight).
20 percent at 4000 ft 95°F (representing high altitude flight).
- GAG cycles: Three engine start/stop cycles per flight hour.

IMPLICATIONS FOR PRODUCTION

The CTS is designed to be a lightweight, low cost, integrated replacement for the AH-64A's metal tail section. As designed, it is attached to the forward fuselage structure at Sta 370 by a double row of HiLok fasteners and requires a modification of the metal airframe at this point. The joint thus formed imposes a small penalty that is well worth accepting in light of the overall benefits of the CTS that are a 71 pound weight saving (including a 7.6 pound weight penalty for the joint) and a \$41,000 production cost saving (including a \$2,500 cost penalty for the joint).

This is the most efficient CTS that can be used, but just before the design work was terminated, a plan was proposed to change to a "mix-and-match" configuration. In this arrangement, any or all of the three composite components could be used interchangeably with the AH-64A metal components. This work was not pursued beyond a preliminary estimate of the design work required and the potential impacts of such a configuration. The unique, integrated design of the CTS that came out of the program is the most effective configuration from a cost and weight standpoint, while the "mix-and-match" design would be easier to introduce into the AAH production line. Table 25 describes the CTS changes needed to accomplish "mix-and-match." Figures 93 and 94 compare the CTS as designed with the two most probable "mix-and-match" arrangements:

- Metal tailboom with composite stabilator and vertical tail
- Composite tailboom, stabilator, and vertical tail

with the basic metal configuration in terms of weight and cost. In addition to weighing more and costing more, the "mix-and-match" design would have the following consequences:

- Reduced vertical tail incidence increases CFTR flapping and potentially reduces its fatigue life
- Reduced stabilator hinge space increases hinge loads and reduces hinge life

TABLE 25. CTS DESIGN CHANGES TO ACHIEVE "MIX-AND-MATCH"

Vertical Tail

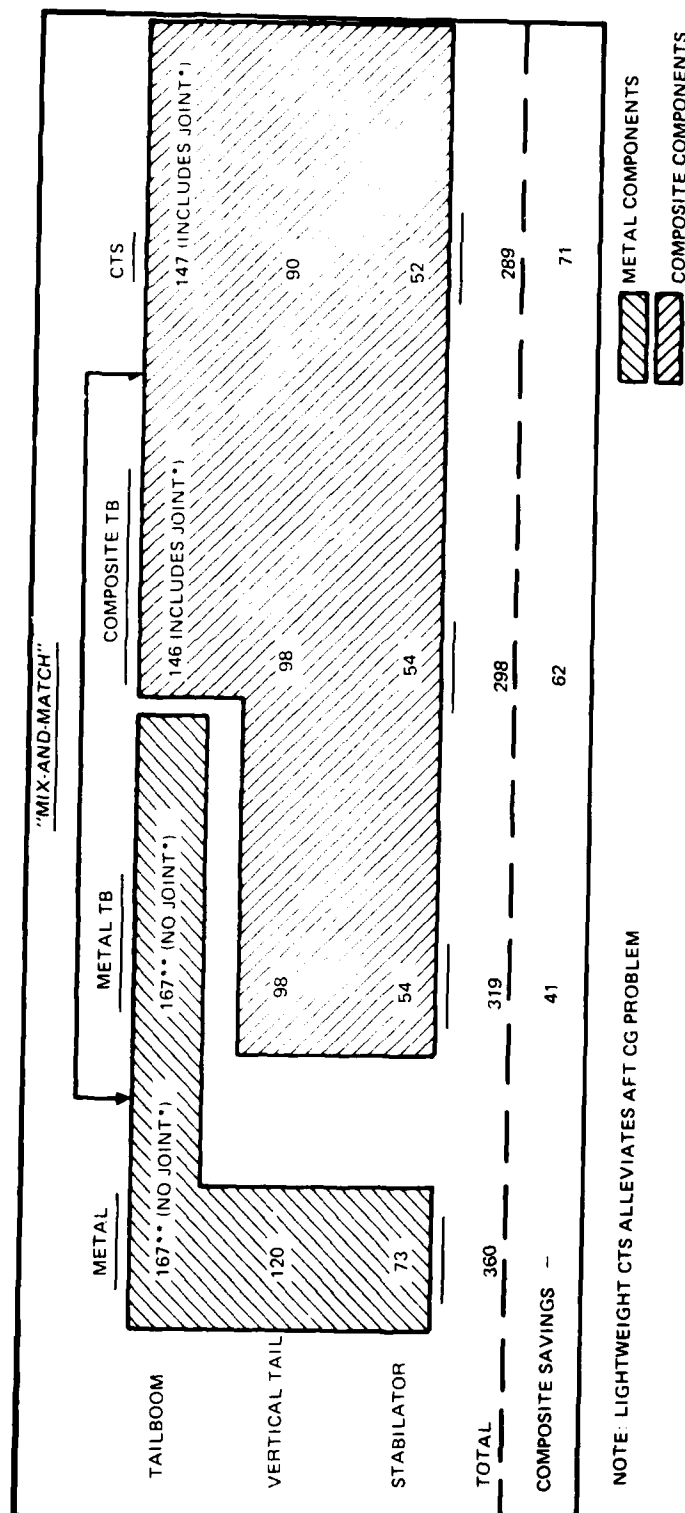
- Reduce incidence to match metal vertical tail
- Locate stabilator hinge fittings on vertical tail spar instead of on tailboom aft bulkhead
- Change root fittings and bolt pattern for attachment to tailboom

Stabilator

- Modify hinge fittings to match fittings on vertical tail spar
- Modify spar/rib structure to accommodate new hinge fitting location

Tailboom

- Change tailboom aft structure and bolt pattern for attaching vertical tail



*FUSELAGE JOINT AT STA 370
 **INCLUDES 6-LB STRENGTH INCREASE OF TAILBOOM FOR COMPOSITE FLEXBEAM TAIL ROTOR

Figure 93. Tail Section Weight Comparison

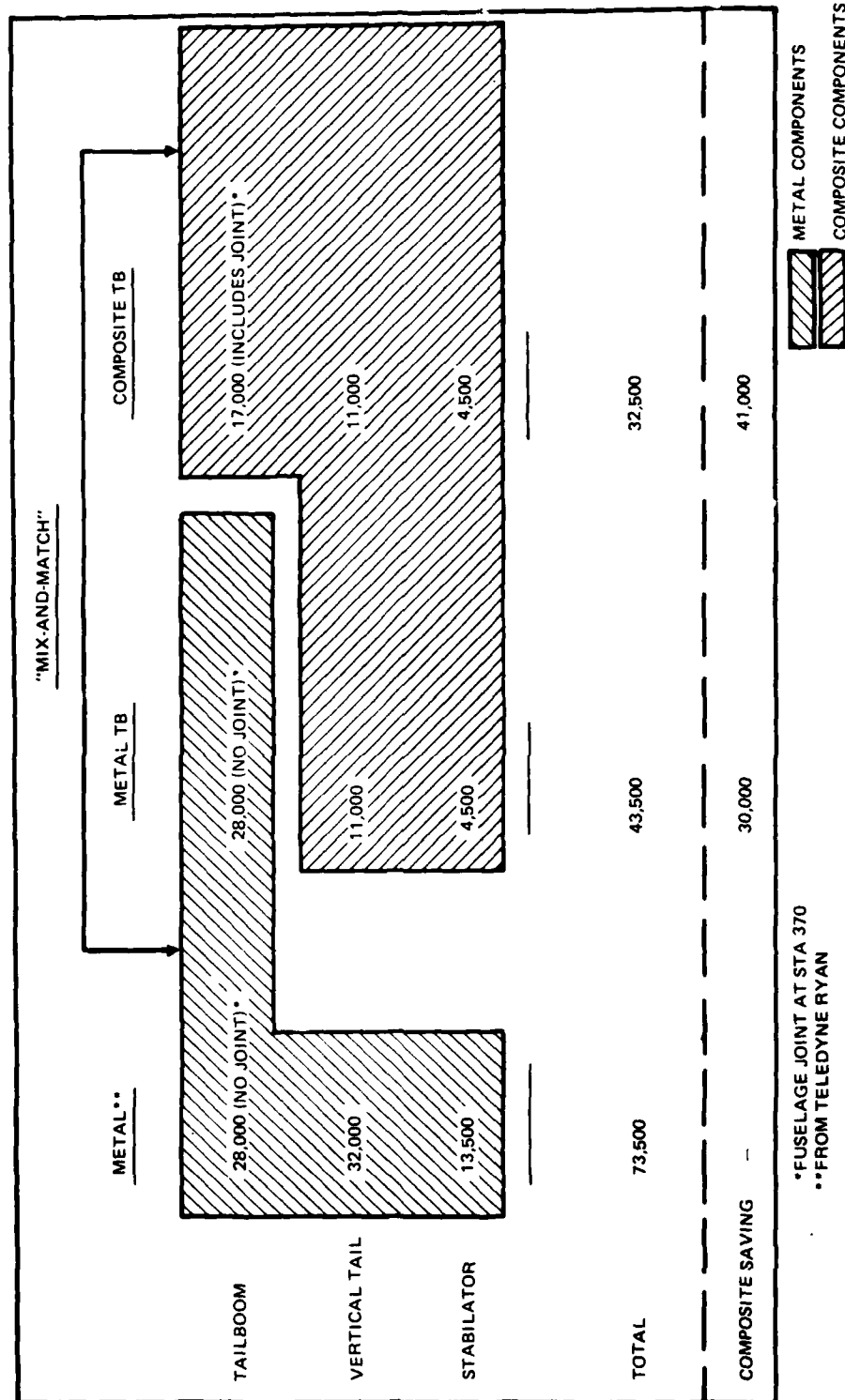


Figure 94. Unit Production Cost Comparison 536 Shipsets -
 Second Quarter 1981 Dollars

CONCLUSIONS

This MM&T program demonstrated how advanced composites technology can be applied to the tail section of the AH-64A helicopter to realize important performance, weight, and cost benefits. Methods that HHI has established are directly applicable to the CTS with the manufacturing refinement segment of the program having shown the way to build this particular configuration.

The CTS structural design is complete, and the tooling design is nearly so. It is recommended that the fabrication and test activities be reinstated in a timely manner so that the CTS can be qualified for installation on the production AH-64A. For maximum savings, the complete CTS offers:

- 71 pounds weight saving
- \$41,000 DTUPC saving (1981 dollars)
- 269 parts count saving
- 9047 fastener count saving
- \$1.1 million fuel saving over the life of the fleet
- \$22 million overall production and life cycle cost saving for the fleet
- 55 fpm vertical rate of climb increase
- Improved reliability and maintainability

As an alternative to funding the entire CTS, a program limited to only the composite stabilator can offer:

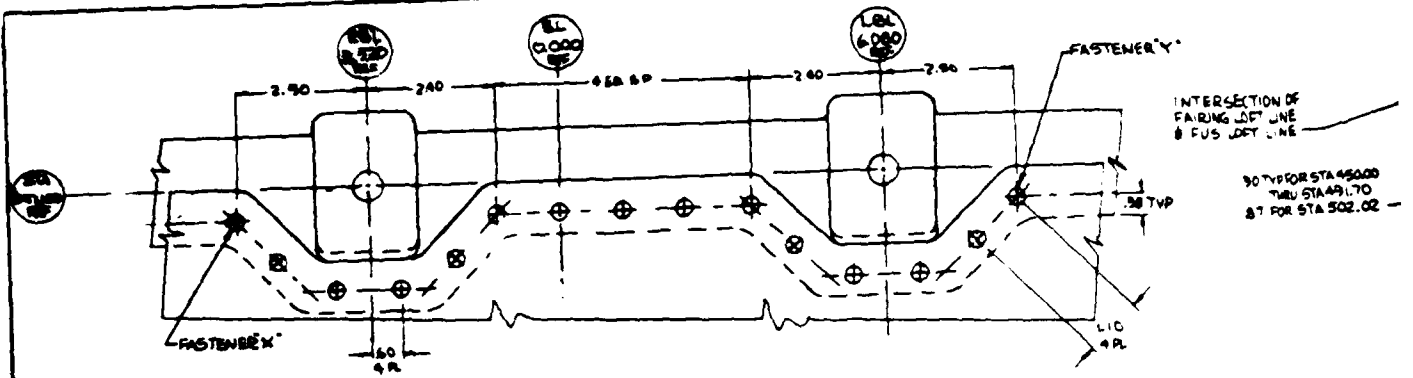
- 19 pounds weight saving
- \$9000 DTUPC saving (1981 dollars)
- 11 parts count saving
- 41 fastener count saving
- \$300,000 fuel saving over the life of the fleet
- \$5.9 million overall production and life cycle cost saving for the fleet
- 15 fpm vertical rate of climb increase
- Improved reliability and maintainability

REFERENCES

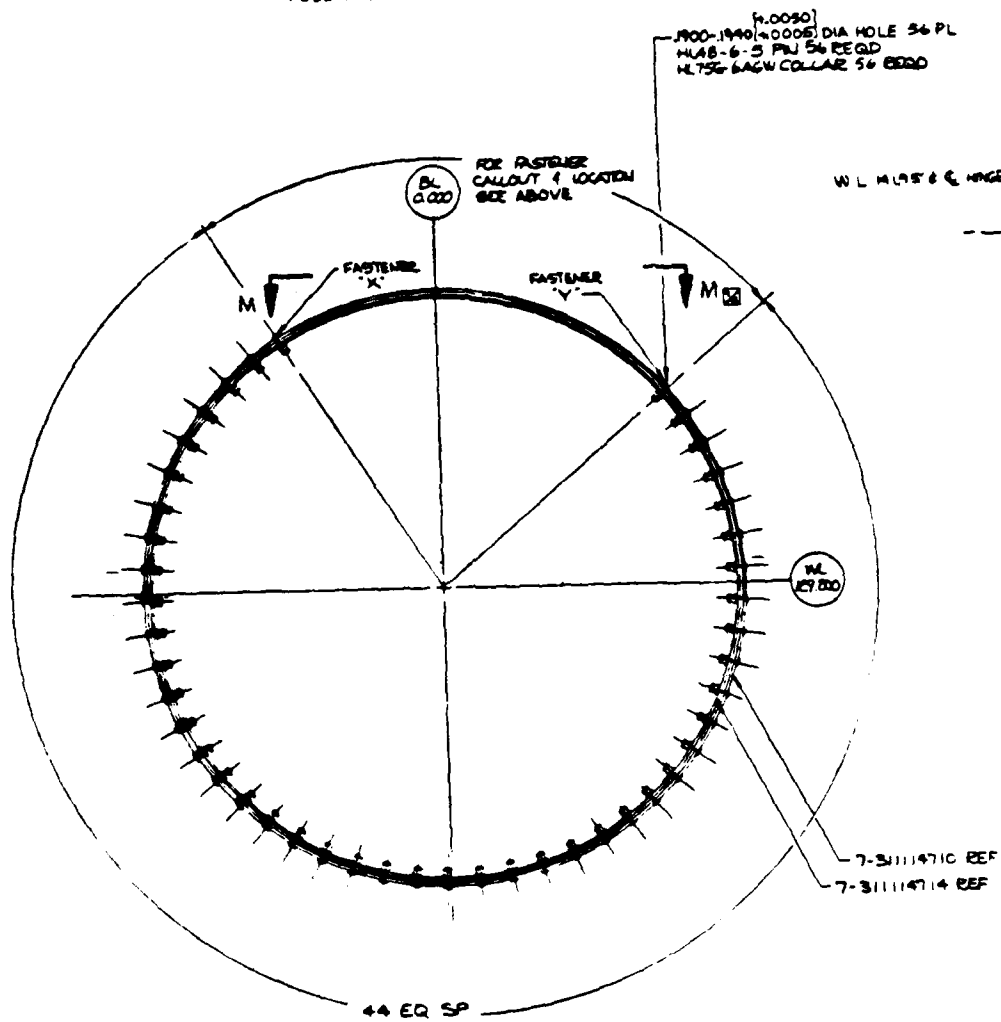
1. Needham, J.F., USAAMRDL TR-76-24: Design, Fabrication, and Testing of an Advanced Composite AH-1G Tail Section (Tailboom/Vertical Fin), February 1976.
2. Head, R.E., USAAMRDL TR-77-19: Flight Test of a Composite Multi-Tubular Spar Main Rotor Blade on the AH-1G Helicopter, August 1977.
3. Goodall, R.E., USAAMRDL TR-77-27: Advanced Technology Helicopter Landing Gear, October 1977.
4. Anon, Design Criteria Report for the YAH-64 Advanced Attack Helicopter, Phase 2 Hughes Helicopters, Inc. Report HH 78-174, revised 15 February 1980.
5. MIL-S8698 (ASG) Military Specification Structural Design Requirements, Helicopters, 28 February 1958.

CTS ASSEMBLY AND SUBASSEMBLY DRAWINGS

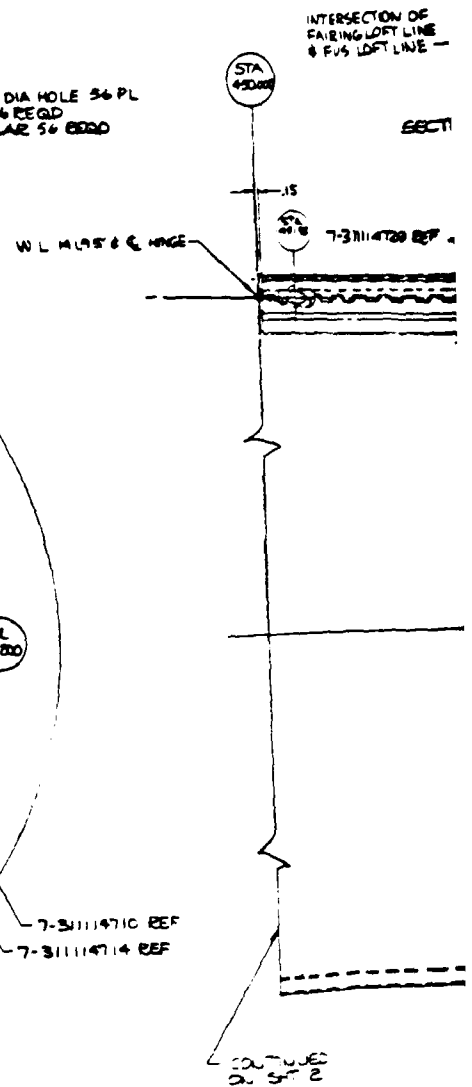
Figure	Title	Drawing Number
95	Tailboom Assembly	7-311114700, Sheet 1
	Tailboom Assembly	Sheet 2
	Tailboom Assembly	Sheet 3
96	Tailboom Subassembly	7-311114710, Sheet 1
	Tailboom Subassembly	Sheet 2
	Tailboom Subassembly	Sheet 3
	Tailboom Subassembly	Sheet 4
97	Vertical Tail Assembly	7-311122700, Sheet 1
98	Vertical Tail Subassembly	7-311122710, Sheet 1
	Vertical Tail Subassembly	Sheet 2
99	Stabilator Assembly	7-311123710, Sheet 1
	Stabilator Assembly	Sheet 2



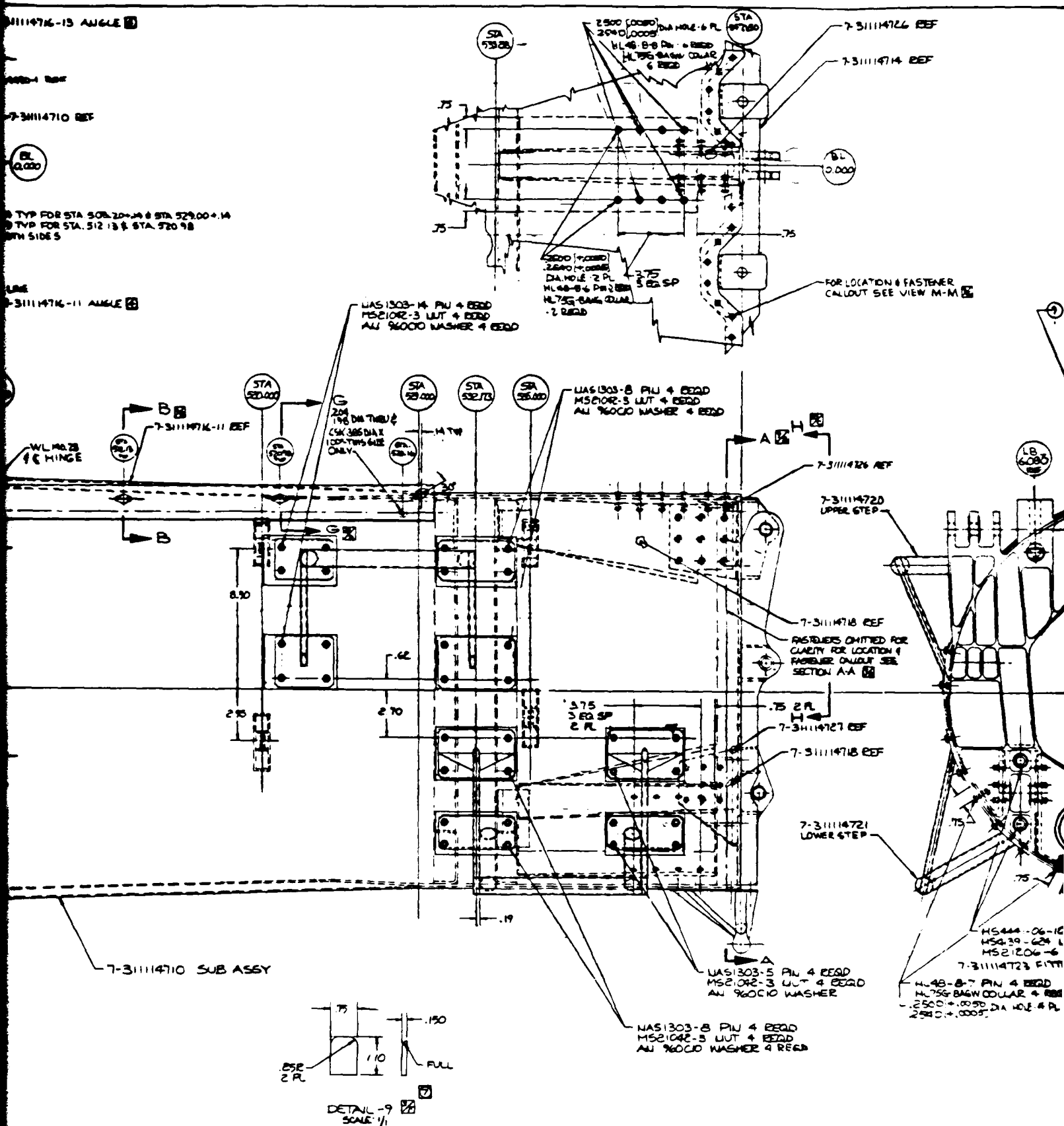
VIEW M-M
FULL SIZE



SECTION A-A
LOOKING AFT



311147K-11 AUG 68

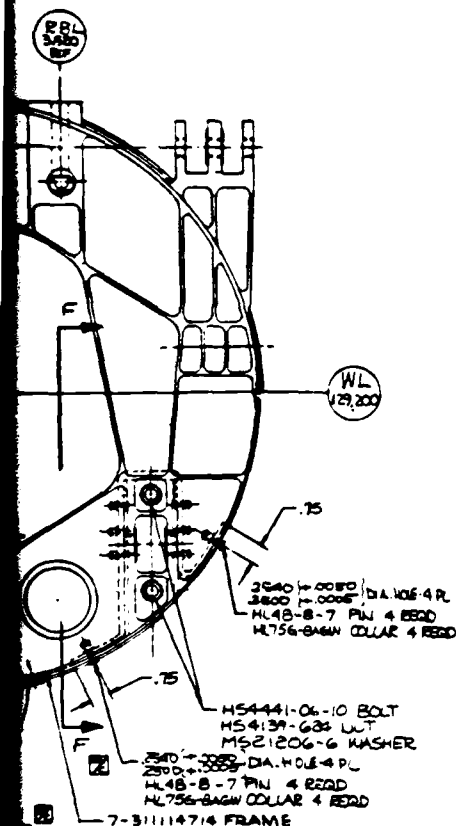


[illegible]

107

7

MS4441-06-10 BOLT
MS4139-624 NUT
MS21206-6 WASHER



PER EPB 4-230
PASTE ADHESIVE CL 1
BULK MIL-C-9084, TYPE VIII
MS2 (010/PLY)
SINE BOND PER HP16-30
6-1111 FILM ADHESIVE CL 6
RING & TOLERANCING PER ANSI Y14.5
THREADED FASTENERS PER HP2-3
N-LOK FASTENERS PER HP3-2
OTHERWISE SPECIFIED

21	MS4430-1	RECEPTACLE			6F
6	MS4447-1082	NUT			2B
6	MS21206-6	WASHER			
16	MS21042-3	NUT			
2	MS21044N3	NUT			5B
6	MS4139-624	NUT			3F
6	MS4441-06-10	BOLT			3F
34	AN960C10	WASHER			25B
2	NAS1635-3-4	SCREW			
4	NAS1305-14	BOLT			
8	NAS1305-8	BOLT			
4	NAS1303-5	BOLT			
16	NAS 9029E7	SCREW			
6	HL48-B-6	PIN			
12	HL48-B-7	PIN			
2	HL48-B-6	PIN			
36	HL48-B-5	PIN			
3	HL48-B-7	PIN			
56	HL48-B-5	PIN			
56	HL756-BAGW	COLLAR			
59	HL756-BAGW	COLLAR			
1	7-311114740	FITTING			2E
1	7-311114739	FITTING			2E
1	7-311114735	INTERCOSTAL			3B
1	7-311114734	BRACKET ASSY			2D
1	7-311114733	BRACKET			2D
1	7-311114731	BRACKET			23D
00	7-311114729	BRACKET			7B
1	7-311114723	FITTING			3B
1	7-311114721	LOWER STEP			4C
1	7-311114720	UPPER STEP			4E
1	7-311114716-13	FAIRING ANGLE			1E
1	7-311114716-11	FAIRING ANGLE			6F
1	7-311114716-9	FAIRING ANGLE			8F
1	7-311114716-7	FAIRING ANGLE			8C
1	7-311114716-5	FAIRING ANGLE			10B
1	7-311114716-3	FAIRING ANGLE			9F
1	7-311114714	REAR FRAME			3B
1	7-311114710	SUB ASSY			5B
2	-2	BARRIER		5	73E
1	-9	BARRIER		5	73D
1	-7	BARRIER		5	73C
21	-15	BARRIER		5	73B
2	-3	HINGE	MS20257-3-4300		5C
1	-11	HINGE	MS20257-3-4000		7C
2	-9	RAD LE BLOCK	201754 20120473 ALUMIN 204-250/4		3E
11	-7	BARRIER		5	5A
44	-3	BARRIER		5	2E

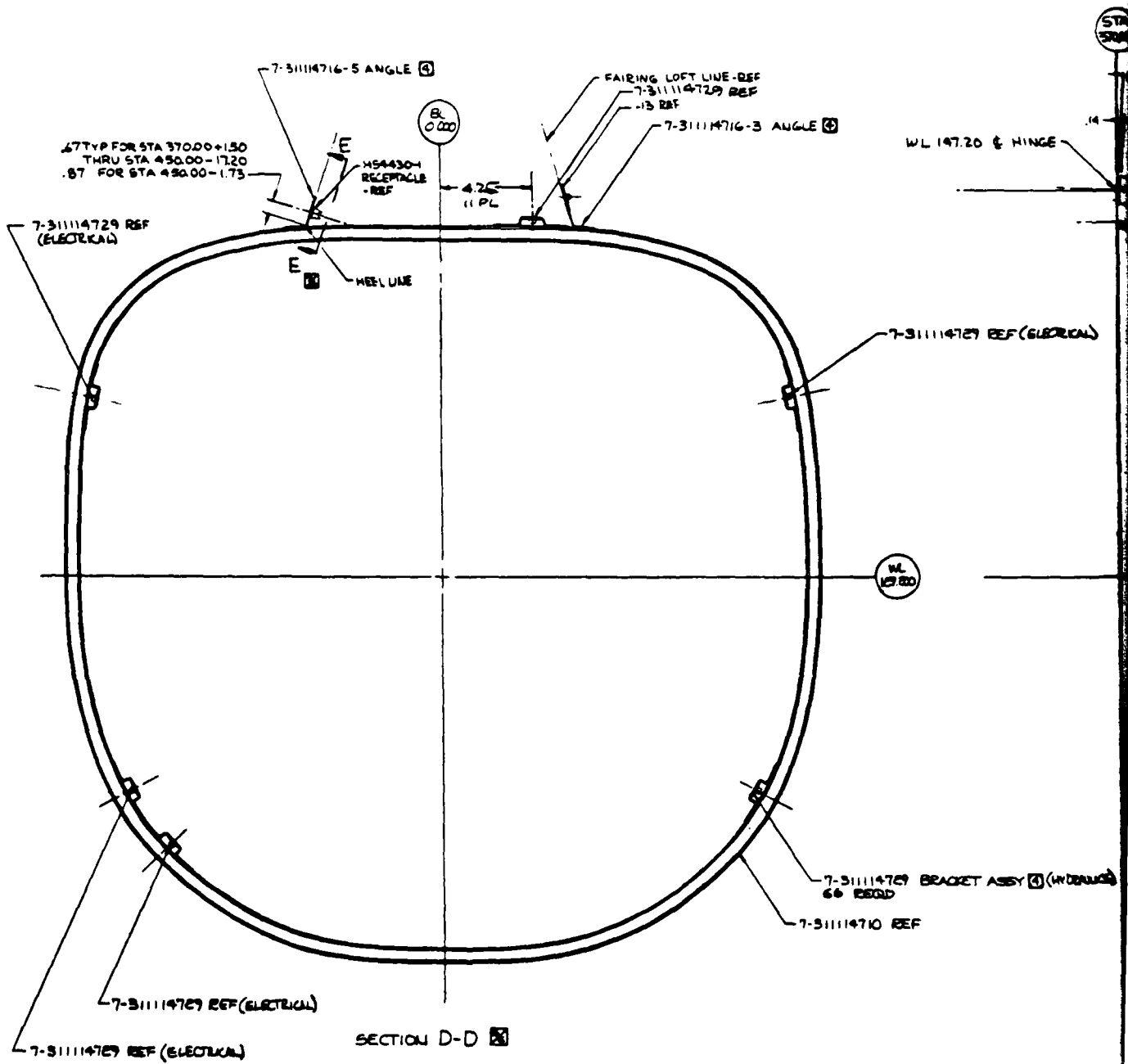
QUANTITY		UNIT		MATERIAL		DESCRIPTION		SPECIFICATION	
02731		J		02731		J		02731	

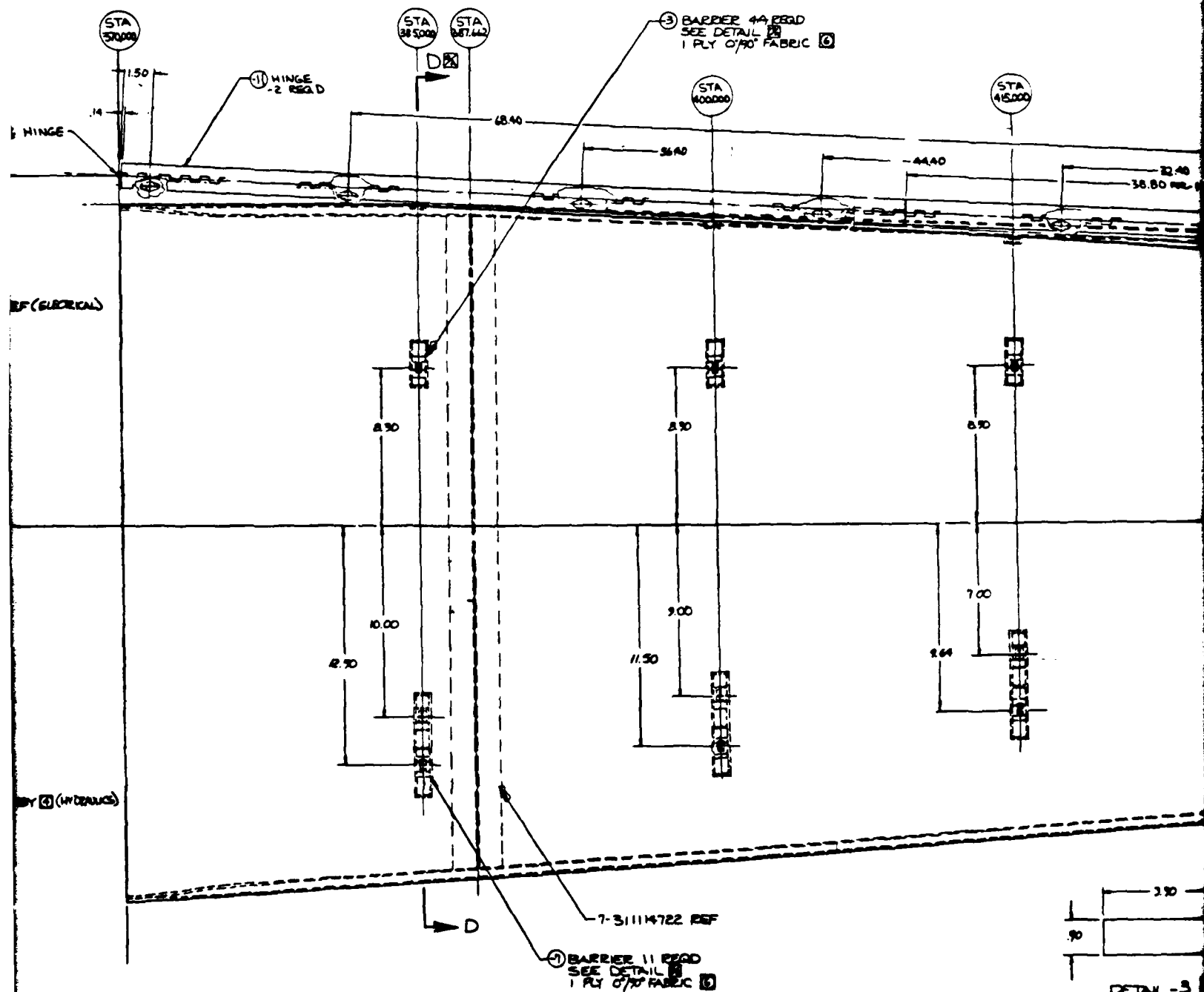
APPLICATION RELATED DATA

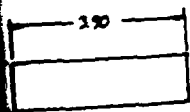
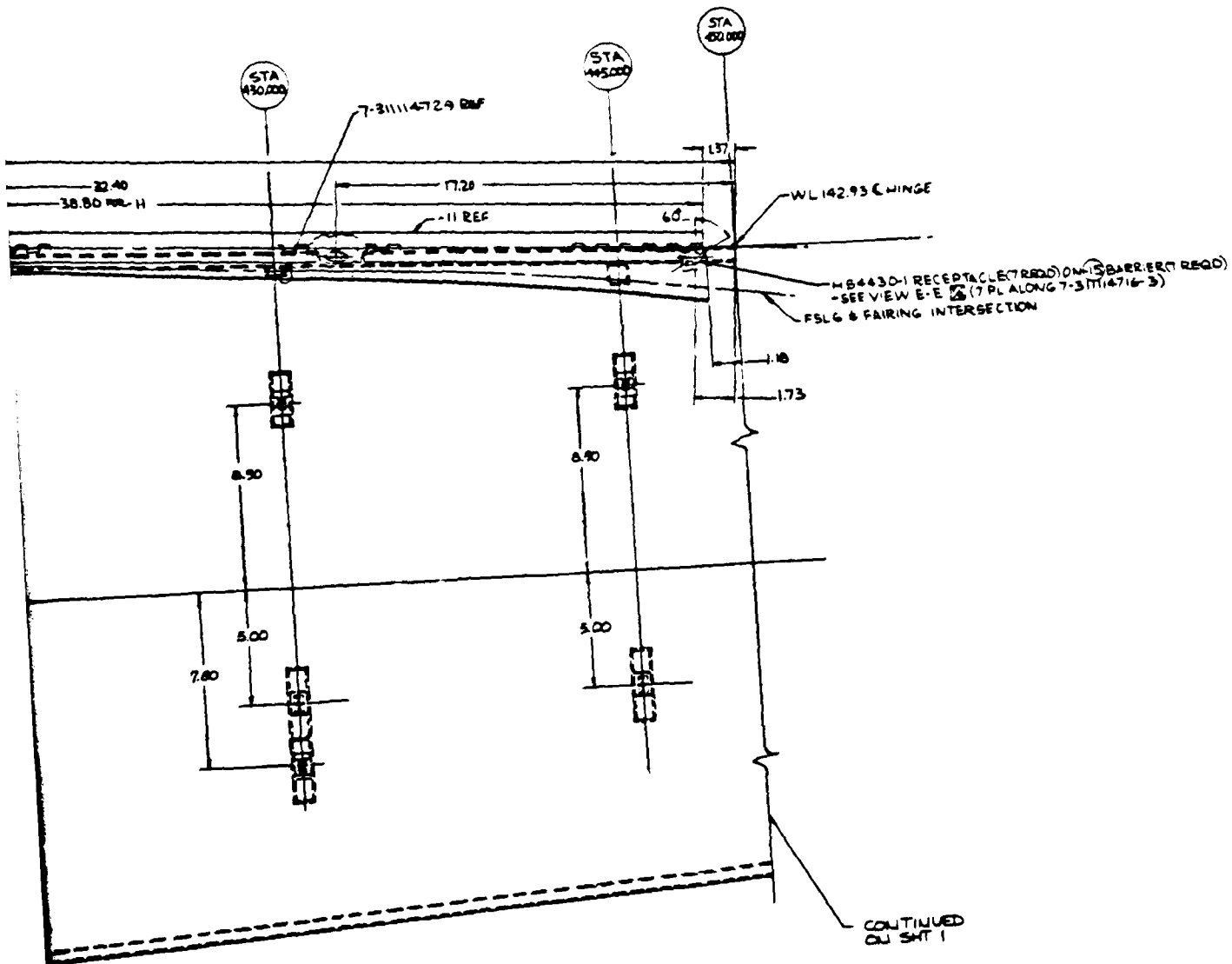
02731 J 02731

Hughes Helicopters
Division of Hughes Aircraft Company

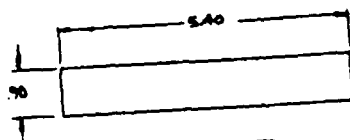
Figure 95. Tailboom Assembly (Sheet 1 of 3)







DETAIL -3



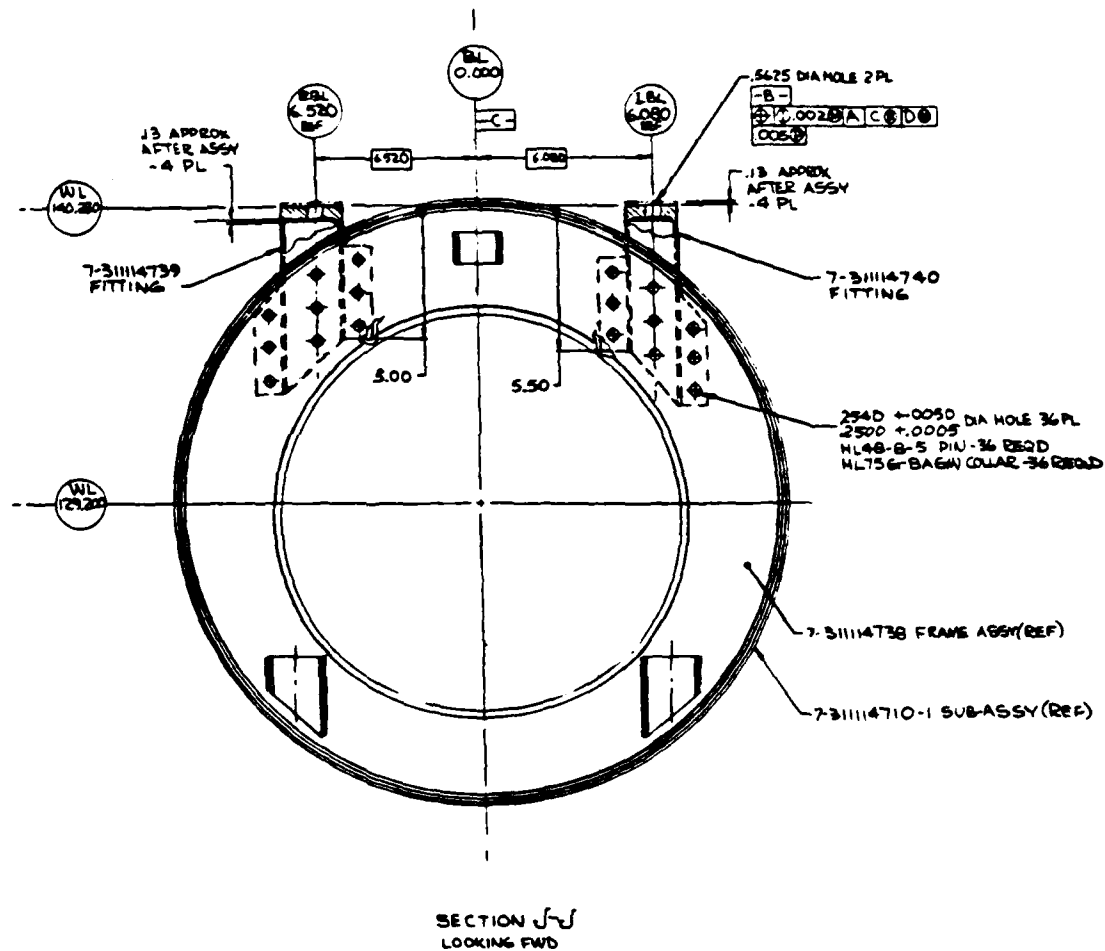
DETAIL -7

MS4430-1 RECEPTACLE (7 REQD) ON 15 BARRIER (7 REQD)
SEE VIEW E-E (7 PL ALONG 7-31114716-3)
6 & FAIRING INTERSECTION

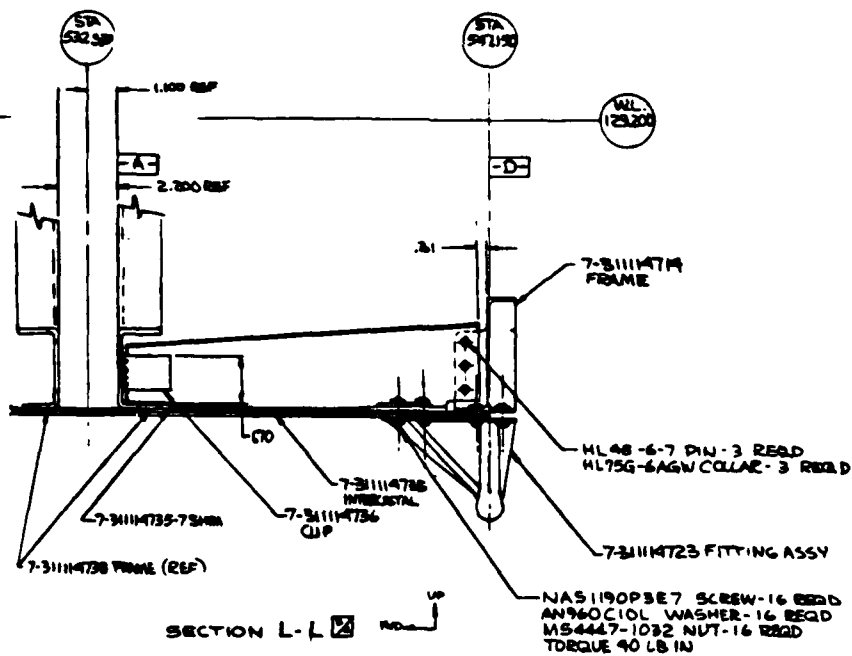
CONTINUED
PAGE 1

QTY	UNIT	DESCRIPTION	REMARKS
<div style="display: flex; justify-content: space-between;"> <div> <p>UNITED STATES OF AMERICA</p> <p>DEPARTMENT OF THE ARMY</p> <p>HEADQUARTERS, WASHINGTON, D.C.</p> </div> <div> <p>OFFICE OF THE CHIEF OF STAFF</p> <p>OFFICE OF THE ADJUTANT GENERAL</p> <p>OFFICE OF THE QUARTERMASTER GENERAL</p> </div> <div> <p>OFFICE OF THE ENGINEER</p> <p>OFFICE OF THE SIGNAL CORPS</p> <p>OFFICE OF THE MEDICAL DEPARTMENT</p> </div> </div>			

Figure 95. Tailboom Assembly (Sheet 2 of 3)

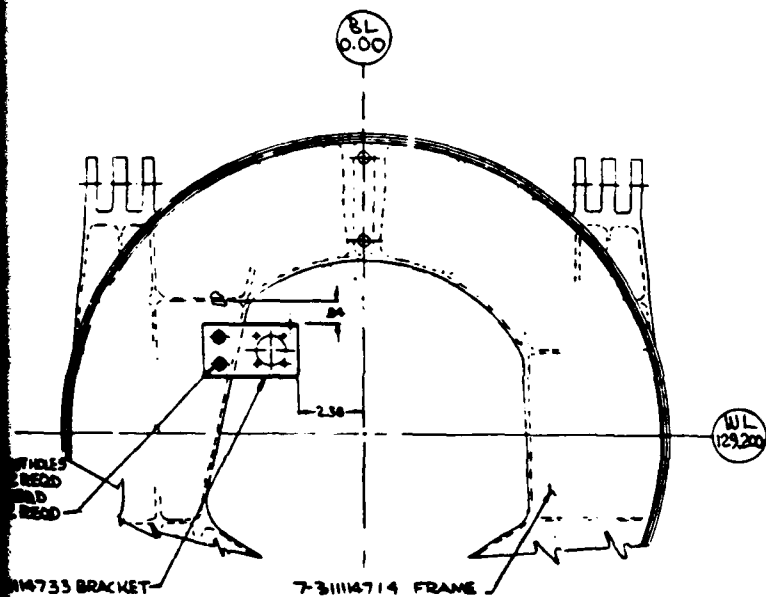


Y(REF)

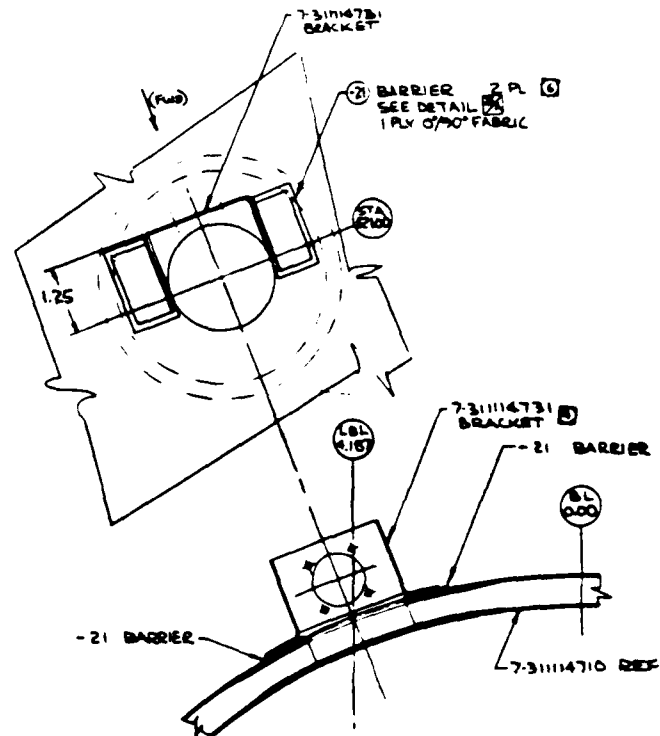


J4 H196 DIA 2 PLTHRU PUTHOLES
 MAG1635-3-4 SCREW 2 RECD
 MS21044 N3 NUT 2 RECD
 AN960C10 WASHER 2 RECD-

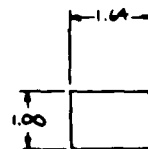
7-31114733 BRACKET-



SECTION H-H
LOOKING AFT



SECTION G-G
SCALE 1/1
LOOKING AFT



DETAIL -21
SCALE 1/1

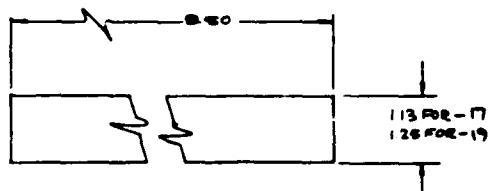
31114731
BRACKET

21 BARRIER 2 PL ②
SEE DETAIL ②
1 PLY 0/90° FABRIC

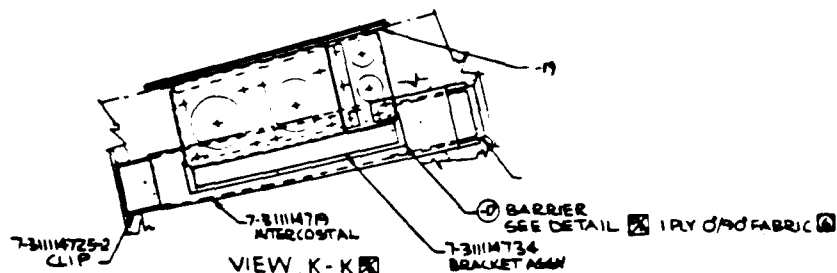
②
21

7-31114731 ②
BRACKET
21 BARRIER
②
0.00
7-31114710 REF

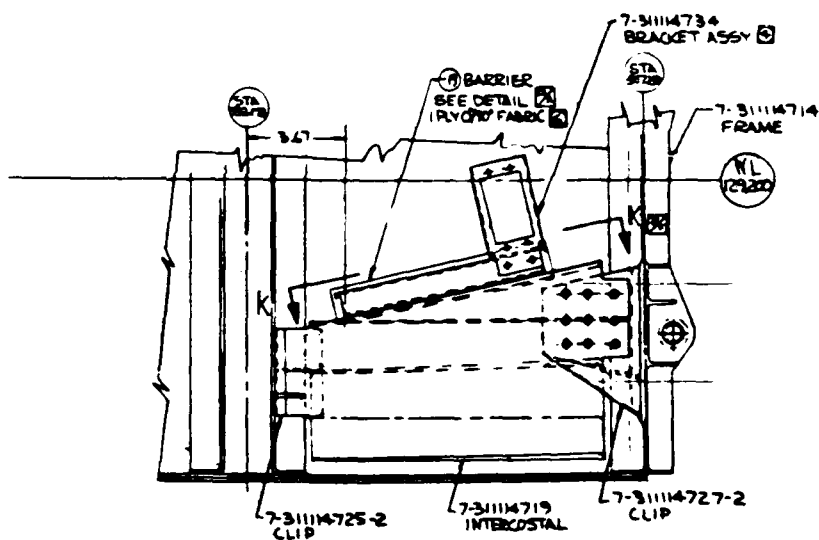
SECTION G-G ②
SCALE 1/1
LOOKING AFT



DETAIL -17 ② -19 ②
SCALE V



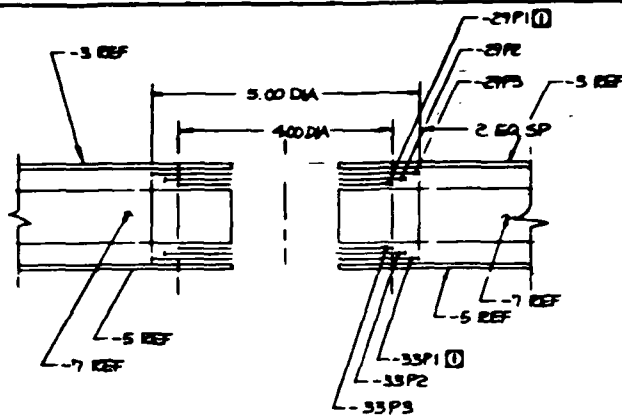
VIEW K-K ②



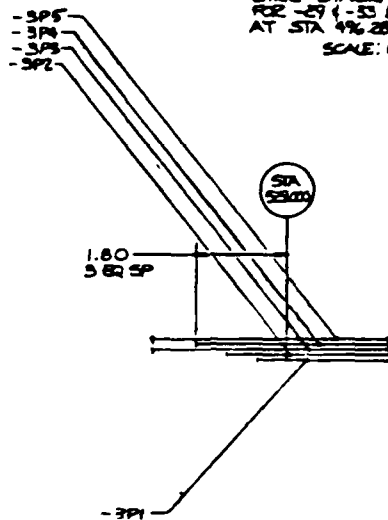
SECTION F-F ②

LIST OF MATERIAL		LIST OF MATERIAL	
ITEM NO.	DESCRIPTION	ITEM NO.	DESCRIPTION
1	7-31114734 BRACKET ASSY ②	1	7-31114734 BRACKET ASSY ②
2	7-31114714 FRAME	2	7-31114714 FRAME
3	21 BARRIER SEE DETAIL ② 1 PLY 0/90° FABRIC	3	21 BARRIER SEE DETAIL ② 1 PLY 0/90° FABRIC
4	7-31114725-2 CLIP	4	7-31114725-2 CLIP
5	7-31114719 INTERCOSTAL	5	7-31114719 INTERCOSTAL
6	7-31114727-2 CLIP	6	7-31114727-2 CLIP
7	7-31114731 BRACKET	7	7-31114731 BRACKET
8	7-31114710 REF	8	7-31114710 REF
9	7-31114725-2 CLIP	9	7-31114725-2 CLIP
10	7-31114719 INTERCOSTAL	10	7-31114719 INTERCOSTAL
11	7-31114727-2 CLIP	11	7-31114727-2 CLIP
12	7-31114731 BRACKET	12	7-31114731 BRACKET
13	7-31114710 REF	13	7-31114710 REF
14	7-31114725-2 CLIP	14	7-31114725-2 CLIP
15	7-31114719 INTERCOSTAL	15	7-31114719 INTERCOSTAL
16	7-31114727-2 CLIP	16	7-31114727-2 CLIP
17	7-31114731 BRACKET	17	7-31114731 BRACKET
18	7-31114710 REF	18	7-31114710 REF
19	7-31114725-2 CLIP	19	7-31114725-2 CLIP
20	7-31114719 INTERCOSTAL	20	7-31114719 INTERCOSTAL
21	7-31114727-2 CLIP	21	7-31114727-2 CLIP
22	7-31114731 BRACKET	22	7-31114731 BRACKET
23	7-31114710 REF	23	7-31114710 REF
24	7-31114725-2 CLIP	24	7-31114725-2 CLIP
25	7-31114719 INTERCOSTAL	25	7-31114719 INTERCOSTAL
26	7-31114727-2 CLIP	26	7-31114727-2 CLIP
27	7-31114731 BRACKET	27	7-31114731 BRACKET
28	7-31114710 REF	28	7-31114710 REF
29	7-31114725-2 CLIP	29	7-31114725-2 CLIP
30	7-31114719 INTERCOSTAL	30	7-31114719 INTERCOSTAL
31	7-31114727-2 CLIP	31	7-31114727-2 CLIP
32	7-31114731 BRACKET	32	7-31114731 BRACKET
33	7-31114710 REF	33	7-31114710 REF
34	7-31114725-2 CLIP	34	7-31114725-2 CLIP
35	7-31114719 INTERCOSTAL	35	7-31114719 INTERCOSTAL
36	7-31114727-2 CLIP	36	7-31114727-2 CLIP
37	7-31114731 BRACKET	37	7-31114731 BRACKET
38	7-31114710 REF	38	7-31114710 REF
39	7-31114725-2 CLIP	39	7-31114725-2 CLIP
40	7-31114719 INTERCOSTAL	40	7-31114719 INTERCOSTAL
41	7-31114727-2 CLIP	41	7-31114727-2 CLIP
42	7-31114731 BRACKET	42	7-31114731 BRACKET
43	7-31114710 REF	43	7-31114710 REF
44	7-31114725-2 CLIP	44	7-31114725-2 CLIP
45	7-31114719 INTERCOSTAL	45	7-31114719 INTERCOSTAL
46	7-31114727-2 CLIP	46	7-31114727-2 CLIP
47	7-31114731 BRACKET	47	7-31114731 BRACKET
48	7-31114710 REF	48	7-31114710 REF
49	7-31114725-2 CLIP	49	7-31114725-2 CLIP
50	7-31114719 INTERCOSTAL	50	7-31114719 INTERCOSTAL
51	7-31114727-2 CLIP	51	7-31114727-2 CLIP
52	7-31114731 BRACKET	52	7-31114731 BRACKET
53	7-31114710 REF	53	7-31114710 REF
54	7-31114725-2 CLIP	54	7-31114725-2 CLIP
55	7-31114719 INTERCOSTAL	55	7-31114719 INTERCOSTAL
56	7-31114727-2 CLIP	56	7-31114727-2 CLIP
57	7-31114731 BRACKET	57	7-31114731 BRACKET
58	7-31114710 REF	58	7-31114710 REF
59	7-31114725-2 CLIP	59	7-31114725-2 CLIP
60	7-31114719 INTERCOSTAL	60	7-31114719 INTERCOSTAL
61	7-31114727-2 CLIP	61	7-31114727-2 CLIP
62	7-31114731 BRACKET	62	7-31114731 BRACKET
63	7-31114710 REF	63	7-31114710 REF
64	7-31114725-2 CLIP	64	7-31114725-2 CLIP
65	7-31114719 INTERCOSTAL	65	7-31114719 INTERCOSTAL
66	7-31114727-2 CLIP	66	7-31114727-2 CLIP
67	7-31114731 BRACKET	67	7-31114731 BRACKET
68	7-31114710 REF	68	7-31114710 REF
69	7-31114725-2 CLIP	69	7-31114725-2 CLIP
70	7-31114719 INTERCOSTAL	70	7-31114719 INTERCOSTAL
71	7-31114727-2 CLIP	71	7-31114727-2 CLIP
72	7-31114731 BRACKET	72	7-31114731 BRACKET
73	7-31114710 REF	73	7-31114710 REF
74	7-31114725-2 CLIP	74	7-31114725-2 CLIP
75	7-31114719 INTERCOSTAL	75	7-31114719 INTERCOSTAL
76	7-31114727-2 CLIP	76	7-31114727-2 CLIP
77	7-31114731 BRACKET	77	7-31114731 BRACKET
78	7-31114710 REF	78	7-31114710 REF
79	7-31114725-2 CLIP	79	7-31114725-2 CLIP
80	7-31114719 INTERCOSTAL	80	7-31114719 INTERCOSTAL
81	7-31114727-2 CLIP	81	7-31114727-2 CLIP
82	7-31114731 BRACKET	82	7-31114731 BRACKET
83	7-31114710 REF	83	7-31114710 REF
84	7-31114725-2 CLIP	84	7-31114725-2 CLIP
85	7-31114719 INTERCOSTAL	85	7-31114719 INTERCOSTAL
86	7-31114727-2 CLIP	86	7-31114727-2 CLIP
87	7-31114731 BRACKET	87	7-31114731 BRACKET
88	7-31114710 REF	88	7-31114710 REF
89	7-31114725-2 CLIP	89	7-31114725-2 CLIP
90	7-31114719 INTERCOSTAL	90	7-31114719 INTERCOSTAL
91	7-31114727-2 CLIP	91	7-31114727-2 CLIP
92	7-31114731 BRACKET	92	7-31114731 BRACKET
93	7-31114710 REF	93	7-31114710 REF
94	7-31114725-2 CLIP	94	7-31114725-2 CLIP
95	7-31114719 INTERCOSTAL	95	7-31114719 INTERCOSTAL
96	7-31114727-2 CLIP	96	7-31114727-2 CLIP
97	7-31114731 BRACKET	97	7-31114731 BRACKET
98	7-31114710 REF	98	7-31114710 REF
99	7-31114725-2 CLIP	99	7-31114725-2 CLIP
100	7-31114719 INTERCOSTAL	100	7-31114719 INTERCOSTAL

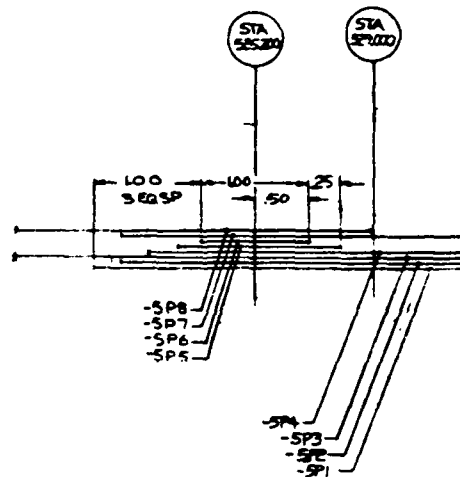
Figure 95. Tailboom Assem



LINE DIAGRAM II
FOR -29 (-33) DOUBLER
AT STA 496.28, 501.70 & 521.00
SCALE: NONE



LINE DIAGRAM I
-3 OUTER SKIN JOINT
@ STA 529.000
NO SCALE



LINE DIAGRAM II
-5 INNER SKIN JOINT
@ STA 529.000
NO SCALE

P3	345°	6	0	.07
P2	070°	6	0	.07
P1	070°	6	0	.07
PLY NO	ORBIT	MATL	PLY THK	

STACKING SEQUENCE
FOR -29 DOUBLER
AT STA 496.28, 501.70 & 521.00
TABLE 4

P3	070°	6	0	.07
P2	070°	6	0	.07
P1	345°	6	0	.07
PLY NO	ORBIT	MATL	PLY THK	

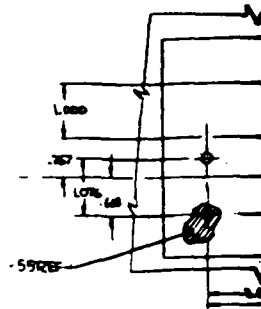
STACKING SEQUENCE
FOR -3 DOUBLER
AT STA 496.28, 501.70 & 521.00
TABLE 3

P5	90°	8	0	.00
P4	345°	8	0	.017
P3	5°	8	0	.020
P2	345°	8	0	.017
P1	345°	8	0	.017
PLY NO	ORBIT	MATL	PLY THK	

STACKING SEQUENCE
FOR -3 OUTER SKIN
AT STA 370.00
TABLE 1

P10	90°	8	0	.010
P9	345°	8	0	.017
P8	070°	8	0	.017
P7	070°	8	0	.017
P6	345°	8	0	.017
P5	345°	8	0	.017
P4	070°	8	0	.017
P3	345°	8	0	.020
P2	345°	8	0	.017
P1	90°	8	0	.010
PLY NO	ORBIT	MATL	PLY THK	

STACKING SEQUENCE
FOR -5 INNER SKIN
AT STA 520.00
TABLE 2



STA 496.28

STA 525.00

STA 527.00

STA 529.00

STA 531.00

STA 533.00

STA 535.00

STA 537.00

STA 539.00

STA 541.00

STA 543.00

STA 545.00

STA 547.00

STA 549.00

STA 551.00

STA 553.00

STA 555.00

STA 557.00

STA 559.00

STA 561.00

STA 563.00

STA 565.00

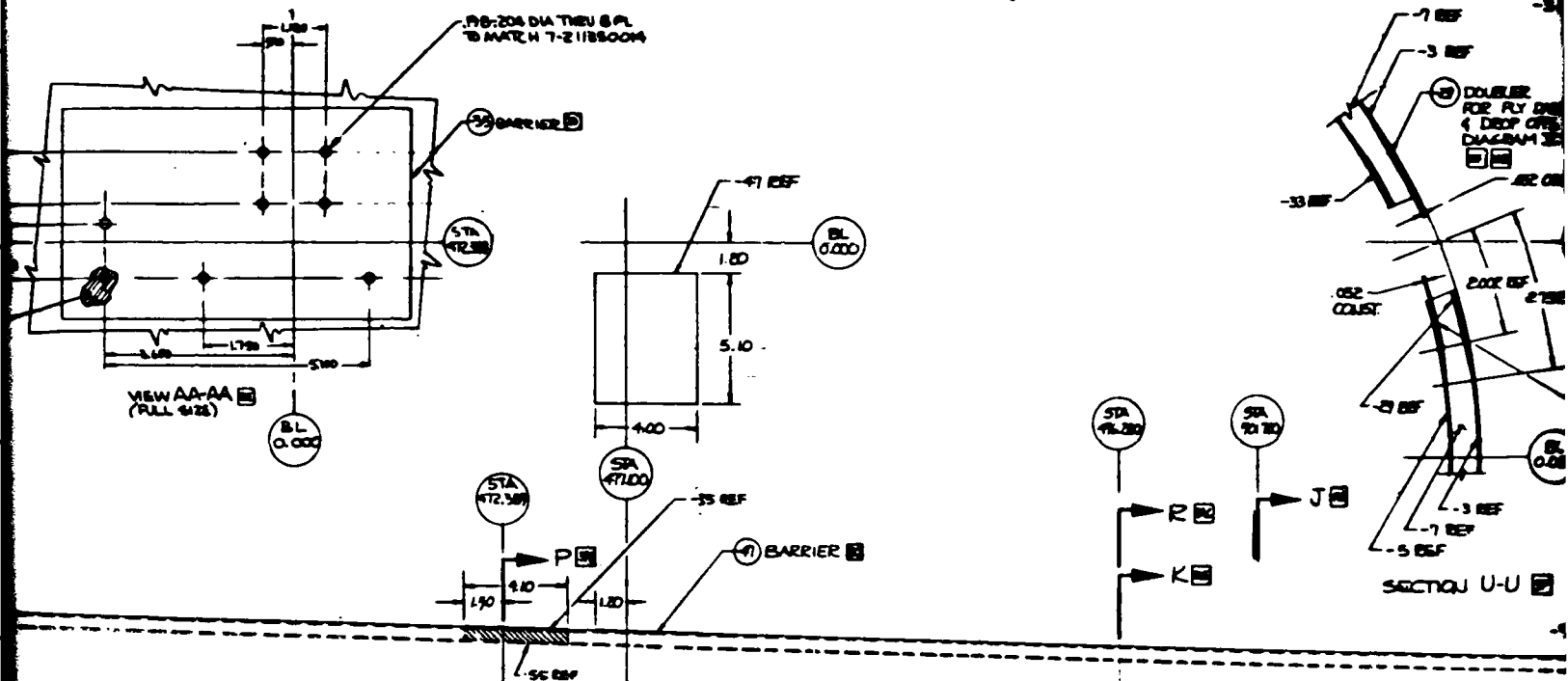
STA 567.00

STA 569.00

STA 571.00

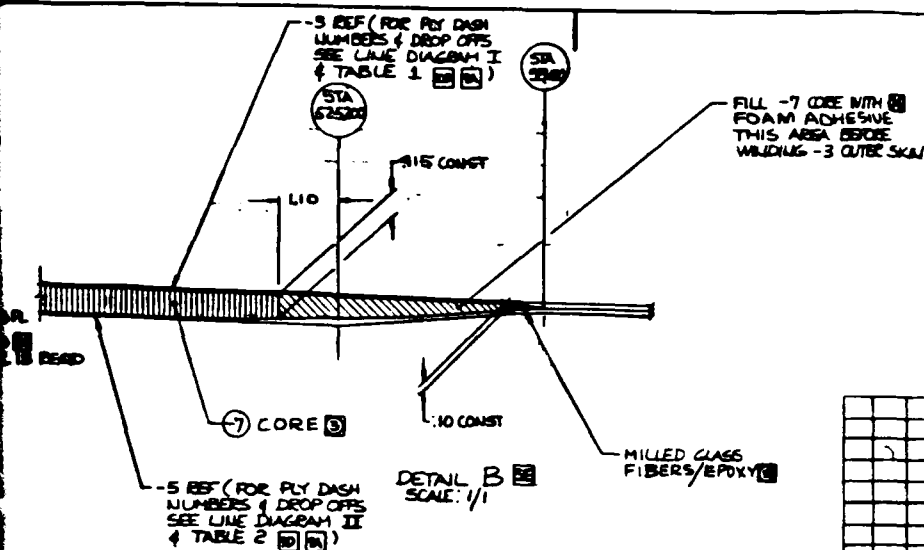
STA 573.00

CONTINUED ON SHEET 2



CONTINUED
ON SHT 2

VIEW LOOKING INBD
BSC ASSY



SEE 978 DA CONSULT TO STA 527.00

1. SOL FASTENERS PER HP 8-10 TYPE II
2. HYBRID - 58 LB. DENSITY ALUMINUM MATERIAL - AMERICAN OXIDANT CO., BLOOMINGDALE PLANT, HANDE DE GRACE, M.D. 21078
3. 50% VOLUME GRAPHITE ROVING & 50% VOLUME KEVLAR ROVING (.020 TOTAL PLY THK)
4. 50% VOLUME GRAPHITE ROVING & 50% VOLUME KEVLAR ROVING (.010/PLY)
5. HMS 16-1060 PASTE ADHESIVE CL 3. APPLY PER HP 6-5
6. HMS 16-1111 FILM ADHESIVE, CL 3
7. MILLED GLASS FIBERS/EPDXY 1/2 LENGTH THALCO, LA
8. FINISH EXTERIOR ONLY CODE E PER EPB 4-230
9. IDENTIFY PER HP 8-5 TYPE I, CL 3 LOC OPT
10. DIMENSIONING & TOLERANCING PER ANSI Y14.5
11. FOAM ADHESIVE PER HMS 16-1111, CL 4
12. E-GLASS FABRIC MIL-C-9084 TYPE III, A CL 2 (.010/PLY)
13. LAYUP PER HP 15-42
14. CORE (NOMEX) HMS 16-1114 TYPE II, CL 1
15. INSTALL HI-LOK FASTENERS PER HP 3-2
16. FOR LOFT LINES SEE DNG 7-11111310105105200
17. EPOXY RESIN SYSTEM HMS 16-1115 TYPE I, CL 1
18. E-GLASS ROVING MIL-R-60946 TYPE I, CL 1 (.010/PLY)
19. GRAPHITE FABRIC HMS 16-1163 TYPE II, CL 1 GR A (.01/PLY)
20. GRAPHITE ROVING HMS 16-1163 TYPE I, CL 1
21. KEVLAR ROVING HMS 16-1164 TYPE I, CL 3
22. FILM ADHESIVE BOND PER HP 16-30
23. FILAMENT WIND PER HP 15-67
24. FIRST PLY GOES AGAINST TOOL FACE

NOTES UNLESS OTHERWISE SPECIFIED

1	-63	DOUBLER	AR	00
1	-61	DOUBLER	AR	00
1	-59	DOUBLER	AR	000
1	-57	DOUBLER	AR	000
18	N225	HL756-6AGW	COLLAR	
18	N225	HL756-6AGW	COLLAR	
18	N215	HLAB-6-7	PIN	
18	N215	HLAB-6-5	PIN	
AR	HMS 16-1111, CL 3	FILM ADHESIVE		
4	SL601-3-3CM	INSERT		
AR	HMS 1068, CL 3	PASTE ADHESIVE		
2	7-311114737	INSERT		
1	7-311114727-2	LOWER FITTING		
1	7-311114727-1	LOWER FITTING		
1	7-311114726	UPPER FITTING		
1	7-311114725-2	UPPER CLIP		
1	7-311114725-1	LOWER CLIP		
1	7-311114724-2	UPPER CLIP		
1	7-311114722	FRAME		
1	7-311114719-2	INNER INTERSTITIAL		
1	7-311114719-1	INNER INTERSTITIAL		
1	7-311114718	UPPER INTERSTITIAL		
2	7-311114736	SHARP CLIP		
1	7-311114735	INTERSTITIAL		
1	7-311114738	FRAME ASBY		
1	-55	WEDGE		
1	-52	DOUBLER		
2	-51	DOUBLER		
1	-49	DOUBLER		
1	-47	BARRIER		
1	-45	BARRIER		
1	-43	BARRIER		
1	-41	DOUBLER		
1	-39	BARRIER		
1	-37	BARRIER		
1	-35	BARRIER		
3	-33	DOUBLER		
1	-31	DOUBLER		
3	-29	DOUBLER		
2	-27	BARRIER		
1	-25	PAD		
1	-23	BARRIER		
21	-21	INSERT ASBY		
2	-19	BARRIER		
1	-17	PAD		
8	-15	INSERT ASBY		
4	-13	BARRIER		
4	-9	BARRIER		
1	-7	CORE	AR	
1	-5	INNER SKIN	AR	
1	-3	OUTER SKIN	AR	

QTY REQD		PART NO.		DATE		REVISION	
1	7-311114700						
ITEM NO		ITEM NAME		ITEM QTY		ITEM UNIT	
1	7-311114700						
APPROVED		DATE		BY		FOR	
02731		J		02/23/10		02/23/10	

Figure 96. Tailboom Subassembly (Sheet

FOR RY DASH
REDS & DROP OFFS
LINE DIAGRAM I
TABLE 1

SA
3040

115 CONST

FILL -7 CORE WITH
FOAM ADHESIVE
THIS AREA BEFORE
WINDING -3 OUTER SKIN

10 CONST

DETAIL B
SCALE: 1/1

MILLED GLASS
FIBERS/EPXY

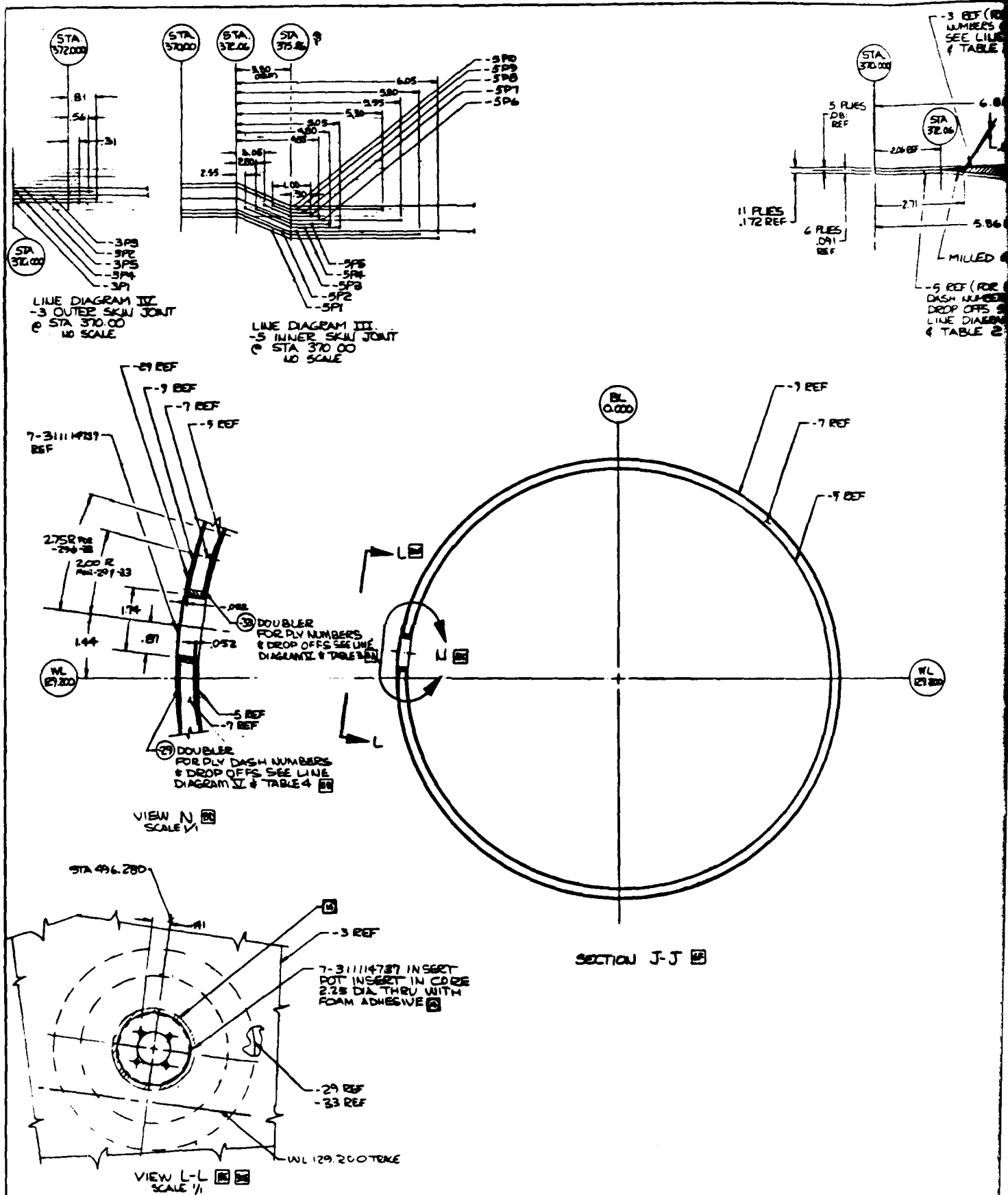
1. 50% FASTENERS PER HP 8-10 TYPE II
2. WIND: 55 LB. DENSITY ALUMINUM MATERIAL -
AMERICAN ORNITHO CO., BLOOMINGDALE PLANT,
HAYES DE GRACE, MD. 21078
3. 50% VOLUME GRAPHITE ROVING &
50% VOLUME KEVLAR ROVING (.020 TYPICAL)
4. 50% VOLUME GRAPHITE ROVING &
50% VOLUME KEVLAR ROVING (.010/PLY)
5. HMS 16-1068 PASTE ADHESIVE CL 3. APPLY PER HP 16-5
6. HMS 16-1111 FILM ADHESIVE, CL 3
7. MILLED GLASS FIBERS/EPXY 1/2 IN. QUANTITY
THALCO, CA
8. FINISH EXTERIOR ONLY
CODE E PER EPB 4-230
9. IDENTIFY PER HPB-5 TYPE I, CL 3 LOC OPT
10. DIMENSIONING & TOLERANCING
PER ANSI Y14.5
11. FOAM ADHESIVE PER
HMS 16-1111, CL 4
12. E-GLASS FABRIC
MIL-C-9084 TYPE III, A CL 2 (.010/PLY)
13. LAYUP PER HP 15-42
14. CORE (NOMEX)
HMS 16-1114 TYPE II, CL 1
15. INSTALL HI-LOK FASTENERS PER HP 3-2
16. FOR LOFT LINES SEE DNG 7-1111131010505200
17. EPOXY RESIN SYSTEM
HMS 16-1119
TYPE I, CL 1
18. E-GLASS ROVING
MIL-R-60946
TYPE I, CL 1 (.00/PLY)
19. GRAPHITE FABRIC
HMS 16-1162 TYPE II, CL 1 GR A (.01/PLY)
20. GRAPHITE ROVING
HMS 16-1163 TYPE I, CL 1
21. KEVLAR ROVING
HMS 16-1164 TYPE I, CL 3
22. FILM ADHESIVE BOLD PER HP 16-30
23. FILAMENT WIND PER HP 15-67
24. FIRST PLY GOES AGAINST TOOL FACE

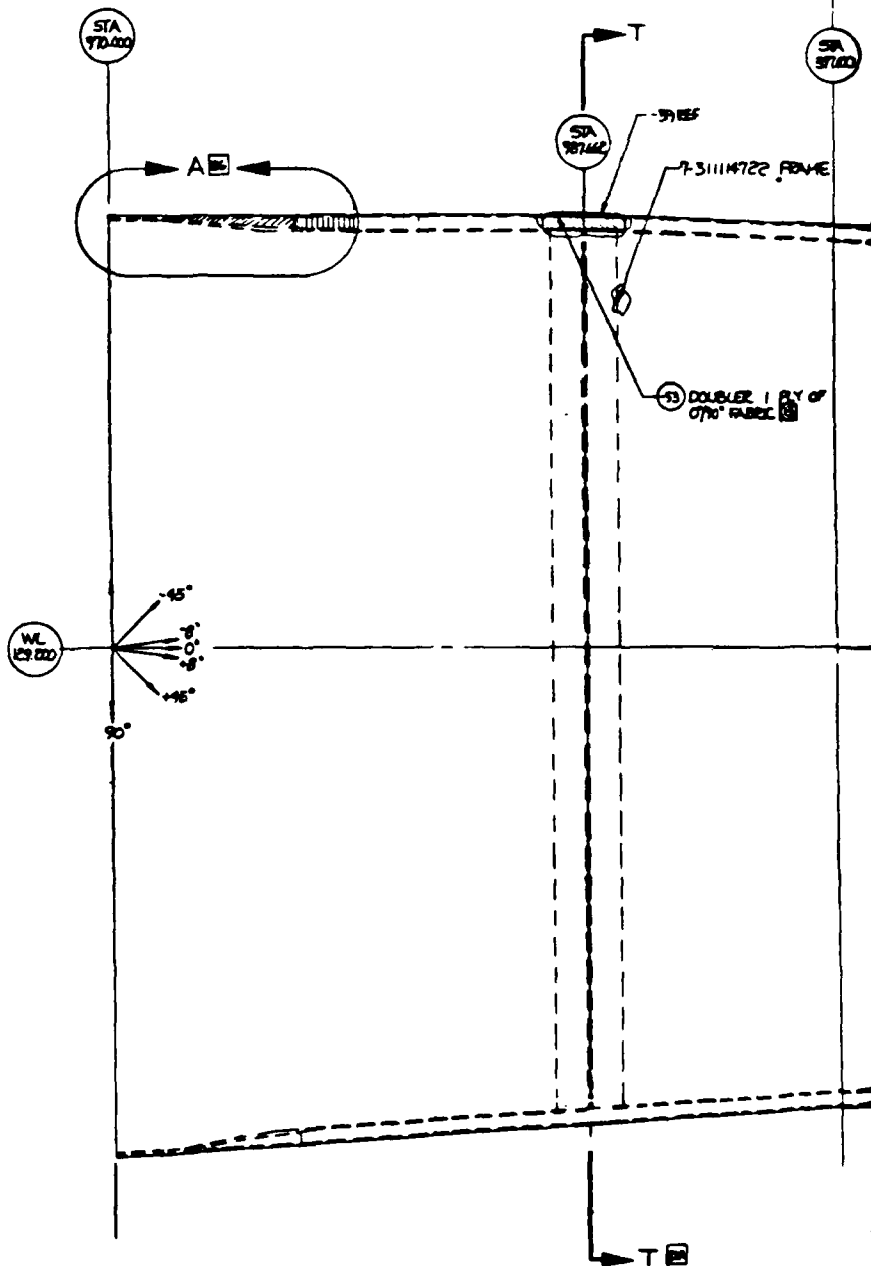
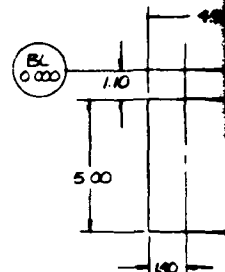
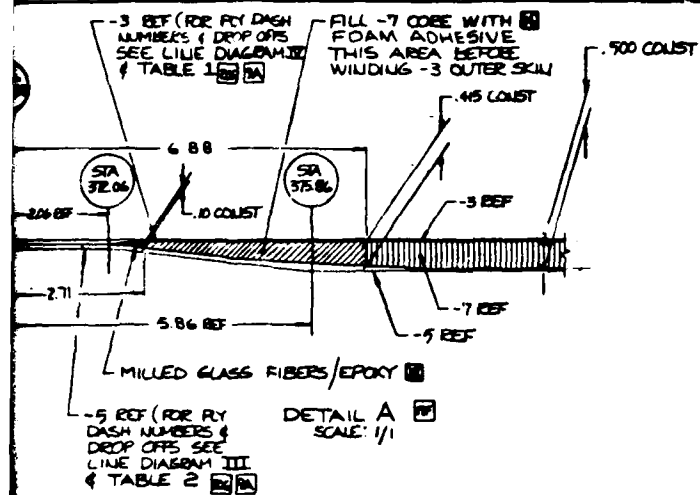
1	-63	DOUBLER	AR	000	33F
1	-61	DOUBLER	AR	000	33C
1	-59	DOUBLER	AR	000	33E
1	-57	DOUBLER	AR	000	33E
18	11215	HL756-BAGW	COLLAR		46
18	11215	HL756-BAGW	COLLAR		4C
18	11215	HLAB-6-7	PIN		46
18	11215	HLAB-6-5	PIN		4C
AR	HMS 16-1111, CL 3	FILM ADHESIVE			
4	SL601-3-3CM	INSERT			33A
AR	HMS 1068, CL 3	PASTE ADHESIVE			
2	7-311114737	INSERT			33A
1	7-311114727-2	LOWER FITTING			33C
1	7-311114727-1	LOWER FITTING			4C
1	7-311114726	UPPER FITTING			4D
1	7-311114725-2	LOWER CLIP			33C
1	7-311114725-1	LOWER CLIP			33C
1	7-311114724-2	UPPER CLIP			4H
1	7-311114722	FRAME			46F
1	7-3111147219-2	LOWER INTERSTIAL			33C
1	7-311114719-1	LOWER INTERSTIAL			4D
1	7-311114718	UPPER INTERSTIAL			4D
2	7-311114786	SHARP CLIP			33C
1	7-311114735	INTERSTIAL			33C
1	7-311114738	FRAME RESIN			4A
1	-55	WEDGE			33E
1	-50	DOUBLER			16E
2	-51	DOUBLER			13B
2	-49	DOUBLER			13E
1	-47	BARRIER			7F
1	-45	BARRIER			46F
1	-43	BARRIER			15F
1	-41	DOUBLER			46E
1	-39	BARRIER			46F
1	-37	BARRIER			46E
1	-35	BARRIER			7E
3	-33	DOUBLER			46F
1	-31	DOUBLER			16E
3	-29	DOUBLER			6F
2	-27	BARRIER	3/4"		24D
1	-25	PAD	3/4"		24D
1	-23	BARRIER			35B
21	-21	INSERT ASSEMBLY			37F
2	-19	BARRIER	1"		18E
1	-17	PAD	1"		24E
8	-15	INSERT ASSEMBLY			22E
4	-13	BARRIER			24D
4	-9	BARRIER			34B
1	-7	CODE	AR	000	33C
1	-5	INNER SKIN	AR	00000	5F
1	-3	OUTER SKIN	AR	00000	5E

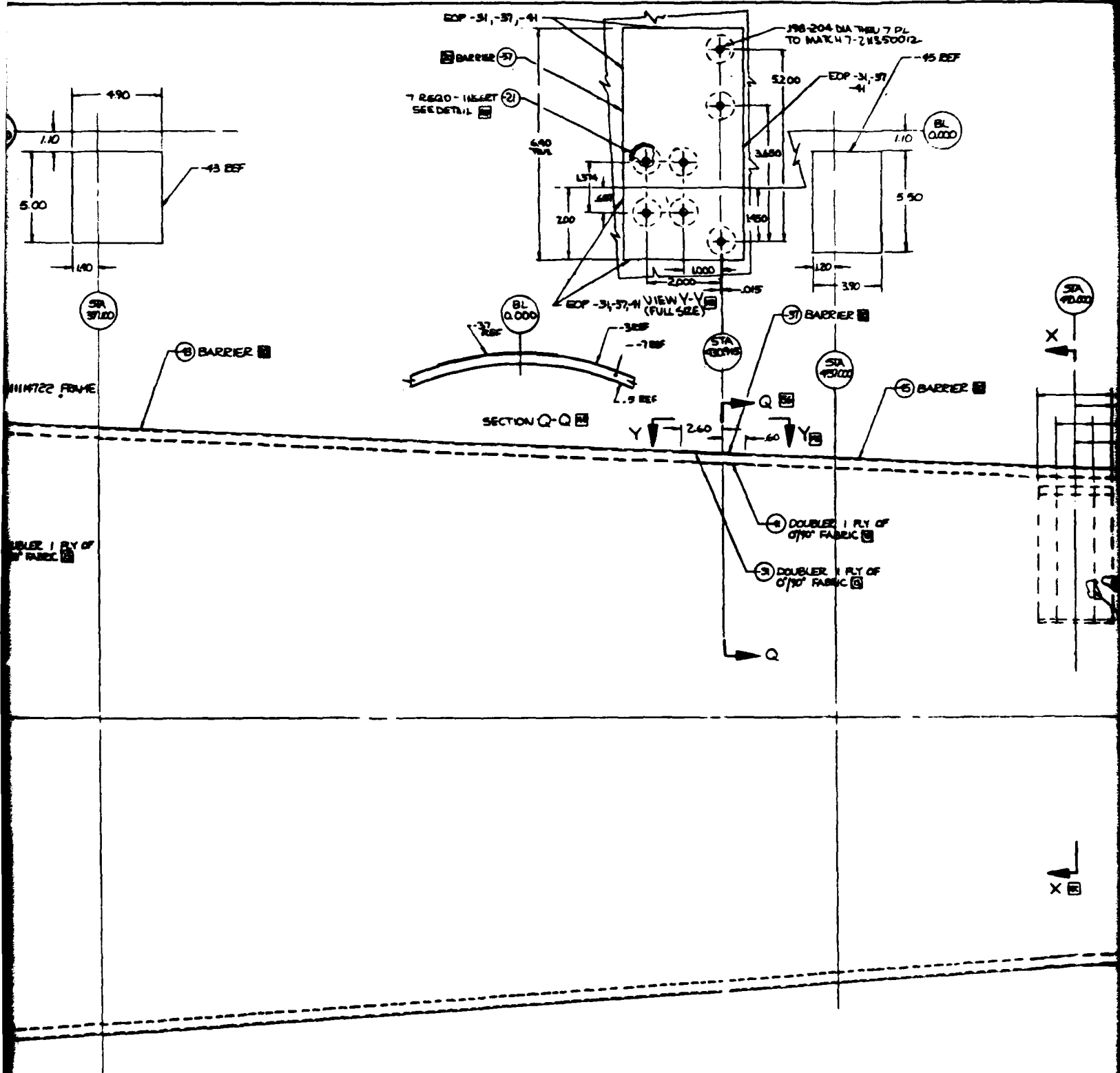
UNLESS OTHERWISE SPECIFIED

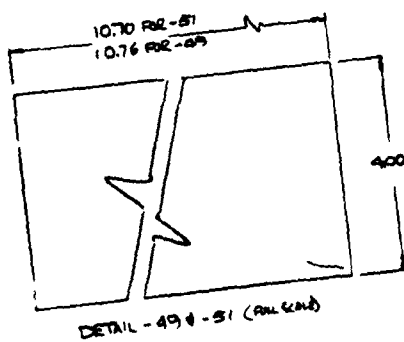
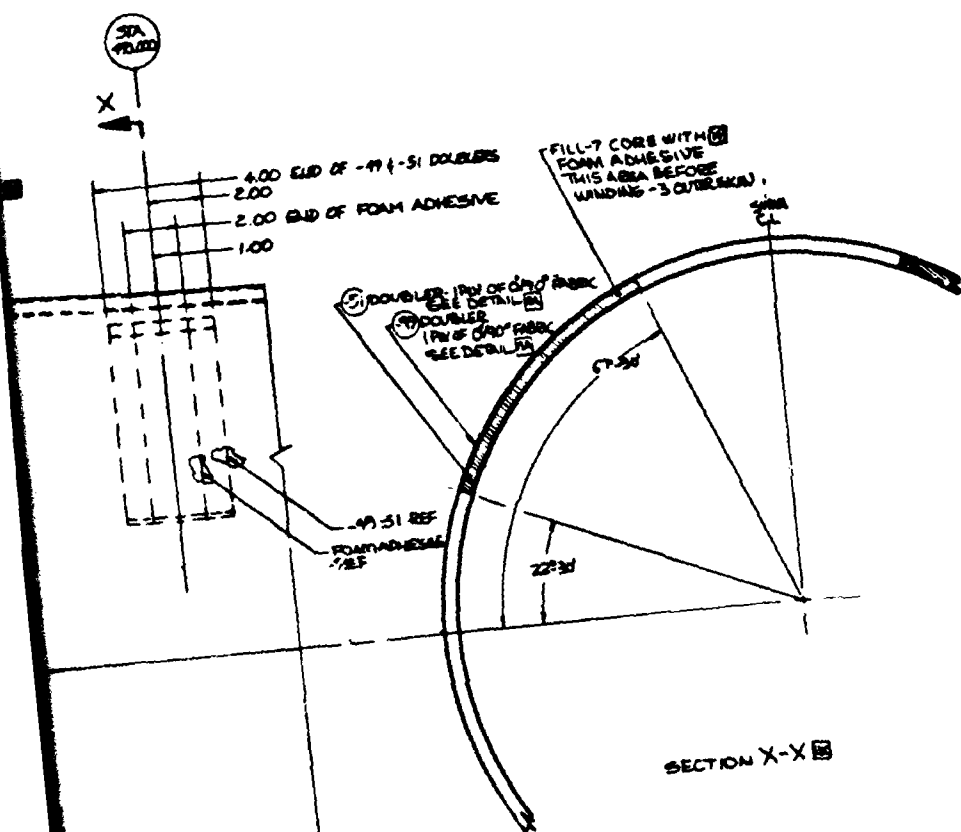
BY: 7-311114700 DATE: 11/77		CHECKED: [Signature] DATE: 11/77	
APPROVED: [Signature] DATE: 11/77		APPROVED: [Signature] DATE: 11/77	
PART NO. 02731		REV. 1	

Figure 96. Tailboom Subassembly (Sheet 1 of 4)





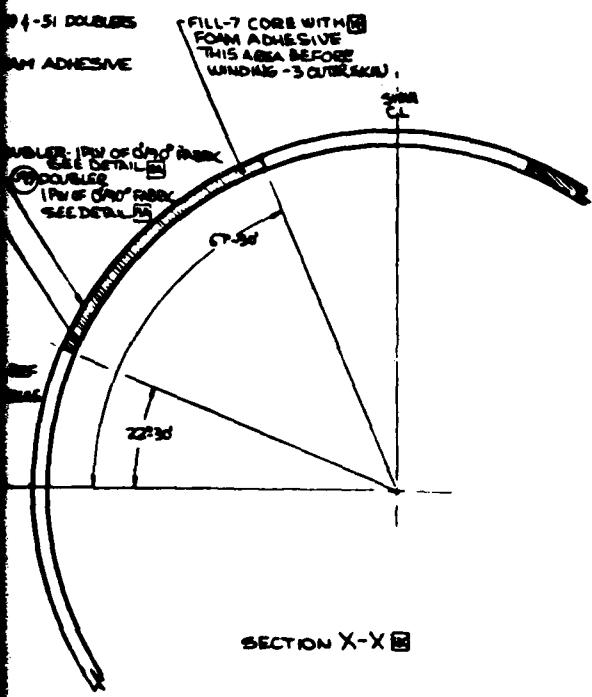




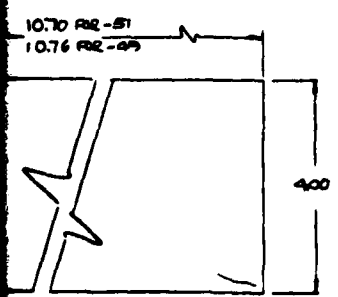
PART NO.		REV	DATE	DESCRIPTION
02731		J		

NO.	DESCRIPTION	DATE	BY	CHKD
1	DESIGNED BY			
2	CHECKED BY			
3	APPROVED BY			

Figure 96. Tailboom Subassembly (Sheet 175)



SECTION X-X



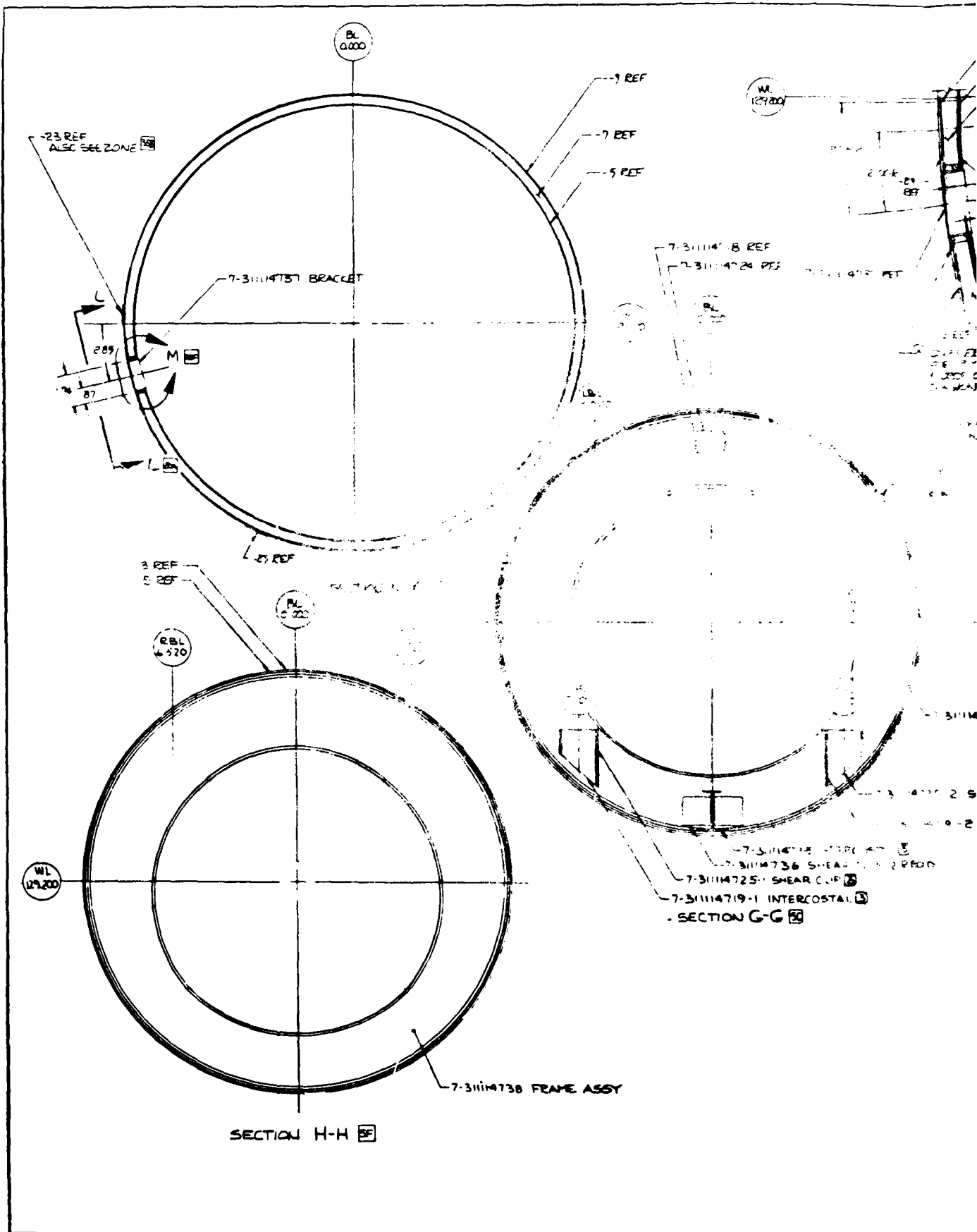
TAIL - 49 - 51 (PWA 6446)

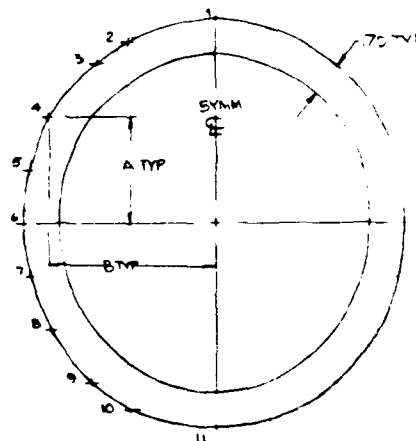
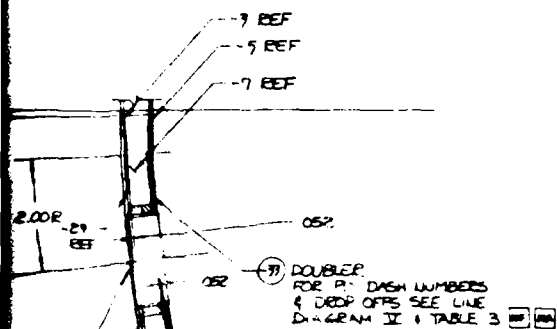
REV		DESCRIPTION	DATE	BY	CHKD	APP'D
1	0	ISSUED FOR CONSTRUCTION	10/1/51	J		
2	1	REVISION				
3	2	REVISION				
4	3	REVISION				
5	4	REVISION				
6	5	REVISION				
7	6	REVISION				
8	7	REVISION				
9	8	REVISION				
10	9	REVISION				

REV	DESCRIPTION	DATE	BY	CHKD	APP'D
1	ISSUED FOR CONSTRUCTION	10/1/51	J		
2	REVISION				
3	REVISION				
4	REVISION				
5	REVISION				
6	REVISION				
7	REVISION				
8	REVISION				
9	REVISION				
10	REVISION				

REV	DESCRIPTION	DATE	BY	CHKD	APP'D
1	ISSUED FOR CONSTRUCTION	10/1/51	J		
2	REVISION				
3	REVISION				
4	REVISION				
5	REVISION				
6	REVISION				
7	REVISION				
8	REVISION				
9	REVISION				
10	REVISION				

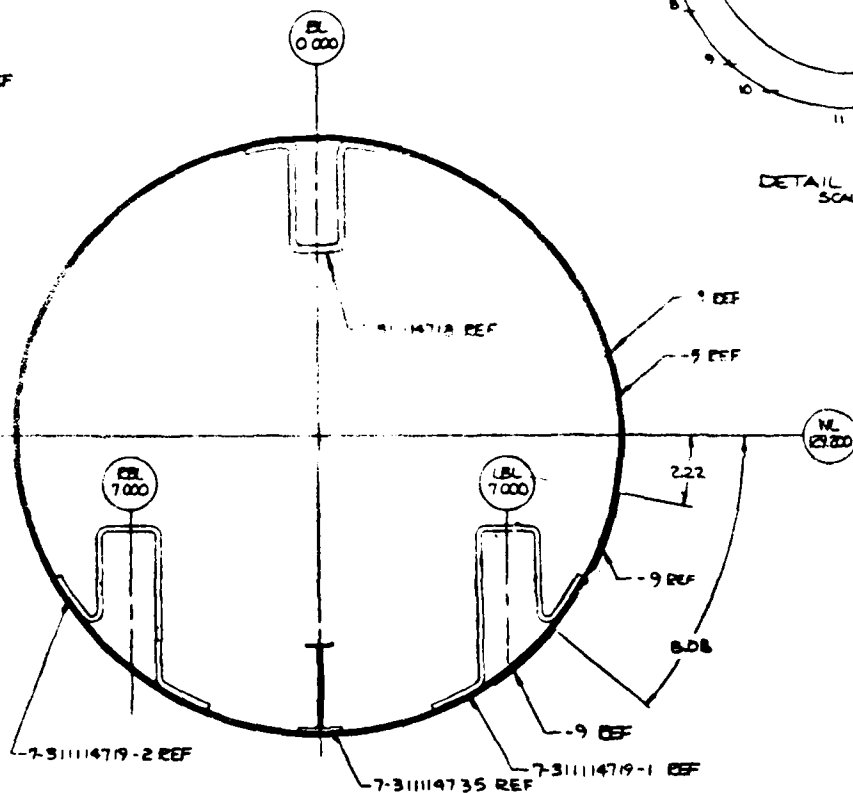
Figure 96. Tailboom Subassembly (Sheet 2 of 4)



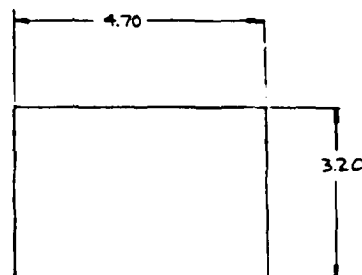


DIMENSION	
1	3.80 6
2	3.50 40
3	3.00 220
4	2.00 3.08
5	1.00 3.44
6	1.00 3.66
7	1.00 3.44
8	2.00 3.08
9	3.00 2.32
10	3.50 64
11	3.80 6

DETAIL -29
SCALE 1/1



SECTION E-E
SECTION F-F



DETAIL -13
SCALE 1/1

AD-A121 172

MANUFACTURING METHODS AND TECHNOLOGY (MANTECH) PROGRAM
MANUFACTURING TECH. (U) HUGHES HELICOPTERS INC CULVER
CITY CA J V ALEXANDER ET AL. OCT 81 HHI-81-367
UNCLASSIFIED USAAVRADCOM-TR-82-F-1 DAAK50-78-G-0004

F/G 1/3

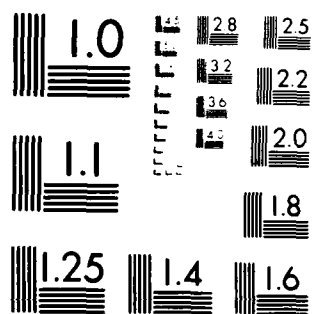
NL

3/3

END

FILED

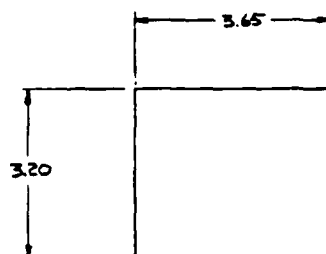
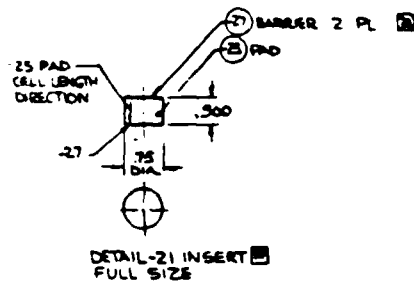
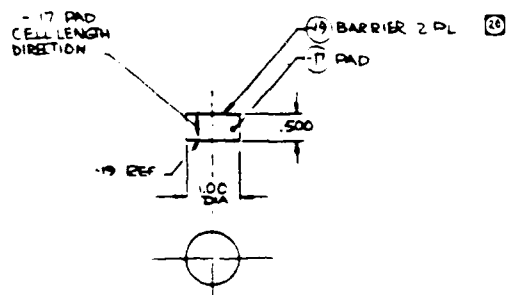
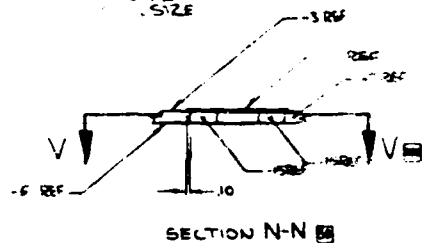
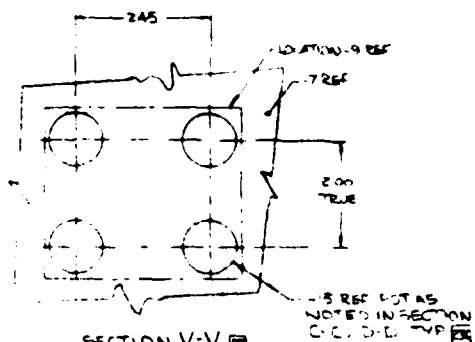
PER



MICROCOPY RESOLUTION TEST CHART
NATIONAL BUREAU OF STANDARDS-1963-A

370 TYP

	A	B
1	3.80	Ø
2	3.50	1.40
3	3.00	2.20
4	2.00	3.08
5	1.00	3.84
6	Ø	3.66
7	1.00	3.64
8	2.00	3.08
9	3.00	2.32
10	3.50	1.64
11	3.80	Ø



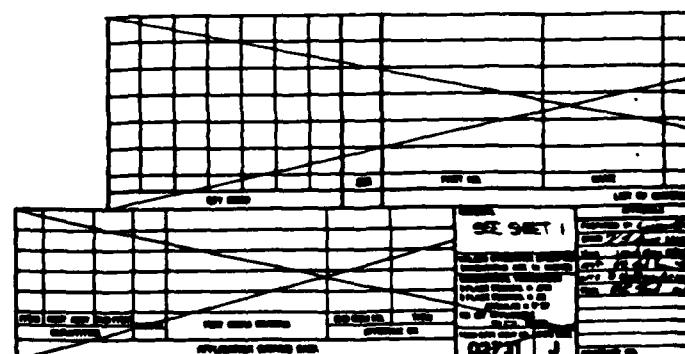
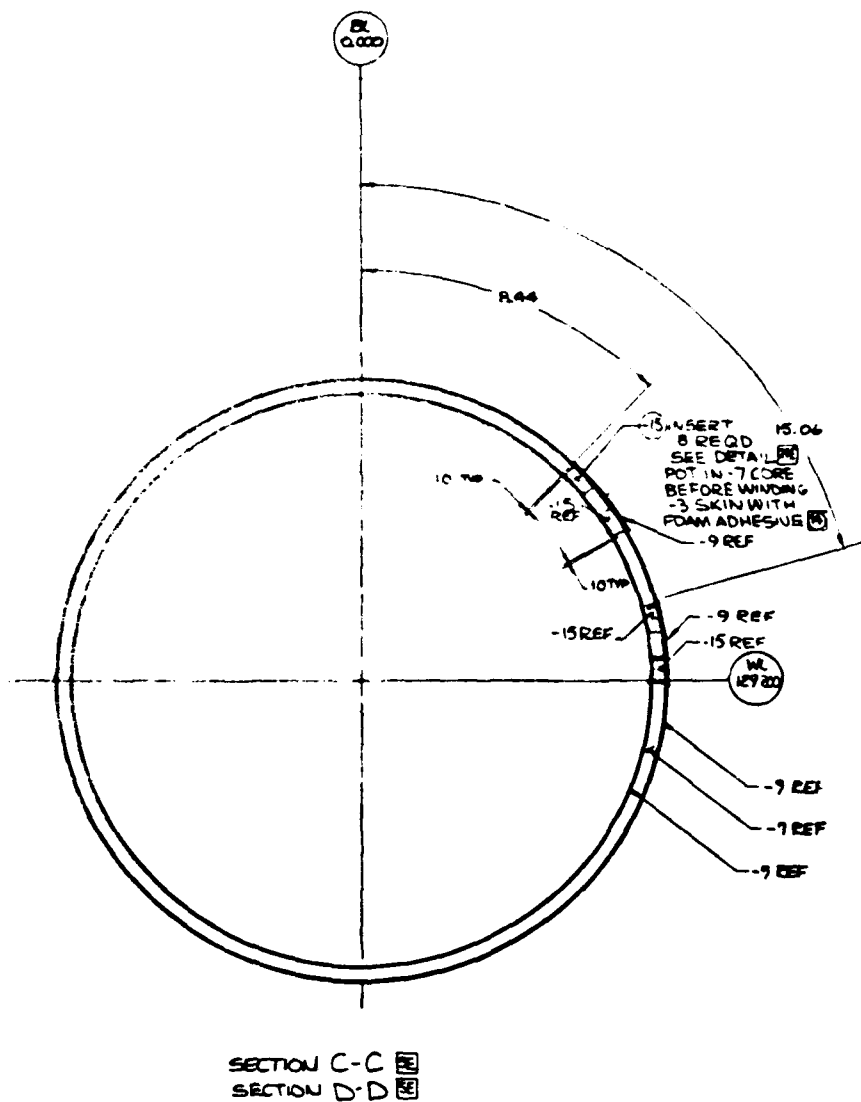
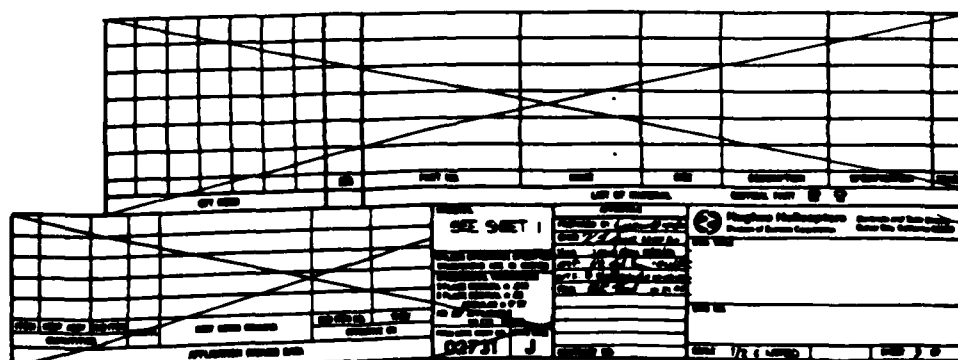
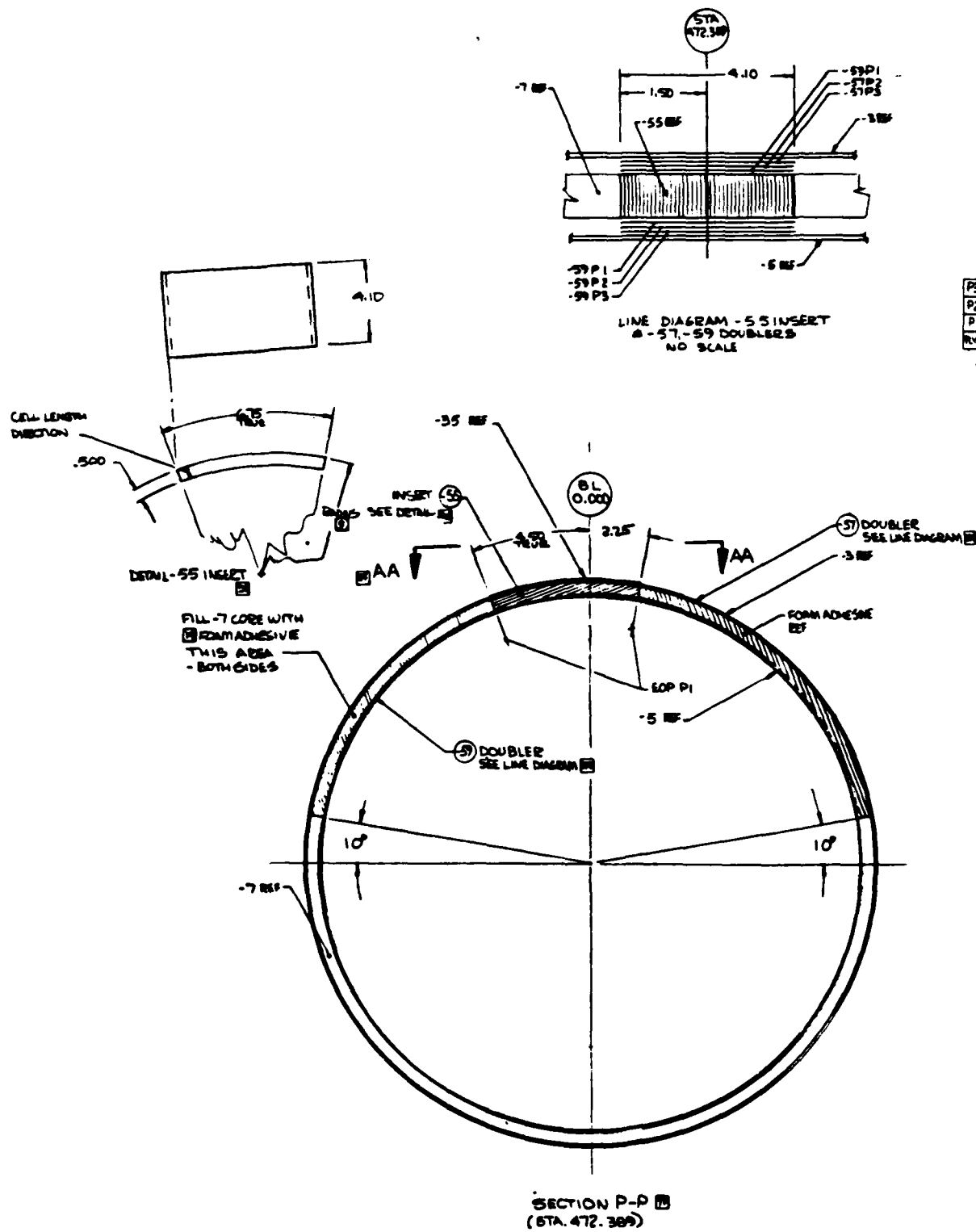


Figure 96. Tailboom Subas



177

5

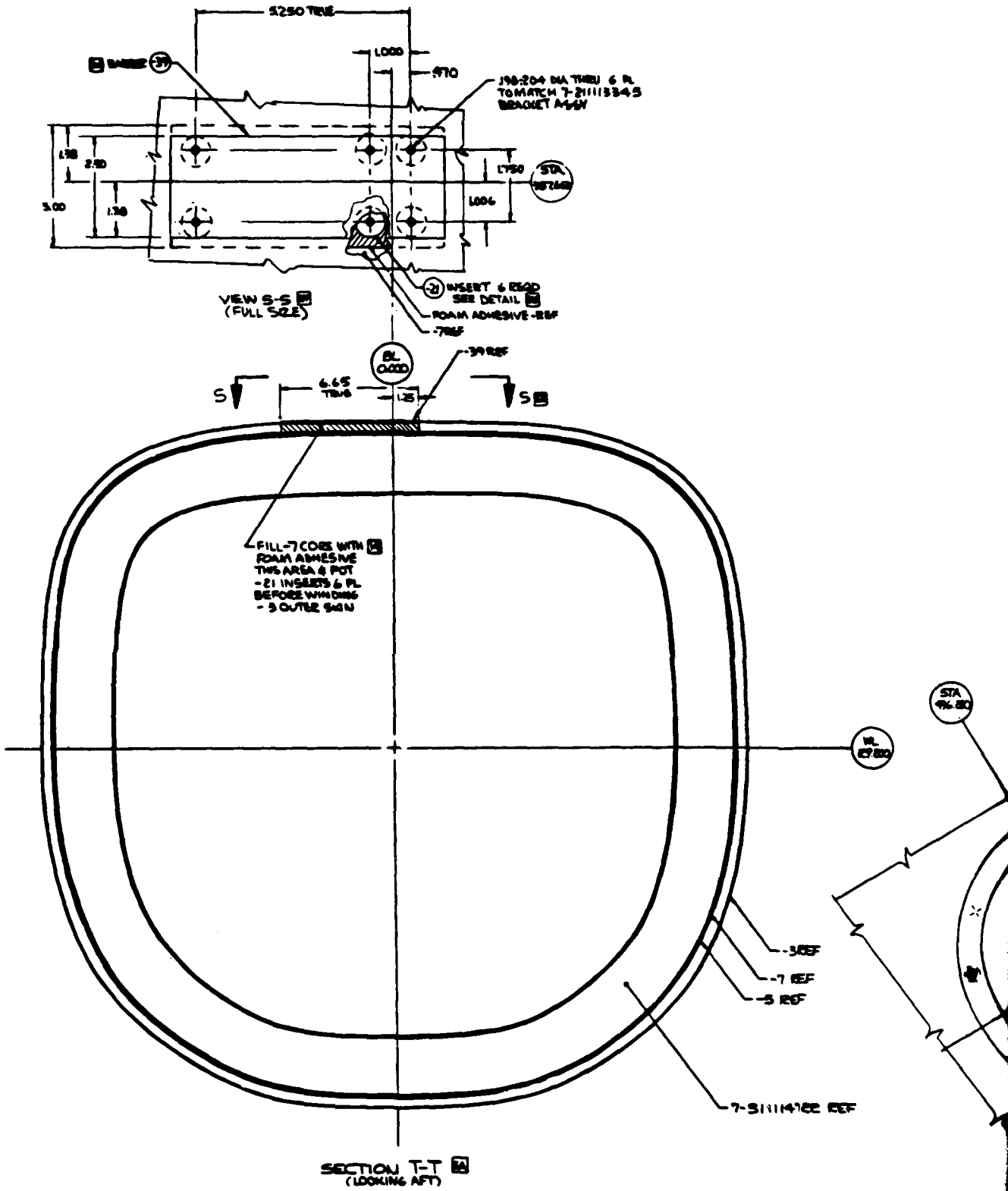


P3	145°	0	U	2
P2	90°	0	U	2
P1	0/90°	0	U	2
RV NO	ORIENT	NATL	IN	

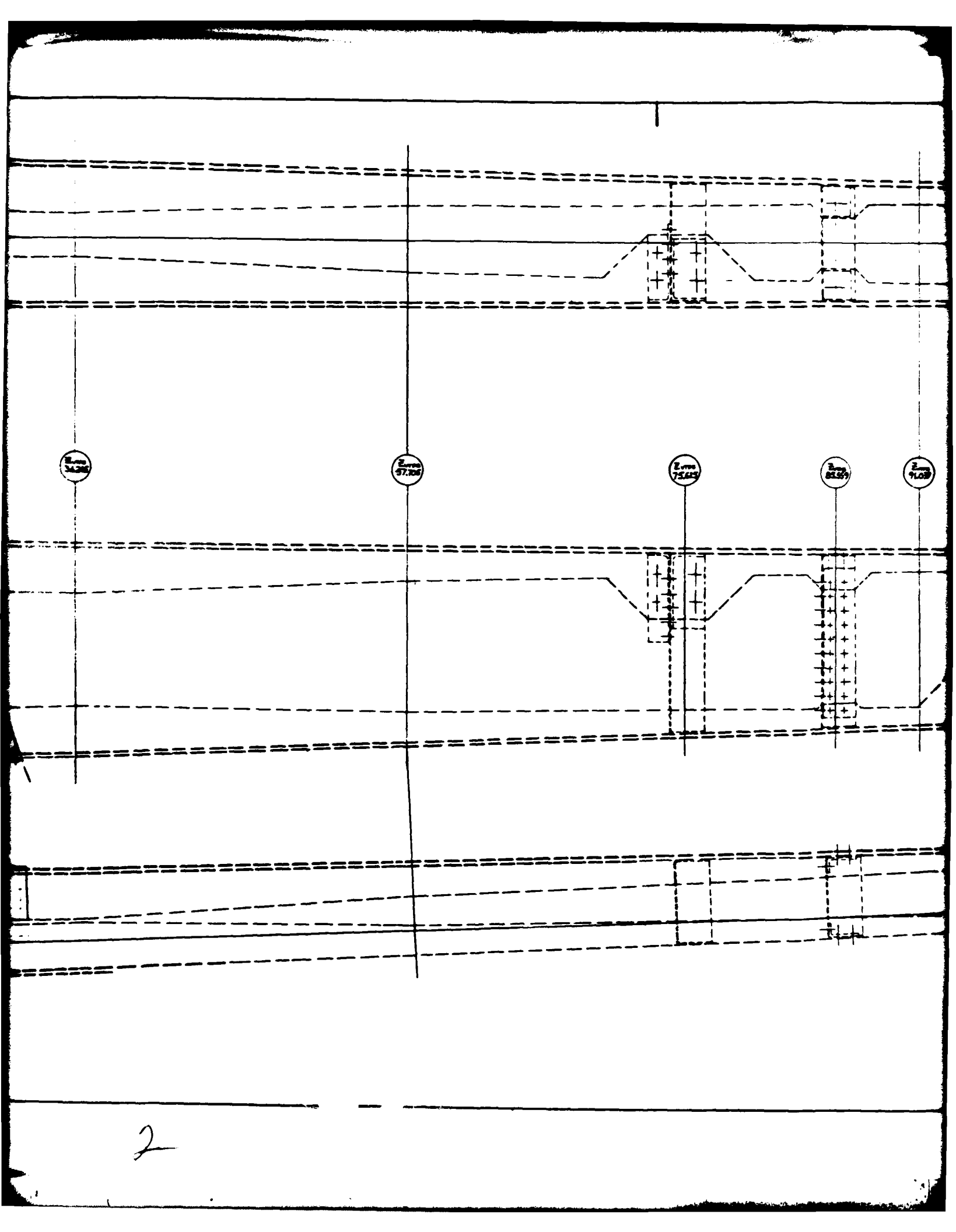
STACKING SEQUE
FOR - 55 INSET
- 57, - 59 DOUBLER

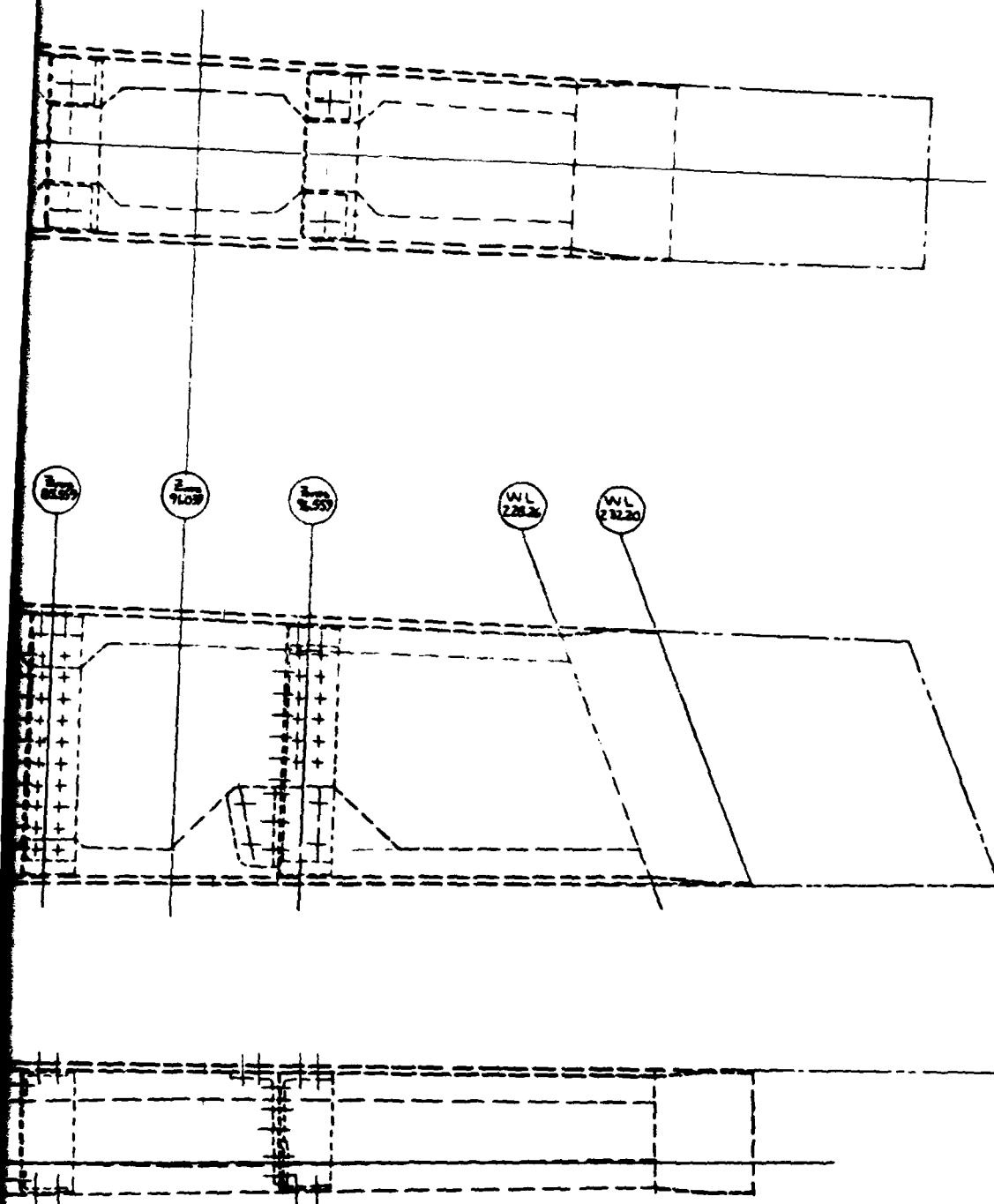
1	145	0	U	.017
2	90	0	U	.050
3	0/90	0	U	.010
4	0/90	0	U	.010

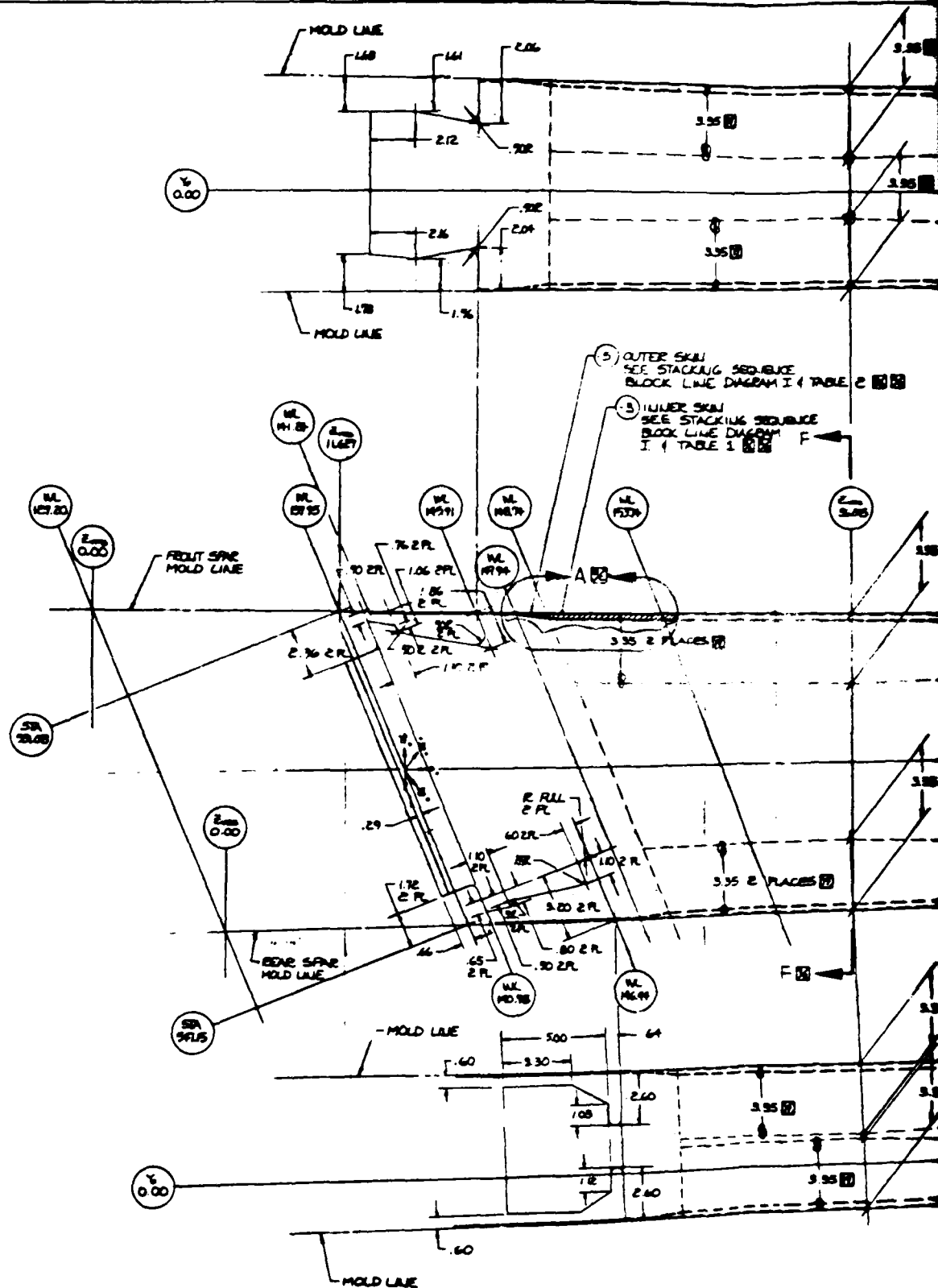
STACKING SEQUENCE
FOR -55 INSERT &
-57-59 DOUBLES

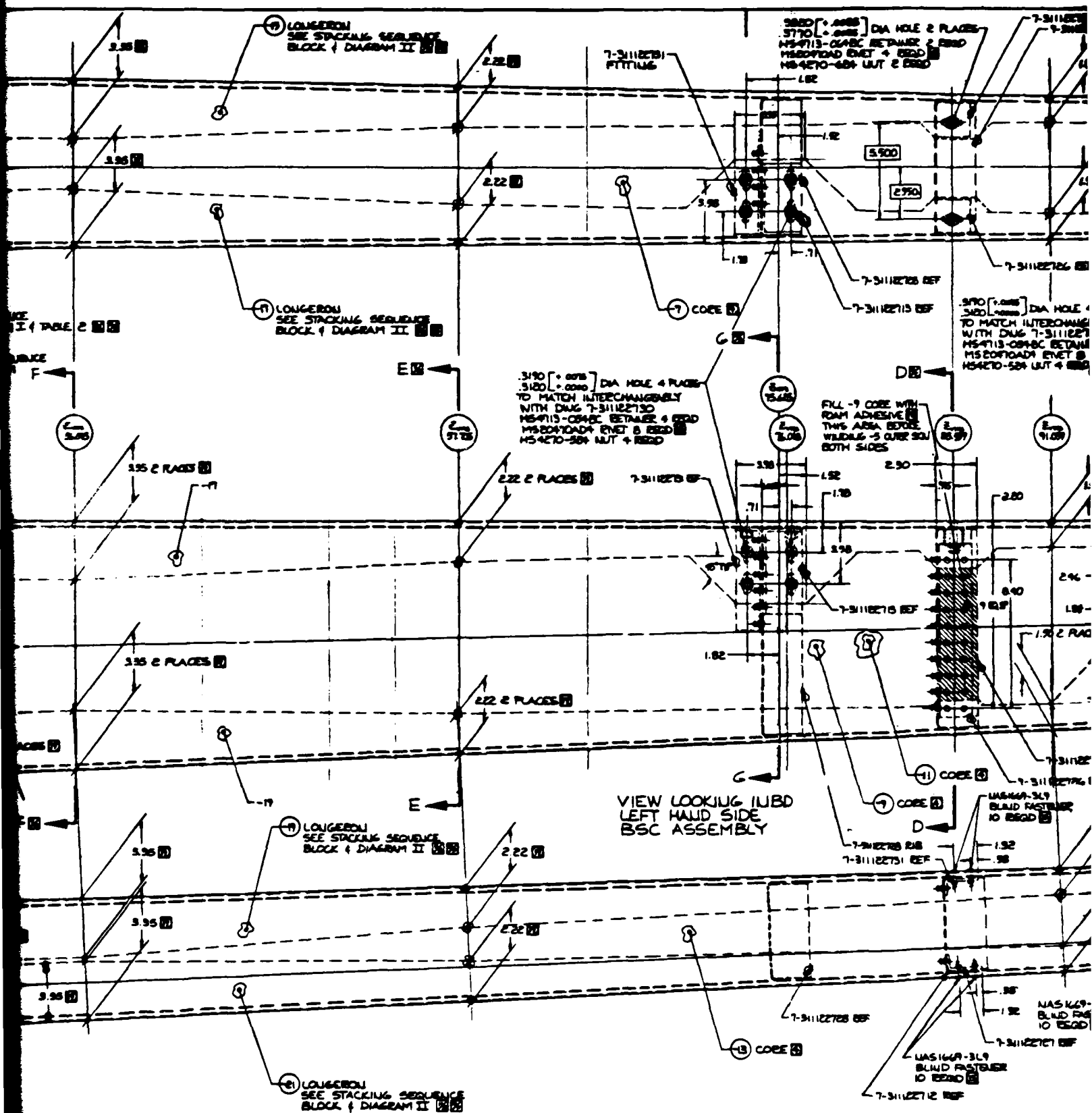


2







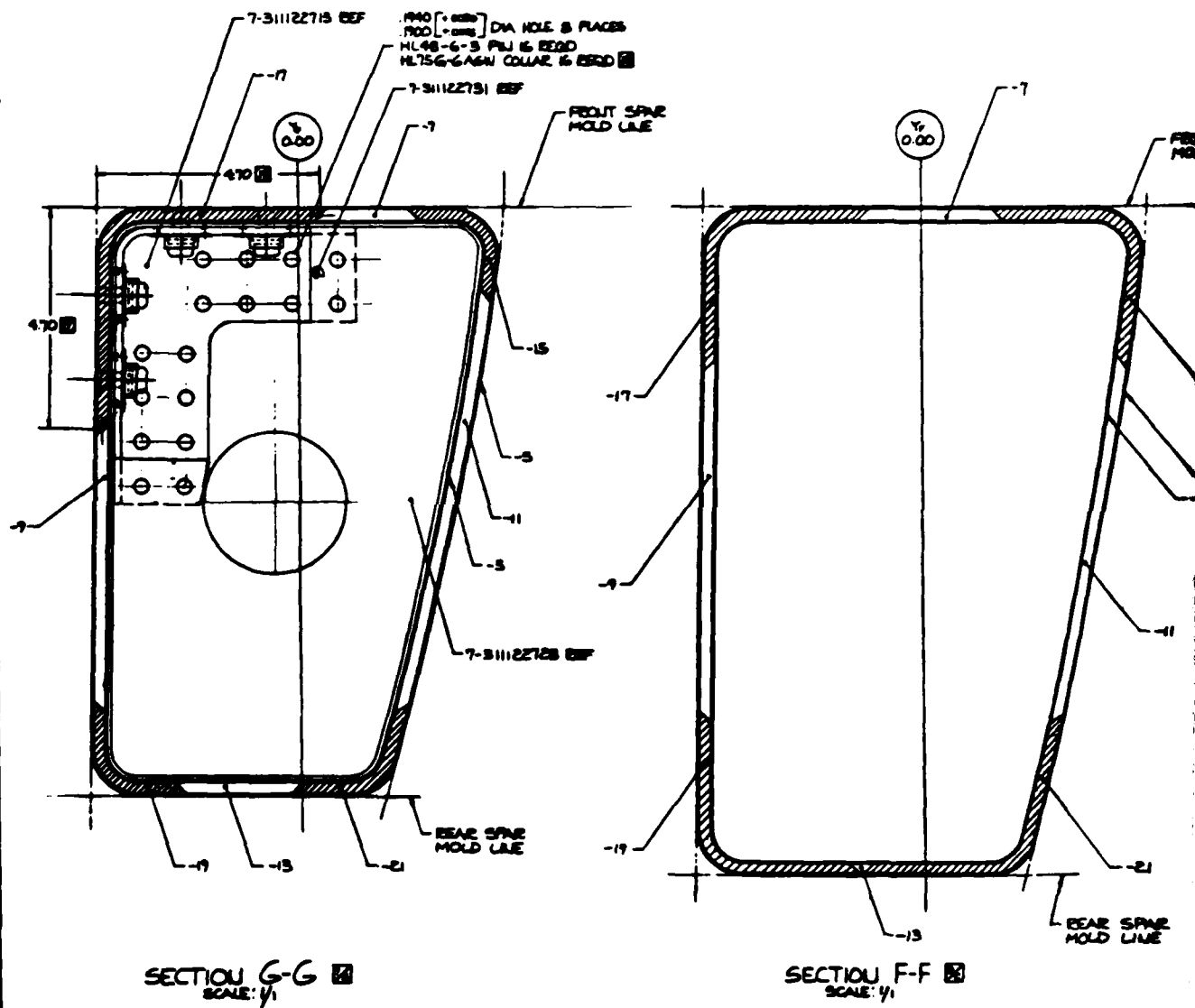


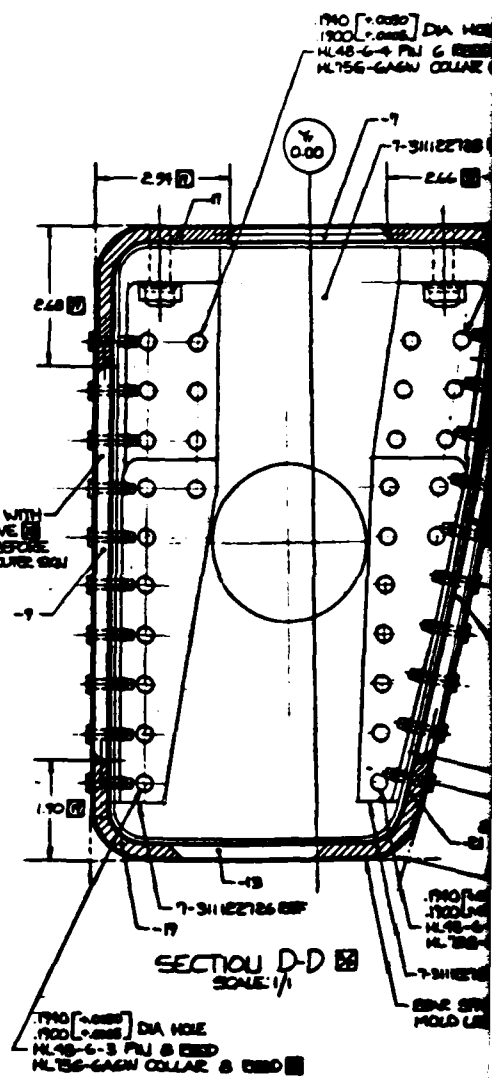
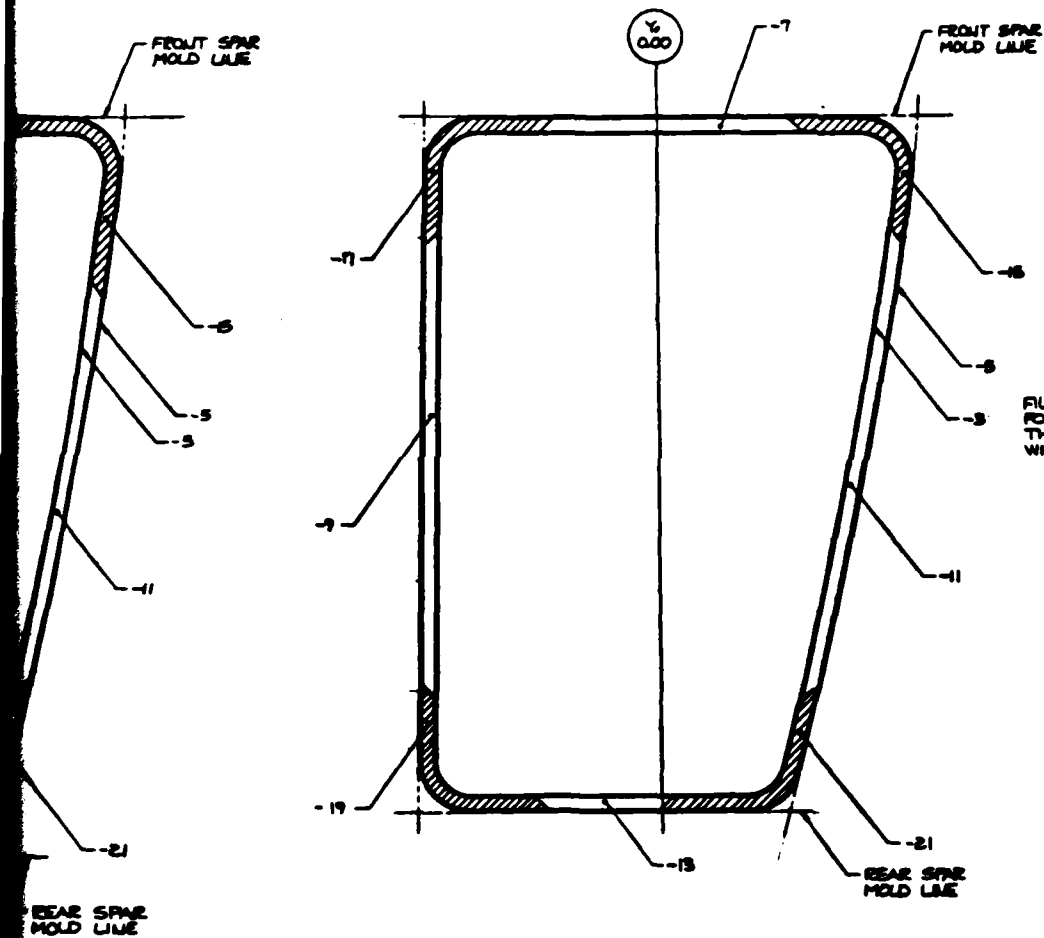


- NOTES: UNLESS OTHERWISE SPECIFIED

[illegible]

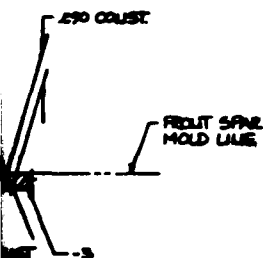
183







LY DASH NUMBERS
OF OFFS SEE LAR
DASH II + TABLE 2



P3	90°	5	6	.0085
P2	225°	5	6	.07
P1	90°	5	6	.0085
PLY 10.	00000	PLY 2	PLY 3	

STACKING SEQUENCE
FOR -3 INNER SKIN
TABLE 1

FE	90°	5	6	.0005
FI	25°	5	6	.001
RY MD.	0.0001	MAX	PER	PER

STACKING SEQUENCE
FOR -5 OUTER SKIN
TABLE 2

[illegible]

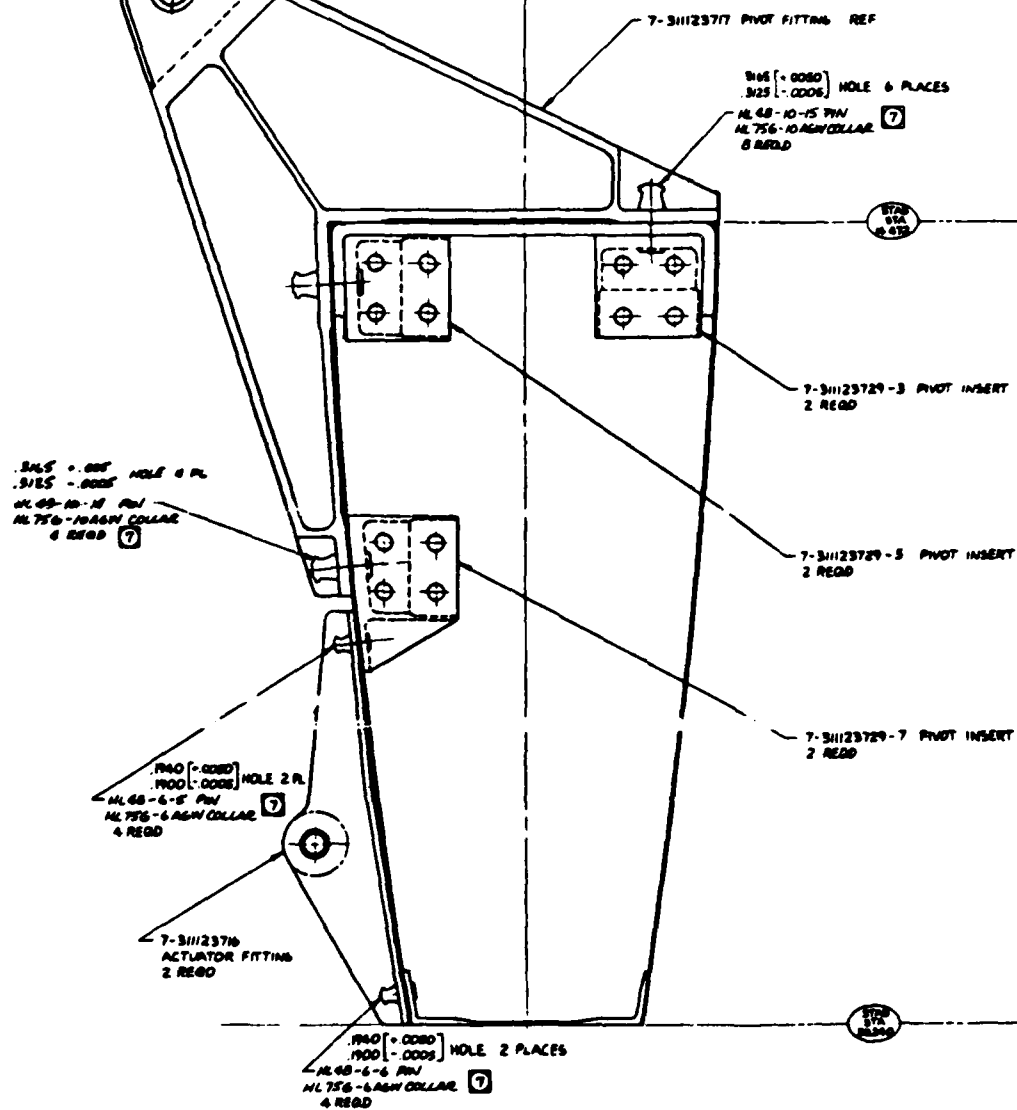
STACKING SEQUENCE
FOR -15, -17, -19, & -21 LONGERON
TABLE 3



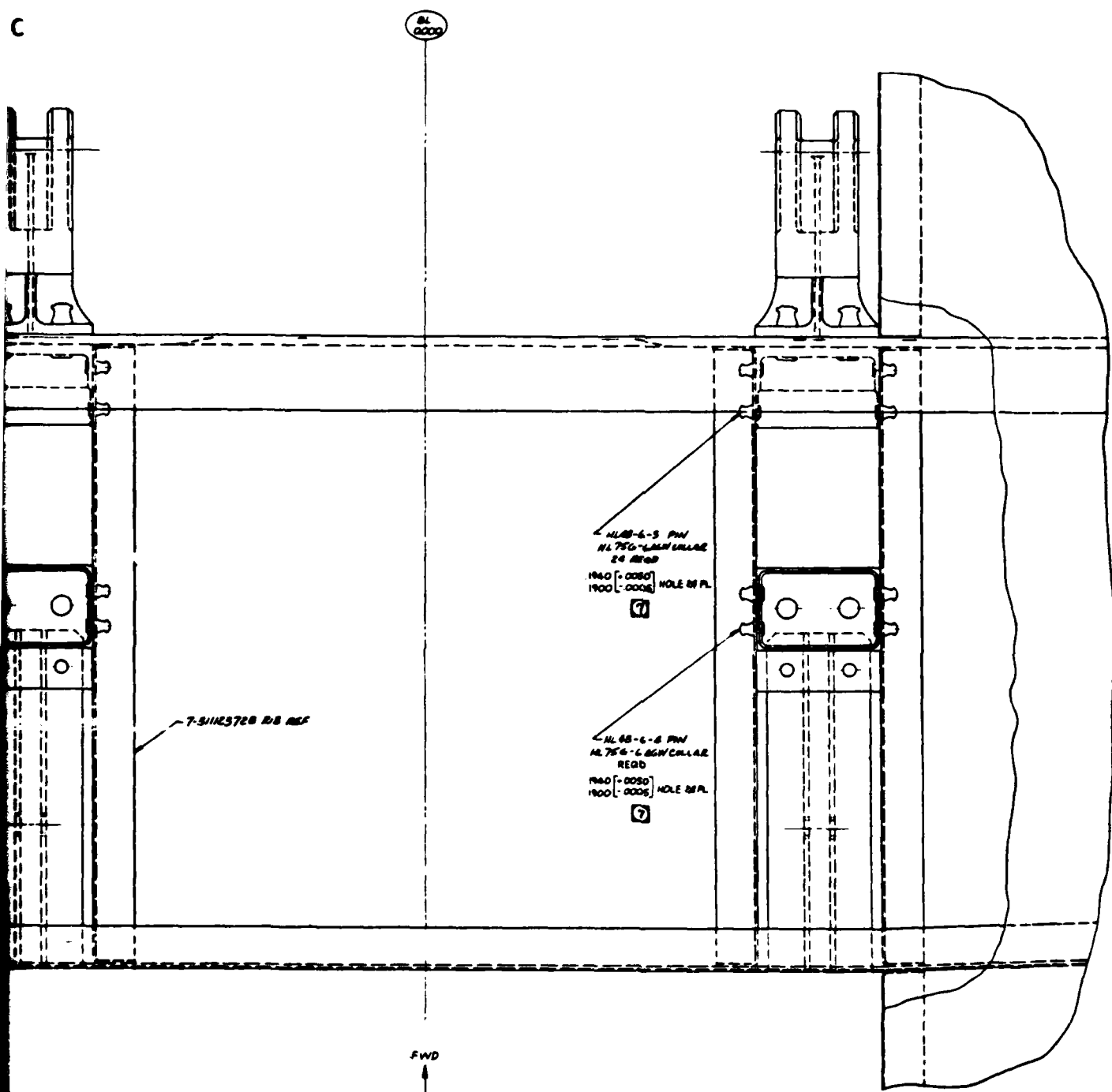
Pages/Story 10

[illegible]

Figure 98. Vertical Tail Subassembly (Sheet 2 of 2)

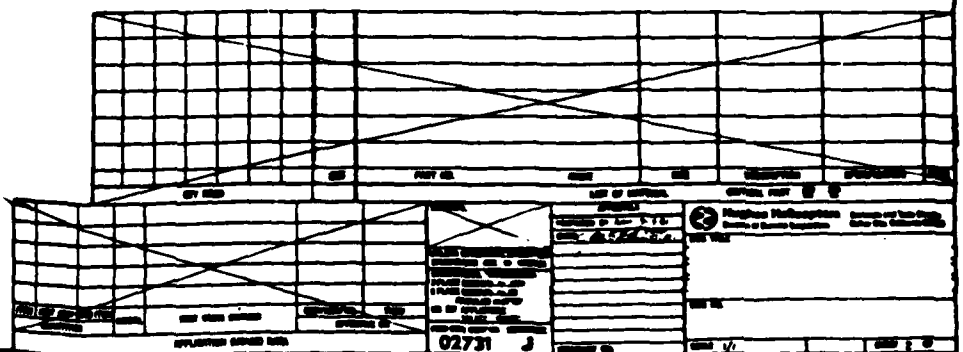


C

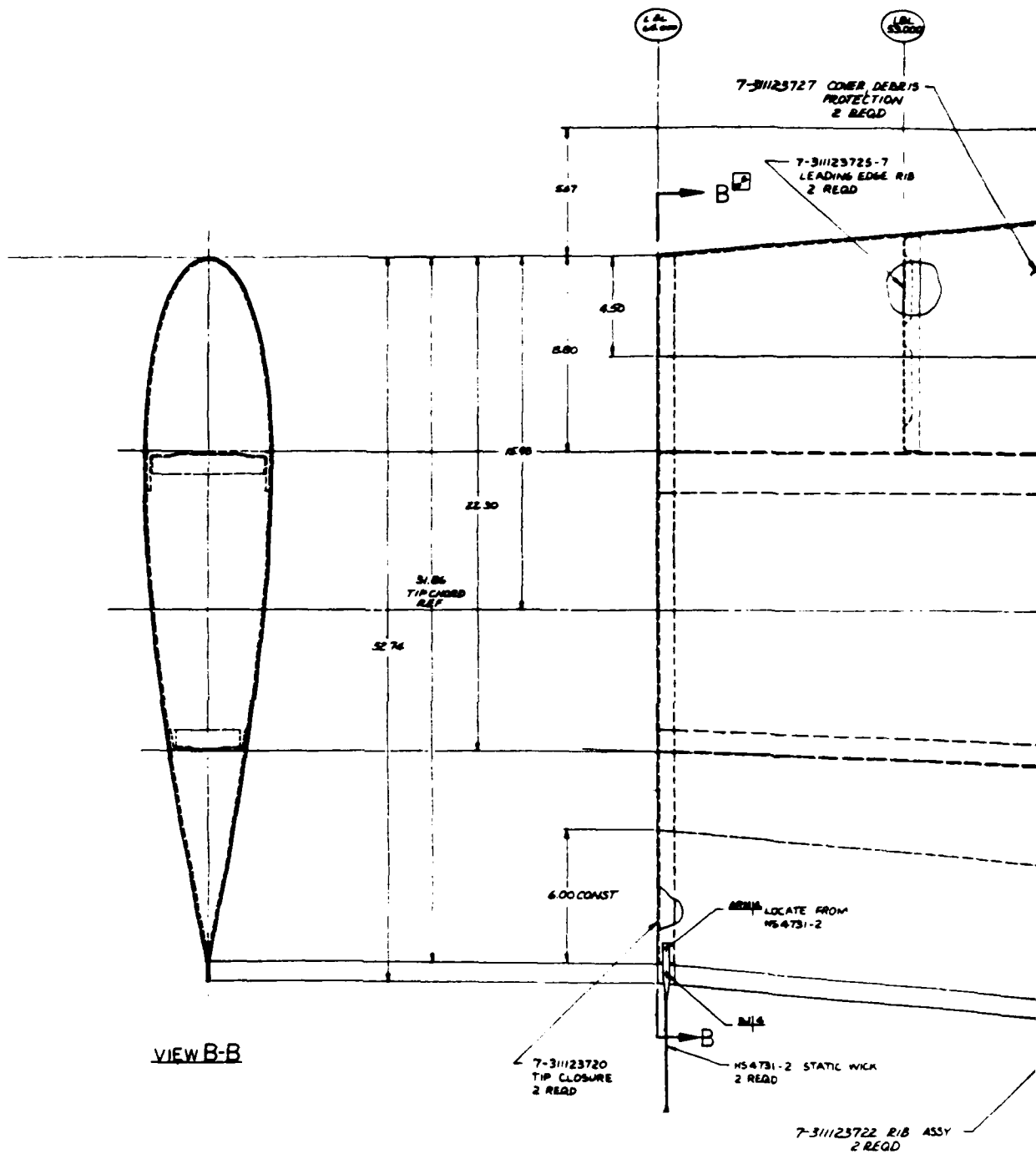


C 2

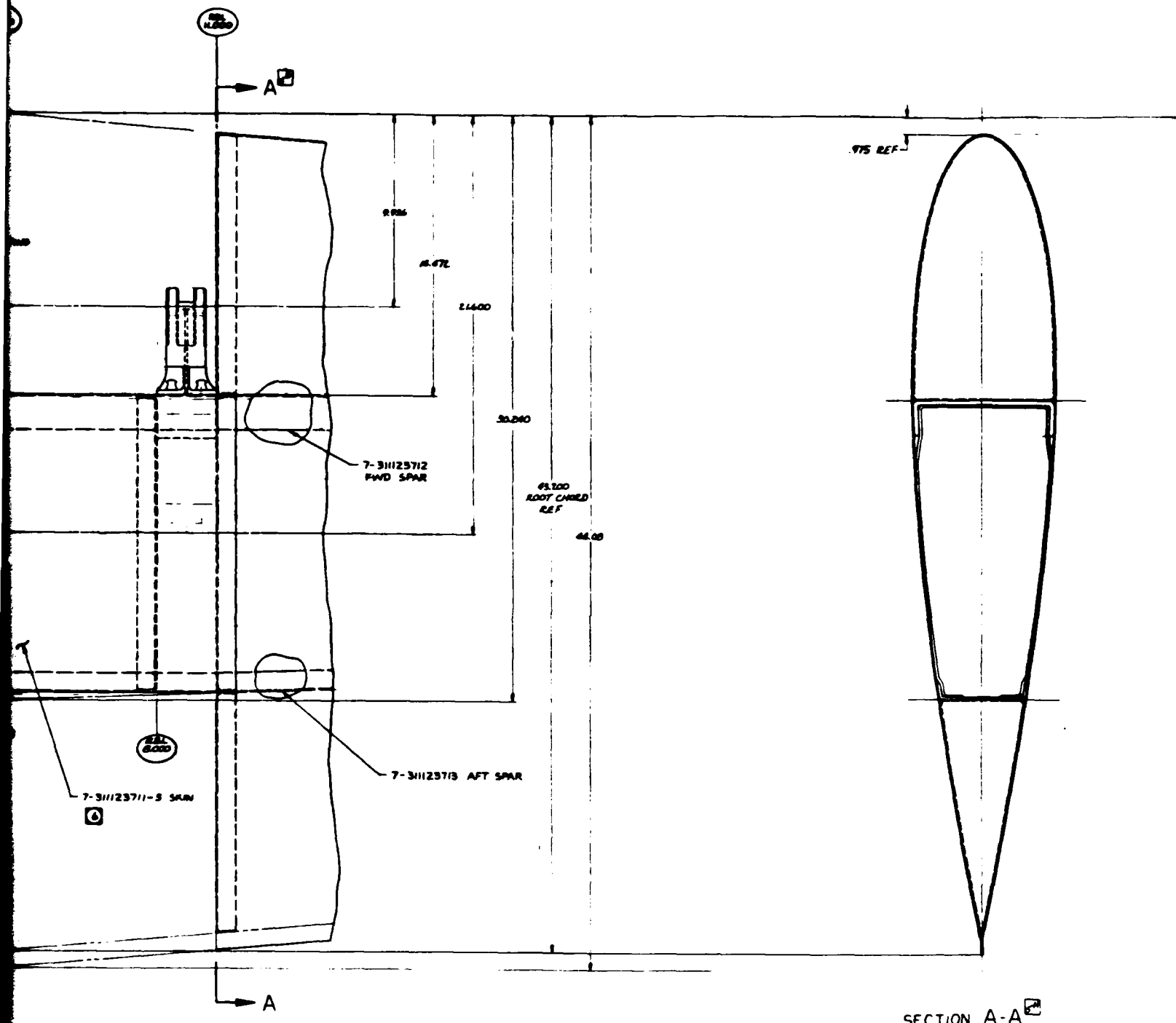
2



3







SECTION A-A

- 1 FINISH AND ED PER EPG 4-230
 - 2 SEAL FASTENERS USING NPSM-1097 PER NPS-10 TYPE III
 - 3 INSTALL NUTS PER NPS-2
 - 4 INSTALL BLIND RIVETS PER NPS-5
 - 5 INSTALL BLIND RIVETS PER NPS-5
 - 6 BOND PER NPS-30
 - 7 DIMENSIONS & TOLERANCES PER ANSI Y14.5
 - 8 IDENTIFY PER NPS-5 TYPE I, CLASS 3 LOCATE APPROX AS SHOWN
 - 9 CONTOUR PER 7-21123600 EXCEPT PLANFORM AS SHOWN
- NOTES: UNLESS OTHERWISE SPECIFIED

QTY	UNIT	DESCRIPTION	REMARKS	DATE	BY
2	AR	CR 3213	ADHESIVE		
2		MS20470AD4	RIVET		
54		NL 756-6 AGW	RIVET		
12		NL 756-10AGW	COLLAR		
4		NL 48-6-6	COLLAR		
4		NL 48-6-5	PIN		
24		NL 48-6-4			
24		NL 48-6-3			
8		NL 48-10-15			
8		NL 48-10-14	PIN		
2		MS4731-2	STATIC WICK		
2		7-31123716	FITTING ACTUATOR		
2		7-31123729	INSERT FITTING		
2		7-31123727	DEBRIS PROTECTING		
2		7-31123728	RIB, BL 8.00		
2		7-31123725	RIB, LEADING EDGE		
2		7-31123722	RIB ASSY, BL 42.00		
2		7-31123721	RIB ASSY, BL 24.00		
2		7-31123720	TIP CLOSEOUT		
2		7-31123717	PIVOT FITTING		
2		7-31123714	RIB ASSY, BL 14.00		
1		7-31123713	SPAR, AFT		
1		7-31123712	SPAR, FWD		
1		7-31123711	SKIN		

Figure 99. Stabilator Assembly (SI

QTY	ITEM	DESCRIPTION	UNIT	REMARKS
2	AR	ADHESIVE	FILM	NMS 16 111 CLASS 2
2	CR 3213	RIVET		
2	MS 20470A04	RIVET		
54	NL 756-6 ASW	COLLAR		
12	NL 756-10 ASW	COLLAR		
4	NL 48-6-6	PIN		
4	NL 48-6-5			
24	NL 48-6-4			
24	NL 48-6-3			
8	NL 48-10-15			
4	NL 48-10-14	PIN		
2	MS 4731-2	STATIC WICK		9C
2	7-31123716	FITTING ACTUATOR		17C
2	7-31123729	INSERT FITTING		AD ME
2	7-31123727	DEBRIS PROTECTIVE		86
2	7-31123728	RIB, BL 42.00		40
2	7-31123725	RIB, LEADING EDGE		7
2	7-31123722	RIB ASSY, BL 42.00		88
2	7-31123721	RIB ASSY, BL 24.00		78
2	7-31123720	TIP CLOSURE		7C
2	7-31123717	PIVOT FITTING		66
2	7-31123714	RIB ASSY, BL 14		68
1	7-31123713	SPAR, AFT		50
1	7-31123712	SPAR, FWD		5F
1	7-31123711	SKIN		78

1097 RFR NPS-10 TYPE 15

PER ANSI Y14.5
CLASS 3 LOCATE APPROX AS SHOWN
DEPT PLATFORM AS SHOWN
REFIED

Figure 99. Stabilator Assembly (Sheet 2 of 2)